UNIVERSITY OF HAWAII
LIBRARY

Geochimica et Cosmochimica Acta

JOURNAL OF THE GEOCHEMICAL SOCIETY

Editors: L. H. AHRENS, *Capetown*. C. W. CORRENS, *Göttingen*. E. INGERSON, *Washington*. S. R. NOCKOLDS, *Cambridge*. F. A. PANETH, *Mainz*. H. C. UREY, *Chicago*. JOHN VERHOOGEN, *Berkeley, Calif.* A. P. VINOGRADOV, *Moscow*. L. R. WAGER, *Oxford*. F. E. WICKMAN, *Stockholm*.

CONTENTS — VOLUME 13, NOS. 2/3 — 1958

PAGE

L. R. WAGER, J. VAN R. SMIT and H. IRVING: Indium content of rocks and minerals from the Skaergaard intrusion, East Greenland 81

JACK GREEN and ARIE POLDERVAART: Petrochemical fields and trends 87

A. A. SMALES, D. MAPPER and A. J. WOOD: Radioactivation analysis of "cosmic" and other magnetic spherules 123

ROY S. CLARKE, JR. and ZALMAN S. ALTSCHULER: Determination of the oxidation state of uranium in apatite and phosphorite deposits 127

AKIMASA MASUDA: Isotopic composition of primeval lead of the earth 143

E. D. GOLDBERG and G. O. S. ARRHENIUS: Chemistry of Pacific pelagic sediments . . 153

GEORGE V. CHILINGAR: Some data on diagenesis obtained from Soviet literature: A summary 213

Geochemical Note:

DONALD L. GRAF and JULIAN R. GOLDSMITH: The solid solubility of $MgCO_3$ in $CaCO_3$: A revision 218

Letters to the Editors:

R. EULER und E. HELLNER: Hydrothermale und röntgenographische Untersuchungen an gesteinsbildenden Mineralen—II. Über hydrothermale Untersuchungen in Druckbomben mit Temperaturgefälle 220

R. EULER und E. HELLNER: Hydrothermale und röntgenographische Untersuchungen an gesteinsbildenden Mineralen—III. Über einen hydrothermal hergestellten Granat (Andradit) 221

News and Notes 223

Papers to appear in future issues 223

In Memoriam 224

PERGAMON PRESS LONDON • NEW YORK • PARIS • LOS ANGELES

GEOCHIMICA ET COSMOCHIMICA ACTA

EDITORS

PROF. L. H. AHRENS *Department of Chemistry, University of Capetown, Rondebosch, Cape Province, South Africa*
PROF. C. W. CORRENS *Sedimentpetrographisches Institut der Universität, Lotzestr.* 13, *Göttingen, Germany*
DR. E. INGERSON *Geochemistry and Petrology Branch, U.S. Geological Survey, Washington* 25, *D.C., U.S.A.*
DR. S. R. NOCKOLDS *Department of Mineralogy and Petrology, The University, Cambridge, England*
PROF. F. A. PANETH, F.R.S. *Max-Planck-Institut für Chemie, Mainz, Saarstrasse* 23, *Germany*
PROF. H. C. UREY, For. Mem. R. S. *The Enrico Fermi Institute for Nuclear Studies, University of Chicago, Illinois, U.S.A.*
DR. JOHN VERHOOGEN *Department of Geology, University of California, Berkeley, California, U.S.A.*
PROF. A. P. VINOGRADOV *Vernatsky Institute, Moscow, U.S.S.R.*
PROF. L. R. WAGER, F.R.S. *Department of Geology and Mineralogy, The University, Oxford, England*
PROF. F. E. WICKMAN *Naturhistoriska Riksmuseets, Mineralogiska Avdelning, Stockholm* 50, *Sweden*

EDITORIAL ADVISORY BOARD

EUROPE

T. BARTH, *Oslo*
L. CAPDECOMME, *Toulouse*
E. J. CONWAY, *Dublin*
P. ESKOLA, *Helsinki*
P. GALLITELLI, *Modena*
A. HADDING, *Lund*
O. HAHN, *Göttingen*
H. W. HARVEY, *Plymouth*
F. HEIDE, *Jena*
A. HOLMES, *Edinburgh*
W. Q. KENNEDY, *Leeds*
PH. H. KUENEN, *Gröningen*
S. LANDERGREN, *Stockholm*
F. MACHATSCHKI, *Vienna*
A. MUIR, *Harpenden*
J. ORCEL, *Paris*
E. RAGUIN, *Paris*
K. RANKAMA, *Helsinki*
E. REINHARD, *Basle*
TH. G. SAHAMA, *Helsinki*
C. E. TILLEY, *Cambridge*
T. VOGT, *Trondheim*
W. WAHL, *Helsinki*

AMERICAN CONTINENT

A. F. BUDDINGTON, *Princeton*
D. GUIMARAES, *Belo Horizonte*
G. E. HUTCHINSON, *New Haven*
B. H. MASON, *New York*
F. WHIPPLE, *Cambridge*
R. WILDT, *New Haven*

FAR EAST

T. WATANABE, *Tokyo*

Publishing Offices: Pergamon Press Ltd., 4 & 5 Fitzroy Square, London W.1 (EUSton 4455)

Four issues per volume, three volumes per year

Subscription *per annum* (including postage) (A) £16. 10s. (U.S.A. $46.50); (B) For individual subscribers who certify that the Journal is for their private use, £10. 10s. (U.S.A. $30.00). Members of the Geochemical Society, or non-members who occasionally publish papers in the Journal, £3. 10s. (U.S.A. $10.00) *per annum.*

Payment must be made in advance

Back numbers, £7 (U.S.A. $19.60) per volume

Copyright © 1958 Pergamon Press Ltd.

PERGAMON PRESS LTD.

4 & 5 FITZROY SQUARE, LONDON W.1 122 EAST 55TH STREET, NEW YORK 22, N.Y.

PRINTED IN NORTHERN IRELAND AT THE UNIVERSITIES PRESS, BELFAST

Geochimica et Cosmochimica Acta, 1958, Vol. 13, pp. 81 to 86. Pergamon Press Ltd., London

Indium content of rocks and minerals from the Skaergaard intrusion, East Greenland

L. R. WAGER, J. VAN R. SMIT* and H. IRVING
University of Oxford

(*Received* 23 *January* 1957)

Abstract—The indium content of rocks and separated minerals from the Skaergaard intrusion, East Greenland, has been determined by radioactivation analyses. The original basic magma contained an average of 0·058 p.p.m. of indium and fractionation resulted in a threefold increase in the ferrogabbros with a subsequent slight decrease in the latest granitic fraction. Analyses of separated minerals of the magmatic stage indicate that indium preferentially enters those containing iron.

INDIUM in VERNADSKY's nomenclature is a dispersed element, nowhere becoming an essential constituent of any mineral. Radioactivation analyses of high sensitivity have recently been made by one of us (J. VAN R. S.) on certain rock-sand minerals from the differentiated Skaergaard intrusion (WAGER and DEER, 1939; WAGER and MITCHELL, 1951). The analyses (Table 1 and also SMALES, SMIT and IRVING, 1957; and IRVING, SMIT and (in part) SALMON, 1957) provide precise evidence of how indium becomes distributed during fractionation of a basic magma.

The composition of the original magma from which the complex, about 300 km^3 in volume, was formed, is represented by chilled marginal gabbro, two examples of which have been analysed for indium (Table 1, first part). The results of separate determinations by two different methods depending on 49 day ^{114}In and 54 min ^{116}In respectively are given and they show that the two rocks have slightly different indium contents. The average indium in the original magma may be taken as 0·058 p.p.m. This is close to the figure of 0·064 p.p.m. obtained for the standard diabase W1 (SMALES, SMIT and IRVING, 1957). SHAW (1952) has given the most recent survey of the geochemistry of indium, based largely on his own spectrographic determinations; for six gabbros and dolerites the range is from 0·02 to 0·078 p.p.m. and for four basalts it is from 0·12 to 0·32 p.p.m.

Rocks of the Skaergaard layered series show an increasing content of indium in successive fractions ranging from 0·060 to 0·18 p.p.m. (Table 1). In the early hypersthene olivine gabbro 5086, where the olivine is Fa_{37} and the pyroxene $Ca_{39}Mg_{42}Fs_{19}$, the amount of indium is 0·06 p.p.m. Earlier layered rocks are not accessible, but there is little doubt that they would have appreciably less indium (see below). The two latest layered rocks, the fayalite ferrogabbros 4327 and 4328, have iron-rich ferromagnesian minerals in about equal amounts and an indium content of 0·15 p.p.m. The rock 4327 is similar to 4328 except that the latter has 2 per cent of iron sulphide (S = 5000 p.p.m.) while the former has only small amounts of sulphide (S = 50 p.p.m.) (WAGER, VINCENT and SMALES, 1957). Indium is regarded as a chalcophile element, and it was expected that it would have entered the sulphides in sufficient amounts to show a distinct increase in the more sulphide-rich rock; this, however, is not the case; apparently, strong concentration

* Now at The National Physical Laboratory, Box 395, Pretoria, South Africa.

Table 1. Indium in rocks and minerals of the Skaergaard intrusion
(Analyst J. van R. Smit)

Rock or mineral	Actual determinations (p.p.m.) (by ^{116}In unless otherwise stated)	Average (p.p.m.)
Chilled marginal gabbro (original magma)		
4507 (south margin)	0·053, 0·058, 0·054, 0·056, 0·053, 0·054, 0·050, 0·053	0·054
	0·052, 0·054, 0·055, (by ^{114}In)	
1825 (east margin)	0·062, 0·062, 0·059, 0·062	0·061
	0·060, 0·062, 0·060, (by ^{114}In)	
Latest differentiates		
Acid granophyre 3058	0·093, 0·089	0·091
Layered series (with height on arbitrary scale		
Fayalite ferrogabbro 4328 (2500 m) with 2% of sulphides	0·18, 0·18, 0·19, 0·17, 0·18, 0·19	0·18
	0·16, 0·19, 0·17, 0·17, 0·194, 0·164, (by ^{114}In)	
Fayalite ferrogabbro 4327 (2455 m)	0·16, 0·17, 0·17, 0·17	0·17
	0·163, 0·170, 0·151, (by ^{114}In)	
Hortonolite ferrogabbro 5181 (1800 m)	0·078, 0·083, 0·077	0·079
Hypersthene olivine gabbro 5086 (280 m)	0·059, 0·062	0·060
Pyroxenes		
From basic hedenbergite granophyre 4332 (2590 m)	1·08, 1·06, 1·06	1·07
From ferrogabbro 5181 (1800 m)	0·18, 0·18	0·18
From hypersthene olivine gabbro 4392 (50 m)	0·16, 0·17	0·17
Minerals from hortonolite ferrogabbro 5181		
Feldspar	0·0034, 0·0030	0·0032
Olivine	0·055, 0·057	0·056
Pyroxene	0·18, 0·18	0·18
Magnetite	0·16, 0·15	0·16
Ilmenite	0·28, 0·29	0·29

of indium in immiscible sulphide liquid in equilibrium with silicate magma has not taken place in this case.

The latest rock of the Skaergaard complex (3058), an acid granophyre or microgranite with 75 per cent SiO_2, was formed from the latest liquid fraction of the Skaergaard gabbro magma. Its indium content is 0·091, a decrease from the values for the latest ferrogabbros, but still much higher than that of the standard granite

G1, which is 0·026 (SMALES, SMIT and IRVING, 1957). SHAW's average figure for granite is given as 0·26, but this is based on values which range from 0·02 to 2 p.p.m. (SHAW, 1952, p. 192).

The distribution of indium in minerals precipitating simultaneously from a late-stage basic magma has been obtained by analysis of the five chief minerals* of the ferrogabbro 5181 (Tables 1 and 2). The amount of indium in the plagioclase is only about a twentieth of that in the ferromagnesian minerals and the iron ores; apparently, indium does not readily occupy any of the positions in the plagioclase structure. Among the ferromagnesian minerals, indium enters pyroxene more readily than olivine. In both minerals it no doubt mainly substitutes for ferrous iron, but as with other tri- and quadri-valent elements, such as chromium, vanadium, scandium, and zirconium, substitution occurs more readily in the augite than the olivine structure (WAGER and MITCHELL, 1951, Table B). Titaniferous magnetite contains approximately the same amount of indium as augite, but ilmenite contains nearly twice as much.

The amounts of the various minerals in the hortonolite ferrogabbro 5181 have been determined by micrometric analysis, and thus the weight of indium in the amount of these minerals in a known weight of the rock may be estimated (Table 2). The summation of the amounts of indium in the individual minerals based on the analysis of the minerals is very close to the figure obtained by analysis of the rock.

Table 2. Indium in hortonolite ferrogabbro 5181 and its constituent minerals and comparisons

	In (p.p.m.)	Proportion of minerals in the rock (wt. %)	Indium in the various minerals (g per metric ton of rock)	Comparison	
				Sc[a] (p.p.m.)	Mn[a,b] (p.p.m.)
Plagioclase	0·0032	54	0·0017	*	50
Olivine	0·056	13	0·0073	*	3200
Pyroxene	0·18	23	0·0414	150	1700
Magnetite	0·16	4·5	0·0072	*	3420
Ilmenite	0·29	5·5	0·0160	*	4800
Rock 5181	0·079		Σ 0·074		

[a] WAGER and MITCHELL (1951) Table 13.
[b] VINCENT and PHILLIPS (1954) Tables 2 and 3.
* Less than 10 p.p.m.

Among high-temperature rock-forming minerals, indium has previously been found in considerable abundance in an augite and a magnetite from a lamprophyre, 0·31 and 0·07 p.p.m. respectively (SHAW, 1952, p. 190) and much less abundantly in hypersthene from the Stillwater complex, 0·017, and in olivine, 0·02 (SHAW, 1952, p. 190). It is interesting to note that GOLDSCHMIDT and HÖRMANN (GOLDSCHMIDT, 1954, p. 333) found indium concentrations in some pyroxene-rich basic rocks, but other pyroxenites, dunites, and peridotites have markedly lower indium contents (SHAW, 1952, p. 191).

* These minerals were separated by J. H. CROCKET, to whom we express our thanks.

Anticipating at least moderate values for indium in the pyroxenes, we selected three for analysis* which had crystallized at different stages of the fractionation process (Table 1). The earliest pyroxene from 4392, $Ca_{40}Mg_{43}Fe_{17}$, contains 0·17 p.p.m. indium; a considerably later pyroxene from 5181, $Ca_{35}Mg_{33}Fe_{32}$, contains 0·18 p.p.m., while one of the latest pyroxenes from 4332, $Ca_{43}Mg_{4}Fe_{53}$, close to hedenbergite, has 1·1 p.p.m. indium. It is clear that the amounts of indium in the pyroxenes depend on the degree of fractionation, the later, more iron-rich and lower-temperature pyroxenes being the richer.

Goldschmidt (1954) has discussed the probable factors controlling the entry of indium into igneous minerals during crystallization of magma, and the results given here broadly support his view that indium commonly substitutes for iron. From a consideration of ionic size and valency, Shaw (1952, p. 197) considered that, during crystal fractionation, indium would enter the early ferromagnesian minerals more readily than the later. His own determinations, as he points out, did not particularly bear this out, nor do the indium figures for the three pyroxenes separated from the Skaergaard intrusion, which show a sixfold concentration in the latest pyroxenes. The behaviour of indium in igneous minerals has some similarity with that of scandium. Thus scandium enters most readily the pyroxenes and there is, at first, an increase with fractionation. The amount in a pyroxene from the hypersthene olivine gabbro at 280 m in the Skaergaard layered series is 30 p.p.m.; in a pyroxene from the hortonolite ferrogabbro at 1800 m, it is 150 p.p.m., and in a later pyroxene from 2500 m it is 80 p.p.m. (Wager and Mitchell, 1952, Table B). In ferromagnesian minerals it seems that trivalent indium (ionic radius† 0·92 Å) tends to replace divalent $Fe^{\cdot\cdot}$ ($r = 0{\cdot}83$ Å) much as trivalent Sc ($r = 0{\cdot}83$ Å) replaces divalent Mg ($r = 0{\cdot}78$ Å). It appears also that indium and divalent manganese, despite valency differences, tend to vary sympathetically in the ferromagnesian minerals, each entering more readily the later, more iron-rich varieties. The present observations, however, suggest that trivalent indium is more abundant in pyroxene than olivine, while the reverse is true of manganese (cf. Table 2).

The over-all behaviour of indium during the differentiation of the Skaergaard gabbro magma may be shown graphically by plotting the amount against the stage of fractionation, estimated as the percentage of the whole intrusion crystallized (Fig. 1). The amount in the whole intrusion based on the composition of the chilled marginal gabbro, is proportional to the rectangle $OPQR$, while the total amount in the successive rocks of the intrusion is indicated by the area below the curve. The earliest rock fraction must have contained less indium than the magma, and indium began to increase in successive residual liquids. Later the amount separating in the various minerals of the rocks increased until more was separating in the crystal phases than was present in the liquid, as shown by the fall in indium in the latest residual magma, the acid granophyre. Concentration of scandium reaches a maximum in the rocks rather earlier than that of indium, that of manganese at apparently the same stage as indium (Fig. 1).

---

* The pyroxenes were separated by G. M. Brown and N. E. Butcher, to whom we express our thanks.

† The ionic radii here used are those of Goldschmidt. The radii for both indium and scandium are both 0·81, according to Ahrens' estimate (1952), and a closer similarity of behaviour of indium and scandium might have been expected.

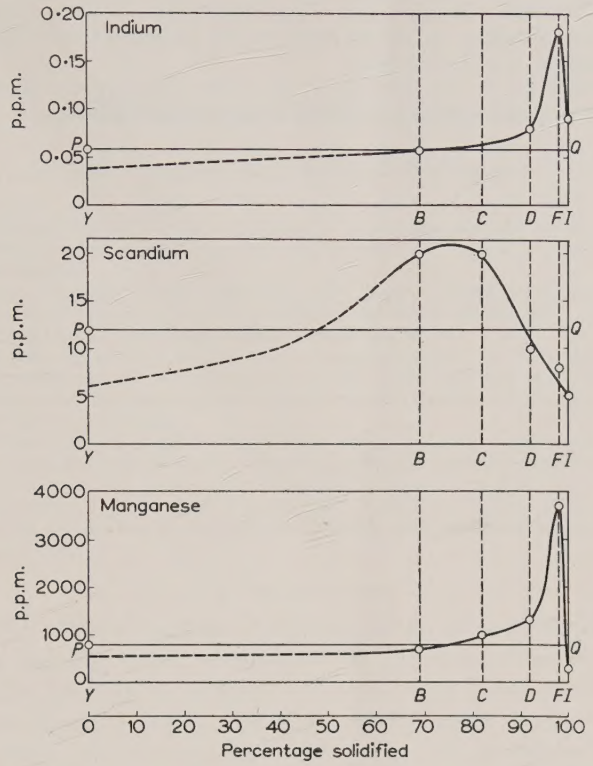

Fig. 1. Indium, scandium, and manganese content of selected rocks of the Skaergaard intrusion, plotted against percentage solidified. *Y*, Chilled marginal gabbro; *B*, Hypersthene olivine gabbro; *C*, Middle gabbro; *D*, Hortonolite ferrogabbro; *F*, Fayalite ferrogabbro; *I*, Acid granophyre.

The average indium content of basic rocks has been estimated as of the order of 0·1 p.p.m. (basalt 0·2, gabbro 0·02; SHAW, 1952, p. 203). Owing to relatively easy entry into the ferromagnesian minerals of basic rocks, indium does not become much enriched in the residual liquids from the fractionation of basic magma, and this is apparently the reason for its low concentration in granites and mineral veins derived from them.

REFERENCES

AHRENS L. H. (1952) The use of ionization potentials. Part 1: Ionic radii of elements. *Geochim. et Cosmochim. Acta* **2,** 155–169.

GOLDSCHMIDT V. M. (1954) *Geochemistry* (Edited by A. MUIR) Oxford.

IRVING H., SMIT J. VAN R. and (in part) SALMON L. (1957) Determination of indium in cylindrite by neutron radioactivation analysis and other methods. *Analyst* **82.** In press.

SHAW D. M. (1952) The geochemistry of indium. *Geochim. et Cosmochim. Acta* **2,** 185–206.

SMALES A. A., SMIT J. VAN R. and IRVING H. (1957) Determination of indium in rocks and minerals by radioactivation. *Analyst* **82.** In press.

VINCENT E. A. and PHILLIPS R. (1954) Iron-titanium minerals in layered gabbros of the Skaergaard intrusion, East Greenland. Part 1: Chemistry and ore-microscopy. *Geochim. et Cosmochim. Acta* **6,** 1–26.

WAGER L. R. and DEER W. A. (1939) The petrology of the Skaergaard intrusion, Kangerdlugssuaq, East Greenland. *Medd. Grønland* **105,** 1–352.

WAGER L. R. and MITCHELL R. L. (1951) The distribution of trace elements during strong fractionation of basic magma—a further study of the Skaergaard intrusion, East Greenland. *Geochim. et Cosmochim. Acta* **1**, 129–208.

WAGER L. R., VINCENT E. A. and SMALES A. A., with appendix by BARTHOLOME P. (1957) *Sulphides in the Skaergaard intrusion, East Greenland.* In preparation.

Geochimica et Cosmochimica Acta, 1958, Vol. 13, pp. 87 to 122. Pergamon Press Ltd., London

Petrochemical fields and trends

JACK GREEN* and ARIE POLDERVAART†

Abstract—Average compositions of igneous, sedimentary, and metamorphic rocks, and of stony meteorites have been recalculated to ionic weight per cent and plotted on diagrams with variables Al, total Fe, Mg, Ca and combined alkalis.

Igneous rocks show a definite trend, indicating that in their formation fractionation predominates over processes which are only locally operative. Na/K ratios show wide scatter, indicating predominance of locally operative processes in sodic versus potassic variations.

Normal and preponderant sediments fall in a well-defined field. Na/K ratios scatter about a mode of 0·54. Na/K ratios in igneous rocks, sediments, and sea-water are used in argument against the derivation of sediments from predominantly mafic source rocks. Storage of Ca near the earth's surface is indicated by the sedimentary averages.

Metamorphic variations from argillite to granitic gneiss indicate addition of alkalis and calcium, with subtraction of iron and magnesium. Low-temperature changes are distinguished from high-temperature metasomatism which grades into formation of granite magma.

Data on stony meteorites are also briefly presented. Variations in composition of different types of stony meteorites can be attributed to oxidation–reduction and fractionation by partial melting, both generally operative processes.

INTRODUCTION

FIVE years ago the writers started a programme to review the chemistry of major elements in the earth's crust, especially to determine what evidence can be used in the elusive puzzles of crustal evolution and development of oceans and continents. Four papers have so far appeared (GREEN, 1953, 1955; GREEN and POLDERVAART, 1955; POLDERVAART, 1955), concerned chiefly with estimates of average compositions of rocks and abundance data of major elements. Publication of NOCKOLDS' reviews of the chemistry of igneous rocks (NOCKOLDS, 1954; NOCKOLDS and ALLEN, 1953; 1954) has greatly helped and accelerated this programme.

In this paper an attempt is made to define a common chemical trend for the progression from mafic to silicic igneous rocks, a field of normal and preponderant sediments, and a trend for the common metamorphic series from argillite to granitic gneiss by progressive feldspathization. Certain assumptions are implicit in these attempts. The treatment is in keeping with an overall dynamic concept of evolution, but it does not necessarily follow that members of a series for which a generalized trend is constructed have evolved from one another.

The quality of the data used varies considerably. For igneous rocks a large number of averages is available, mostly computed by DALY (1933) and NOCKOLDS (1954). NOCKOLDS' averages represent more closely defined rock types and are probably superior to those calculated by DALY. The averages include common rock types as well as igneous rocks sparsely distributed in the earth's crust. Data for sedimentary and metamorphic rocks do not compare with those for igneous rocks; they are few in number and generally less closely defined. For stony meteorites the writers have used the compilations of UREY and CRAIG (1953) and

* California Research Corporation, La Habra, California.
† Department of Geology, Columbia University, New York, N.Y.

WIIK (1956). No attempt is made to qualify the data in the figures, but interpretations based in the diagrams are warranted in terms of both distribution of all data used and distribution of data for common rock types.

IGNEOUS ROCKS

All igneous rocks have crystallized from magma. There is close agreement between the effects of fractionation of artificial melts and observed differentiation in igneous bodies (BOWEN, 1954). Hence it seems likely that fractionation is the most important single process in producing the diversity of igneous rocks. Fractionation is a generally operative process which affects all magmas in the same manner (though not to the same extent), irrespective of geologic time, geographic location or position in the earth's crust.* Superimposed on this common pattern of igneous differentiation are the effects of locally operative processes which vary with depth, amounts of water and other fluxes in different magmas, shape and size of igneous bodies, and nature of country rocks surrounding these bodies.

The existence of a compositional trend common to igneous rocks indicates that the combined effects of locally operative processes are small relative to those of fractionation. Conversely, the scatter of points in chemical diagrams furnishes indications of the respective roles played by fractionation and locally operative processes in the formation of igneous rocks. Some constituents may be more sensitive to the latter processes, while others may show the effects of the former process more clearly. A series of diagrams showing variations of different constituents of igneous rocks may therefore exhibit different degrees of scatter of points which in themselves are significant.

A common igneous trend of evolution has meaning only for the progression from mafic to felsic rocks. Ultramafic averages are also shown on the diagrams but the trend is not extended to the ultramafic rocks. In the mantle, magma is formed by partial melting. Migration of this magma into the crust results in the residual material of the mantle becoming yet more ultramafic. A regressive series for the mantle that may be suggested is stony meteorite–peridotite–dunite. These averages are indicated in Fig. 4. The trend direction in the mantle is necessarily different from that of the crustal series from mafic to felsic rocks. Ultramafic crystal accumulates are formed in the crust by gravity differentiation. The effects show a strong dependence on size, shape, and depth of the intrusives.

Fractional crystallization of ferromagnesian minerals results in iron enrichment of residual magmas, while fractionation of feldspars results in alkali enrichment. The effects of these two competing trends are most clearly shown on a type of diagram suggested by SIMPSON (1954), modified by the writers to ionic weight per cent.

Fig. 1 shows the result of plotting 201 averages of igneous rocks on this diagram. (See Table 1 and its index.) Between mafic and felsic rocks the averages fall along a reasonably well-defined zone which spreads in the ultramafic rocks. At the felsic end the zone appears to curve toward the right to include averages of

*At depths exceeding 100 km the effects of fractional crystallization or partial melting may be entirely different (cf. VERHOOGEN, 1954), but this affects the mantle rather than the crust.

Table 1. Averages of igneous rocks

Index No.	Si	Ti	Al	Fe^{3+}	Fe^{2+}	Mn	Mg	Ca	Na	K	P	O
1	12·3	3·6	1·2	9·2	22·4	0·3	13·3	0·4	0·3	0·1	tr	36·9
2	16·3	1·8	7·4	4·3	3·5	0·2	4·0	15·4	3·4	2·4	0·8	40·5
3	16·6	0·0	0·8	0·0	29·7	0·6	13·4	1·0	0·2	tr	0·0	37·7
4	17·7	2·0	4·4	3·7	5·7	0·1	10·0	11·9	1·7	1·2	0·4	41·2
5	17·8	2·1	6·0	3·7	5·3	0·3	8·3	10·7	2·7	1·1	0·5	41·5
6	18·2	0·8	2·3	4·0	3·6	0·1	21·0	5·4	0·3	1·0	0·4	42·9
7	18·3	1·1	3·3	4·9	3·7	0·2	5·0	21·1	1·7	0·2	0·2	40·3
8	18·6	2·4	6·9	6·2	5·0	0·2	3·8	10·3	3·1	1·7	0·3	41·5
9	18·6	1·2	3·0	5·7	2·9	0·1	17·6	5·3	0·3	2·2	0·3	42·8
10	18·7	1·9	7·3	5·6	2·8	0·3	5·1	11·5	2·7	2·1	0·2	41·8
11	18·8	1·7	4·4	4·7	3·5	0·2	9·1	11·2	1·0	3·5	0·3	41·6
12	18·9	0·1	0·5	1·3	9·3	0·2	26·2	0·5	0·2	0·1	0·0	42·7
13	18·9	1·9	7·1	3·8	5·8	0·2	5·5	9·5	2·5	2·7	0·3	41·8
14	19·0	1·8	6·1	3·4	6·0	0·2	8·1	9·4	2·4	1·2	0·3	42·1
15	19·2	2·4	7·3	4·7	5·6		5·1	9·5	2·3	1·4	0·4	42·1
16	19·4	1·5	11·0	2·7	4·0	0·1	2·2	7·3	6·5	2·5	0·2	42·6
17	19·5		0·5	2·0	4·4	0·2	28·8	0·5	0·1		0·0	44·0
18	19·5	2·0	3·9	4·8	6·1	0·2	7·9	12·2	1·0	0·6	0·3	41·5
19	19·6	0·8	4·0	3·1	7·4	0·2	15·3	5·3	0·8	0·5	0·2	42·8
20	19·9	1·7	6·1	3·7	8·1	0·2	7·6	8·2	1·4	0·7	0·1	42·3
21	19·9	1·4	6·6	4·6	3·4	0·2	3·3	12·1	3·9	2·3	0·6	41·7
22	20·1	1·6	8·9	3·4	4·6	0·2	2·7	7·7	4·1	4·3	0·3	42·1
23	20·1	0·9	9·9	2·8	3·3	0·2	2·0	8·2	7·2	2·1	0·7	42·6
24	20·2	0·5	5·2	3·9	7·2	0·2	12·6	6·0	0·9	0·3	0·1	42·9
25	20·2	0·6	3·0	1·9	7·8		18·9	3·5	0·6	0·4	0·0	43·1
26	20·2	0·9	8·0	2·9	4·1	0·1	9·2	10·0	0·6	0·3	0·0	43·7
27	20·3	0·2	2·2	1·5	7·4	0·2	22·1	2·1	0·3	0·1	0·0	43·6
28	20·3	0·2	14·8	1·8	1·5	0·1	0·4	3·2	10·7	3·2	0·2	43·6
29	20·5	0·5	2·1	1·8	7·7	0·2	20·7	2·5	0·4	0·2	0·0	43·4
30	20·6	1·3	4·8	2·4	7·4	0·1	12·0	6·6	1·1	0·6	0·1	43·0
31	20·6	0·4	7·2	1·6	7·2	0·1	12·0	5·9	1·0	0·5	0·1	43·4
32	20·6	1·0	3·3	3·2	6·8	0·1	13·7	7·3	0·6	0·6	0·1	42·7
33	20·6	1·5	5·5	3·6	4·6	0·1	8·4	7·7	1·6	3·4	0·3	42·7
34	20·6	1·5	4·0	3·9	4·5	0·1	8·7	11·2	0·5	2·3	0·3	42·4
35	20·7	1·7	7·9	3·1	6·1	0·1	5·7	8·9	1·7	0·8	0·2	43·1
36	20·7	1·6	8·0	2·6	6·2	0·2	4·1	8·7	3·6	1·3	0·2	42·8
37	20·9	0·1	1·5	0·6	5·8	0·1	25·0	1·8	0·1			44·1
38	21·0	1·1	9·4	2·6	5·8	0·2	2·3	6·1	5·5	3·0	0·4	42·6
39	21·1	0·6	2·3	3·2	6·3	0·1	11·5	12·1	0·3	0·2		42·3
40	21·1	1·3	6·0	3·4	3·4		5·2	14·4	0·6	2·1	0·0	42·5
41	21·3	1·6	8·3	3·0	5·2	0·1	4·5	7·5	4·0	1·1	0·2	43·2
42	21·4	1·1	4·5	3·6	6·1	0·2	10·3	8·7	0·8	0·3	0·1	42·9
43	21·5	0·1	12·3	4·6	1·6	0·1	0·3	0·7	13·9	1·4	0·0	43·5
44	21·6	1·6	7·8	2·2	6·8	0·2	5·7	7·7	2·0	0·8	0·2	43·4
45	21·6	0·4	9·0	2·8	3·4		3·1	7·8	1·8	7·3	0·2	42·6
46	21·6	2·2	7·4	3·9	4·1	0·1	5·0	7·2	3·5	1·0	0·4	43·6
47	21·6	1·4	8·9	2·1	6·5	0·2	3·5	7·5	3·8	1·2	0·1	43·2
48	21·9	1·6	7·9	3·1	6·0	0·1	4·7	7·6	2·2	1·0	0·2	43·7
49	21·9	1·5	9·3	3·9	3·1	0·1	3·9	7·1	3·8	1·1	0·3	44·0
50	22·0	1·8	8·0	2·6	6·3	0·1	4·8	7·8	2·0	0·8	0·1	43·7

Table 1—*continued*

Index No.	Si	Ti	Al	Fe^{3+}	Fe^{2+}	Mn	Mg	Ca	Na	K	P	O
51	22·0	1·8	7·8	2·6	6·2	0·1	4·1	8·9	1·9	0·9	0·2	43·5
52	22·0	1·0	7·5	2·4	2·7	0·1	5·0	8·0	1·3	6·8	0·3	42·9
53	22·0	0·6	9·3	1·3	6·4	0·1	6·1	8·2	1·5	0·3	0·1	44·1
54	22·0	0·7	5·5	1·8	3·0	0·0	8·1	10·6	0·7	4·5	0·1	43·0
55	22·1	1·3	7·9	3·7	3·6	0·2	3·0	6·3	4·6	3·6	0·6	43·1
56	22·1	1·6	8·4	3·2	5·6	0·2	3·4	7·1	2·9	1·8	0·3	43·4
57	22·1	1·7	9·1	2·6	4·7	0·1	3·0	6·9	3·8	2·2	0·2	43·6
58	22·1	0·9	8·6	2·5	4·5	0·1	3·8	7·8	1·8	4·5	0·3	43·1
59	22·3	1·3	8·9	2·8	5·9	0·2	3·8	6·5	3·1	1·2	0·2	43·8
60	22·3	0·8	8·4	3·2	3·6	0·2	3·2	8·0	1·5	5·6	0·2	43·0
61	22·3	1·5	8·9	3·2	4·5	0·2	3·1	6·2	4·0	2·2	0·3	43·6
62	22·4	1·7	7·8	2·8	6·1	0·1	4·4	6·8	2·8	1·0	0·2	43·9
63	22·5	1·5	8·6	3·1	5·1	0·2	3·4	6·0	3·4	2·1	0·3	43·8
64	22·5	1·0	8·6	4·0	4·1	0·2	2·1	5·1	5·8	3·0	0·3	43·4
65	22·5	1·0	6·3	1·6	7·7	0·1	8·5	6·7	1·2	0·5	0·1	43·8
66	22·6	1·7	8·5	2·4	5·8	0·1	3·7	6·3	3·0	1·6	0·3	44·0
67	22·7	0·9	9·2	2·1	6·0	0·1	4·5	7·8	1·7	0·5	0·1	44·4
68	22·7	1·2	8·3	2·1	6·1	0·1	5·0	7·6	1·9	0·8	0·1	44·1
69	22·8	0·8	9·0	1·8	6·2	0·1	4·9	8·0	1·7	0·5	0·1	44·1
70	22·8	1·1	8·3	2·0	6·3	0·1	5·2	7·7	1·7	0·6	0·1	44·1
71	22·8	1·0	8·3	1·2	3·9	0·1	4·1	8·8	1·4	4·6	0·2	43·6
72	23·0	1·2	8·8	2·2	6·3	0·2	4·1	6·9	2·3	0·8	0·1	44·1
73	23·0	0·5	2·4	1·4	3·8	0·1	9·3	15·7	0·4	0·3	0·0	43·1
74	23·1	0·7	8·0	1·5	3·4	0·1	4·0	8·5	1·1	5·8	0·2	43·6
75	23·2	1·3	7·5	2·6	7·8	0·2	4·1	6·9	1·9	0·6	0·1	43·8
76	23·3	0·4	3·7	1·9	7·2	0·1	13·8	4·7	0·5	0·1	0·1	44·2
77	23·3	0·8	8·5	3·8	5·1	0·2	3·8	6·5	2·4	1·3	0·2	44·1
78	23·4	0·6	8·9	2·6	5·3	0·2	2·5	7·2	1·9	2·9	0·4	44·0
79	23·5	0·1	15·4	0·6	1·1	0·1	0·5	10·1	2·0	0·4	0·0	46·2
80	23·5	0·8	9·8	1·5	3·9	0·1	2·7	6·0	1·8	5·6	0·2	44·1
81	23·6	1·4	8·7	2·8	4·9	0·2	2·7	6·0	3·2	2·0	0·3	44·2
82	23·6	0·5	5·9	2·4	4·5	0·1	6·0	7·0	1·6	4·4	0·4	43·6
83	23·6	0·5	9·4	0·9	5·8	0·1	5·6	7·0	1·5	0·5	0·1	45·0
84	23·6	0·7	7·0	3·0	4·1	0·3	4·3	6·2	2·2	4·5	0·3	43·8
85	23·7	0·3	2·2	1·7	5·8	0·1	13·2	8·6	0·3	0·2	0·0	43·9
86	23·8	0·5	10·2	2·5	2·7	0·2	1·7	5·7	2·5	5·9	0·2	44·1
87	23·8	0·8	8·3	0·8	7·6	0·2	4·2	7·5	1·6	0·8	0·1	44·3
88	23·9	0·7	8·3	1·6	5·8	0·1	5·1	7·8	1·6	0·5	0·1	44·5
89	23·9	1·5	10·7	2·0	3·1	0·1	1·3	4·4	4·8	3·4	0·2	44·7
90	23·9	0·7	7·2	2·3	3·7	0·1	4·9	6·8	1·7	4·5	0·3	43·9
91	24·0	1·2	7·5	2·0	7·1	0·1	3·9	7·5	1·7	0·7	0·1	44·2
92	24·1	0·7	9·6	2·4	4·5	0·1	3·6	7·2	2·1	0·7	0·1	44·9
93	24·1	1·4	8·9	2·3	5·1	0·1	2·6	5·2	3·6	2·0	0·3	44·4
94	24·3	1·6	7·0	2·4	7·6	0·2	3·2	6·3	2·4	0·9	0·2	43·9
95	24·3	0·7	7·9	1·3	5·4	0·2	4·5	6·1	2·0	3·3	0·2	44·1
96	24·4	0·2	2·4	1·6	5·7	0·1	13·0	7·9	0·4	0·1	0·0	44·2
97	24·4	0·9	8·8	1·9	5·5	0·1	3·7	6·1	2·5	1·1	0·2	44·8
98	24·5	1·0	6·8	1·9	5·4	0·2	4·4	5·9	1·9	3·7	0·3	44·0
99	24·7	0·4	11·9	0·9	0·4	0·0	0·1	1·3	1·1	15·6	0·0	43·6
100	24·7	0·8	8·3	1·6	5·4	0·1	4·2	6·2	2·4	1·2	0·2	44·9

Table 1—*continued*

Index No.	Si	Ti	Al	Fe^{3+}	Fe^{2+}	Mn	Mg	Ca	Na	K	P	O
101	25·0	1·0	9·7	1·4	4·9	0·1	2·9	5·5	2·6	1·4	0·2	45·3
102	25·1	0·7	8·6	1·9	3·6	0·1	2·9	5·5	2·6	4·0	0·2	44·8
103	25·1	0·9	10·3	2·3	2·3	0·2	1·2	3·9	4·9	3·7	0·2	45·1
104	25·3	0·5	9·6	1·8	4·5	0·1	3·3	6·0	2·5	0·8	0·1	45·5
105	25·3	0·6	10·2	1·8	2·3	0·2	1·2	2·5	6·0	4·8	0·3	44·8
106	25·4	0·7	8·3	6·4	1·4	0·5	0·4	1·9	8·1	2·6	0·0	44·3
107	25·4	0·3	11·6	1·8	3·1	0·1	0·4	1·9	6·5	3·3	0·1	45·5
108	25·5	0·7	9·2	2·7	3·1	0·1	2·4	4·9	2·5	3·7	0·2	45·0
109	25·5	0·8	9·6	2·2	3·6	0·1	2·1	5·1	2·9	2·7	0·2	45·2
110	25·6	1·1	8·8	2·1	5·3	0·1	1·5	3·6	4·2	2·3	0·3	45·1
111	25·6	0·8	9·2	2·5	4·3	0·1	2·7	5·7	2·7	0·9	0·1	45·4
112	25·6	0·1	1·2	0·6	6·7	0·1	18·8	1·2	0·1	0·1	0·0	45·5
113	25·7	0·5	11·5	2·2	1·3	0·1	0·3	1·7	6·0	5·3	0·1	45·3
114	25·7	0·3	13·7	0·6	1·1	0·0	0·5	6·9	3·5	0·9	0·1	46·7
115	25·7	0·9	9·2	2·3	3·6	0·1	2·0	4·2	3·8	3·0	0·2	45·0
116	25·7	0·9	8·7	2·3	4·1	0·1	2·3	4·7	3·1	2·7	0·2	45·2
117	25·7	0·7	9·0	2·3	4·2	0·1	2·4	5·0	2·8	2·3	0·2	45·3
118	25·7	0·5	9·0	2·1	3·7	0·1	2·3	4·8	2·6	4·0	0·2	45·0
119	25·9	0·8	8·9	2·4	4·3	0·1	2·4	4·9	2·6	2·3	0·2	45·2
120	25·9	0·5	10·7	2·4	1·7	0·3	0·5	1·8	6·2	4·6	0·1	45·3
121	25·9	0·9	9·5	2·2	3·9	0·1	1·3	3·9	4·3	2·3	0·3	45·4
122	26·0	0·7	10·8	1·5	1·9	0·1	0·6	2·7	5·7	4·6	0·1	45·3
123	26·0	0·7	8·8	1·8	3·6	0·1	2·2	4·9	2·6	3·9	0·2	45·2
124	26·1	0·5	11·3	1·6	1·8	0·1	0·3	1·8	6·3	4·8	0·1	45·3
125	26·2	0·4	11·4	1·7	1·6	0·2	0·4	1·4	6·6	4·5	0·1	45·6
126	26·3	0·5	8·8	2·2	4·6	0·1	2·0	4·6	3·1	2·5	0·1	45·2
127	26·3	0·7	9·2	2·1	3·9	0·1	2·1	4·9	2·7	2·4	0·2	45·4
128	26·4	0·2	11·5	1·9	1·0	0·2	0·2	1·0	7·5	4·1	0·0	46·0
129	26·4	0·8	9·0	2·6	3·4	0·1	2·1	5·0	2·7	2·2	0·2	45·5
130	26·5	0·7	9·1	2·1	3·2	0·1	2·0	4·7	2·8	3·2	0·2	45·6
131	26·6	0·7	11·0	1·8	1·6	0·2	0·4	1·1	6·6	4·1	0·0	45·9
132	26·7	0·9	9·4	2·0	3·5	0·2	1·2	3·8	3·9	2·6	0·2	45·6
133	26·8	1·0	9·5	1·6	3·3	0·1	0·9	3·2	4·3	3·4	0·3	45·6
134	26·9	0·5	8·9	2·2	3·5	0·1	2·5	4·9	2·5	1·8	0·1	46·1
135	26·9	0·4	10·8	1·6	1·5	0·2	0·4	1·4	6·6	4·6	0·1	45·8
136	27·1	0·3	12·2	0·5	1·9	0·2	0·2	0·7	6·5	4·4	0·0	46·0
137	27·2	0·6	8·9	1·6	3·2	0·1	2·0	4·1	2·7	3·7	0·2	45·8
138	27·4	0·7	9·3	2·8	2·5	0·0	0·8	3·0	4·3	3·1	0·3	46·0
139	27·4	0·4	9·6	1·8	1·6	0·1	1·3	3·1	2·9	6·2	0·1	45·5
140	27·4	0·3	11·1	1·7	0·8	0·1	0·2	1·1	6·7	4·4	0·1	46·2
141	27·4	0·8	8·3	2·4	3·1	0·1	1·5	4·0	2·6	3·8	0·2	45·8
142	28·0	0·5	9·1	1·5	2·2	0·1	1·2	2·9	2·9	5·5	0·2	45·9
143	28·1	0·7	8·3	2·2	3·0	0·1	2·1	3·7	2·9	2·7	0·1	46·1
144	28·2	0·5	9·3	2·4	2·4	0·2	1·7	4·2	2·7	1·7	0·1	46·6
145	28·7	0·2	9·5	1·9	2·1	0·1	0·7	2·2	3·3	4·8	0·1	46·4
146	28·9	0·4	9·3	1·3	2·4	0·1	0·5	1·7	4·2	5·0	0·1	46·1
147	29·0	0·3	7·8	3·2	2·9	0·2	0·4	1·3	5·0	3·9	0·1	45·9
148	29·0	0·3	9·2	2·2	1·4	0·2	0·3	1·1	5·2	4·8	0·1	46·2
149	29·0	0·1	9·1	1·7	3·4	0·0	1·7	4·0	2·0	1·9	0·1	46·9
150	29·1	0·4	9·0	1·6	2·1	0·1	0·6	1·8	4·1	4·9	0·1	46·2

Table 1—*continued*

Index No.	Si	Ti	Al	Fe^{3+}	Fe^{2+}	Mn	Mg	Ca	Na	K	P	O
151	29·1	0·4	9·6	1·6	1·2	0·1	0·4	1·4	4·9	4·6	0·1	46·6
152	29·2	0·4	8·7	1·8	3·0	0·1	1·7	3·9	2·5	1·8	0·1	46·9
153	29·2	0·4	8·4	2·1	2·6	0·2	1·8	3·6	2·5	2·2	0·1	46·9
154	29·4	0·8	8·4	1·1	3·4	0·1	1·7	3·4	2·5	2·2	0·1	46·9
155	29·4	0·5	8·1	1·4	3·4	0·1	1·9	3·9	2·4	2·2	0·1	46·6
156	29·8	0·5	8·7	2·9	1·0	0·1	1·1	3·1	2·5	3·2	0·1	47·1
157	29·9	0·4	8·9	1·6	2·4	0·1	1·3	4·0	3·0	1·2	0·1	47·1
158	30·0	0·4	8·2	2·9	1·2	0·1	0·2	1·1	5·4	3·9	0·1	46·5
159	30·0	0·6	8·3	1·2	3·6	0·1	1·5	3·8	2·6	1·0	0·1	47·2
160	30·4	0·3	8·3	1·5	1·9		1·5	3·1	2·6	3·1	0·1	47·2
161	30·7	0·4	8·5	1·2	2·1	0·1	1·2	3·2	2·7	2·3	0·1	47·5
162	30·8	0·4	8·3	1·2	2·2	0·1	1·1	3·0	2·9	2·5	0·1	47·4
163	31·0	0·5	8·0	1·2	2·1	0·1	0·8	2·4	2·6	3·9	0·1	47·3
164	31·1	0·4	8·3	1·0	2·7	0·1	1·2	3·3	2·9	1·2	0·1	47·7
165	31·2	0·4	8·7	1·7	1·5	0·1	0·9	2·5	3·0	2·3	0·1	47·8
166	31·2	0·4	8·2	1·5	1·8	0·1	1·0	2·7	3·1	2·5	0·1	47·4
167	31·5	0·3	8·3	0·9	2·0	0·1	1·0	2·6	2·9	2·6	0·1	47·7
168	31·5	0·3	8·3	1·4	1·5	0·1	0·9	2·5	2·6	3·1	0·1	47·8
169	31·6	0·4	6·5	3·0	2·4	0·1	0·2	1·2	4·0	3·7	0·0	46·9
170	32·3	0·5	7·4	1·0	2·5	0·0	0·6	2·2	2·2	3·4	0·1	47·8
171	32·4	0·3	7·7	1·2	1·7	0·1	0·7	1·9	2·9	3·2	0·1	47·8
172	32·5	0·3	8·3	0·8	1·6	0·1	0·7	2·2	2·8	2·6	0·1	48·0
173	32·5	0·3	7·8	0·9	1·8	0·1	0·6	1·8	2·5	3·8	0·1	47·8
174	32·6	0·3	8·0	0·8	2·4	0·1	0·6	2·2	3·5	1·2	0·1	48·2
175	33·0	0·3	7·7	1·2	1·2	0·1	0·4	1·6	2·7	3·8	0·1	47·9
176	33·1	0·2	7·6	0·8	1·9	0·0	0·1	0·9	3·1	4·3	0·0	48·0
177	33·1	0·2	7·7	1·1	1·4	0·1	0·5	1·4	2·6	3·4	0·1	48·4
178	33·1	0·2	8·3	0·4	1·7	0·0	0·4	1·4	3·1	3·0	0·1	48·3
179	33·1	0·3	5·8	4·3	0·7	0·1	0·1	0·7	4·0	3·4	0·0	47·5
180	33·2	0·2	7·5	0·6	1·9	0·1	0·3	1·2	2·7	4·5	0·0	47·8
181	33·2	0·2	8·4	0·6	1·1	0·0	0·5	2·0	3·7	1·4	0·1	48·8
182	33·4	0·2	6·0	3·0	1·7	0·1	0·2	0·6	3·7	3·5	0·0	47·6
183	33·4	0·2	7·6	0·7	1·5	0·1	0·5	1·4	2·5	3·9	0·1	48·1
184	33·5	0·6	6·7	0·6	2·8	0·0	0·2	1·3	2·3	4·2	0·0	47·8
185	33·5	0·2	7·4	1·3	1·0	0·1	0·2	0·5	4·2	3·3	0·0	48·3
186	33·6	0·2	5·2	3·8	2·2	0·1	0·2	0·5	3·3	3·4	0·0	47·5
187	33·7		7·6	0·8	1·6		0·5	1·3	2·6	3·6		48·3
188	33·7	0·2	7·8	0·4	1·2	0·1	0·3	0·9	2·2	4·6	0·1	48·5
189	33·8	0·2	7·9	0·5	1·3	0·0	0·4	1·1	2·4	3·9	0·1	48·4
190	33·9	0·2	7·4	0·6	1·3	0·1	0·3	1·0	2·3	4·6	0·1	48·2
191	34·0	0·3	5·8	2·1	1·9	0·1	0·1	0·5	3·9	3·7	0·0	47·6
192	34·3	0·1	5·6	2·1	2·3	0·2	0·1	0·4	3·2	3·7	0·0	48·0
193	34·4	0·2	7·1	0·6	1·1	0·0	0·3	0·8	2·2	4·6	0·1	48·6
194	34·6	0·2	7·1	1·0	0·8	0·1	0·2	0·9	2·5	3·9	0·0	48·7
195	34·7	0·1	7·3	0·6	0·9	0·0	0·2	0·5	2·6	4·3	0·1	48·7
196	34·7	0·1	7·2	0·9	0·6	0·0	0·2	0·8	2·2	4·5	0·0	48·8
197	34·7	0·1	7·6	0·2	0·6	0·0	0·1	0·5	2·7	4·4	0·1	49·0
198	35·1	0·1	6·7	0·9	0·8	0·0	0·1	0·4	3·1	4·0	0·0	48·8
199	35·1	0·1	7·4	0·4	0·7	0·0	0·2	0·4	2·3	4·3	0·1	49·0
200	35·2	0·1	7·0	0·7	0·7	0·1	0·1	0·4	2·6	4·2	0·1	48·8
201	35·3	0·2	7·0	0·4	0·3	0·1	0·2	0·8	2·7	4·0	0·0	48·3

INDEX TO TABLE 1

1. Ore dunite (7), Nockolds (1954, p. 1023).
2. Turjaite (5), *ibid* (p. 1029).
3. Hortonolite dunite (2), *ibid* (p. 1023).
4. Olivine melilitite (10), *ibid* (p. 1029).
5. Olivine-melilite nephelinite (8), *ibid* (p.1029).
6. Basaltic kimberlite (10), *ibid* (p. 1023).
7. Uncompahgrite (2), *ibid* (p. 1029).
8. Nephelinite (8), *ibid* (p. 1028).
9. Micaceous kimberlite (4), *ibid* (p. 1023).
10. Melilite nephelinite (3), *ibid* (p. 1029).
11. Olivine-melilite leucitite (5), *ibid* (p. 1031).
12. *Dunite* (9), *ibid* (p. 1023).
13. Olivine etindite (7), *ibid* (p. 1031).
14. Olivine nephelinite (21), *ibid* (p. 1028).
15. Titanaugite melteigite (3), *ibid* (p. 1028).
16. Titanaugite ijolite (3), *ibid* (p. 1028).
17. *Dunite* (10), Daly (1933, p. 20).
18. Alkali pyroxenite (21), Nockolds (1954, p. 1022).
19. Alkali peridotite (22), *ibid* (p. 1023).
20. Hornblendite (15), *ibid* (p. 1022).
21. Melteigite (9), *ibid* (p. 1028).
22. Etindite (6), *ibid* (p. 1031).
23. Ijolite (11), *ibid* (p. 1028).
24. Picrite (14), Daly (1933, p. 19).
25. Hornblende peridotite (5), Nockolds (1954, p. 1023).
26. Ariégite (9), *ibid* (p. 1022).
27. Pyroxene peridotite (11), *ibid* (p. 1023).
28. Urtite (6), *ibid* (p. 1028).
29. *Peridotite* (23), *ibid* (p. 1023).
30. Olivine-rich alkali basalt (31), *ibid* (p. 1021).
31. Troctolite (9), *ibid* (p. 1020).
32. *Ultramafic igneous rocks* (182), *ibid* (p. 1032).
33. Olivine leucitite (11), *ibid* (p. 1031).
34. Biotite pyroxenite (17), *ibid* (p. 1022).
35. Alkali gabbro (42), *ibid* (p. 1020).
36. Bekinkinite (4), *ibid* (p. 1028).
37. *Peridotite bombs in basalt* (2), Hess in Poldervaart (1955, p. 134).
38. Soda amphibole-pyroxene malignite (6), Nockolds (1954, p. 1025).
39. Olivine pyroxenite (8), *ibid* (p. 1022).
40. Puglianite (2), *ibid* (p. 1030).
41. Nepheline tephrite (8), *ibid* (p. 1027).
42. Olivine hornblendite (5), *ibid* (p. 1022).
43. Tawite (3), *ibid* (p. 1029).
44. *Normal alkali basalt and dolerite* (96), *ibid* (p. 1021).
45. Melilite leucitite (2), *ibid* (p. 1031).
46. Olivine analcitite (8), *ibid* (p. 1028).
47. Theralite (6), *ibid* (p. 1027).
48. Atlantic olivine basalt (25), Green and Poldervaart (1955, p. 182).
49. Analcite tephrite (7), Nockolds (1954, p. 1027).
50. *Pacific olivine basalt* (116), Green and Poldervaart (1955, p. 179).
51. Alkali basalt without olivine (22), Nockolds (1954, p. 1021).
52. Mesotype missourite (6), *ibid* (p. 1030).
53. Olivine gabbro (53), *ibid* (p. 1020).
54. Melanocratic missourite (5), *ibid* (p. 1031).
55. Pyroxene-biotite malignite (9), *ibid* (p. 1025).
56. Alkali mangerite of Hurum type (36), *ibid* (p. 1018).
57. Essexite (15), *ibid* (p. 1027).
58. Leucite tephrite (31), *ibid* (p. 1030).
59. Teschenite (8), *ibid* (p. 1027).
60. Leucitite (7), *ibid* (p. 1031).
61. Ordanchite (27), *ibid* (p. 1027).
62. Alkali andesite (37), *ibid* (p. 1019).
63. Glenmuirite (13), *ibid* (p. 1027).
64. Malignite (25), *ibid* (p. 1024).
65. Tholeiitic olivine basalt (28), *ibid* (p. 1021).
66. Volcanic equivalent of Hurum-type alkali mangerite (40), *ibid* (p. 1018).
67. Hornblende gabbro (15), *ibid* (p. 1020).
68. *Mafic igneous rocks including nepheline types* (721), *ibid* (p. 1032).
69. Gabbro (160), *ibid* (p. 1020).
70. *Mafic igneous rocks excluding nepheline types* (637), *ibid* (p. 1032).
71. Leucite mangerite (3), *ibid* (p. 1030).
72. Hornblende-, and hornblende-augite diorite (10), *ibid* (p. 1019).
73. Augite pyroxenite (7), *ibid* (p. 1022).
74. Sommaite (4), *ibid* (p. 1030).
75. Plateau basalt (43), Daly (1933, p. 17).
76. Hornblende hypersthenite (4), Nockolds (1954, p. 1022).
77. Basalt (198), Daly (1933, p. 17).
78. Tephrite (24), *ibid* (p. 23).
79. Anorthosite, localized (8), Nockolds (1954, p. 1020).
80. Leucite ordanchite (12), *ibid* (p. 1030).
81. Alkali mangerite (53), *ibid* (p. 1018).
82. Olivine-augite-biotite shonkinite (9), *ibid* (p. 1016).
83. Norite (39), *ibid* (p. 1020).
84. Augite-biotite shonkinite (8), *ibid* (p. 1016).
85. *Pyroxenite* (46), *ibid* (p. 1022).
86. Leucite latite, including vicoite and campanite (16,) *ibid* (p. 1030).
87. *Tholeiite* (102), Green and Poldervaart (1955, p. 185).
88. Pyroxene gabbro (38), Nockolds (1954, p. 1020).
89. Nepheline monzonite (7), *ibid* (p. 1024).
90. Alkali trachyte equivalent to shonkinite (6), *ibid* (p. 1016).
91. *Normal tholeiitic basalt and dolerite* (137), *ibid* (p. 1021).
92. Central basalt (56), *ibid* (p. 1021).
93. *Alkali doreite* (76), *ibid* (p. 1018).
94. *Tholeiitic andesite* (26), *ibid* (p. 1019).
95. Augite-biotite-olivine monzonite (6), *ibid* (p. 1017).
96. Two-pyroxene pyroxenite (20), *ibid* (p. 1022).
97. *Diorite* (50), *ibid* (p. 1019).
98. Mesotype and melanocratic calc-alkali syenite (6), *ibid* (p. 1016).
99. Italite (2), *ibid* (p. 1030).
100. Pyroxene-mica diorite (11), *ibid* (p. 1019).
101. Hornblende-mica diorite (16), Nockolds (1954, p. 1019).
102. Augite-biotite monzonite (11), *ibid* (p. 1017).
103. Nepheline latite (16), *ibid* (p. 1024).
104. *Parental calc-alkali magma* (calc.), Nockolds and Allen (1953, p. 139).
105. Augite-biotite nepheline syenite (5), Nockolds (1954, p. 1025).

INDEX TO TABLE 1—*continued*

106. Aegirine malignite (4), *ibid* (p. 1025).
107. Soda amphibole-biotite nepheline syenite (6), *ibid* (p. 1025).
108. Latite (42), *ibid* (p. 1017).
109. Augite-biotite mangerite (7), *ibid* (p. 1018).
110. Mugearite (10), *ibid* (p. 1018).
111. *Andesite* (49), *ibid* (p. 1019).
112. Bronzite pyroxenite (9), *ibid* (p. 1022).
113. Aegirine augite-biotite nepheline syenite (14), *ibid* (p. 1025).
114. Anorthosite, in massifs (9), *ibid* (p. 1020).
115. *Intermediate igneous rocks including nepheline types* (810), *ibid* (p. 1032).
116. *Intermediate igneous rocks excluding nepheline types* (635), *ibid* (p. 1032).
117. Mangerite (56), *ibid* (p. 1018).
118. Pyroxene-hornblende-biotite monzonite (9), *ibid* (p. 1017).
119. Pyroxene-biotite mangerite (11), *ibid* (p. 1018).
120. Nepheline syenite (43), DALY (1933, p. 14).
121. Volcanic equivalent of Aker-type alkali mangerite (26), NOCKOLDS (1954, p. 1018).
122. Titanaugite-soda amphibole nepheline syenite (3), *ibid* (p. 1025).
123. *Monzonite* (46), *ibid* (p. 1017).
124. Soda amphibole nepheline syenite (11), *ibid* (p. 1025).
125. Nepheline syenite (80), *ibid* (p. 1024).
126. Pyroxene-hornblende-biotite mangerite (10), *ibid* (p. 1018).
127. Hornblende-biotite mangerite (9), *ibid* (p. 1018).
128. Soda pyroxene nepheline syenite (24), *ibid* (p. 1025).
129. *Doreite* (38), *ibid* (p. 1018).
130. *Monzonite* (27), DALY (1933, p. 13).
131. Aegirine-soda amphibole nepheline syenite (9), NOCKOLDS (1954, p. 1025).
132. Alkali mangerite of Aker type (17), *ibid* (p. 1018).
133. Larvikite (15), *ibid* (p. 1017).
134. *Diorite* (70), DALY (1933, p. 16).
135. *Phonolite* (47), NOCKOLDS (1954, p. 1024).
136. Biotite nepheline syenite (6), *ibid* (p. 1025).
137. *Latite* (10), DALY (1933, p. 13).
138. *Trachyandesite* (12), *ibid* (p. 13).
139. *Calc-alkali trachyte* (24), NOCKOLDS (1954, p. 1016).
140. *Phonolite* (25), DALY (1933, p. 14).
141. Hornblende-biotite monzonite (5), NOCKOLDS (1954, p. 1017).
142. Calc-alkali syenite (18), *ibid* (p. 1016).
143. *Igneous rock* (calc.), CLARKE (1924, p. 29).
144. *Andesite* (87), DALY (1933, p. 16).
145. *Trachyte* (48), *ibid* (p. 11).
146. Ferrohastingite syenite (11), NOCKOLDS (1954, p. 1016).
147. Peralkaline syenite (47), *ibid* (p. 1016).
148. Peralkaline trachyte (12), *ibid* (p. 1016).
149. *Tonalite* (10), DALY (1933, p. 15).
150. Alkali syenite (25), NOCKOLDS (1954, p. 1016).
151. *Alkali trachyte* (15), *ibid* (p. 1016).
152. *Quartz diorite* (55), DALY (1933, p. 15).
153. *Cordilleran-Appalachian igneous rock* (calc.), KNOPF (1916, p. 622).
154. Hypersthene granodiorite (10), NOCKOLDS (1954, p. 1014).
155. *Igneous rock* (calc.) WICKMAN (1954, p. 105).
156. *Quartz latite* (12), DALY (1933, p. 13).
157. *Dacite and dacite obsidian* (50), NOCKOLDS (1954, p. 1015).
158. Aegirine syenite (13), *ibid* (p. 1016).
159. Hornblende-biotite tonalite (22), *ibid* (p. 1015).
160. *Plutonic igneous rock* (calc.), VOGT (1931, p. 47).
161. *Granodiorite* (40), DALY (1933, p. 15).
162. Hornblende-biotite granodiorite (65), NOCKOLDS (1954, p. 1014).
163. Hornblende-biotite adamellite (41), *ibid* (p. 1014).
164. *Tonalite* (58), *ibid* (p. 1015).
165. *Dacite* (90), DALY (1933, p. 15).
166. *Rhyodacite and rhyodacite obsidian* (115), NOCKOLDS (1954, p. 1014).
167. *Granodiorite* (137), *ibid* (p. 1014).
168. *Quartz monzonite* (20), DALY (1933, p. 15).
169. Laneite-aegirine granite (8), NOCKOLDS (1954, p. 1013).
170. Hypersthene adamellite (11), *ibid* (p. 1014).
171. *Felsic igneous rock* (794), *ibid* (p. 1032).
172. Biotite granodiorite (36), *ibid* (p. 1014).
173. *Adamellite* (121), *ibid* (p. 1014).
174. Biotite tonalite (11), *ibid* (p. 1015).
175. *Dellenite and dellenite obsidian* (58), *ibid* (p. 1014).
176. Ferrohastingite granite (7), *ibid* (p. 1012).
177. *Granite* (546), DALY (1933, p. 9).
178. Muscovite-biotite granodiorite (20), NOCKOLDS (1954, p. 1014).
179. Aegirine granite (11), *ibid* (p. 1013).
180. Biotite-hornblende granite (6), *ibid* (p. 1012).
181. Muscovite-biotite tonalite (9), *ibid* (p. 1015).
182. Peralkaline granite (53), *ibid* (p. 1013).
183. Biotite adamellite (45), *ibid* (p. 1014).
184. Hypersthene granite (4), *ibid* (p. 1012).
185. Arfvedsonite-aegirine granite (9), *ibid* (p. 1013).
186. Riebeckite-aegirine granite (14), *ibid* (p. 1013).
187. Granite (74), LAPADU-HARGUES (1945, p. 276).
188. Muscovite-biotite granite (21), NOCKOLDS (1954, p. 1012).
189. Muscovite-biotite adamellite (22), *ibid* (p. 1014).
190. *Calc-alkali granite* (72), *ibid* (p. 1012).
191. Peralkaline rhyolite and rhyolite obsidian (39), *ibid* (p. 1013).
192. Riebeckite (or osannite) granite (10), *ibid* (p. 1013).
193. Biotite granite (37), *ibid* (p. 1012).
194. *Rhyolite* (102), DALY (1933, p. 9).
195. Alkali granite (48), NOCKOLDS (1954, p. 1012).
196. *Calc-alkali rhyolite and rhyolite obsidian* (22), *ibid* (p. 1012).
197. Muscovite granite (6), *ibid* (p. 1012).
198. Alkali rhyolite and rhyolite obsidian (21), *ibid* (p. 1012).
199. Muscovite-biotite alkali granite (17), *ibid* (p. 1012).
200. Biotite alkali granite (12), *ibid* (p. 1012).
201. Granite aplite (15), DALY (1933, p. 27).

strongly sodic granites and sodic syenites. This probably results from increased solubility of Fe^{3+} in highly sodic melts (Bowen, Schairer, and Willems, 1930, p.p. 424–425). At the mafic end the zone terminates in average basalts. Average chondrite (point SM) is included in Fig. 1. The series chondrite–peridotite (point P)–dunite (point D) is in opposite direction and displaced with respect to the series basalt–granite.

By contouring Fig. 1 a line can be constructed to pass through the high concentration areas, as shown in Fig. 2. Averages of common igneous rocks fall on or near this trend. It is a straight line with a steep slope, indicating that fractionation of feldspars is usually more than twice as effective as fractionation of ferromagnesians. Also indicated in Fig. 2 are several specific examples of magmatic differentiation. The Skaergaard trend (Wager and Deer, 1939) is an extreme example of strong fractionation of ferromagnesians with little fractionation of feldspars. That of the southern California batholith (Larsen, 1948) is a typical example of the calc–alkaline series (Nockolds and Allen, 1953). The trend of the Hawaiian series alkali basalt–trachyte (Macdonald, 1949) is an example of the alkaline series (Nockolds and Allen, 1954). The three series fall to the right of the igneous trend but this is accidental and only shows that the examples chosen have slightly higher mafic/felsic ratios than most igneous rocks.

Fig. 3 is a Ca–Na–K diagram and shows a wide scatter of points distributed about equally on either side of the line joining the Ca corner with a point midway along the Na–K side of the diagram. Most widely distributed intermediate and mafic rocks fall on the sodic side of the line and only in felsic rocks are there common rock types represented by points on the potassic side of the line. It appears from this figure that in the production of sodic versus potassic rocks, the effects of locally operative processes predominate over those of fractionation. As a generally operative process, fractionation alone apparently tends to produce rocks with a Na/K ratio of 1. This is also approximately the Na/K ratio for the minimum of the Na–K feldspar solid solution series. Added interest is given these observations by recognition of a series basalt–latite–trachyte–phonolite (trend A), typical of the oceanic domain, while the series basalt–andesite–dacite–rhyolite (trend B) may be regarded as characteristic of continents. The two series are indicated in Fig. 3. Since this work is aimed at finding a general trend of evolution of igneous rocks, combined alkalis have been used as a variable which is less sensitive to the effects of locally operative processes than Na and K as separate variables.

Fig. 4 shows igneous averages plotted on a series of eleven triangular diagrams, expressed as ionic weight per cent.

The first figure of the series is an Si–Al–Mg diagram and is an example of diagrams including Si. Both early and late products of magmatic consolidation are emphasized in such diagrams, at the expense of intermediate stages of crystallization. The figure shows therefore little of interest. The crystal chemistry of silicates indicates that they consist of (SiO_4) tetrahedra arranged in a limited number of fundamental patterns, which form a structural skeleton for different minerals. The (SiO_4) tetrahedra have therefore been called the "building bricks" of silicates (Buerger, 1948). The interstitial cations determine the pattern of

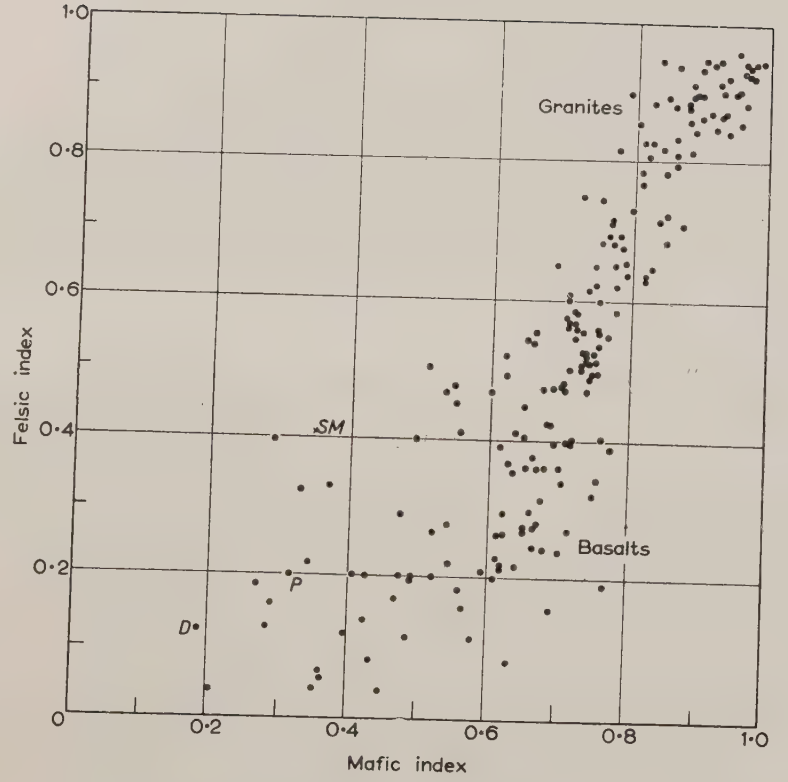

Fig. 1. Igneous rocks plotted on diagrams of mafic index. $\left(\frac{Fe_{total}}{Mg + Fe_{total}}\right) \times 100$ vs. felsic index $\frac{(Na + K)}{Ca + Na + K} \times 100$

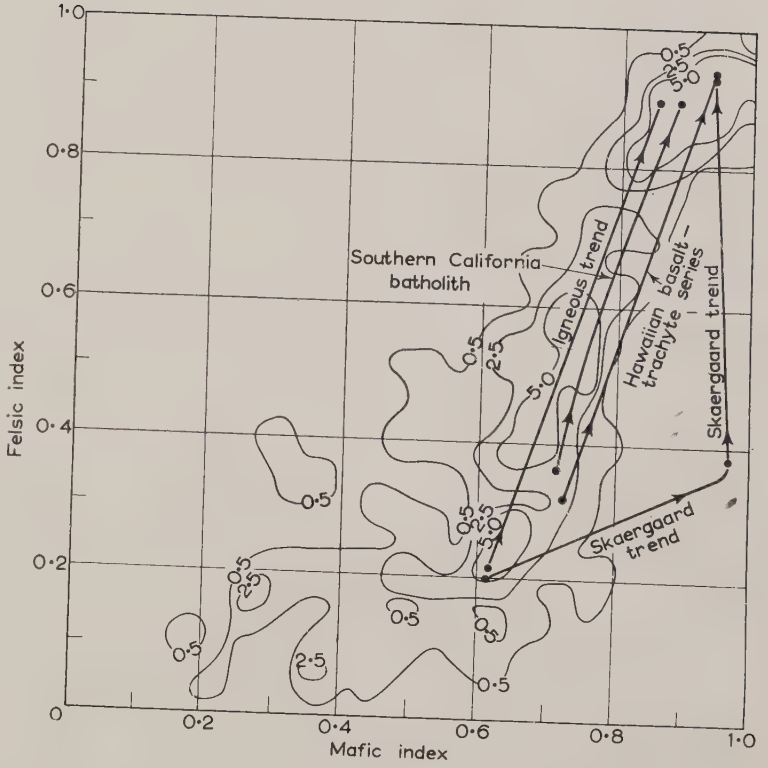

Fig. 2. Trends of igneous rocks on diagram of mafic index vs. felsic index.

(SiO_4) tetrahedra and give identity to a mineral. In an analogous manner, Si can be regarded as playing a more or less passive role in magmatic differentiation, while the interstitial cations are of greater significance in tracing the evolution of igneous rocks.

This leaves five variables which are major constituents of igneous rocks; Al, total Fe, Mg, Ca and (Na + K). Possible combinations of these five variables are represented in the next ten diagrams. Three groups can be distinguished:

Group 1. Three diagrams with corner Fe, Mg, or Ca, and with a side Al–(Na + K), in which igneous rocks fall in a zone extending toward a point midway

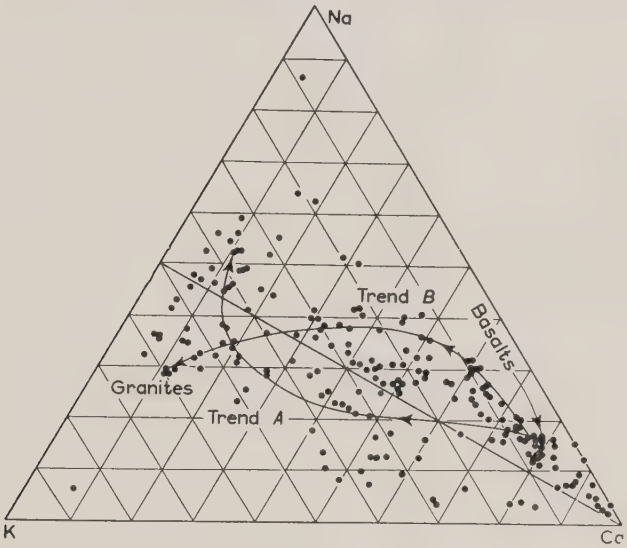

Fig. 3. Ca–Na–K diagram for igneous rocks.

along the Al–(Na + K) side. The points show generally more scatter than in diagrams of groups 2 and 3. The igneous trend is shown on all the diagrams, arrows marking the progression from mafic to felsic rocks. Variations in ultramafic rocks are indicated by averages of stony meteorites, peridotites, and dunites. In the Al–(Na + K)–Ca diagram quite a number of points show low Ca content but fall on the (Na + K) side of the igneous trend. These points represent peralkaline granites and syenites. The diagram also shows a series of rocks (including pyroxenites) enriched in Ca which departs from the main igneous trend and is directed toward the Ca corner.

Group 2. Three diagrams with corner Al, Ca, or (Na + K), and with a side Fe–Mg. The igneous rocks again fall in a well-defined zone which starts from a point along the Fe–Mg side, approximately at Mg : Fe = 3 : 1. In the Fe–Mg–Al diagram the zone curves toward the Al corner, is convex toward the Fe corner, and ends at a point along the Al–Fe side, approximately at Al : Fe = 9 : 1. In the Fe–Mg–Ca diagram the zone curves toward the Fe corner where it ends, and is convex toward the Ca corner. In the familiar Fe–Mg–(Na + K) diagram the zone curves toward the (Na + K) corner, is convex toward the Fe corner, and

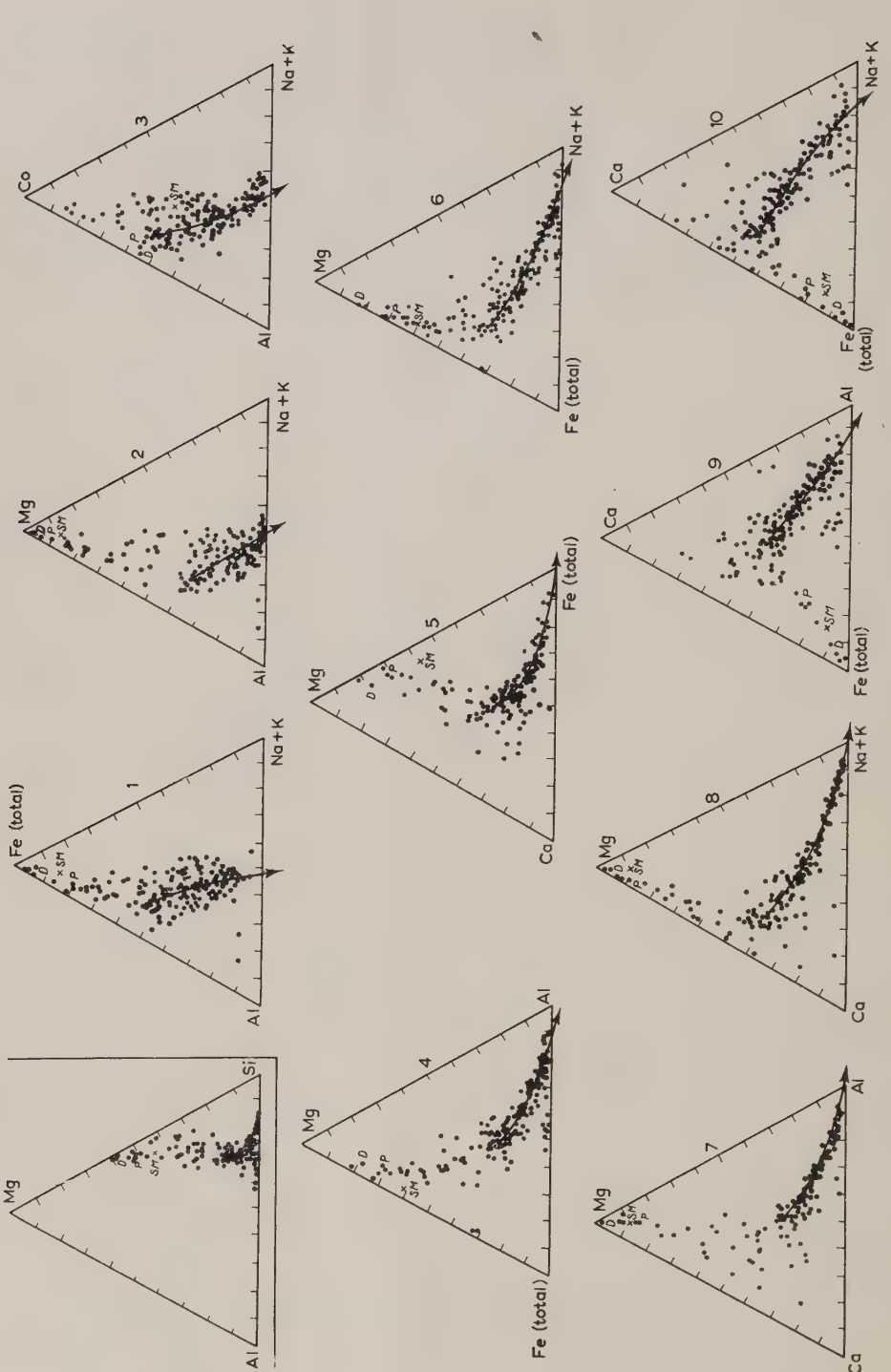

Fig. 4. Si–Al–Mg diagram and diagrams with variables Al, total Fe, Mg, Ca, and combined alkalis for igneous rocks.

ends at a point along the Fe–(Na + K) side, approximately at (Na + K) : Fe = 8·5 : 1·5. The igneous trend is again shown for the progression from mafic to felsic rocks only. In both the Fe–Mg–Al and Fe–Mg–(Na + K) diagrams there is a group of points with low proportions of Mg but with distinctly higher Fe than corresponds with other igneous rocks of comparable Mg content. The points again represent strongly sodic granites and sodic syenites and their anomalous position reflects the increased solubility of Fe^{3+} in highly sodic melts.

Group 3. Four diagrams with Ca in one corner, and without either of the pairs Al–(Na + K) or Fe–Mg. Here the igneous rocks fall in a zone which is convex toward the Ca corner and curves between the other two corners. In the Al–Mg–Ca and Mg–Ca–(Na + K) diagrams the zone passes through the Mg corner and respectively the Al and (Na + K) corners. The Mg–Ca–(Na + K) diagram shows the least scatter of points of these ten diagrams. In the Al–Fe–Ca and Fe–Ca–(Na + K) diagrams the zone passes through the Fe corner and respectively a point along the Al–Fe side at about Al : Fe = 9 : 1, and a point along the Fe–(Na + K) side at about (Na + K) : Fe = 8·5 : 1·5. Both diagrams show some scatter toward the Fe corner at the felsic end of the igneous trend, produced by averages of strongly sodic granites and sodic syenites. The progression from mafic to felsic rocks is again indicated as a trend which is not extended to the ultramafic rocks.

If desired, the ten diagrams can be combined in five tetrahedra to show the igneous trend for any four of the five variables. This is not done in the present paper.

The existence of a general trend of evolution of igneous rocks demonstrates that for the variables considered, the effects of fractionation predominate over those produced by locally operative processes. Studies of fractional crystallization of artificial melts are progressing from simple to more complicated systems. Eventually the results of these investigations should be capable of calculation in terms of the same five variables and should then coincide with the igneous trend shown here.

In diagrams with the pair Fe–Mg, the ultramafic rocks start at a ratio Mg : Fe = 3 : 1, which seems to be the mean Mg/Fe ratio of early crystallizing ferromagnesians (although earliest crystals of olivine and bronzite may have a ratio Mg : Fe = 5 : 1). Similarly, in diagrams with the pair Al–(Na + K), the igneous trend ends at or near a ratio Al : (Na + K) = 1 : 1, which is the Al/(Na + K) ratio of alkali feldspars. Corresponding diagrams with Fe or with Mg (e.g. Fe–Ca–Al and Mg–Ca–Al) are not quite identical, as they would be if Mg and Fe were mutually dependent variables. Ca and (Na + K) are also independent variables. Remarkable is the strong curvature of the zone occupied by igneous rocks convex toward Ca in diagrams which include this element with either Mg or Fe. Ca is gained in the mantle progression from ultramafic to mafic rocks, but in the crustal progression from mafic to felsic rocks Ca is lost.

Detailed interpretation of the igneous trend cannot be attempted here. A full evaluation will require many comparisons with detailed studies of magmatic differentiation in single intrusions, variations in igneous rocks in magmatic provinces, and experimental results obtained for synthetic melts. Statistical analysis

of the results, with due consideration of relative abundances of the various rock types in the earth's crust, is also desirable. A general synthesis of this type stands in danger of masking trends of importance which do not result from generally operative processes. The writers believe that the igneous trend portrayed here adequately reflects the progression from mafic to felsic igneous rocks in terms of the variables used. However, by omitting Si the alkalic series of igneous rocks has been made to coincide in large part with the calc–alkalic series. This raises the interesting question whether the alkalic series is really so different from the calc–alkalic series. Further, by combining alkalis instead of representing Na and K separately, important aspects of igneous evolution toward sodic or potassic differentiates have been neglected. These obvious defects in the present analysis require careful attention, especially in considerations of crustal evolution.

The series of diagrams is also useful as a guide to future investigations of chemical variation in igneous rocks. Evidently the Mg–Ca–(Na + K), Fe–Ca–(Na + K), and Fe–Mg–(Na + K) diagrams are the most suitable to show chemical variation in igneous rock series, since they show the widest spread and least scatter.

SEDIMENTARY ROCKS

Chemical differentiation effected in sedimentary processes is remarkably efficient and can be compared with the methodology of quantitative silicate analysis (GOLDSCHMIDT, 1922). Main stages in the differentiation are the formation of resistates, hydrolysates, oxidates, carbonates, evaporates, and redusates (cf. MASON, 1952). Many writers have emphasized the greater range in content of various major elements in sediments as compared with igneous rocks. This applies especially to Si (as dioxide), Al and Fe (as hydrated oxides), and Ca and Mg (as carbonates).

As in the case of igneous rocks, one may regard sediments as having formed in response to generally operative processes, as well as to processes of local application only. It is immediately evident that local factors play a much greater role in weathering, transport, and deposition of sediments than they do in the production of igneous rocks. The distribution of the various types of sediments depends on a myriad of different physical and chemical factors. These are winds, waves, currents, climatic conditions, partial CO_2 pressures, salinity, redox potential, hydrogen ion concentration, shoreline geometry, topography of source highlands and sea floor, nature of source rocks, type and role of organisms, presence of barriers, regressive or transgressive seas, etc. All play vital roles in various combinations at different places and at diverse times. Attempts to derive a general sedimentary trend are therefore foredoomed to failure.

Chemical adjustments in rock-weathering tend to produce new mineral phases in equilibrium with surface temperatures and pressures, and in accord with the chemical composition of the system. This is a generally operative process which sets sediments apart from high-temperature igneous and metamorphic rocks. A link may be provided by low-temperature phases of igneous and metamorphic

Table 2. Averages of sedimentary rocks

Index No.	Si	Ti	Al	Fe^{3+}	Fe^{2+}	Mn	Mg	Ca	Na	K	P	C	O
1*							3·7	1·2	30·8	1·1			5·4
2	4·1	0·1	0·7	0·6		0·1	3·8	58·3	0·1	0·4			31·8
	2·4	0·1	0·4	0·4		0·1	2·2	34·3	0·1	0·3		11·2	48·5
3	4·2	0·1	0·7	0·6		0·1	8·3	52·9	0·1	0·4			32·6
	2·4	0·1	0·4	0·4		0·1	4·8	30·7	0·1	0·3		11·4	49·3
4	4·3	0·1	0·7	0·6		0·1	13·9	46·1	0·1	0·4			33·7
	2·4	0·1	0·4	0·4		0·1	8·0	26·4	0·1	0·3		11·7	50·1
5	5·9	0·2	3·4	4·4		0·6	0·8	49·1	1·5	1·0	0·2		32·9
	4·6	0·1	2·7	3·4		0·5	0·6	38·2	1·2	0·8	0·1	6·1	41·8
6	12·5	0·2	3·8	3·8		0·4	1·2	39·7	0·6	0·9	0·1		36·8
	8·8	0·2	2·7	2·7		0·3	0·8	27·9	0·4	0·6	0·1	8·1	47·4
7	15·8	0·3	4·7	5·6		0·6	1·0	30·9	1·2	1·1	0·1		38·7
8	16·4	0·3	5·2	4·4		0·5	1·3	30·4	0·7	1·2	0·1		39·5
	13·3	0·2	4·3	3·5		0·5	1·1	21·8	0·6	1·0	0·1	6·2	47·4
9	21·0	0·5	7·1	4·4		0·5	1·2	20·6	0·8	1·4	0·0		42·5
	18·3	0·5	6·2	3·9		0·4	1·0	17·9	0·7	1·2	0·0	3·5	46·4
10	23·1	0·5	7·0	3·7	0·5	0·3	1·7	17·2	0·9	1·7	0·1		43·3
	20·2	0·4	6·1	3·2	0·5	0·2	1·5	15·1	0·8	1·5	0·0	3·4	47·1
11	24·0	0·4	6·7	3·2	0·8	0·3	1·8	16·3	0·9	1·8	0·1		43·7
	20·8	0·4	5·8	2·8	0·7	0·2	1·6	14·1	0·8	1·6	0·0	3·7	47·5
12	25·8	0·5	9·2	9·4		1·0	1·2	4·4	1·1	1·7	0·1		45·6
	25·0	0·5	8·9	9·1		1·0	1·2	4·3	1·0	1·7	0·1	0·8	46·4
13	25·8	0·7	8·9	3·5	1·7	0·1	1·3	10·0	0·8	1·8	0·1		45·3
	23·6	0·7	8·1	3·2	1·6	0·1	1·2	9·2	0·7	1·7	0·1	2·4	47·4
14	25·9	0·7	8·9	5·3		0·6	1·5	8·8	1·0	1·7	0·1		45·5
15	25·9	0·5	9·1	6·6		0·9	1·8	5·8	1·3	2·3	0·1		45·7
	24·7	0·5	8·7	6·3		0·8	1·8	5·5	1·3	2·2	0·1	1·3	46·8
16	27·4	0·3	6·8	2·1	1·8		2·6	10·2	1·1	2·3	0·1		45·3
	24·3	0·3	6·0	1·8	1·6		2·3	9·0	1·0	2·0	0·0	3·1	48·6
17	27·5	0·6	8·5	6·0		0·5	2·2	4·5	1·4	2·4	0·1		46·3
18	27·8	0·3	8·6	4·3		0·6	1·5	7·5	0·8	2·0	0·1		46·5
	25·9	0·3	8·0	4·1		0·5	1·4	6·9	0·7	1·8	0·1	1·9	48·4
19	27·9	0·5	7·7	4·5	0·8	0·6	1·1	7·2	1·3	2·3	0·1		46·0
20	28·3	0·4	5·9	2·3	1·4	0·1	1·1	11·4	1·3	2·4	0·1		45·3
	24·9	0·3	5·2	2·0	1·2	0·1	1·0	10·1	1·2	2·2	0·1	3·7	48·0
21	29·0	0·3	8·8	5·0	0·7	0·1	2·1	4·0	1·0	2·0	0·0		47·0
	27·9	0·3	8·4	4·8	0·6	0·1	2·0	3·9	1·0	1·9	0·0	1·1	48·0
22	29·0	0·5	8·8	5·1			2·1	2·3	1·6	3·4	0·1		47·1
23	29·2	0·3	8·2	3·2	1·6		1·8	4·8	1·5	2·5	0·1		46·8
	27·7	0·3	7·8	3·0	1·5		1·8	4·6	1·4	2·4	0·1	1·3	48·1
24	29·4	0·9	10·1	3·9	2·0	0·1	1·4	1·6	1·8	0·9	0·1		47·8
	28·8	0·8	9·8	3·9	1·9	0·1	1·4	1·6	1·8	0·9	0·1	0·6	48·3
25	29·9	0·4	9·0	3·1	2·1		1·6	2·4	1·1	3·0	0·1		47·3
	29·1	0·4	8·7	3·0	2·0		1·6	2·4	1·0	2·9	0·1	0·7	48·1
26	30·1	0·4	7·9	2·7	1·8		1·8	4·7	0·9	2·6	0·1		47·0
	28·2	0·4	7·4	2·5	1·7		1·7	4·4	0·9	2·5	0·1	2·2	48·0
27	30·2	0·5	9·4	1·9	3·2		1·6	1·3	1·4	3·0			47·5
	29·7	0·5	9·3	1·9	3·1		1·6	1·3	1·4	3·0		0·5	48·7
28	30·2	0·5	8·7	5·9		0·2	1·4	1·9	1·8	1·4	0·1		47·9
	29·6	0·5	8·6	5·8		0·2	1·3	1·9	1·8	1·4	0·1	0·6	48·2

Table 2—*continued*

Index No.	Si	Ti	Al	Fe^{3+}	Fe^{2+}	Mn	Mg	Ca	Na	K	P	C	O
29	30·2	0·5	9·4	3·1	2·4		1·5	1·1	0·8	3·2	0·1		47·7
	29·8	0·5	9·3	3·0	2·4		1·5	1·1	0·8	3·2	0·1	0·4	47·9
30	30·4	0·4	7·4	6·8		0·9	2·0	2·3	0·8	1·4	0·1		47·5
	29·8	0·4	7·2	6·6		0·9	2·0	2·2	0·7	1·4	0·1	0·5	48·2
31	30·6	0·4	7·7	2·6	1·7		1·7	4·4	0·9	2·6	0·1		47·3
	28·8	0·4	7·3	2·5	1·6		1·6	4·1	0·9	2·5	0·1	2·1	48·1
32	31·3	0·3	7·7	0·7	3·4	0·1	1·8	2·6	2·7	1·7	0·0		47·7
	30·8	0·3	7·6	0·7	3·4	0·1	1·8	2·6	2·6	1·7	0·0	0·4	48·0
33	31·5	0·3	5·2	1·9	1·0		1·9	8·4	0·7	1·9	0·1		47·1
	28·3	0·2	4·7	1·7	0·9		1·8	7·6	0·6	1·7	0·0	2·7	49·8
34	31·6	0·4	7·6	4·7		0·8	1·7	1·6	1·6	2·0	0·1		47·9
35	32·5	0·4	8·3	0·7	2·7	0·2	1·1	1·7	2·0	1·8	0·1		48·5
36	35·5	0·4	6·1	2·6		0·1	0·9	1·7	1·2	2·1	0·1		49·3
	34·9	0·4	6·0	2·6		0·1	0·9	1·6	1·2	2·1	0·1	0·4	49·7
37	35·7		6·1	1·7		0·2	0·1	1·2	1·5	4·8			48·7
	35·6		6·1	1·7		0·2	0·1	1·1	1·5	4·7		0·1	48·9
38	37·1	0·4	5·1	0·6	2·1	0·2	1·0	0·9	1·6	1·3	0·1		49·6
	36·9	0·4	5·1	0·6	2·1	0·2	1·0	0·9	1·6	1·3	0·1	0·1	49·7
39	38·2	0·2	2·9	1·7		0·1	1·2	5·4	0·1	0·1	0·0		50·1
	36·3	0·2	2·7	1·6		0·1	1·1	5·2	0·1	0·1	0·0	1·4	51·2
40	38·6	0·2	2·6	1·6		0·1	1·1	5·6			0·0		50·2
41	39·3	0·2	2·7	0·8	0·3		0·8	4·2	0·4	1·1	0·0		50·2
	37·3	0·2	2·5	0·8	0·2		0·7	4·0	0·4	1·1	0·0	1·4	51·4
42	39·5		3·4	1·6	0·9		0·4	1·2	0·6	1·5	0·3		50·6
	39·1		3·4	1·6	0·9		0·4	1·2	0·6	1·5	0·3	0·3	50·7
43	44·2		0·7	0·1	0·2		0·1	2·2	0·1	0·1			52·3
	43·2		0·7	0·1	0·2		0·1	2·1	0·1	0·1		0·6	52·8

* Cl 55·4, S 2·3

processes which result in hydrothermal alteration minerals (cf. FREDERICKSON and Cox, 1954).

Even on this basis of surface-equilibrium phases it is difficult to define a characteristic field for sedimentary rocks. Difficulties are threefold:

(1) It is not easy to decide which sediments are thoroughly representative and which are not. Metastable sediments may be formed in near-equilibrium with peculiar local conditions. Conglomerates, grits, and arkoses are probably not sedimentary equilibrium phases, but the position of laterites and bauxites is more problematical. Evaporates are probably metastable in the sense of generally operative processes. However, it is questionable whether dolomite-formation is a sedimentary process or the result of metasomatism.

(2) Complete equilibrium can only be the exception on the surface of the restless earth. Successive sedimentary cycles undoubtedly add continually to equilibrium phases in sediments. But acting against this are the incidence and effects of compaction, lithification, metasomatism, igneous action, and metamorphism which again disturb the sedimentary equilibria.

(3) The composition of the atmosphere has probably changed markedly in

geologic time (RUBEY, 1951, 1955; UREY, 1952). Undoubtedly this has affected chemical differentiation in sedimentary processes (cf. NANZ, 1953). Chemical adjustments in rock-weathering probably have not acted in the same directions throughout geologic time.

While recognizing these problems, the writers have attempted to use the geologic record since the Cambrian and the distribution of average compositions as guides to delineate a sedimentary field. This field includes normal and preponderant sediments such as muds, shales, limestones, graywackes, subgraywackes, and sandstones, but excludes conglomerates, grits, arkoses, laterites, bauxites, evaporates, and dolomite or dolomitized limestones. Thus defined the sedimentary field reflects compositions and stabilities of sediments *normally* attained on the earth's surface in contact with an oxidizing atmosphere.

Fig. 5 shows sedimentary averages plotted according to a system suggested by MASON (1952, pp. 130–131) and adopted by RUBEY (in preparation) in his compilation of sediments in the United States. (Al + Fe) does not exceed 40 per cent of (Si + Al + Fe + Mg + Ca) in normal sediments, and only reaches more than 30 per cent in sediments with more than 50 per cent Si.

INDEX TO TABLE 2*

1. Dissolved solids in sea-water (calc.), RUBEY (1951, p. 1126).
2. Devonian—Pleistocene limestone (calc.), RUBEY (personal communication).†
3. Limestone (345, comp. anal.), CLARKE (1924, p. 30).
4. Precambrian—Silurian limestone (calc.), RUBEY (personal communication).†
5. Globigerina ooze (66 sta.), SUJKOWSKI (1952, p. 373).
6. Globigerina—pteropod ooze (49–75), RUBEY (personal communication).
7. Modern oceanic sediment (calc.), SUJKOWSKI (1952, p. 373).
8. Pelagic sediment (calc.), POLDERVAART (1955, p. 125).
9. Hemipelagic sediment (calc.), POLDERVAART (1955, p. 131).
10. Suboceanic sediment (calc.), POLDERVAART (1955, p. 131).
11. All sediment (calc.), POLDERVAART (1955, p. 132).
12. Red clay (45 sta.), SUJKOWSKI (1952, p. 373).
13. Terrigenous clay (52), SVERDRUP *et al.* (1946, p. 1006).
14. Terrigenous mud (53–88), RUBEY in POLDERVAART (1955, p. 131).
15. Red clay (61–85), RUBEY in POLDERVAART (1955, p. 125).
16. Sediment of young folded belts (calc.) POLDERVAART (1955, p. 130).
17. All sediment (calc.), KUENEN (1950, p. 125).
18. Siliceous ooze (6–17), RUBEY in POLDERVAART (1955, p. 125).
19. All sediment (calc.) SUJKOWSKI (1952, p. 361).
20. Continental sediment (calc.) SUJKOWSKI (1952, p. 361).
21. Clay and soil (12), CLARKE (1924, p. 631).
22. Norwegian glacial and post-glacial clays (78), GOLDSCHMIDT (1933, p. 124).
23. Mesozoic—Cenozoic shale (27, comp. anal.), CLARKE (1924, p. 552).
24. Terrigenous mud (52, comp. anal.), CLARKE (1924, p. 518).
25. Shale (78, comp. anal.), CLARKE (1924, p. 30).
26. All sediment (calc.), LEITH and MEAD (1915, p. 82).
27. Pelitic rock (155), SHAW (1956, p. 928).
28. Blue mud (13 sta.), SUJKOWSKI (1952, p. 373).
29. Paleozoic shale (51, comp. anal.), CLARKE (1924, p. 552).
30. Radiolarian ooze (7 sta.), SUJKOWSKI (1952, p. 373).
31. All sediment (calc.), CLARKE (1924, p. 33).
32. Graywacke (11), PETTIJOHN (1949, p. 250).
33. Continental Shield sediment (calc.), POLDERVAART (1955, p. 129).
34. Pacific diatom ooze (2 sta.), SUJKOWSKI (1952, p. 373).
35. Graywacke (30), TYRRELL (1933, p. 26).
36. Mississippi silt (235, comp. anal.), CLARKE (1924, p. 509).
37. Arkose (3), PETTIJOHN (1949, p. 259).
38. Subgraywacke (3), PETTIJOHN (1949, p. 256).
39. All diatom ooze (calc.), POLDERVAART, from SUJKOWSKI (1952, p. 373).
40. Antarctic diatom ooze (4 sta.), SUJKOWSKI (1952, p. 373).
41. Sandstone (253, comp. anal.), CLARKE (1924, p. 30).
42. Quartzite (?), SEDERHOLM (1925, p. 4).
43. Orthoquartzite (7), PETTIJOHN (1949, p. 241).

* Although original sources are quoted, many of these averages have been modified in recalculations by the writers.

† After CLARKE (1924, p. 30), modified for Ca/Mg ratios after DALY (1909, p. 20).

Table 2(a). Clays of the Russian Platform (recomputed from VINOGRADOV and RONOV, 1956, pp. 6–7.)

Index letter*	Si	Ti	Al	Fe^{+3}	Mg	Ca	Na	K	C	O	Ca/Mg†
Pϵ	29·2	0·6	10·4	6·3	1·5	0·4	0·6	3·5		47·6	
	28·8	0·6	10·3	6·2	1·4	0·4	0·6	3·5	0·3	47·9	0·28
ϵ	30·0	0·5	10·0	5·0	1·4	0·6	0·4	4·3		47·8	
	29·8	0·5	10·0	5·0	1·4	0·6	0·4	4·2	0·2	48·0	0·44
S	25·6	0·4	7·6	4·4	2·9	9·5	0·7	4·1		44·8	
	23·0	0·4	6·8	4·0	2·6	8·5	0·6	3·7	2·8	47·7	3·17
D	25·6	0·6	9·2	5·4	2·5	7·2	0·5	3·5		45·5	
	23·7	0·6	8·5	5·0	2·3	6·6	0·5	3·2	2·1	47·6	2·81
C	27·6	0·6	10·3	5·1	2·0	3·5	0·5	3·6		46·8	
	26·4	0·5	9·8	4·9	1·9	3·3	0·5	3·5	1·2	48·0	1·71
P	24·1	0·4	7·3	4·9	4·1	11·1	1·2	2·7		44·3	
	21·2	0·4	6·4	4·3	3·6	9·8	1·0	2·4	3·3	47·7	2·63
TR	26·5	0·5	8·7	4·8	2·5	8·1	0·9	2·1		45·9	
	24·5	0·4	8·1	4·4	2·3	7·5	0·8	2·0	2·1	48·0	3·17
J	28·8	0·5	9·7	4·9	1·3	3·8	1·2	2·9		47·0	
	27·5	0·5	9·4	4·7	1·3	3·6	1·1	2·8	1·1	48·1	2·80
K	29·2	0·5	9·4	4·6	1·2	4·5	1·1	2·2		47·3	
	27·8	0·5	9·0	4·4	1·2	4·2	1·0	2·1	1·3	48·5	3·59
T	30·2	0·4	6·9	4·9	1·5	5·9	1·0	2·2		47·1	
	28·4	0·4	6·5	4·6	1·4	5·5	0·9	2·1	1·7	48·6	3·89
Q	30·4	0·4	7·8	4·6	2·0	3·9	0·6	2·9		47·5	
	29·1	0·4	7·5	4·4	1·9	3·7	0·6	2·7	1·2	48·6	1·85
Ave.‡	27·9	0·5	8·8	5·0	2·1	5·3	0·8	3·1		46·5	
	26·4	0·5	8·4	4·7	1·9	4·9	0·7	2·9	1·6	48·0	2·51

* Shown on Figs. 5 and 6.
† From the original (VINOGRADOV and RONOV, 1956, p. 11).
‡ Average plotted on Fig. 7.

INDEX TO TABLE 2(a)

Pϵ Late Precambrian. Average of 17 composites based on 765 individual specimens.
ϵ Cambrian. Average of 14 composites based on 436 individual specimens.
S Silurian. Average of 14 composites based on 729 individual specimens.
D Devonian. Average of 94 composites based on 2543 individual specimens.
C Carboniferous. Average of 36 composites based on 508 individual specimens.
P Permian. Average of 28 composites based on 730 individual specimens.
TR Triassic. Average of 4 composites based on 121 individual specimens.
J Jurassic. Average of 16 composites based on 328 individual specimens.
K Cretaceous. Average of 12 composites based on 255 individual specimens.
T Tertiary. Average of 12 composites based on 352 individual specimens.
Q Quaternary. Average of 5 composites based on 28 individual specimens.
Ave. Average of the above 11 averages giving equal weight to each geologic period. This average differs from the anhydrous equivalent of the original which is a weighted average based on number of composites. The difference is within 0·5 per cent for each constituent. Mn and P are not listed separately in the original. The averages are, therefore, computed Mn and P free. However, the sum of Mn and P in non-pelagic clays normally does not exceed 1 per cent.

The Ca–Na–K diagram shown in Fig. 6 shows a strong scatter of points widening toward the Na–K side, with a median line which intersects the Na–K side at approximately Na : K = 7 : 13, as compared with Na : K = 1 : 1 for igneous rocks and Na : K = 28 : 1 for sea-water. If it be assumed that Na and K in sea-water result solely from rock weathering, it can be calculated from these three ratios that sedimentary processes affecting igneous source rocks in which Na equals K, result in storage of roughly 47 per cent Na and 1·7 per cent K in sea-water, while 53 per cent Na and 98·3 per cent K are retained in the sediments formed. If the igneous source rocks are basalt with Na = 2·5 K, sedimentary processes similarly would result in storage of 79·6 per cent Na and 7·1 per cent K in sea-water, while 20·4 per cent Na and 92·9 per cent K would be retained in the derived sediments.

With the assumption that chemical differentiation in sedimentary processes has remained the same throughout geologic time, these percentages may be compared with total amounts of Na and K in all sea-water (respectively 17,232 $\times 10^{12}$ tons and 619 $\times 10^{12}$ tons). This assumption is probably not warranted but results are nonetheless instructive. Thus for igneous source rocks with Na = K the amounts of Na and K in all sea-water are equivalent to 19,432 $\times 10^{12}$ tons Na and 35,793 $\times 10^{12}$ tons K retained in all sediments. For basaltic source rocks with Na = 2·5 K, the equivalents are 4416 $\times 10^{12}$ tons Na and 8099 $\times 10^{12}$ tons K. Taking Poldervaart's (1955, p. 132) average composition of unmetamorphosed sediments as a basis, the amounts of Na and K for igneous source rocks with Na = K represent 1800 $\times 10^{15}$ tons of sediment, while for basaltic source rocks with Na = 2·5 K the amounts of Na and K represent 400 $\times 10^{15}$ tons of sediment. In contrast, Poldervaart has calculated that there exist at present 1700 $\times 10^{15}$ tons of sediment in an unmetamorphosed or slightly metamorphosed condition.

These calculations completely fail to explain the enormous amounts of sediments found as metamorphic rocks in Archean shields. To the writers it seems likely that the total amount of sediments produced in geologic time is three to ten times the amount calculated. Possible solution of the problem involves one or more of the following assumptions. (1) Estimates on which the calculations are based are completely wrong and should be rejected. (2) Chemical differentiation by sedimentary processes has changed markedly in geologic time and in particular differentiation of Na and K was decidedly less efficient in the Archean than in geologically more recent times. (3) Throughout geologic time considerable proportions of sediments have consisted of intermediate to felsic tuffs with Na $\leqslant$ K. (4) Throughout geologic time source materials for sediments have consisted predominantly of rocks with Na $\leqslant$ K. (5) The Na and K in sea-water have not resulted solely from rock weathering; appreciable proportions may have been added to the oceans by degassing of the mantle.

The writers consider a combination of the last four assumptions most likely. The geochemistry of Na and K is incompatible with a theory of evolution of continents by weathering and sedimentation of basaltic source rocks. On the one hand there is too much sediment, on the other there is not enough Na and K in sea-water.

Fig. 7 shows the same series of 11 triangular diagrams as Fig. 4 for igneous

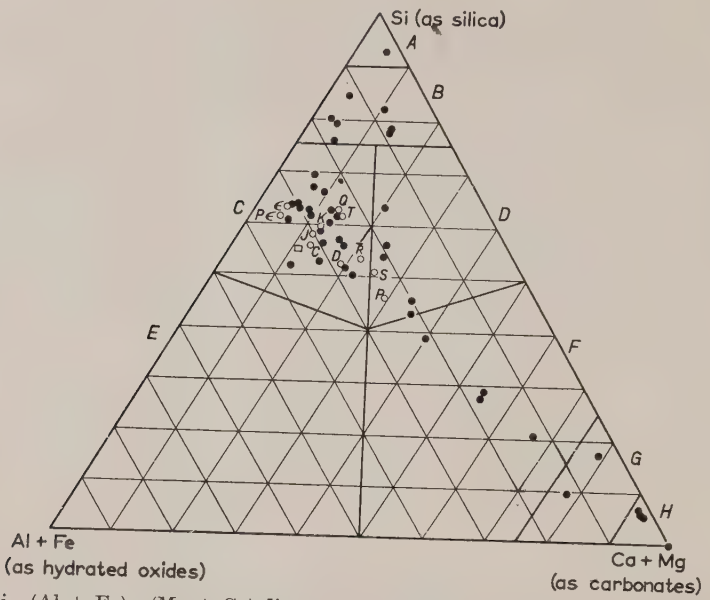

Fig. 5. Si—(Al + Fe)—(Mg + Ca) diagram for sedimentary rocks. Open circles represent clays of the Russian Platform: Pϵ—Late Precambrian, ϵ—Cambrian, S—Silurian, D—Devonian, C—Carboniferous, P—Permian, TR—Triassic, J—Jurassic, K—Cretaceous, T—Tertiary, Q—Quaternary. See note added in proof. Open square represents an anhydrous average of 21 Pacific pelagic clays exclusive of calcareous or diatomaceous cores Cap. 32-33HG, Ck-8-9, and NH9 (recalculated from GOLDBERG and ARRHENIUS, 1957). Weight percentages and s.d. in parentheses are as follows: Si 24·4 (2·4); Ti 0·65 (0·32); Al 9·6 (1·3); Fe 5·4 (0·9); Mn 1·0 (0·7); Mg 1·9 (0·3); Ca 2·8 (1·6); Na 3·6 (0·9); K 2·6 (0·5). Data for 17 additional elements in original reference.

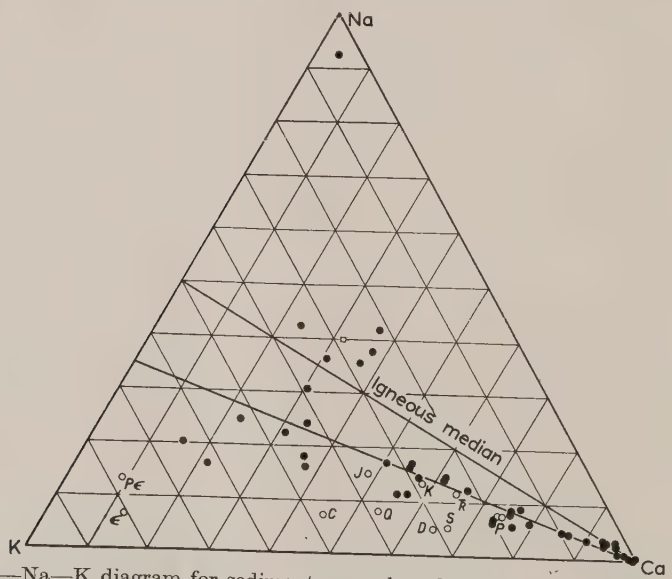

Fig. 6. Ca—Na—K diagram for sedimentary rocks. Open circles represent clays of the Russian Platform. Symbols as in Fig. 5. See note added in proof. Open square represents average of 21 Pacific pelagic clays exclusive of calcareous or diatomaceous types (GOLDBERG and ARRHENIUS, 1957). The position of the open square relative to the open circles reflects in part the degree of influence of basaltic source for these pelagic clays versus a predominantly non-basaltic source for the Russian terrestrial clays.

rocks. The Si–Al–Mg diagram shows few instructive features. Most points are near the Si corner and their grouping suggests that for the same Si–Al values, sediments have slightly higher Mg than igneous rocks.

The next ten diagrams show the variation of Al, total Fe, Mg, Ca, and (Na + K). For comparison the igneous trend from mafic to felsic rocks has been added to the diagrams. In diagrams which include Ca, the sedimentary averages fall in a zone fanning out from the Ca corner and widening toward the opposite side. Median lines for these zones intersect the side as follows:

Diagram	Intersection on side opposite Ca corner	
Ca–Al–Fe	Al : Fe	= 60 : 40
Ca–Al–Mg	Al : Mg	= 85 : 15
Ca–Al–(Na + K)	Al : (Na + K)	= 70 : 30
Ca–Fe–Mg	Fe : Mg	= 75 : 25
Ca–Fe–(Na + K)	Fe : (Na + K)	= 60 : 40
Ca–Mg–(Na + K)	Mg : (Na + K)	= 30 : 70

The zone is relatively narrow in the Ca–Al–(Na + K) and Ca–Al–Mg diagrams, but widest in the Ca–Fe–(Na + K) diagram. The width of the zone in each diagram reflects the degree of coherence of the two contrasted constituents in normal sediments. Points outside the generalized zones represent arkose, solids in sea-water, diatom ooze, and dolomitized limestone.

In diagrams which exclude Ca, the sedimentary averages fall within a well-defined field. This field is most nearly circular in the Al–Fe–(Na + K) diagram, but more elliptical in the other three diagrams, with greatest length of longer axis in the Fe–Mg–(Na + K) diagram. Arkose, solids in sea-water, diatom ooze, and dolomitized limestones again fall outside this field.

Although not done in this paper, the triangular diagrams can be combined in five tetrahedra to show the variation for any combination of four of the five variables. In the four tetrahedra which include Ca, the sedimentary field is a cone which issues from the Ca corner and widens toward the opposite side of the tetrahedron. In the Al–Fe–Mg–(Na + K) tetrahedron the sedimentary field is an ellipsoid of revolution.

Metamorphic Rocks

As the term is used here, metamorphism encompasses all processes, exclusive of weathering, whereby pre-existing rocks are changed mineralogically, texturally, and/or chemically after their first formation or deposition. Thus it includes low-temperature processes such as diagenesis in sediments and hydrothermal alteration of rocks, as well as high-temperature changes effected by plutonic processes.

Many metamorphic rocks have only recrystallized without significant variation in proportions of major and minor elements. In other rocks metamorphism has changed the water content without significant differences in other major constituents, although the content of particular trace elements may be materially

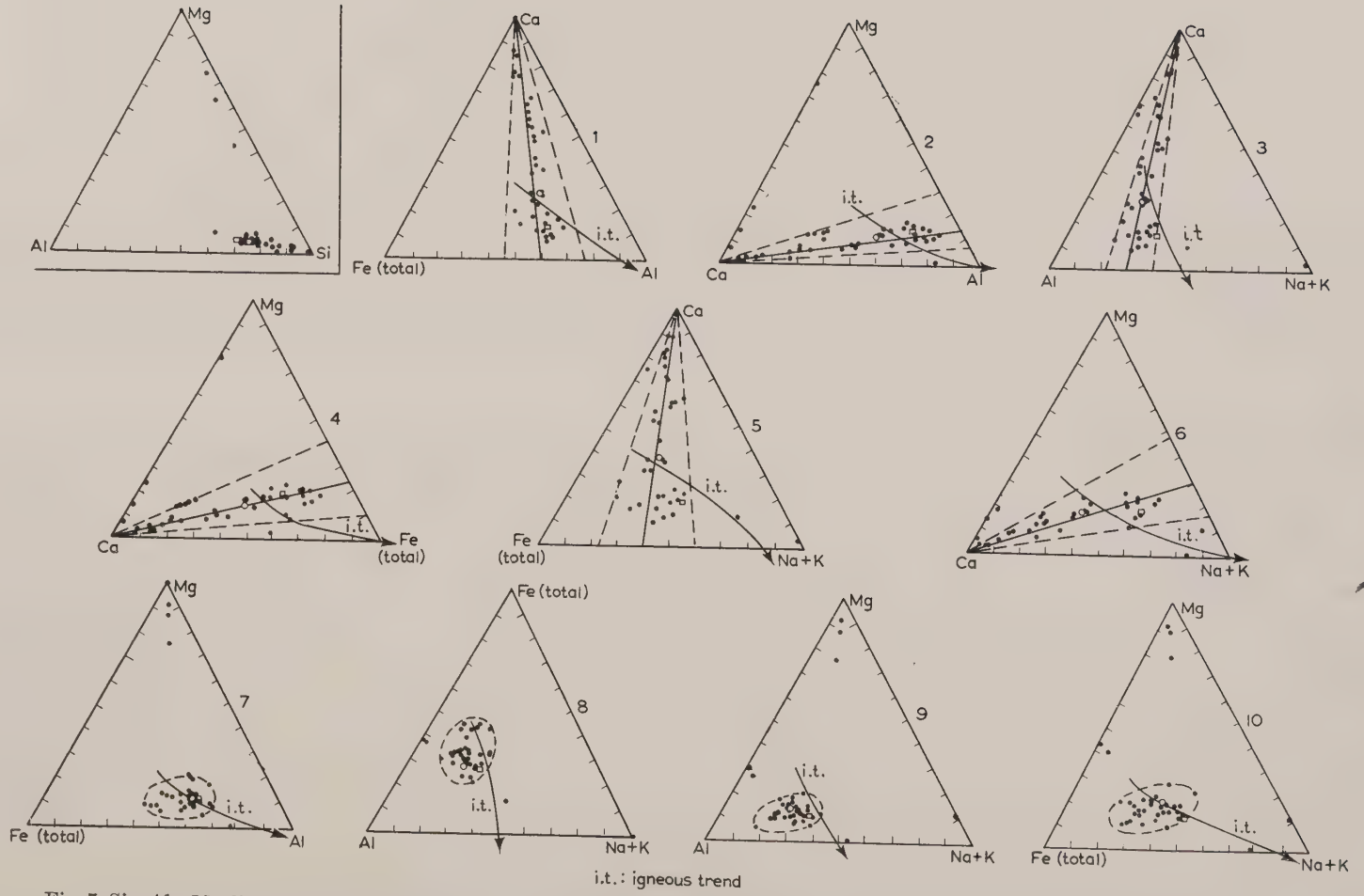

Fig. 7. Si—Al—Mg diagram and diagrams with variables Al, total Fe, Mg, Ca, and combined alkalis for sedimentary rocks. Open circle represents over-all average of clays of the Russian Platform. See note added in proof. Open square represents non-calcareous and non-diatomaceous Pacific pelagic-clays. (GOLDBERG and ARRHENIUS, 1957). In the Si—Mg—Al and Al—Fe—Mg triads the circle falls within the small cluster of solid points.

Table 3. Averages of metamorphic rocks.

Index No.	Si	Ti	Al	Fe^{3+}	Fe^{2+}	Mn	Mg	Ca	Na	K	P	O
1	22·9		7·7	2·7	7·1		5·4	8·2	1·9	0·6		43·5
2	23·5	1·0	8·3	2·5	6·1	0·2	4·2	6·8	2·2	0·9	0·1	44·2
3	23·5		8·8	2·6	6·9		4·2	7·2	2·2	0·6		44·0
4	28·1	0·7	11·0	2·1	3·7	0·1	1·8	0·9	1·5	3·3	0·1	46·7
5	28·2		12·8	2·0	2·8		1·2	0·6	1·3	3·7		47·4
6	28·2	0·5	9·8	2·9	5·2	0·1	1·6	0·8	1·0	3·4	0·1	46·4
7	28·9	0·4	10·1	2·3	4·2	0·2	1·8	0·7	1·3	3·2	0·0	46·9
8	28·9		10·9	2·8	3·4		1·8	1·0	1·0	3·0		47·2
9	29·9	0·5	9·0	1·7	2·3		1·1	2·9	2·7	2·6	0·1	47·2
10	29·9		10·7		5·4		1·3	0·3	1·1	3·9		47·4
11	30·1	0·6	9·3	1·5	3·6	0·1	1·6	1·4	1·4	3·1	0·1	47·2
12	30·2		10·2	1·9	2·6		1·6	1·1	1·2	3·5		47·7
13	30·3		10·2	2·7	1·9		1·0	2·0	1·0	3·2		47·7
14	30·3	0·5	9·2	2·0	3·0		1·9	0·8	2·0	2·7		47·6
15	31·0	0·4	8·2	1·3	2·2	0·1	1·2	2·7	2·6	2·7	0·1	47·5
16	31·0	0·4	8·4	1·6	3·6	0·1	1·8	1·0	1·9	2·7	0·0	47·5
17	31·6	0·4	9·5	1·4	2·6		1·2	0·9	1·3	2·8	0·0	48·3
18	31·7		8·8	1·3	2·6		1·1	1·4	2·3	2·9		47·9
19	31·8		8·1		5·3		2·1	0·9	1·0	3·2		47·6
20	32·0	0·2	7·8	0·9	2·5		1·0	2·4	2·3	3·0	0·0	47·9
21	32·1	0·2	8·7		2·8		1·1	1·8	2·0	3·2	0·0	48·1
22	32·9		7·8	1·4	1·6		0·7	1·4	2·6	3·6		48·0
23	33·0	0·2	8·5	0·6	1·4		0·4	2·1	3·2	2·0	0·0	48·6
24	33·1	0·3	7·7	1·1	1·6	0·1	0·7	1·6	2·4	3·2	0·1	48·1
25	34·5	0·1	7·0	1·0	1·2	0·1	0·6	1·1	2·4	3·1	0·0	48·9
26	37·5		5·1	1·6	1·0		0·6	0·8	1·4	2·2		46·2

INDEX TO TABLE 3*

1. Eclogite (34), Lapadu-Hargues (1953, p. 166).
2. Amphibolite (200), Poldervaart (1955, p. 136).
3. Amphibolite (89), Lapadu-Hargues (1953, p. 161).
4. Phyllite (50), Poldervaart (1955, p. 136).
5. Sericite (muscovite) schist (25), Lapadu-Hargues (1945, p. 267).
6. Precambrian slate (33), Nanz (1953, p. 57).
7. Slate (61), Poldervaart (1955, p. 136).
8. Slate and phyllite (27), Lapadu-Hargues (1945, pp. 261–2).
9. Canadian Shield (calc.), Grout (1938, p. 502).
10. Norwegian phyllite (29), Goldschmidt (1933, p. 130).
11. Mica schist (103), Poldervaart (1955, p. 136).
12. Biotite—muscovite schist (37), Lapadu-Hargues (1945, pp. 265–7).
13. U.S. roofing slate (36), Eckel (1904, p. 26).
14. Slate (22), Clarke (1924, p. 631).
15. Continental crystallines (calc.), Poldervaart (1955, p. 127).
16. Kinzigite (15), Poldervaart (1955, p. 136).
17. Mica schist (5), Clarke (1924, p. 631).
18. Biotite—muscovite gneiss (51), Lapadu-Hargues (1945, pp. 267–71).
19. Norwegian mica schist (53), Goldschmidt (1933, p. 130).
20. Finnish Shield (calc.), Sederholm (1925, p. 10).
21. Finnish mica schist (?), Sederholm (1925, p. 4).
22. Plutonic gneiss (64), Lapadu-Hargues (1945, pp. 271–6).
23. Greenland gneiss (12), Ramberg (1951, p. 31).
24. Quartzofeldspathic gneiss (250), Poldervaart (1955, p. 135).
25. Leptite and hälleflinta (112), Poldervaart (1955, p. 135).
26. Metaquartzite (18), Lapadu-Hargues (1945, pp. 296–7).

* Although original sources are quoted, many of these averages have been modified in recalculations by the writers.

altered (cf. Eckelmann and Poldervaart, 1957). Of greatest chemical interest are metamorphic changes that are accompanied by significant variation in bulk chemical composition. These are usually called metasomatic to distinguish them from metamorphic effects in which there is no appreciable change in major chemical constituents other than water.

Probably the most important low-temperature metasomatic change in sediments is dolomitization of limestone. Daly (1909) has estimated the Ca/Mg ratio in all pre-Devonian limestone at 3·35 and in all Devonian to Recent limestone at 20·01. This may be compared with a Ca/Mg ratio of 0·50 in Precambrian slate (Nanz, 1953), 0·73 in Paleozoic shale, and 2·67 in Mesozoic and Cenozoic shale (Clarke, 1924). Undoubtedly the biosphere has played a major role in this distribution of Ca and Mg in geologic time (cf. Kuenen, 1950, pp. 392–394). However, dolomitization of limestone and the Mg content of argillites may also be influenced by the salinity and pH of water (Rivière, 1939, 1940; Millot, 1949; Sander, 1951).

Several authors have remarked on the enormous amounts of Ca now stored as carbonates in sediments. Usually this is attributed to derivation of sediments from predominantly mafic igneous rocks, but this supposition appears less likely if amounts of Mg and Fe are also considered. There is "not enough" Mg and Fe in sediments and sea-water combined. Consideration of Na/K ratios in igneous rocks, sediments, and sea-water renders derivation of sediments from basaltic source rocks even more unlikely. The alternative is that Ca is continually stored as carbonates at or near the earth's surface, similar to the continual storage of Na in sea-water. If CO_2 is combined with Ca for $CaCO_3$ in Poldervaart's (1955, p. 132) average sediment, the remainder when recalculated to 100 per cent and adjusted for Na/K ratio, comes remarkably close to average granodiorite, not average basalt.

Dolomitization is not the only indication of displacement of Ca in rocks. Ground-water dissolves and redistributes Ca in buried rocks, while it often deposits $CaCO_3$ nearer the surface. Studies of hydrothermal alteration frequently indicate solution of Ca at depth and deposition of $CaCO_3$ at higher levels. Plutonic processes may also redistribute Ca and perhaps this accounts for the relative scarcity of marbles in plutonic terranes and the decrease in Ca implicit in the formation of para-amphibolites from limestones or dolomitic shales (cf. Adams, 1909; Backlund, 1953).

Excellent studies are available of hydrothermal alteration of rocks, but the changes are not easily analysed quantitatively. Changes induced by low-temperature metasomatism often run contrary to trends of magmatic differentiation. Late residual magmas are usually poor in Ca, Mg, and Fe, yet accompanying hydrothermal solutions frequently dissolve these elements from igneous rocks and deposit them elsewhere as calcite, dolomite, illite, sericite, chlorite, nontronite, or iron oxides (cf. Lovering, 1949; Schwartz, 1950; Stringham, 1953; Jaffe, 1955; Kerr *et al.*, 1955). In these respects low-temperature metasomatism resembles chemical differentiation produced by sedimentary processes.

Somewhat more is known of high-temperature chemical changes effected by plutonic processes. The overall change from shale, slate, or phyllite to schist,

gneiss, and granitic gneiss by progressive feldspathization is well-known and has been a *cause célèbre* in the granite controversy. Marked chemical changes in the plutonic series from argillite to granitic para-gneiss can hardly be denied and have been demonstrated repeatedly in different localities. LAPADU-HARGUES (1945) has discussed these changes on the basis of averages computed by him. Averages of metamorphic rocks calculated by POLDERVAART (1955) are based on larger numbers of analyses, yet are not significantly different from LAPADU-HARGUES' (1945, 1953) results. However, averages are still too few in number and thorough chemical studies of particular regions affected by plutonic processes are also

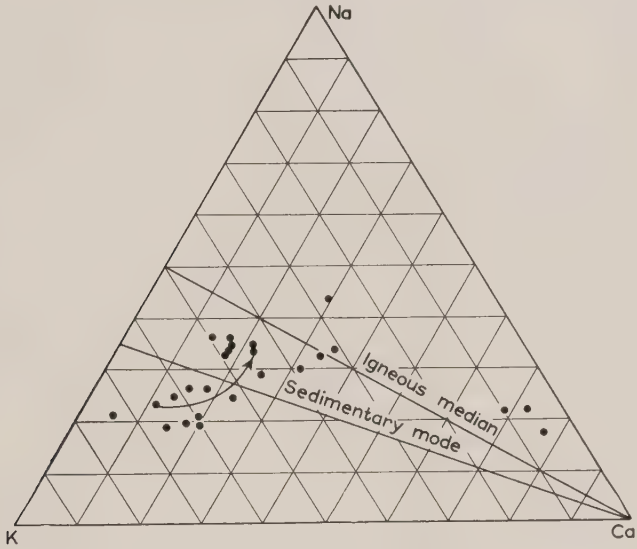

Fig. 8. Ca–Na–K diagram for metamorphic rocks.

scarce. It is therefore only possible to analyse the main chemical changes which attend feldspathization. At present details cannot be discussed quantitatively.

A change from argillite to granitic gneiss involves a compositional trend directed toward granite on the igneous trend. Fig. 8 shows averages of metamorphic rocks plotted on a Ca–Na–K diagram. The igneous and sedimentary medians are also indicated. The trend shown is that for a series from normal potassic shale to granitic para-gneiss, and indicates progressive relative enrichment in both Na and Ca. The three points near the Ca corner represent averages for amphibolites and eclogites. The points nearly coincide with the position of average basalts. If such rocks are feldspathized and converted into granitic gneiss, the compositional trend would be entirely different and involve progressive enrichment in Na and K, with decrease in Na/K ratio. Thus a number of different trends could be drawn, of which the trend of the series shale-granitic gneiss is only one example. This particular series has been selected because it is believed to be most common in plutonic regions.

Fig. 9 shows the same eleven diagrams used for igneous and sedimentary rocks. The Si–Al–Mg diagram is again not instructive and metamorphic averages

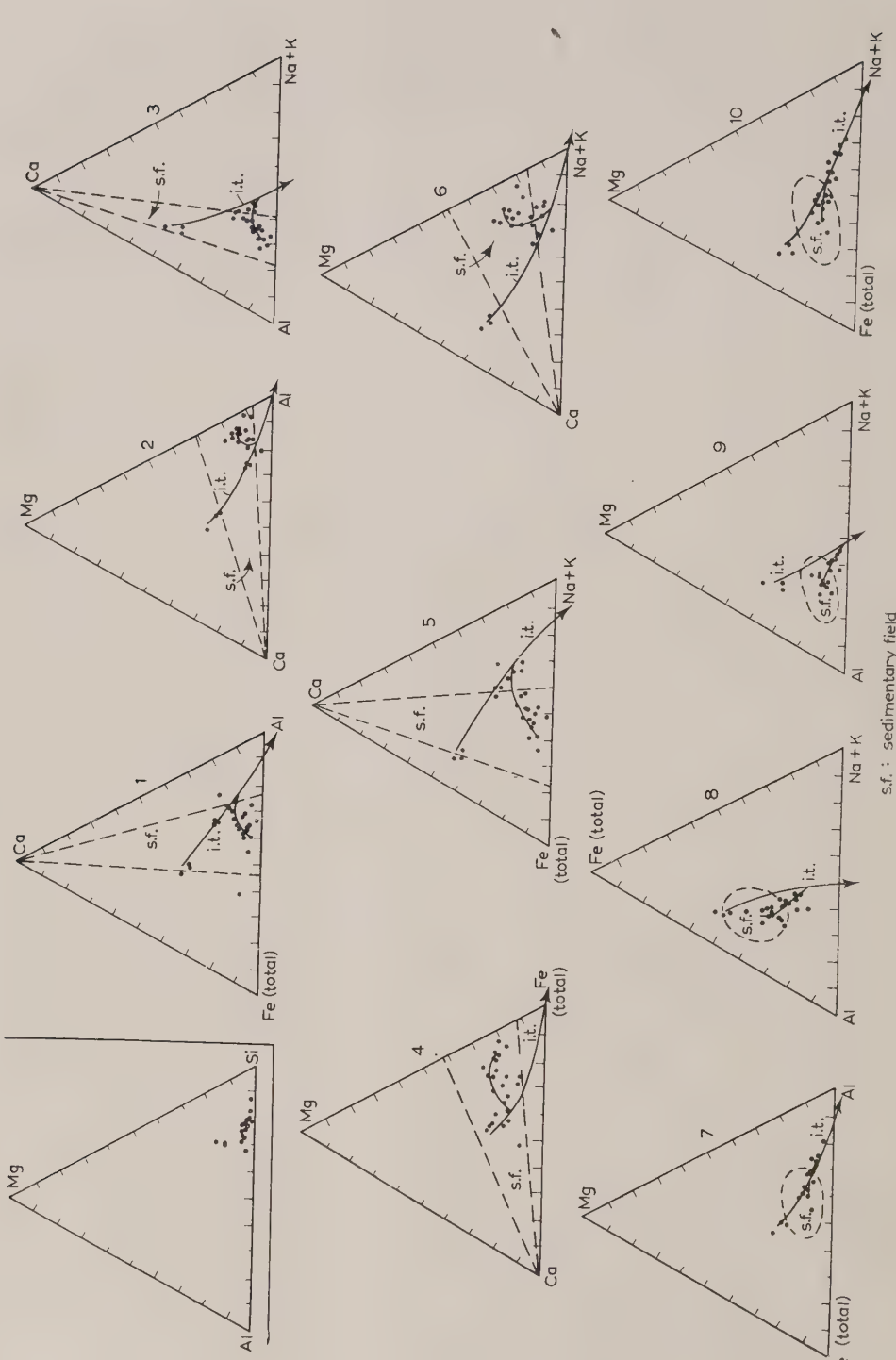

Fig. 9. Si–Al–Mg diagram and diagrams with variables Al, total Fe, Mg, Ca, and combined alkalis for metamorphic rocks.

are nearly in the same positions as igneous rocks and sediments. The other ten diagrams are more satisfactory. In these diagrams the igneous trend is shown as well as the field of normal sediments. The beginning of the igneous trend is the position of average basalts and in all diagrams the three averages for amphibolites and eclogites fall near this point. The additional trend shown is that from average shale to granitic gneiss.

Combined alkalis consistently increase in all the diagrams. Likewise, iron consistently decreases, except in the Fe–Mg–Ca diagram. Ca increases gradually relative to iron and magnesium (Ca–Fe–Mg diagram), but in the other five diagrams which include calcium, there is a small initial increase, after which there is no significant change in proportions of calcium. Aluminium increases relative to iron, but decreases relative to combined alkalis. Relative to calcium, aluminium shows at first a small decrease, probably due to initial increase in calcium content, after which both aluminium and calcium retain about the same proportions. Magnesium increases relative to iron but decreases relative to aluminium. Relative to calcium and combined alkalis, the proportion of magnesium varies little initially but decreases in the change from biotite schist to granitic gneiss. These variations indicate that in the metasomatic transformation of argillites into granitic gneiss: (1) combined alkalis are added, (2) initially a little calcium is also added, and (3) iron and magnesium are diminished, with first decreases of iron preceding first decreases of magnesium.

Addition of combined alkalis probably means that the fluid medium for metasomatism contains Na, K, Al, and Si, roughly in the proportions of alkali feldspar, but with a small excess of alkalis (cf. Morey and Chen, 1955). Although in the transformation of argillites there is apparently preferred fixation of Na rather than K, it does not follow that the metasomatizing fluid contains more Na than K. In the same terrain one often finds feldspathized argillites (preferred fixation of Na) associated with feldspathized amphibolites (preferred fixation of K). The initial small increase in Ca is probably not very significant. Thick sedimentary wedges usually contain calcarenites, and in the initial stage of metamorphism Ca may well be redistributed throughout the sedimentary sequence, as well as subtracted from the sequence as a whole. These adjustments can easily account for small gains in Ca in argillitic members while at the same time Ca is lost in more calcareous members of the same succession. The decrease in Fe and Mg has greater import. In part this decrease is probably a dilution effect and reflects continued addition of feldspar-making material. However, there is evidently also removal of Mg and Fe in the feldspathization of argillites.

Lapadu-Hargues (1945), Reynolds (1946), and others have emphasized the development of mafic fronts in regional feldspathization. The writers believe that the problem of basification is essentially one of time and place and not necessarily in contradiction to regional homogenization. Chemical changes proceed during initial heating of sediments when dehydration occurs (cf. Yoder, 1955). These initial metasomatic phases of plutonism have relatively low temperatures and may in part be compared with hydrothermal alteration. Originally existing chemical contrasts between rocks may be accentuated during these phases and this may result in geochemical culminations and depressions. Ultimately these

initial effects are smoothed out by continued high-temperature metasomatism, but in any particular terrain this may not have advanced far enough to result in complete homogenization. Probably mafic fronts are developed in early phases of plutonism in any particular place, but gradually there is a shift toward the development of mafic rears as feldspathization continues and magmatic conditions are approached. In intermediate phases mafic fronts are represented by scattered relicts (skialiths) in thoroughly feldspathized and homogenized terrains.

Table 4. Averages of silicate phase of stony meteorites

Index No.	Si	Ti	Al	Cr	Fe	Mn	Mg	Ca	Na	K	P	C	O
1	21·6	0·1	1·6	0·3	13·5	0·2	17·3	1·6	0·9	0·2	0·1	—	42·6
2	22·2	0·1	1·7	0·3	10·5	0·2	18·5	1·9	0·9	0·2	0·1	—	43·4
A	21·9	0·1	1·7	0·3	12·3	0·2	17·8	1·7	0·8	0·1	0·1	—	43·0
3	27·8	0·1	1·6	0·2	1·0	0·2	19·4	1·1	1·1	0·2	0·1	—	47·2
4	17·5	0·1	1·6	0·4	19·6	0·2	15·6	1·9	0·8	0·1	0·2	3·2	38·8
5	25·1	0·1	0·6	0·5	7·8	0·3	19·7	0·8	0·3	0·0	0·0	—	44·8
6	22·9	0·3	6·4	0·3	12·6	0·4	5·9	7·8	0·3	0·1	0·0	—	43·0
B	21·5	0·1	1·8	0·4	13·2	0·3	16·5	2·1	0·8	0·2	0·2	—	42·9

INDEX TO TABLE 4

1.* Low total iron chondrites (56)
2.* High total iron chondrites (40)
A* Average chondrite (96)
3. Enstatite chondrites (6)
4. Carbonaceous chondrites (15)
5. Chondritic-type achondrite (12)
6. Basaltic-type achondrite (22)
B Stony meteorite (107), BROWN and PATTERSON (1947, p. 407).

* Exclusive of enstatite—and carbonaceous chondrites, inclusive of two amphoteric chondrites; Manbhoom (modified analysis by UREY and CRAIG, 1954, p. 63) and Vavilovka (UREY and CRAIG, 1953, p. 55).

The peak of plutonism is represented by partial melting (palingenesis) of the rocks. The less refractory (salic) constituents then form new magmas which migrate and intrude rocks elsewhere in the crust, while the more refractory (femic) constituents remain behind as mafic rears. During the intermediate phases of regional feldspathization, mafic constituents (Ca, Fe, Mg), removed from the feldspathized rocks, may migrate with the metasomatizing fluid toward lower temperature regions in the crust where the effects of their passage are shown as hydrothermal alteration.

Although present data only allow analysis of the transformation of argillites into granitic gneiss, it is apparent from the literature that all types of pre-existing rocks affected by plutonic processes tend to change toward the composition of granite. The plutonic series is extended from these autochthonous granites into parautochthonous granites, and finally into migmatic and magmatic intrusive granites (cf. READ, 1955).

STONY METEORITES

Table 4 lists averages of six types of stony meteorites. Na and K for averages A, 5 and 6 have been corrected in accordance with EDWARDS and UREY (1955)

and Edwards (1956). Together with 151 individual analyses of stony meteorites, these data form the basis for the following discussion.

Prior (1916, p. 26) has noted that a low metallic iron phase in chondrites is associated with a high percentage of iron in the silicate phase. Urey and Craig

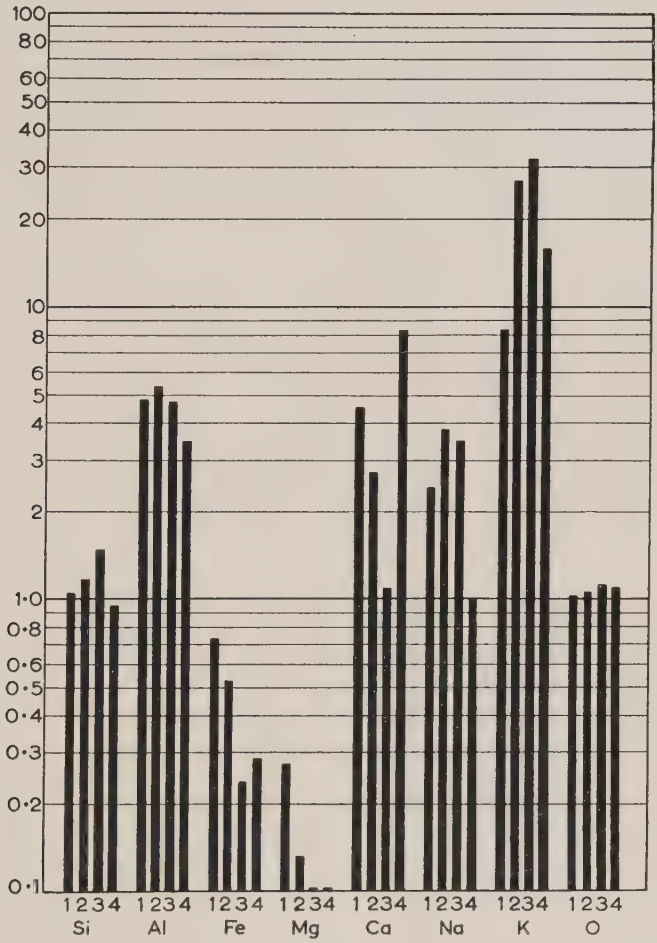

Fig. 10. Concentration ratios of average chondrite and averages of Pacific basalt, intermediate and silicic igneous rocks, and sediment.
(1) Average Pacific olivine basalt.
(2) Average intermediate igneous rock.
(3) Average silicic igneous rock.
(4) Average unmetamorphosed sediment.

(1953, p. 58) and Wiik (1956, p. 282) have recorded a bimodal distribution of total iron (silicate, sulphide, and metal phases) in superior chondrite analyses. Thus chondrites are divided into a high total iron group and a low total iron group. The distribution of iron in the silicate phase of these superior analyses also shows a bimodal distribution, but this has a reciprocal relationship to the distribution of iron. Hence the high total iron group of chondrites has less iron in the silicate phase than the low total iron group. Enstatite chondrites have a

high total iron content, a high percentage of metallic iron, but a low percentage of iron in the silicate phase. Carbonaceous chondrites have a high total iron content, a low percentage of metallic iron, and a high percentage of iron in the silicate phase. Chondritic-type achondrites are low in calcium, contain oligoclase, and have an Fe/Mg ratio of about 0·4. Basaltic-type achondrites are high in calcium, contain calcic plagioclase, and have an Fe/Mg ratio of about 2·1.

Fig. 10 illustrates differences in main elements between average chondrite (A of Table 4) and Pacific olivine basalt (Green and Poldervaart, 1955, p. 179), intermediate and silicic igneous rocks (Nockolds, 1954, p. 1032), and average sediment (Poldervaart, 1955, p. 132). Differences are expressed as concentration ratios relative to average chondrite, and are plotted on a logarithmic scale. Al shows a fourfold enrichment in terrestial rocks; Fe and Mg are impoverished in these rocks. Ca has a range from about 1 in silicic igneous rocks to about 8 in average sediment. K has a range from about 7 in Pacific olivine basalt to about 30 in silicic igneous rocks.

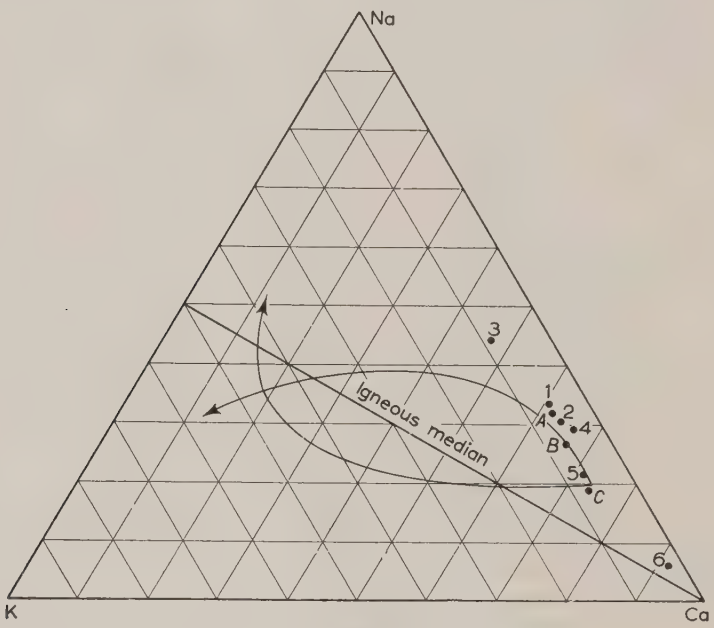

Fig. 11. Ca–Na–K diagram for silicate phase of stony meteorites.

In Figs. 11 and 12 the six types of stony meteorites have been plotted on the same diagrams used in earlier sections. The igneous trend is shown on the diagrams for comparison.

Fig. 11 is a Ca–Na–K diagram on which the eight averages of Table 4 have been plotted in addition to Pacific olivine basalt (C), the median line for igneous rocks, and the igneous trends basalt–latite–trachyte–phonolite and basalt–andesite–dacite–rhyolite (Fig. 3). The diagram illustrates the lack of Na–K fractionation in stony meteorites. The position of point C relative to point 6 (basaltic-type

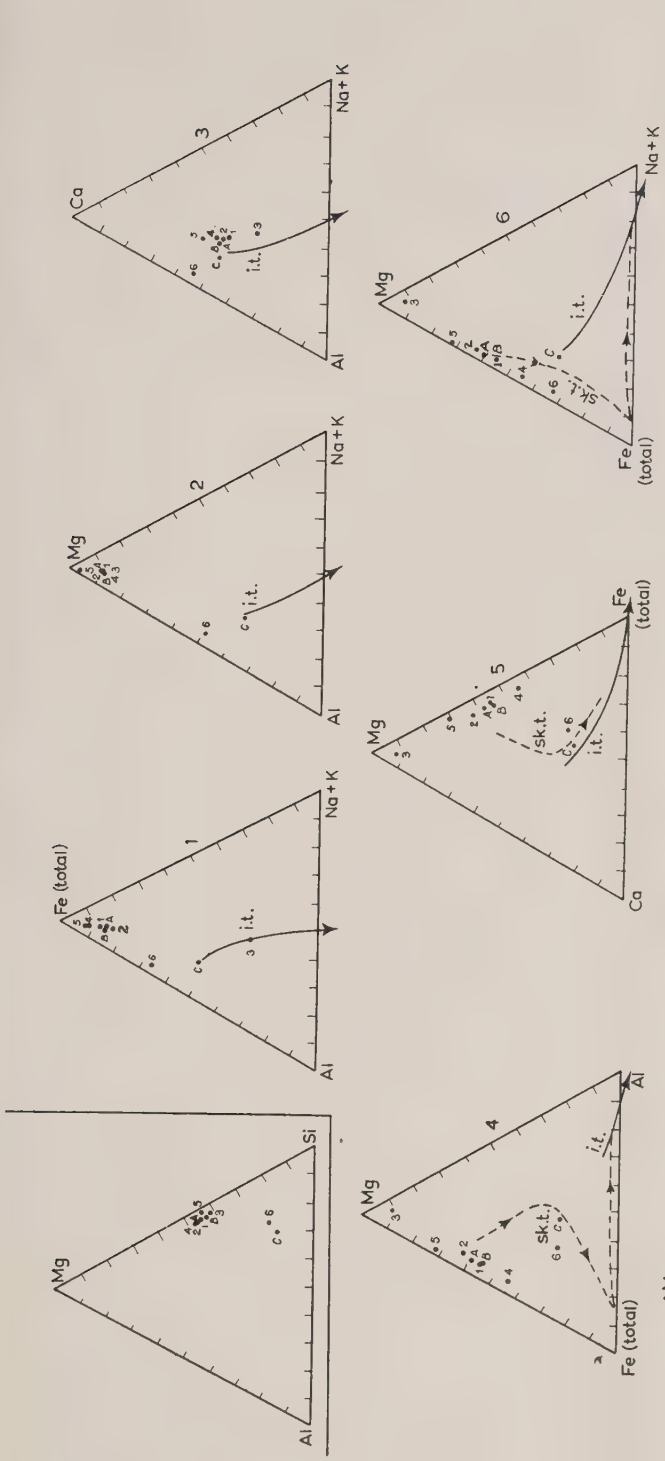

Fig. 12. Si–Al–Mg diagrams and diagrams with variables Al, total Fe, Mg, Ca, and combined alkalis for silicate phase of stony meteorites.

achondrite) is noteworthy. The writers consider the term "basaltic-type achondrite" as misleading; compositions of these meteorites do not resemble those of basalts.

Fig. 12 shows eleven diagrams arranged in the same order used for igneous rocks (Fig. 4). The Si—Mg—Al diagram shows all points, including the point for basaltic-type achondrite (6). Point C again represents Pacific olivine basalt. The following 10 diagrams show the 8 meteorite averages, as well as the igneous trend (Fig. 4) and Pacific olivine basalt (point C).

Group 1. Three diagrams with side Al–(Na + K). The meteorite averages in these diagrams group together, but the point for basaltic-type achondrite (6) is outside the group in all three diagrams while the point for enstatite chondrite (3) falls outside the group in two of the diagrams. The tendency to cluster reflects the lack of alkali enrichment in stony meteorites.

Group 2. Three diagrams with side Fe–Mg. These diagrams reflect the major role of Fe–Mg differentiation in stony meteorites in the wide spread of the points along the side Fe–Mg of the diagrams. For comparison the Skaergaard trend (WAGER and DEER, 1939) has been added to the diagrams as a broken line. The point for basaltic-type achondrite (6) deviates from the alignment of the meteorite points in the first two diagrams of this group, but conforms with the other points in the Mg–Fe–(Na + K) diagram.

Group 3. Four diagrams with corner Ca and without the pairs Al–(Na + K) or Fe–Mg. The points are again grouped together, with the points for basaltic-type achondrite (6) outside the group in all four diagrams and the point for enstatite chondrite (3) outside the group in the two diagrams which include Fe.

PRIOR (1916, pp. 39–40) has expressed the opinion that progressive oxidation has been of major importance in the formation of stony meteorites, and is reflected in variations in the metallic iron phase. UREY and CRAIG (1953, p. 56) have postulated an initially oxidized state with subsequent reduction by hydrogen and oxidation by water, to produce observed variations in the metallic iron phase. However, the last two authors point out that the bimodal distribution of total iron in chondrites cannot be explained by differences in oxidation or reduction. They suggest a theory involving selective collision of asteroids to account for the two groups of chondrites.

The diagrams of Fig. 12 indicate to the writers that compositional differences between the various types of stony meteorites have resulted from generally operative processes and not from chance collisions between asteroids. This impression is further strengthened if all 151 individual analyses are plotted on the diagrams. In the Skaergaard intrusive of eastern Greenland (WAGER and DEER, 1939), high concentrations of iron in silicates have resulted from fractional crystallization. In many respects the Skaergaard trend resembles differences shown by stony meteorites, except that in the latter alkali enrichment is negligible. Thus the writers favour a theory of fractional melting to account for observed differences in iron content of stony meteorites.

In the formation of stony meteorites, three phases can be distinguished: (1) accretion, (2) condensation and compaction, and (3) fragmentation. During accretion an oxidizing environment may have prevailed. Condensation and

compaction with attendant increase in pressure and temperature, may have resulted in partial expulsion of water and a change from an oxidizing to a reducing environment. Radioactive heating (Urey, 1955)* and compaction finally resulted in fractionation by partial melting. Several arguments (Kuiper, 1955, 1956; Urey, 1955) indicate that at least the larger asteroids had differentiated shortly (less than 10^9 year) after their formation and before fragmentation. Fragments which reach the earth are probably differentiates and mixtures of differentiates (cf. Hess and Henderson, 1949; Wahl, 1952). Thus the iron enrichment shown by stony meteorites is thought by the writers to reflect fractionation by partial melting. In contrast, the igneous trend from mafic to silicic igneous rocks shows the effects of fractionation by partial crystallization. Here iron enrichment at first competes with and ultimately yields to alkali enrichment.

Stony meteorites are believed to reflect also the early steps in the differentiation of the primitive earth during the first billion years after its formation. One of the writers (Poldervaart, 1955, p. 140) has pointed out that this is probably also the time of formation of most of the silicic to intermediate crustal material now concentrated in the continental plates. Thus the problem of stony meteorite differentiation is complementary to that of the chemical evolution of the earth's crust.

Acknowledgements—The writers gratefully acknowledge receipt of a grant from the Kemp Fund of Columbia University to aid in the preparation of diagrams and manuscript. The writers also wish to express their appreciation of the splendid co-operation of W. W. Rubey in making his unpublished average compositions of oceanic sediments available. They are further indebted to H. H. Hess and D. M. Shaw for unpublished data used in averages given here. Finally they acknowledge critical reading of the manuscript by A. F. Buddington and H. H. Hess, who made many valuable suggestions incorporated in the paper.

Note added in proof: Some recent Russian publications relating to the distribution of the major elements in the common rock types have appeared in the literature (Vinogradov, Ronov and Ratynskii, 1952; Vinogradov, 1956; Vinogradov and Ronov, 1956). Analytical data from the latter reference are in appended Table 2(a) and are included in Figs. 5, 6 and 7.

Na/K ratios obtained from this table show an increase with time and relate to argument on the improbability of basaltic source rocks for sediments during the bulk of geologic time. Grouped data by Vinogradov and Ronov (1956, p. 11) show a Na/K ratio of 0·17 for Paleozoic clays and shales (203 composites based on 5720 individual specimens) and a Na/K ratio of 0·42 for Mesozoic clays and shales (32 composites based on 704 individual specimens). Vinogradov and Ronov (1956) believe that low Na/K ratios in the early Paleozoic are possibly due to more intensive formation of weathering products enriched in potassium.

Relative to discussion on low temperature metasomatic changes in sediments, attention is called to the increase in Ca/Mg ratio with time in both clays and carbonates (Vinogradov, Ronov and Ratynskii, 1952) of the Russian Platform.

* Recent analytical data have presuaded Urey (1956, p. 891) to believe that radioactive heating is a minor factor in the melting of minerals in chondrites.

The graphed data appear on pages 173 and 274 of volume 12 of *Geochimica et Cosmochimica Acta* in reviews prepared by Chilingar. The ratios show considerable fluctuation. The major "break" in Ca/Mg ratio for clays occurs in the early Paleozoic and does not coincide with the major "break" for carbonates which is in the latter half of the Mesozoic. Discussion of the tectonic, paleotemperature, and biochemical factors producing these fluctuations cannot be attempted here. Extrapolation of these data to other areas should be done with caution and only after statistical analysis of comparable numbers and distribution of samples.

References

Adams F. D. (1909) On the origin of the amphibolites of the Laurentian area of Canada. *J. Geol.* **17**, 1–18.

Backlund H. G. (1953) The granitization problem. *Estud. Geol. Inst. Mallada* **9**, 71–106.

Bowen N. L. (1954) Experiment as an aid in the understanding of the natural world. *Proc. Acad. Nat. Sci. Philad.* **106**, 1–12.

Bowen N. L., Schairer J. F. and Willems H. W. V. (1930) The ternary system Na_2SiO_3–Fe_2O_3–SiO_2. *Amer. J. Sci.* 5th Ser. **20**, 405–455.

Brown H. S. and Patterson C. (1947) The composition of meteoritic matter: I, The composition of the silicate phase of stony meteorites. *J. Geol.* **55**, 405–411.

Buerger M. J. (1948) The role of temperature in mineralogy. *Amer. Mineral.* **33**, 101–121.

Clarke F. W. (1924) The data of geochemistry. *U.S. Geol. Surv.*, 5th ed., Bull. **770**, 841 pp.

Daly R. A. (1909) First calcareous fossils and the evolution of the limestones. *Bull. Geol. Soc. Amer.* **20**, 153–170; (1933) *Igneous Rocks and the Depths of the Earth.* 598 pp. McGraw-Hill, New York.

Eckel E. C. (1904) On the chemical composition of American shales and roofing slates. *J. Geol.* **12**, 25–29.

Eckelmann F. D. and Poldervaart A. (1957) Research on Archean rocks of Beartooth Mountains (Montana–Wyoming). I. Origin and structure of granitic gneiss and migmatite in Quad Creek area. *Bull. Geol. Soc. Amer.* **68**.

Edwards G. (1956) Sodium and potassium in meteorites. *Geochim. et Cosmochim. Acta* **8**, 285–294.

Edwards G. and Urey H. C. (1955) Determination of alkali metals in meteorites by a distillation process. *Geochim. et Cosmochim. Acta* **9**, 154–168.

Frederickson A. F. and Cox J. E. (1954) "Solubility" of albite in hydrothermal solutions. *Amer. Min.* **39**, 738–749.

Goldberg E. D. and Arrhenius G. O. S. (1957) Chemistry of Pacific pelagic sediments. *Geochim. et Cosmochim. Acta* **13**, 153–211

Goldschmidt V. M. Der Stoffwechsel der Erde. Norsk Videnskapsselskapets Skrifter. I. Mat.-naturv. Klasse, **11**, 1–25; (1933) Grundlagen der quantitativen Geochemie. *Fortschr. Min.* **17**, 112–156.

Green J. (1953) Geochemical table of the elements for 1953. *Bull. Geol. Soc. Amer.* **64**, 1001–1012; (1955) Conversion factors for silicate analyses. *N.Y. Acad. Sci. Ann.* **62**, 295–326.

Green J. and Poldervaart A. (1955) Some basaltic provinces. *Geochim. et Cosmochim. Acta* **7**, 177–188.

Grout F. F. (1938) Petrographic and chemical data on the Canadian Shield. *J. Geol.* **46**, 486–504.

Hess H. H. and Henderson E. P. (1949) The Moore County meteorite; a further study with comment on its primordial environment. *Amer. Min.* **34**, 494–507.

Jaffe F. C. (1955) Les ophiolites et les roches connexes de la région du Col des Gets. *Suisse Min. Pet. Bull.* **35**, fasc. 1, 150 pp.

Kerr P. F., Kelley D. R., Keys W. S. and Bodine M. W. Jr., (1955) Annual Report for June 30, 1954 to April 1, 1955. Part 3. Collapse features, Temple Mountain uranium area, Utah. *U.S. Atomic Energy Comm.* R.M.E.-3110 (pt. 3), 138 pp.

Knopf A. (1916) The composition of the average igneous rock. *J. Geol.* **24**, 620–622.

Kuenen P. H. (1950) *Marine Geology.* 568 pp. John Wiley, New York.
Kuiper G. P. (1955) On the origin of the lunar surface features. *Proc. Nat. Acad. Sci. Wash.* **40,** 1096–1112; (1956) The formation of the planets. Pts. I–III, *Roy. Astron. Soc. Canada J.* **50,** 57–68, 105–121, 158–176.
Lapadu-Hargues (1945) Sur l'existence et la nature de l'apport chimique dans certaines séries crystallophylliènnes. *Soc. Géol. France Bull.*, 5th sér., **15,** 255–310; (1953) Sur la composition chimique des amphibolites. *Soc. Géol. France Bull.* (6th sér.), **3,** 153–173.
Larsen E. S. (1948) Batholith and associated rocks of Corona, Elsinore, and San Luis Rey quadrangles, Southern California. *Bull. Geol. Soc. Amer.* Mem. **29,** 182 pp.
Leith C. K. and Mead W. J. (1915) *Metamorphic Geology.* 337 pp. Holt, New York.
Lovering T. S. (1949) Rock alteration as a guide to ore—East Tintic District, Utah. *Econ. Geol.* Monograph 1, 65 pp.
Macdonald G. A. (1949) Hawaiian petrographic province. *Bull. Geol. Soc. Amer.* **60,** 1541–1595.
Mason B. (1952) *Principles of Geochemistry* 276 pp. John Wiley, New York.
Millot G. (1949) Relations entre la constitution et la genèse des roches sédimentaires argileuses. *Géol. Appl.* **2,** no. 2–4, 352 pp.
Morey G. W. and Chen W. T. (1955) The action of hot water on some feldspars. *Amer. Min.* **40,** 996–1000.
Nanz R. H., Jr. (1953) Chemical composition of pre-Cambrian slates with notes on the evolution of lutites. *J. Geol.* **61,** 51–64.
Nockolds S. R. (1954) Average chemical composition of some igneous rocks. *Bull. Geol. Soc. Amer.* **65,** 1007–1032.
Nockolds S. R. and Allen R. (1953) The geochemistry of some igneous series. *Geochim. et Cosmochim. Acta* **4,** 105–142; (1954) The geochemistry of some igneous rock series, part II. *Geochim. et Cosmochim. Acta* **5,** 245–285.
Pettijohn F. J. (1949) *Sedimentary rocks* 526 pp. Harper & Brothers, New York.
Poldervaart A. (1955) Chemistry of the earth's crust. *Geol. Soc. Amer.* Special Paper **62,** 119–144.
Prior G. T. (1916) On the genetic relationship and classification of meteorites. *Miner. Mag.* **18,** 26–44.
Ramberg H. (1951) Remarks on the average chemical composition of granulite facies and amphibolite—to epidote amphibolite facies gneisses in West Greenland. *Dansk. Geologisk Forening. Middelelser.* **12,** 27–34.
Read H. H. (1955) Granite series in mobile belts. *Geol. Soc. Amer.* Special Paper **62,** 409–429.
Reynolds D. L. (1946) The sequence of geochemical changes leading to granitization. *Quart. J. Geol. Soc. Lond.* **102,** 389–446.
Rivière A. (1939) Sur la dolomitisation des sédiments calcaires. *C. R. Acad. Sci., Paris.* **209,** 597–599; (1940) L'eau de mer et les sédiments calcaires. *C. R. Soc. Géol. France.* **5,** 40–42.
Rubey W. W. (1951) Geologic history of sea-water. *Bull. Geol. Soc. Amer.* **62,** 1111–1148; (1955) Development of the hydrosphere and atmosphere, with special reference to probable composition of the early atmosphere. *Geol. Soc. Amer.* Special Paper **62,** 631–650; (in preparation) Compilation of published chemical analyses of sedimentary rocks of the United States. *U. S. Geol. Surv., Wash. D.C.*
Sander B. (1951) Contributions to the study of depositional fabrics. (Translated by Knopf E. B.) *Amer. Assoc. Petrol. Geol.* 160 pp.
Schwartz G. M. (1950) Problems in relation of ore deposits to hydrothermal alteration. *Colo. Sch. Min. Quart.* **45,** 197–208.
Sederholm J. J. (1925) The average composition of the earth's crust in Finland. *Bull. Comm. géol. Finl.* **12,** No. 70, 20 pp.
Shaw D. M. (1956) Geochemistry of pelitic rocks. Part III: Major elements and general geochemistry. **67,** 919–934.
Simpson E. S. W. (1954) On the graphical representation of differentiation trends in igneous rocks. *Geol. Mag.* **91,** 238–244,
Stringham B. (1953) Granitization and hydrothermal alteration at Bingham, Utah. *Bull. Geol. Soc. Amer.* **64,** 945–992.

SUJKOWSKI ZB. L. (1952) Average chemical composition of the sedimentary rocks. *Amer. J. Sci.* **250,** 360–374.

SVERDRUP H. U., JOHNSON M. W. and FLEMING R. H. (1946) *The Oceans* 1060 pp. Prentice Hall, New York.

TYRRELL G. W. (1933) Greenstone and greywackes. *Réunion Intern. pour l'Etude précamb.* 1931, *C.R.* 24–26.

UREY H. C. (1951) *The Planets. Their Origin and Development* 245 pp. Yale Univ. Press, New Haven, Conn.; (1955) The cosmic abundance of potassium, uranium, and thorium and the heat balances of the earth, the moon, and Mars. *Nat. Acad. Sci. Proc.* **41,** 127–144.

UREY H. C. (1956) The cosmic abundance of potassium, uranium and thorium and the heat balances of the earth, the moon and Mars. *Proc. Nat. Acad. Sci.* **42,** 889–891.

UREY H. C. and CRAIG H. (1953) The composition of the stone meteorites and the origin of the meteorites. *Geochim. et Cosmochim. Acta* **4,** 36–82.

VERHOOGEN J. (1954) Petrological evidence on temperature distribution in the mantle of the earth. *Trans. Amer. Geophys. Un.* **35,** 85–92.

VINOGRADOV A. P. (1956) Distribution regularity of chemical elements in the earth's crust. *Geokhim.* No. 1, pp. 6–52.

VINOGRADOV A. P. and RONOV A. B. (1956) Evolution of chemical composition of clays of the Russian Platform. *Geokhim.* No. 2, pp. 3–18.

VINOGRADOV A. P., RONOV A. B. and RATYNSKII V. M. (1952) Variation in the chemical composition of carbonate rocks of the Russian Platform. *Izv. Akad. Nauk. SSSR Geol. Ser.* No. 1, pp. 33–50. Cited from review prepared by G. CHILINGAR in *Geochim. et Cosmochim. Acta* **12,** 273–276.

VOGT J. H. L. (1931) On the average composition of the earth's crust, with particular reference to the contents of phosphoric and titanic acid. *Skr. Norske Vidensk. Akad. I, Mat.-naturv. Kl.,* **7,** 48 pp.

WAGER L. R. and DEER W. A. (1939) Geological investigations in East Greenland. Part 3. The petrology of the Skaergaard intrusion, Kangerdlugssaug, East Greenland. *Medd. Grönland,* Bd. **105,** Nr. 4, 335 pp.

WAHL W. (1952) The brecciated stony meteorites and meteorites containing foreign fragments. *Geochim. et Cosmochim. Acta* **2,** 91–117.

WICKMAN F. E. (1954) The "total" amount of sediments and the composition of the "average igneous rock". *Geochim. et Cosmochim. Acta* **5,** 97–110.

WIIK H. B. (1956) The chemical composition of some stony meteorites. *Geochim. et Cosmochim. Acta* **29,** 279–289.

YODER H. S., JR. (1955) Role of water in metamorphism. *Geol. Soc. Amer.* Special Paper **62,** 505–524.

Geochimica et Cosmochimica Acta, 1958, Vol. 13, pp. 123 to 126. Pergamon Press Ltd., London

Radioactivation analysis of "cosmic" and other magnetic spherules

A. A. Smales D. Mapper and A. J. Wood

(*Received* 11 *July* 1957)

Abstract—The published methods of the authors for the determination of cobalt, nickel, and copper by neutron activation analysis, have been used to determine trace quantities of these elements in "cosmic" and other magnetic spherules, in order to obtain quantitative evidence of their possible extra-terrestrial origin. Since the amount of spherules available for analysis ranged from ~10 to 250 μg only, special techniques, using a micro-manipulator for transferring the spherules to polythene strips for irradiation, had to be used, and these are described. The quantity of iron present was also determined by a spectrophotometric method.

The nickel content of the spherules ranged from <0·03 to 3·9 μg, the cobalt from <0·01 to 0·3 μg, and the copper from 0·0006 to 0·53 μg. From the nickel/copper, nickel/cobalt, copper/cobalt, and nickel/iron ratios it is shown that two of the samples—those obtained from deep-sea cores—are closely similar to iron meteorites. In the case of the other two samples, one from the roof of a collecting station off the coast of Sweden, and the other separated from sand obtained from the River Danube, there is no correspondence in the above ratios, and they appear to be quite different in chemical composition from the spherules from deep-sea cores.

1. Introduction

We have been able to apply the extremely sensitive methods of radioactivation analysis to determine the nickel, copper, and cobalt contents of firstly, some spherules found in the deep-sea sediment cores collected by the Swedish Deep Sea Expedition of 1947–1948, under the leadership of Professor H. Pettersson, and secondly, some spherules obtained from other sources. It was thought that such quantitative analytical information would yield valuable evidence on the origin of these spherules, whether extra-terrestrial or otherwise, a subject which has recently attracted much attention (Pettersson, 1955; Laevastu and Mellis, 1955; Bruun, Langer and Pauly, 1955; Öpik, 1955). Smales and Wiseman (1955), investigating Pettersson and Rotschi's (1952) suggestion on the possible cosmic origin of part of the nickel found in deep-sea deposits, showed that the ratios of nickel/cobalt, nickel/copper and copper/cobalt, determined on these deposits, were quite different from the corresponding ratios determined on meteoritic material, and therefore a cosmic origin of the bulk of the nickel was unlikely. The radioactivation methods which we have used for the nickel, copper and cobalt determinations in the rocks, marine sediments and meteorites have been published (Smales, Mapper and Wood, 1957) and they have now been applied to the determination of these elements in the spherules, with a similar end in view.

Radioactivation analysis was particularly suitable in the present case, since the total weight of sample available for the analyses was between 10 and 250 μg only.

Fredriksson and Pettersson, in the Oceanografiska Institutet, Göteberg, have magnetically extracted from deep-sea cores several hundred black spherules greater than 35 μ in diameter, per kg of dry sediment. Fredriksson (1956), from microscopic examination of these spherules, concluded that they were of cosmic origin, and it is these spherules, extracted from core 71, collected in the Pacific

Ocean (07° 38′ S, 152° 53′ W) at a depth of 4990 m, which we have analysed. In addition, some spherules extracted from a manganese crust also found in one of the deep-sea cores and some supposedly similar spherules collected from other sources, were also available. The latter samples consisted of, firstly, spherules separated from rainwater collected on the roof of a research station at Bornö in Gullmar Fjord, 60 km NNW of Göteberg, and secondly some spherules separated from a heavy fraction of sand from the River Danube, near Vienna.

2. Experimental

The spherules, which will be distinguished as core 71, Mn-crust, Bornö, and River Danube, presented some difficulties in handling for analysis, but an adequate technique for dealing with them was finally evolved. On arrival in our laboratory, the Canada balsam, in which the spherules were embedded in small glass beakers, was removed by gentle heating, and then, using a micro-manipulator, the spherules were transferred, under the microscope, to a thin sheet of polythene, to which they were fixed with a minute spot of "microscope" oil. The polythene was then cut so that the "oil spot" containing the spherules was in the centre of a narrow strip, and this was now fixed in a small polythene container, in such a way that the strip though suspended was not free to move within the tube. The "oil spot" was thus prevented from coming in contact with the sides of the tube. Similar strips of polythene containing the same amount of oil, but no spherules, were used as blanks. After irradiation in the Harwell Pile, BEPO, for one week, the polythene tubes were carefully cut open, the narrow strip removed, and the smallest possible piece, about 2 mm square of polythene, surrounding the "oil spot," cut from the strip. Examination of the "oil spot" under the microscope showed the spherules intact and undamaged by the irradiation, but after dissolution in nitric and hydrochloric acids no spherules could be seen on re-examining the piece of polythene. The blanks were treated in the same way, and then nickel, copper, and cobalt were determined by the methods described fully elsewhere (Smales, Mapper and Wood, 1957). In addition, the iron present was determined by measuring spectrophotometrically the colour complex formed with thioglycollic acid. However, blank difficulties made the iron determination less precise than the activation determinations for nickel, copper and cobalt, where the blank contributions from the polythene and oil, due to the technique described above, were extremely small.

3. Results

The results obtained are given in Table 1, the ratios Ni/Cu, Ni/Co, Cu/Co, and Ni/Fe are given in Table 2, and the corresponding ratios for meteoritic matter are given in Table 3.

The ratios for iron meteorites in Table 3 have been calculated from the analytical results for nickel given by Goldberg, Uchiyama and Brown (1951) and for copper and cobalt by Lovering, Nichiporuk, Chodos and Brown (1957), in their recent studies of iron meteorites. The ratios for meteoritic material in Table 3 have been calculated from the values, published by Rankama and Sahama (1950), for the average composition of meteoritic matter.

Table 1. Nickel, cobalt, copper and iron contents of spherules

Sample	Ni found (μg)	Co found (μg)	Cu found (μg)	Fe found (μg)
Magnetic spherules, deep-sea core 71, Pacific Ocean	0·83	0·05	0·0006	~10
Magnetic spherules from Mn-crust, deep-sea core, Pacific Ocean	3·9	0·31	0·0038	~30
Magnetic spherules, rainwater, Bornö	(a) <0·03 (b) <0·03	<0·003 <0·01	0·017 <0·005	~10 ~60
Magnetic spherules from heavy fraction of sand, River Danube, Vienna	0·29	0·08	0·53	240
Activation blank	<0·03	<0·003	<0·0002	

Table 2. Nickel/copper, nickel/cobalt, copper/cobalt and nickel/iron ratios experimentally found in the spherules

Sample	$\frac{Ni}{Cu}$	$\frac{Ni}{Co}$	$\frac{Cu}{Co}$	$\frac{Ni}{Fe}$
Magnetic spherules, deep-sea core 71, Pacific Ocean	~1400	17	0·012	~0·08
Magnetic spherules from Mn-crust, deep-sea core, Pacific Ocean	~1000	13	0·012	~0·13
Magnetic spherules, rainwater, Bornö	(a) $\gtrsim 2$ (b) —	— —	— —	~0·003 ~0·001
Magnetic spherules from heavy fraction of sand, River Danube, Vienna	0·55	3·6	6·6	0·001

Table. 3. Nickel/copper, nickel/cobalt, copper/cobalt and nickel/iron ratios in iron meteorites and average meteoritic material

	$\frac{Ni}{Cu}$	$\frac{Ni}{Co}$	$\frac{Cu}{Co}$	$\frac{Ni}{Fe}$
Iron meteorites	~210 to 1650	~7·3 to 43·4	~0·013 to 0·069	~0·06 to 0·17
Average meteoritic material	92	13·1	0·14	0·054

4. Conclusions

A comparison of the ratios given in Tables 2 and 3 shows that the spherules from core 71 and those from the Mn-crust are very similar indeed to iron meteorites. Although only a small quantity of the Bornö sample was available, these spherules show no similarity to meteoritic matter. A microscopic examination of the River Danube sample showed that 2 of the 19 spherules analysed, representing 70 per cent by volume of the total sample, were quite different in appearance from the other 17, being dull brown rather than shiny black, and here again the results on this sample indicate a composition quite different from the spherules of core 71 and the Mn-crust. When we consider the method of collection and place of origin of the Bornö and River Danube spherules, it is apparent that an artificial origin for these particles is not unlikely.

Fredriksson (1956) has pointed out the great caution required in interpreting data obtained on magnetic spherules collected on the continents, and he has informed us that spherules similar to those collected at Bornö were much more abundant in the industrialized centre of Göteberg. The results of our experiments indicate the considerable differences which exist among these spherules, and it seems likely that it is this confusion between spherules of artificial and cosmic origin which has led some investigators to give such high figures for the rate of accretion of extra-terrestrial material on the earth's surface.

Since completing our work, we have learned that Hecht and Patzak (1957) have also analysed similar spherules, using conventional methods on a micro-scale, for iron, nickel and cobalt. From the iron/nickel ratio and the fact that they were able to detect cobalt, these workers also conclude that the spherules from deep-sea sediments are similar to iron meteorites.

Acknowledgements—We are indebted to Professor H. Pettersson and Mr. K. Fredriksson for supplying the spherules and for the interest they have shown in our experiments. We are especially indebted to Mr. L. Peaple, of the Health Physics Division, A.E.R.E., Harwell, for his invaluable assistance in the manipulation of the spherules.

References

Bruun A. F., Langer E. and Pauly H. (1955) *Deep-Sea Res.* **2,** 230.
Fredriksson K. (1956) *Nature, Lond.* **177,** 32.
Goldberg E., Uchiyama A. and Brown H. (1951) *Geochim. et Cosmochim. Acta* **2,** 1.
Hecht F. and Patzak R. (1957) *Astronautica Acta* **III,** 47.
Laevastu T. and Mellis O. (1955) *Trans. Amer. Geophys. Un.* **36,** 385.
Lovering J. F., Nichiporuk W. Chodos, A. and Brown H. (1957) *Geochim. et Cosmochim. Acta* **11,** 276.
Öpik E. J. (1955) *Nature, Lond.* **176,** 926.
Pettersson H. (1955) *Naturwissenschaften* **42,** 387.
Pettersson H. and Rotschi H. (1952) *Geochim. et Cosmochim. Acta* **2,** 81.
Rankama K. and Sahama T. G. (1950) *Geochemistry* p. 39. University of Chicago Press.
Smales A. A., Mapper D. and Wood A. J. (1957) *Analyst* **82,** 75.
Smales A. A. and Wiseman J. D. H. (1955) *Nature, Lond.* **175,** 464.

Geochimica et Cosmochimica Acta, 1958, Vol. 13, pp. 127 to 142. Pergamon Press Ltd., London

Determination of the oxidation state of uranium in apatite and phosphorite deposits*

Roy S. Clarke, Jr. and Zalman S. Altschuler
U.S. Geological Survey, Washington 25, D.C.

(*Received* 23 *May* 1957)

Abstract—Geological and mineralogical evidence indicate that the uranium present in apatite may proxy for calcium in the mineral structure as U(IV). An experimental investigation was conducted and chemical evidence was obtained that establishes the presence of U(IV) in apatite.

The following analytical procedure was developed for the determination of U(IV). Carbonate–fluorapatite is dissolved in 1·5 M orthophosphoric acid at a temperature of 5°C or slightly below and fluorapatite is dissolved in cold 1·2 M hydrochloric acid (approximately 5°C) containing 1·5 g of hydroxylamine hydrochloride per 100 ml. Uranium(IV) is precipitated by cupferron using titanium as a carrier. The uranium in the precipitate is separated by use of the ethyl acetate extraction procedure and determined fluorimetrically. The validity and the limitations of the method have been established by spike experiments.

Introduction

The ubiquitous occurrence of uranium as a trace constituent of apatite and the fact that apatite is a prominent accessory mineral in almost all classes of rocks make the nature of this trace occurrence an important geochemical problem. Igneous apatite generally has from 10 to 100 p.p.m. of uranium and sedimentary apatite typically contains about 100 p.p.m. of uranium, although generally ranging from 50 to 300 p.p.m. (Altschuler *et al.*, in press). In many limestones and shales, apatite is the major uranium host, and phosphorites are now commercial sources of uranium.

Several mechanisms have been proposed to explain the role of uranium in phosphorites. Hendricks and Hill (1950) have suggested that the uranium occurs as chemically adsorbed ions or radicals at internal discontinuities in the apatite structure. Moore (1954) has shown that natural apatite can remove appreciable uranyl ion from solution in the laboratory. Neuman *et al.* (1949) have demonstrated that uranyl ions removed from solution by treated bone are fixed on the surface of such bone by displacement of two calcium ions per uranyl radical, and that two phosphate radicals are rendered non-exchangeable for each uranyl radical emplaced. They have proposed the formation of uranyl pyrophosphate to account for these experimental results. Recently, Bowie and Atkin (1956) have adopted Neuman's suggestion to explain the surface concentration of uranium in fossil and nodular apatite.

In studies of the petrology of uraniferous phosphorite, Altschuler *et al.* (1956) have found that uranium and calcium oxide contents parallel one another in their distribution through sections of leached and altered phophorite. They also noted that uranium occurs preferentially in the calcium phosphate, apatite, to a lesser extent in the calcium–aluminium phosphate, crandallite, and that it is least prominent in the pure aluminium phosphate wavellite. To explain the above facts,

* Publication authorized by the Director, U.S. Geological Survey.

they suggested that uranium proxies for calcium in the apatite structure. The substitution of uranium for calcium is crystallographically plausible only in terms of the uranous ion (I.R. = 0·97 Å), which is virtually identical to the calcium ion (I.R. = 0·99 Å) (Green, 1953) in size. Based on this theoretical plausibility, other writers have also proposed the substitution of uranous uranium for calcium (Goldschmidt, 1954; McKelvey and Nelson, 1950).

With the development of petrologic evidence favouring the structural substitution of tetravalent uranium in apatite, it became important to determine the oxidation state of the uranium present in phosphorites. None of the available chemical methods was directly applicable for such determination with any assurance that the inherent valence state of traces of uranium would be unaltered during the course of analysing the impure natural materials. As a result, an experimental investigation was undertaken to develop a chemical method that would indicate if U(IV) is present in natural apatite and in what quantity it occurs. The present study describes this investigation and the resulting method of analysis.

There are two general classes of apatite that have been considered in this work. The first is carbonate–fluorapatite (Altschuler *et al.*, 1952), which may be represented by the formula $Ca_{10}(PO_4,CO_3)_6F_{2-3}$. Apatite from the sedimentary phosphorites, such as those from Florida, the north-western United States, and Morocco, are examples of this type. The second class of apatite is fluorapatite, which has the general formula $Ca_{10}(PO_4)_6F_2$. This is normally an accessory mineral in igneous rock. Carbonate–fluorapatite generally contains from 0·01 to 0·02 per cent uranium and is readily soluble in cold 1·5 M phosphoric acid. Fluorapatites generally contain slightly less uranium and are difficultly soluble in 1·5 M phosphoric acid.

In Table 1, a general description of the various materials used in this work is given.

The solution of apatite for analysis is a critical step in the determination of U(IV). Naturally occurring apatite contains small quantities of elements that may interfere by either oxidizing or reducing the uranium initially present in the solid material. Specimens of both fluorapatite and carbonate–fluorapatite can be hand-picked to a fair degree of mineralogical purity. However, even with the greatest possible care, minor elements may be present in rather large concentrations relative to the uranium. The nature of these minor constituents is evident from the semi-quantitative spectrographic analyses (Waring and Annell, 1953) of selected representative materials (Table 2). The chemical value for uranium is inserted in the table in its proper position to show its abundance relative to the other elements present.

The spectrographic analyses, of course, indicate nothing of the oxidation state of the elements that are present. However, it does show for the carbonate–fluorapatite sample (B.L.-3, Florida) that elements capable of acting as oxidizing or reducing agents towards uranium are present in quantities comparable to or greater than uranium. Manganese and chromium are present in the same general concentration as uranium. Iron, which as Fe(III) is used in analytical work to oxidize U(IV), is also present in much larger amounts than the uranium. In the

Table 1. Materials used in this investigation

Sample	Description	Locality and reference
AP-2	Synthetic fluorapatite, clear macrocrystalline	
AP-3	Synthetic fluorapatite, clear macrocrystalline	
B.L.-3	Carbonate–fluorapatite, nodules cryptocrystalline	Bonny Lake mine, Ridgewood, Florida
Va.-7	Carbonate–fluorapatite, nodules cryptocrystalline	Varn mine, Ft. Meade, Florida
Wa.-10	Carbonate–fluorapatite, nodules cryptocrystalline	Watson mine, Ft. Meade, Florida
P.V.-5	Carbonate–fluorapatite, nodules cryptocrystalline	Peace Valley mine, Homeland, Florida
Ho.-20	Carbonate–fluorapatite, pebbles, cryptocrystalline	Homeland mine Homeland, Florida
Mor.-11	Carbonate–fluorapatite, nodules, cryptocrystalline	Khouribga, French Morocco, daily production sample
Durango	Fluorapatite, clear, macrocrystalline	Cerro Mercado, Durango Mexico (Foshag, 1929)
G-25	Fluorapatite, clear, macrocrystalline	Mountain Pass, California (Olson *et al.*, 1954)
F.K.-3	Fluorapatite, clear, macrocrystalline, contain Th and R.E.	Smith mine, Mineville New York (McKeown and Klemic, 1956)
G.P.-19	Fluorapatite, clear, macrocrystalline	Boulder Creek batholith, Magnolia, Colorado
W-3841	Carbonate-fluor-hydroxyl-apatite, fossil bone	Montana, locality unknown

fluorapatite (Durango, Mexico) and the fluorapatite (G-25, Mountain Pass, California) samples the situation becomes more complex. It is clear that precautions must be taken if U(IV) analyses are to be performed on material of this complexity.

Fortunately, in most apatite the total amounts of uranium and of the elements

Table 2. Semi-quantitative spectrographic analyses of minor constituents in apatite samples

Range per cent	Carbonate–fluorapatite B.L.3* Florida	Fluorapatite		Synthetic apatites	
		Durango,† Mexico	G-25,* Mountain Pass, Calif.	AP-2*	AP-3*
1–5	Al		Ce Sr La		
0·5–1		Ce La Na Y Si	Nd Na Si		
0·1–0·5	Mg Fe Na		Mg Al Y Fe Pr	Mg	Mg
0·05–0·1	Sr Ti	Mg Sr Al Fe Nd Mn	Ba Pb	Al	Al
0·01–0·05	Pb Mn Cr [U]		Gd Zr Ti Mn	Si Rb	Si Sr
0·005–0·01	Ba	V Ni Ba Ti Se Yb [U]	Dy B Er Yb [U]	Fe Sr	Fe Na
0·001–0·005	Cu V Y		Eu Cu Se V	Cr	Ba
0·0005–0·001	Zr	Cr Cu	Cr	Ba	Cr Ti Cu
0·0001–0·0005	Yb			Ti Cu	Ag

* Analyst, Katherine V. Hazel, U.S. Geological Survey.
† Analyst, Helen W. Worthing, U.S. Geological Survey.

that may act to change its oxidation state on solution are small. This results in a concentration factor that could be expected to lead to relatively slow attainment of equilibrium. It could also be expected that equilibrium would be more slowly attained if the temperature of the system were held as low as possible. If an appreciable delay in reaching equilibrium could be attained in practice, the U(IV) separated from solution would be inherent to the solid apatite and not merely a result of oxidation–reduction reactions in solution. To demonstrate the conditions under which interferences of this type could be considered negligible, synthetic apatite, relatively free of interfering elements, was prepared (Table 2, AP-2 and AP-3) for use in test experiments.

The organic precipitant cupferron can be used in acid solutions to separate quantitatively insoluble U(IV) cupferrate from the soluble U(VI) cupferrate. When only very small quantities of uranium are present, a carrier such as Ti may be required to give the precipitate sufficient bulk to be handled conveniently. Using this carrier technique, it was possible to recover U(IV) additions quantitatively from a phosphoric acid solution of synthetic apatite. This leads to a straightforward procedure for the determination of U(IV) in apatite readily soluble in phosphoric acid if elements normally present in apatite can be prevented from interfering. Toohey and Kaufman (1954) have shown that this type of interference can lead to completely erroneous conclusions.

The first experimental problem was to determine conditions under which

Table 3. Recoverability of U(IV) in presence of dissolved apatite. (50 ml quantities of 1·5 M H_3PO_4 containing 100 mg of sample were used.)

Sample	U(IV) present (μg)	U(IV) added (μg)	U(IV) determined (μg)	Per cent recovery
Synthetic apatite, AP-3	—	50	50	100
Carbonate–fluorapatite, B.L.-3*	13	50	61	97

* Total U equals 16 μg

materials could be dissolved and the U(IV) precipitated without appreciable oxidation or reduction of the uranium. The second problem was to establish, in a general way, the accuracy of the results obtained. This was carried out by means of a series of spike experiments. In these experiments known additions, or spikes, were added to solutions of pure synthetic materials and to solutions of natural materials. It was found from these experiments that the results obtained from natural materials were similar to those obtained from synthetic mixtures, when temperature was kept low and elapsed time was at a minimum. This indicates that the method developed is a valid determination of U(IV) when properly applied to selected materials.

General Procedure

Carbonate–fluorapatite is readily soluble in cold 1·5 M orthophosphoric acid (~5°C). Baes (1953) has shown that at this concentration of phosphoric acid the tendency of Fe(II) to reduce U(VI) is at a minimum. Experiments that are discussed in detail below (Table 4) show that the oxidation of U(IV) by Fe(III) at this acid concentration may also be held at a minimum by properly controlling

Table 4. The effect of Fe(III) concentration and temperature on the recoverability of U(IV) in the presence of dissolved apatite. (50 ml quantities of 1·5M H_3PO_4 containing 100 mg of synthetic apatite, AP-3, were used.)

U(IV) added (μg)	Fe(III) added (μg)	Time of standing before precipitation (hr)	U recovered (μg)	
			~25°C	~5°C
48	100	1	41	50
48	100	2	37	50
48	100	17	8	47
48	100	4		48
48	100	4		48
48	200	4		44
48	500	4		42
48	1000	4		34

temperature and elapsed time. As Fe(III) is the most common interfering ion and the one generally present in the largest quantity, a solution of this concentration is a favourable medium for the solution of apatite without change of oxidation state of the uranium present.

Schreyer (1954) has shown that U(IV) orthophosphate is sufficiently soluble so that no phosphate precipitate of the small quantities of U(IV) found in carbonate–fluorapatite forms during the dissolution of the sample. Schreyer also points out that U(IV) in phosphoric acid solution is more stable to air oxidation than in hydrochloric or sulphuric acid solutions.

Phosphoric acid dissolves the well-crystallized fluorapatite from crystalline rocks so slowly that oxidation of U(IV) took place when using this solvent. For this reason, samples of igneous or similar apatite were dissolved in cold 1·2 M hydrochloric acid (~5°C) containing 1·5 g of hydroxylamine hydrochloride ($NH_2OH{\cdot}HCl$) per 100 ml. Experimental data indicate that hydroxylamine hydrochloride functions to suppress the oxidation of U(IV) without reducing U(VI).

An outline of the procedure that was used to test the method for the determination of U(IV) follows. The sample is dissolved in cold 1·5 M phosphoric acid (~5°C) if it is readily soluble or, if not, in 1·2 M hydrochloric acid containing 1·5 g of hydroxylamine hydrochloride per 100 ml. The cold solution is filtered to remove any insoluble residue. A titanium solution is added and the cupferrates precipitated by the addition of 6 per cent aqueous cupferron. The precipitate is filtered, washed, and ignited. The ignited residue is dissolved with $HF–HNO_3$ mixture, taken to dryness with HNO_3, and finally made to volume in 7 per cent HNO_3. Uranium is determined by the ethyl acetate extraction-fluorimetric procedure (Grimaldi *et al.*, 1952).

When U(IV) spikes were used they were added either as the samples were being dissolved or after they had been dissolved. Spike solutions were prepared so that only a small volume, generally 1 ml or less, would have to be added to 50 or 100 ml of sample solution. The concentration of the U(IV) spike solutions was checked with each group of experiments performed. The same precipitation technique that was used on samples was used on an aliquot of U(IV) spike solution in a corresponding volume of 1·5 M H_3PO_4 or 1·2 M HCl to give the actua concentration of the U(IV) solution at the time of use.

Preparation of Synthetic Fluorapatite

The synthetic fluorapatites, AP-2 and AP-3, were prepared by thoroughly mixing stoicheiometric quantities of $Ca_3(PO_4)_2$ (18·6 g) and CaF_2 (1·56 g). The mixture was placed in a platinum dish and covered with a platinum sheet. The dish was placed in a cold furnace and rapidly taken to 1250°C, at which temperature it was held for 2 hr. The temperature was slowly reduced to 950°C over a period of 6 hr before the furnace was turned off. The material was left in the furnace until it reached room temperature.

The indices of refraction of the resulting apatite were $\varepsilon = 1{\cdot}630$ and $\omega = 1{\cdot}632$. The structure was checked by X-ray diffraction, and the pattern was that of fluorapatite without recognizable impurities present. The semi-quantitative spectrographic analyses of these materials are given in Table 2.

Experiments

To test the method for the determination of U(IV) in natural apatite one must know precisely how much U(IV) is present in such apatite or rely on synthetic

mixtures of known composition. As apatite of known U(IV) content was not available the experimental procedure was applied to spiked samples of dissolved synthetic and natural apatite.*

The fact that U(IV) spikes added to synthetic and natural apatite could be recovered quantitatively is established by the following experiment. Spikes were added to cold (~5°C) solutions of synthetic fluorapatite (AP-3) and carbonate–fluorapatite (B.L.-3, Florida) and after standing an hour in the cold, U(IV) was determined. The results of this experiment together with the U(IV) value obtained when sample B.L.-3 is analysed without a U(IV) spike are given in Table 3. Sample B.L.-3 contains 0·016 per cent U, or 16 μg per 100 mg of material. Experience at other levels of U(IV) concentration also support the conclusion that complete recovery is obtained.

As the most common impurities associated with apatite are Fe(III) oxides and hydrous oxides in the form of hematite, limonite, and goethite, it is important to establish the range of tolerance of Fe(III). Its oxidizing effect on U(IV) in the presence of dissolved apatite at approximately 25°C and 5°C over different periods of time was investigated. The results of this experiment are given in Table 4.

Most iron incrustations also contain some Fe(II). The total Fe content and Fe (II) content of several samples of Florida apatite are givenin Table 5. Total Fe

Table 5. Per cent total Fe and Fe(II) in some Florida apatite samples

Sample	Total Fe (per cent)	Fe(II) (per cent)
B.L.-3	0·26	0·14
Va.-7	0·33	0·06
Wa.-10	0·60	0·04
P .V.-5	1·0	0·06

was determined by the *o*-phenanthroline method (Sandell, 1950). An estimation of the Fe(II) content was made by the same general procedure. The sample was dissolved in acid without heating and the *o*-phenanthroline-ferrous complex was developed without the addition of a reducing agent.

In an experiment similar to that reported in Table 4 the reducing effect of Fe(II) on U(VI) spikes was studied. This experiment, the results of which are given in Table 6, was conducted at room temperature.

The small quantity of uranium recovered (Table 6) in the experiment with Fe(II) and U(VI) is undoubtedly only partly due to reduction. The last few per cent of the uranium present are often not separated due probably to incomplete washing and other mechanical problems. Had this experiment been carried out at 5°C, any reduction effect would undoubtedly have been less.

Having established the independent effect of both Fe(II) on U(VI)- and

* To keep the effect of oxidation reactions at a minimum, experiments were performed on solutions that were maintained at a low temperature (~5°C). The time elapsed during solution of sample and precipitation of the cupferrates was also kept at a minimum, generally less than 1 hr.

Fe(III) on U(IV)-spiked synthetic apatite, the effect of addition of both of these forms of iron to a U(IV)-spiked natural carbonate–fluorapatite (B.L.-3, Florida) was examined (Table 7). Sample B.L.-3 contains significant and approximately equal amounts of Fe(II) and Fe(III) (Table 5). In this experiment cold (~5°C) sample solutions that stood for approximately 1 hr before precipitation were used.

Table 6. The effect of Fe(II) concentration on U(VI) in the presence of dissolved apatite. (50 ml quantities of 1.5 M H_3PO_4 containing 100 mg of the synthetic apatite, AP-3 were used.)

U(VI) added (μg)	Time of standing before precipitation (hr)	Fe(II) added (μg)	U in precipitate (μg)
30	1	—	1·1
30	4	100	2·5
60	4	500	5·0

Table 7. The effect of Fe(II) and Fe(III) additions on U(IV) in the presence of dissolved natural apatite. (50 ml quantities of 1·5 M H_3PO_4 containing 100 mg of the natural apatite, B.L.-3, Florida, were used.)

U(IV) added (μg)	Fe(III) added (μg)	Fe(II) added (μg)	U(IV) determined (μg)	Per cent recovery of U(IV)
Unspiked B.L.-3	—	—	13, 13, 15	—
42	—	—	56, 55	100
48	100	—	60	97
48	—	100	56	91

The conclusions that can be drawn from the experiments reported in Tables 4 to 7 should be emphasized. These experiments show that interference of ferric iron can be the cause of serious error unless the conditions of the experiment are carefully controlled. In Table 4, 100 μg of Fe(III) is equivalent to 0·1 per cent Fe in a 100 mg sample of apatite. At this level of Fe(III) concentration, very little oxidation has resulted after even 4 hr. If samples are dissolved in cold acid and the precipitation carried out after a reasonably short period of time (1 hr or less), it would be expected that several tenths of a per cent Fe(III) could be tolerated without seriously influencing the results.

The results for the carbonate–fluorapatite sample (B.L.-3, Florida) are in agreement with the results for the synthetic material. The recovery figure on the addition of 100 μg of Fe(II) is low (Table 7), but the expected effect would be to increase the U(IV) figure. Sample B.L.-3 contains 16 to 17 μg of total uranium per 100 mg, therefore, presumably 3 to 4 μg of U(VI) that could be reduced.

The problem of solution of materials that are not readily soluble in cold (~5°C) 1·5 M H_3PO_4 was overcome by using cold (~5°C) 1·2 M HCl. Treatment with this

acid readily dissolves all apatite in a short time. Table 8 shows the per cent U(IV) obtained when five natural apatite samples are dissolved in cold 1·2 M HCl. This table also includes data on percentages obtained when these materials are dissolved in 1·2 M HCl containing 1·5 per cent hydroxylamine hydrochloride. The use of $NH_2OH{\cdot}HCl$ gave either comparable or higher results than those obtained with HCl alone. The presence of the hydroxylamine hydrochloride seems to add stability to the U(IV) in solution and reproducibility to the analytical results on most apatite samples. An obvious exception to this is the result on the complex fluorapatite F.K.-3 (New York). This type of behaviour is discussed below.

A series of experiments was performed to establish the recovery and reproducibility of the recovery of U(IV) spikes added to solutions of apatite in 1·2 M hydrochloric acid containing 1·5 per cent hydroxylamine hydrochloride. Two different levels of U(IV) were first precipitated from acid solution containing hydroxylamine hydrochloride without apatite being present. In these blank determinations essentially complete recovery was obtained. Synthetic apatite AP-2, which contains no uranium, and three natural carbonate–fluorapatite samples were analysed for U(IV). These materials were re-analysed for U(IV) after known additions of U(IV) were made to the sample solution. In the presence of apatite less than complete recovery of U(IV) spikes was obtained. The results of this experiment are given in Table 9. In summary, the average per cent recovery for these 12 analyses on 4 different samples is 79, with a range of values from 67 to 87. Despite the fact that the spikes varied from 20 to 500 μg of uranium, the standard deviation from the average per cent recovery is only 5·4.

Katz and Rabinowitch (1951) point out that there is evidence for U(IV)-fluoride ion complex formation, and Ahrland and Larsson (1954) have made a detailed study of U(IV) complexes with chloride, bromide, and thiocyanate ions. It is possible that the formation of a U(IV)-fluoride ion complex causes the consistent 20 per cent low recovery in the above experiments (Table 9). The apatite used contained from 3 to 4 per cent fluorine, the carbonate–fluorapatite being at the high end and the fluorapatite being at the low end of this range.

An indication of possible complexing action was obtained by an experiment using the carbonate–fluorapatite sample B.L.-3 (Florida). The U(IV) was precipitated and filtered in the normal way and the filtrate from this operation was checked for additional U(IV). A value of 0·010 per cent U(IV) was obtained from the first precipitation (a low value for this sample). An additional 0·0028 per cent U(IV), which was obtained from the second precipitation, accounts for 47 per cent of the uranium remaining in solution.

That a 20 per cent deficiency in recovery could be attributed to a U(IV)-fluoride complex was established by comparing the recoveries of known spikes of U(IV) from solutions of tricalcium phosphate and calcium fluoride. The concentrations of calcium phosphate and calcium fluoride used were equivalent to those obtained upon dissolving apatite as in the normal experimental procedure. In calcium phosphate alone the spike was completely recovered, whereas with calcium fluoride alone only 80 per cent of the spike was recovered. These experiments would seem to establish that a U(IV)-fluoride ion complex is operating to cause the low recoveries.

Table 8. U(IV) values for natural apatite dissolved in 1·2 M HCl and in 1·2 M HCl containing 1·5 per cent $NH_2OH{\cdot}HCl$

Sample	Per cent U(IV)	
	HCl as solvent	HCl containing $NH_2OH{\cdot}HCl$ as solvent
B.L.-3 Florida	0·012	0·012
Durango, Mexico	0·0002	0·0002
G.P.-19, Colorado	0·0008	0·0009
F.K.-3, New York	0·0015	0·020
G-25, California	0·0014	0·0019

Table 9. Recovery of U(IV) spikes from solutions of apatite in 1·2 M HCl containing 1·5 per cent $NH_2OH{\cdot}HCl$

Sample 0·100 g	U(IV) in spike (μg)	U(IV) determined (μg)	Total U(IV) recovered (per cent)
Blank	20	20	100
Blank	100	97	97
AP-2 (synthetic, no U)	0	0	—
AP-2 (synthetic, no U)	20	15	75
AP-2 (synthetic, no U)	40	35	87
AP-2 (synthetic, no U)	100	84	84
AP-2 (synthetic, no U)	500	400	80
B.L.-3, Florida	0	12	—
B.L.-3, Florida	20	25	78
B.L.-3, Florida	40	41	79
B.L.-3, Florida	100	88	79
B.L.-3, Florida	500	370	72
Va.-7, Florida	0	4·0	—
Va.-7, Florida	20	20	83
Va.-7, Florida	40	36	82
Wa.-10, Florida	0	1·6	—
Wa.-10, Florida	20	17	77
Wa.-10, Florida	40	28	67

Experiments to study the effect on U(IV) values of changing the hydroxylamine hydrochloride concentrations in 1·2 M hydrochloric acid were performed. The data from these experiments are given in Table 10. Several different materials were used and 100 mg portions were allowed to stand in the cold acid solutions with occasional stirring for 1 hr. To the solutions containing the synthetic fluorapatite, AP-3, 1·0 ml of a spike solution that contained approximately 20 μg of

Table 10. U(IV) values obtained on solution of samples in 1·2 M HCl containing various concentrations of $NH_2OH{\cdot}HCl$

Per cent $NH_2OH{\cdot}HCl$ in 1·2 M HCl	Per cent U(IV)			
	AP-3* spiked to contain ~0·02 per cent U(IV)	B.L.-3, Florida (total U 0·016 per cent)	Durango, Mexico (total U 0·00087 per cent)	F.K.-3, New York (total U 0·074 per cent)
0	0·015	0·012	0·0002	0·0015
0·15	0·019	0·012	0·00025	0·0010
0·75	0·019	0·012	0·00030	0·015
1·5	0·020	0·013	0·0002	0·020
3·0	0·018	0·012	0·00032	0·022
15	0·019	0·013	0·00034	0·030

* Uranium-free.

U(IV) per ml was added. Sample B.L.-3 (Florida), a carbonate–fluorapatite, was used because a fluorapatite of simple chemical composition at this relatively high level of U(IV) content was not available. The Durango (Mexico) fluorapatite is of relatively simple composition whereas the fluorapatite F.K.-3 (New York) is of more complex composition. The compositions of AP-3, B.L.-3, and Durango are given in Table 2 and that of F.K.-3 is given by McKeown and Klemic (1956).

The U(IV) values obtained for the spiked synthetic AP-3 and sample B.L.-3 (Florida) are essentially constant over the range of hydroxylamine hydrochloride concentrations studied. This constancy demonstrates that the 1·5 per cent hydroxylamine hydrochloride concentration, selected for use as a solvent for fluorapatite, is well within a range of concentrations that can be varied without causing variation in U(IV) values for a number of materials. The results on the Durango (Mexico) material probably fall, in a general way, into the pattern of AP-3 and B.L.-3. However, the data on Durango are not conclusive because of the low level of U in this material.

The U(IV) values obtained for the complex material F.K.-3 (New York) increase markedly with increasing hydroxylamine hydrochloride concentration. This kind of response is a general indication of unsuitability of a particular apatite specimen or group to this type of U(IV) analysis.

The lack of constancy of U(IV) values in sample F.K.-3 (New York) is not surprising when its chemical composition is considered. The material contains over 10 per cent rare earths (more than 1 per cent Ce) and several elements such as Fe, Mn, and As in the 0·0X to 0·X per cent range which could act to change the oxidation state of uranium. This material also contains Co in the 0·0X per cent range and Cu in the 0·00X per cent range. Pannell (1950) has shown that both Co and Cu, along with Mo and silicate, catalyse the air oxidation of uranium.

A possible explanation of the behaviour observed with sample F.K.-3 (New York) is that hydroxylamine hydrochloride in the presence of an unknown catalytic agent reduces some U(VI) to U(IV), resulting in an increase in apparent U(IV)

with increased hydroxylamine hydrochloride concentration. That this type of behaviour does not usually occur is shown by the results with AP-3 and B.L.-3 (Florida). It should be noted that for sample B.L.-3 an essentially constant U(IV) value was obtained with all the various solvents used in this work (1·2 M HCl, 1·2 M HCl containing various concentrations of $NH_2OH{\cdot}HCl$, Table 10, and 1·5 M H_3PO_4, Table 7). It should also be noted that there is appreciable uranium, 25 per cent of the total, in sample B.L.-3 that is not accounted for as U(IV). This uranium is presumably present as U(VI).

An experiment was conducted to see if Fe(II) spikes could reduce U(VI) when the samples are dissolved in 100 ml of hydrochloric acid–hydroxylamine hydrochloride solution. The synthetic apatite, which is essentially iron free, and a natural apatite, B.L.-3 (Florida), containing 0·26 per cent total Fe and 0·14 per cent Fe(II) were used. The iron and U(VI) spikes were added with stirring to the cold (~5°C) sample solution. The cupferron precipitation was made after approximately 1 hr. The results are given in Table 11. This experiment demonstrates that relatively large quantities of Fe(II), as compared to uranium, can be tolerated under these conditions.

Table 11. The effect of Fe(II) additions on U(IV) values for samples dissolved in 100 ml of 1·2 M HCl containing 1·5 per cent $NH_2OH{\cdot}HCl$

100 mg sample	Treatment	Per cent U(IV)
AP-2	15 μg U(VI) + 0·12 mg Fe(II)	0·00030*
AP-2	15 μg U(VI) + 0·12 mg Fe(II) + 0·06 mg Fe(III)	0·00035*
B.L.-3, Florida	0·31 mg Fe(II)	0·013†
B.L.-3, Florida	3·1 mg Fe(II)	0·014†

* Less than 2·5 per cent of total uranium present.
† Unspiked values run from 0·011 to 0·013 per cent U(IV).

Table 12. Comparison of U(IV) values of natural materials using two different methods of sample solution

Sample	Dissolved in HCl—$NH_2OH{\cdot}HCl$		Dissolved in H_3PO_4	
	Per cent U(IV)	Per cent of total U in reduced state	Per cent U(IV)	Per cent of total U in reduced state
B.L.-3 Florida	0·012	71	0·013	82
Va.-7 Florida	0·0040	45	0·0055	57
Wa.-10 Florida	0·0016	21	0·0028	37
P.V.-5 Florida	0·0024	34	0·0029	39
Ho.-20 Florida	0·011	48	0·015	65
Mor.-11 Morocco	0·0009	9	0·0005	5
W-3841 Montana	0·40	48	0·50	60

A comparison of results obtained on natural materials that are soluble in both the phosphoric acid and the hydrochloric acid–hydroxylamine hydrochloride solutions is given in Table 12. With the exception of sample Mor.-11 (carbonate–fluorapatite, Morocco), the results of phosphoric acid solution of the sample are higher than those of hydrochloric acid–hydroxylamine hydrochloride. This fits in with the data on fluoride-complex formation in the hydrochloric acid–hydroxylamine hydrochloride medium. On the average these determinations are lower by 12 per cent than those using phosphoric acid. This is not far out of line with the 80 per cent recovery figure on U(IV) spike experiments. Perhaps the values obtained using phosphoric acid are also a little low.

The carbonate–fluorapatite sample Mor.-11 (Morocco) is an oxidized material containing an appreciable amount of goethite and therefore would be expected to contain little U(IV). When 50 μg of U(IV) spike was added to a phosphoric acid solution of Mor.-11 and the U(IV) precipitated, only 46 μg of uranium was recovered rather than the 51 μg that would be expected—a 90 per cent recovery.

Reagents

All chemicals used were reagent grade.

1·5 M orthophosphoric acid.

1·2 M hydrochloric acid containing 1·5 g of hydroxylamine hydrochloride ($NH_2OH{\cdot}HCl$) per 100 ml.

6 per cent aqueous cupferron.

Wash solution: Add 25 ml of 6 per cent cupferron solution and 60 ml of hydrochloric acid to water and dilute to 1 l.

Titanium solution: 0·437 g of titanium dioxide, TiO_2, was fused with 5 g of potassium pyrosulphate. The product of the fusion was dissolved in 200 ml of water containing 25 ml of concentrated sulphuric acid. This solution was diluted to 250 ml, yielding a solution containing 1·0 mg of Ti per ml.

Uranium (IV) spike solution: A solution of 200 μg of uranium per ml in 5 per cent H_2SO_4 prepared from 99·9 per cent U_3O_8 was reduced on a Jones reductor and was stored in a refrigerator when not in use. Solutions of various strengths were prepared from it by dilution with cold (~5°C) 5 per cent H_2SO_4. Fresh solutions were prepared every few days because of appreciable oxidation.

Detailed Analytical Procedure

The choice of solvent depends on the nature of the sample. Cold (~5°C) phosphoric acid should be used for carbonate–fluorapatite and any other material that will dissolve in this medium. The use of hydrochloric acid–hydroxylamine hydrochloride solution is required for apatite of igneous origin or other highly crystalline fluorapatite.

Solution of sample in phosphoric acid

The sample is ground to a fine powder, 0·100 g is weighed, put into a 100 ml beaker, and 50 ml of 1·5 M phosphoric acid that has been chilled to at least 5°C is added. The acid is stirred to suspend the sample, the beaker is covered and placed in a cold-water bath regulated at 4–5°C for 1 hr. The suspension is stirred several times during this period. More frequent stirring is required for less readily soluble samples.

Solution of sample in hydrochloric acid–hydroxylamine hydrochloride solution

The sample is ground to a fine powder, 0·100 g is weighed, put into a 250 ml beaker, and 100 ml of a solution of 1·2 M hydrochloric acid containing 1·5 per cent hydroxylamine hydrochloride that has been chilled to 5°C, or below, is added. The solvent is stirred to suspend the sample, the beaker is covered and placed in the cold-water bath regulated at 4–5°C. The sample is stirred at frequent intervals until it is in solution. This can take from 20 min to 1 hr.

Cupferron precipitation

The cold sample solution (either method of preparation) is filtered with suction through a 2·1 cm glass fibre filter paper in a Gooch crucible. The beaker and crucible are washed twice with small quantities of water. The filtrate is received in a 150 ml beaker sitting in ice water.

Immediately 3·0 ml of a cold solution of 1·0 mg of Ti per ml in 10 per cent sulphuric acid is added. This is followed by the addition, with stirring, of 3·0 ml of a cold aqueous 6 per cent cupferron solution. The beaker containing the cupferrate is placed in the freezing compartment of a refrigerator for 10–15 min before filtration with suction through a 9 cm close-textured filter paper. The precipitate is washed a total of eight times with a cool solution of 6 per cent hydrochloric acid and 0·15 per cent cupferron. The paper containing the precipitate is placed in a 25 ml platinum crucible and charred under an infra-red lamp and then ignited over a burner.

Determination of uranium

The ignited residue must be put into a 7 per cent by volume nitric acid solution for extraction of the uranium. This may be done by two methods, either (a) potassium pyrosulphate fusion or (b) HF–nitric acid treatment.

(a) Add 0·5 g of potassium pyrosulphate to the residue and heat over an open flame at as low a temperature as possible until solution is complete.

(b) Add 5 ml of (1 + 1) nitric acid and 5 ml of HF to the residue. Evaporate to dryness on the steam-bath. Add 1 ml of (1 + 1) nitric acid and again take to dryness.

Take up the residue from either method of treatment with enough 1 + 1 nitric acid to yield on dilution a convenient volume of 7 per cent by volume nitric acid. Warm on the steam-bath to dissolve the material and transfer the solution and any insoluble material to a volumetric flask and dilute to volume. A 5·0 ml aliquot of this solution is added to a glass-stoppered test tube containing 9·5 g aluminium nitrate of low uranium content. Uranium is then determined by a standard ethyl acetate extraction-fluorimetric procedure (Grimaldi *et al.*, 1952).

It may be convenient when working with small amounts of material or with materials that are quite low in uranium to take up the whole sample in a volume of 5 ml of 7 per cent by volume nitric acid. If this is to be done, 9·5 g aluminium nitrate of low uranium content is added directly to the crucible containing the residue from either treatment (a) or (b) given above. Five millilitres of 7 per cent by volume nitric acid is added and the crucible and contents heated on the steam-bath until the salt dissolves and as much as possible of the residue is in solution. The contents of the crucible are then transferred (without washing) to a glass-stoppered test tube for extraction.

Summary

The data obtained by spike experiments demonstrate that the method outlined in this paper can be used to estimate the U(IV) content of selected apatite samples. The purity of the sample material determines the applicability of the method. Spectrographic analyses or other suitable tests are suggested to check on unusual content of elements that may act either to oxidize or to reduce uranium.

Materials of the carbonate–fluorapatite type can be put into solution with the phosphoric acid treatment. Analyses based on this method of solution are on a more secure footing than those based on solution of sample in hydrochloric acid–hydroxylamine hydrochloride. For this reason, phosphoric acid solution is used whenever the sample is readily soluble in it. Hydrochloric acid–hydroxylamine hydrochloride solution is used only on the less soluble materials.

U(IV) results should be evaluated in terms of all the information available on a particular material. Knowledge of the general chemical composition of the material, particularly with reference to iron and other elements that may act as oxidizing or reducing agents, is helpful.

The reliability of particular analysis may be checked by use of a U(IV) spike.

The spike should be recovered nearly completely if phosphoric acid is used to dissolve the sample. If the more drastic hydrochloric acid–hydroxylamine hydrochloride treatment is required, the spike should be recovered at about the 80 per cent level. It should also be noted that values obtained when using this latter solvent are probably some 20 per cent low.

Experience indicates that little confidence can be placed on any U(IV) figure that is less than 10 per cent of the total uranium present in the material analysed. Only when spiking experiments indicate that it is a valid result should any significance be attributed to such a low value.

The analytical procedure developed has been advantageously applied to several types of apatite in the course of a study of the geochemistry of uranium in apatite and phosphorite samples; this study will be the subject of a later report.

Conclusions

Analytical data collected on a variety of apatite materials have shown that virtually all marine and igneous apatites have some U(IV). The data are discussed elsewhere (Altschuler, Clarke and Young, in press). The following, however, may be cited as representative of the more significant results.

The U(IV) contents of marine sedimentary apatites studied range from 3 to 91 per cent of the total uranium. Geologically young and unweathered material contains significantly higher per cents of U(IV). Thus, black pebbles from the Pliocene Bone Valley formation contain from 63 to 91 per cent of their uranium as U(IV) and nodules dredged from the sea floor off Southern California contain from 59 to 71 per cent of their uranium as U(IV). These facts are interpreted to signify that the uranium initially fixed in marine apatite is dominantly U(IV) and that subsequent weathering oxidizes some of this to U(VI). The U(IV) contents of igneous apatites studied thus far range from 10 to 66 per cent of the total uranium.

Acknowledgement—The authors wish to acknowledge their indebtedness to Frank S. Grimaldi of the U.S. Geological Survey for his valuable suggestions and criticisms throughout the course of these studies. This work is part of the programme conducted by the U.S. Geological Survey on behalf of the Division of Raw Materials of the U.S. Atomic Energy Commission.

References

Ahrland S. and Larsson R. (1954) The complexity of uranium(IV) chloride, bromide, and thiocyanate. *Acta Chem. Scand.* **8,** 137–150.

Altschuler Z. S., Cisney E. A. and Barlow I. H. (1952) X-ray evidence of the nature of carbonate-apatite (abs.). *Bull. Geol. Soc. Amer.* **63,** 1230–1231.

Altschuler Z. S., Clarke R. S. and Young E. J. The geochemistry of uranium in apatite and phosphorite. In press.

Altschuler Z. S., Jaffe E. B. and Cuttitta F. (1956) The aluminum phosphate zone of the Bone Valley formation and its uranium deposits. *U. S. Geol. Survey Prof. Paper* 300, pp. 495–504.

Baes C. F., Jr. (1953) The reduction of uranium(VI) by ferrous iron in phosphoric acid solution: The formal electrode potential of the U(IV)/(VI) couple: *ORNL*–1581 U. S. Atomic Energy Comm. Tech. Inf. Service Extension, Oak Ridge, Tenn.

Bowie S. H. U. and Atkin D. (1956) An unusually radioactive fossil fish from Thurso, Scotland. *Nature, Lond.* **177,** 487–488.

Foshag W. F. (1929) Mineralogy and geology of Cerro Mercado, Durango, Mexico *Proc. U.S. Nat. Mus.* **74,** 1–27.

Goldschmidt V. M. (1954) *Geochemistry*. Oxford University Press.

Green J. (1953) Geochemical table of the elements for 1953. *Bull. Geol. Soc. Amer.* **64,** 1001–1012.

Grimaldi F. S., May I. and Fletcher M. H. (1952) U.S. Geological Survey fluorimetric methods for uranium analysis. *U.S. Geol. Survey Circ.* 199, 1–20.

Hendricks S. B. and Hill W. L. (1950) The nature of bone and phosphate rock. *Proc. Nat. Acad. Sci. Wash.* **36,** 731–737.

Katz J. J. and Rabinowitch E. (1951) The chemistry of uranium. Part 1. The element, its binary and related compounds. *National Nuclear Energy Ser.* Div. VIII, Vol. 5, p. 358. McGraw-Hill, New York.

McKelvey V. E. and Nelson J. M. (1950) Characteristics of marine uranium-bearing sedimentary rocks. *Econ. Geol.* **45,** 35–53.

McKeown F. A. and Klemic H. (1956) Rare-earth-bearing apatite at Mineville, Essex County, New York. *U.S. Geol. Survey Bull.* 1046–B

Moore G. W. (1954) Extraction of uranium from aqueous solution by coal and other materials. *Econ. Geol.* **49,** 652–658.

Neuman W. F., Neuman M. W., Main F. R. and Mulryan B. J. (1949) The deposition of uranium in bone, V—Ion exchange studies. *J. Biol. Chem.* **179,** 335–340.

Olson J. C., Shawe D. R., Pray L. C. and Sharp W. N. (1954) Rare-earth mineral deposits of the Mountain Pass district, San Bernardino County, California. *U.S. Geol. Survey Prof. Paper* 261, 1–75.

Pannell J. H. (1950) Air oxidation of uranous solutions. *MITG*–261. U.S. Atomic Energy Comm. Tech. Inf. Service Extension, Oak Ridge, Tenn.

Sandell E. B. (1950) *Colorimetric Determination of Traces of Metals* (2nd Ed.) p. 375. Interscience, New York.

Schreyer J. M. (1954) The chemistry of uranium (IV) orthophosphate solutions: Part 1. The solubility of uranium (IV) orthophosphates in phosphoric acid solutions. *ORNL*–1747. U.S. Atomic Energy Comm. Tech. Inf. Service Extension, Oak Ridge, Tenn.

Toohey J. G. and Kaufman D. (1954) The relationship between oxidation reduction potential and valence state of iron, vanadium, and uranium in sulfuric acid leach liquors. *ACCO*–60 U.S. Atomic Energy Comm. Tech. Inf. Service Extension, Oak Ridge, Tenn.

Waring C. L. and Annell C. S. (1953) Semiquantitative spectrographic method for analysis of minerals, rocks and ores. *Analyt. Chem.* **25,** 1174–1179.

Geochimica et Cosmochimica Acta, 1958, Vol. 13, pp. 143 to 152. Pergamon Press Ltd., London

Isotopic composition of primeval lead of the earth

Akimasa Masuda
Institute of Earth Sciences, Nagoya University, Nagoya, Japan

(*Received* 8 *April* 1957)

Abstract—Based upon the variation of isotopic composition of lead ores from the same site, the age of the earth is estimated to be 4·55 billion years (b.y. = 10^9 years). By assuming a fixed heterogeneity of two radioactive elements, thorium and uranium, we can obtain a self-consistent primeval lead with $^{204}Pb : {}^{206}Pb : {}^{207}Pb : {}^{208}Pb = 1 : 9{\cdot}05 : 9{\cdot}81 : 29{\cdot}45$. These figures demonstrate for the first time that the isotopic composition of earth's primeval lead does not differ essentially from that of primeval lead of meteorites or troilite lead. It is the chief advantage of this approach that no knowledge of deposition time for the vast majority of samples is required.

Although common igneous rocks are accountable for lead ores, mafic rock is of greater importance than felsic.

Introduction

Naturally occurring stable lead isotopes consist of ^{204}Pb, ^{206}Pb, ^{207}Pb, and ^{208}Pb. As is well known, ^{238}U decays to ^{206}Pb, ^{235}U to ^{207}Pb, and ^{232}Th to ^{208}Pb, after each has passed through a particular chain of successive nuclear transformations, and thus the natural composition of lead isotopes has been changing at a regular rate, while ^{204}Pb has not yet been known to be produced in appreciable amounts by any natural nuclear reaction except through the process of birth of elements. McCrady (1952) remarks that no nuclear reaction other than the decay processes just mentioned has affected the natural abundances of lead isotopes. This field of study owes its opening and development largely to Nier and his co-workers.

An attempt to estimate the age of the earth and the isotopic composition of primeval lead by means of the disintegration of ^{238}U, ^{235}U, and ^{232}Th to lead isotopes was initiated by Holmes (1946,1947) and independently by Houtermans (1947), the presumptions and practices of whom are identical in principle. They used Nier's isotopic analyses of twenty-five lead ores (common leads) of different formation ages from the oldest to most recent times. Holmes' treatment results in giving the age of earth's crust as 3·35 b.y., and Houtermans' as 2·9 b.y. Thereafter other researchers published their estimates as follows, all fundamentally on the same basis: Using the least squares method, 3·29 b.y. was obtained by Bullard and Stanley (1949); 3·5 b.y. by Collins, Russell, and Farquhar (1953) also using the least squares method; 3 b.y. as a first approximation by Vinogradov, Zadorozhnyi, and Zykov (1952). Collins *et al.* and Vinogradov *et al.* used their own analyses in addition to Nier's data.

In 1953 Patterson, Brown, Tilton, and Inghram published isotopic analyses of meteoritic leads. Their elaborate study showed that the isotopic composition of troilite lead differs considerably from previous estimates for terrestrial primeval lead, and gives the age of the earth of 4·5 b.y. as calculated by Houtermans (1953).* This difference provoked arguments, and even some attempts were made

* The stone meteorites have also their ages of 4·5 b.y. (Patterson, 1955).

to place significance on it. But Russell and Allan (1955) seem to have almost settled the matter of age discrepancy; they obtained 4·3 b.y. as the earth's age just from measurements of Postcambrian leads. Bate (1955), on the other hand, obtained a value close to but larger than this, 4·8 b.y. He assumed troilite lead to be a terrestrial primeval lead, as did Houtermans, and proposed a model embodying continuous differentiation of the earth's crust.

As for isotopic composition of primeval lead of the earth itself, no re-study has been made since the report on meteoritic leads by Patterson *et al.* The main object of this paper is to re-examine the problem of the earth's primeval lead based upon the data on terrestrial leads exclusively and from a new standpoint. The chief causes which have misled previous investigators are the scarcity of data and the unreliability of estimated geological times for samples, particularly for Precambrian deposits. Ahrens (1955) pointed out that the geological time dated by lead method is prone to be more or less seriously underestimated. Thus it is necessary to collect as much data on ore lead as is available, and to find out a procedure free from unreliability of the geological time of ore deposition.

Although our hypothesis is similar to those presented by several authors, such as Holmes, Houtermans, and others, our way of treating the data as an approach to the problem is quite distinct from theirs.

The data on isotopic analyses of common leads used in this paper are taken from the following references: Nier (1938); Nier, Thompson, and Murphey (1941); Collins, Farquhar, and Russell (1952); Vinogradov, Zadorozhnyi, and Zykov (1952); Allan, Farquhar, and Russell (1953); Collins, Russell, and Farquhar (1953); Ehrenberg (1953); Collins, Farquhar, and Russell (1954); Geiss (1954); Begemann, Geiss, Houtermans, and Buser (1954); Russell, Farquhar, Cumming, and Wilson (1954); Wilson, Farquhar, Gretener, Russell, and Shillibeer (1954); and Sakai, Honda, and Minami (1955). Lead isotope analyses made by Carbide and Carbon Co. of Tennessee for the U.S. Geological Survey are listed in *Nuclear Geology* (1954) edited by H. Faul. These analyses are used by us with permission of John Wiley Inc. Through the courtesy of Prof. J. T. Wilson of the University of Toronto, Canada, a great many analyses which were carried out by Drs. R. M. Farquhar, G. L. Cumming, and C. B. Collins up to 1 March 1955 have come to hand. Thus nearly 300 isotopic analyses of lead, exclusive of erratic and abnormal, are used in our calculations.

Fundamental Hypothesis

Here "primeval" refers to the latest period when the isotopic composition of lead was homogeneous in all parts of the globe. Although due to various cosmological viewpoints not all may agree on the primordial state and subsequent development of the earth, "primeval" here may be considered that time when the earth's silicate shells, or layers, were formed from its liquid state. In the course of solidification and concurrent differentiation of the material phases, three elements, lead, uranium, and thorium, here under consideration were presumably distributed throughout the solid phases in various amounts according to their geochemical specificities as were other elements. The heterogeneity of these three elements thus caused and fixed in the lithosphere could have continued producing wider variations of lead isotope composition with elapsing time. While there are some criticisms on fixed heterogeneity, this premise is not only indispensable to further calculations, but it may be statistically valid. For convenience, it is assumed here that the lithosphere consists of innumerable closed systems of various chemical

composition, and that their interaction takes place during the activity of magma. Since lead ore is a residual of magma (transient molten silicate), it is granted that the lead isotope composition in the very parent silicate mass was frozen within the lead ore itself without undergoing any tangible isotopic fractionation during its deposition.

Primeval Age of the Earth

For the purpose of estimating the composition of primeval lead, it is first necessary to get a reliable estimate of primeval age. Of the values thus far obtained from terrestrial lead alone, Russell and Allan's is certainly the most reliable and may well be close to the truth. However, theirs is probably a little low. We shall follow a modified path.

Nuclide balance equations for the decays concerned can be expressed as follows: Let $^{206}Pb_0$, $^{207}Pb_0$, and $^{208}Pb_0$ represent the primeval number of each nuclide relative to non-radiogenic ^{204}Pb taken as unity. Let $^{238}U_0$, $^{235}U_0$, and $^{232}Th_0$ represent the primeval number of each nuclide relative to ^{204}Pb in a supposedly closed system. Then the numbers of ^{206}Pb, ^{207}Pb, and ^{208}Pb at the time $= T$ years since the primeval era, each denoted by subscript T, are given by

$$^{206}Pb_T = {}^{206}Pb_0 + {}^{238}U_0(1 - e^{-\lambda 238 T}) \tag{1}$$

$$^{207}Pb_T = {}^{207}Pb_0 + {}^{235}U_0(1 - e^{-\lambda 235 T}) \tag{2}$$

$$^{208}Pb_T = {}^{208}Pb_0 + {}^{232}Th_0(1 - e^{-\lambda 232 T}) \tag{3}$$

$$= {}^{208}Pb_0 + \kappa\,{}^{238}U_0(1 - e^{-\lambda 232 T}) \tag{3'}$$

where λ_{238}, λ_{235}, and λ_{232} are the disintegration constants of nuclides, $^{238}U(1{\cdot}54 \times 10^{-10}$ year$^{-1})$, $^{235}U(9{\cdot}78 \times 10^{-10}$ year$^{-1})$, and $^{232}Th(0{\cdot}499 \times 10^{-10}$ year$^{-1})$, respectively, and κ is the ratio of $^{232}Th_0$ to $^{238}U_0$, which consequently bears on the supposed system. Implication of κ will be discussed in more detail further on.

A combination of equations (1) and (3) gives another useful formula

$$\frac{^{206}Pb_{r,t}}{^{207}Pb_{r,t}} = \frac{^{206}Pb_t - {}^{206}Pb_0}{^{207}Pb_t - {}^{207}Pb_0} = 139 \times \frac{(e^{\lambda 238 T_0} - e^{\lambda 238 t})}{(e^{\lambda 235 T_0} - e^{\lambda 235 t})} = \beta_t \tag{4}$$

where T_0 is the primeval age of the earth, t the time from the ore deposition to the present, 139 the present day ratio of natural abundance of ^{238}U to ^{235}U, subscript r stands for "radiogenic" and other notations are all similar to equations (1), (2), (3), and (3'). It is self-evident from the definition that $T + t = T_0$. This equation or its modification has been employed most frequently and usefully by earlier authors. It also underlies "isochron" method of Houtermans. Equation (4) states that samples of the same age should fall on a straight line in a plot of ^{206}Pb against ^{207}Pb and that T_0 can be calculated from its slope which corresponds to β_t. As a matter of fact, however, the points representing samples of the same age do not fall strictly on a straight line, but are found to be more or less scattered. This is the reason the least squares method has been generally employed. Clear as is the mathematical meaning of this method, caution should be used in its application to cases where the points are scattered. Such consideration has resulted in use of a modified method, i.e. special attention is directed toward

the variation of lead isotope composition found in a set of lead ores from the same mine or locality. The following two interpretations of such variation may be accepted: That (1) the great silicate mass which yielded magma had not been homogeneous in relative contents of U to ^{204}Pb and was followed by differential evolution of each part of its melt; that (2) an arising primary magma reacted upon and mixed with (assimilated) various relative amounts of surrounding rocks which had contained uranium in amounts differing from that in primary

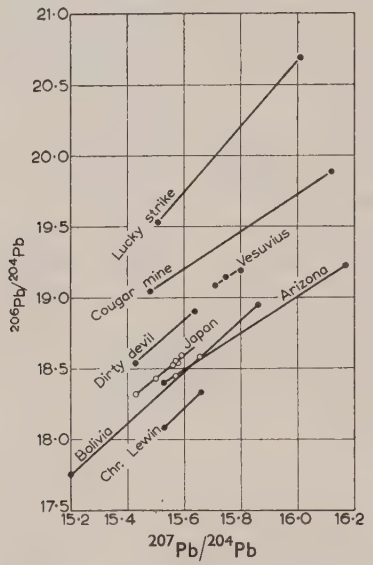

Fig. 1. Variations of $^{206}Pb/^{204}Pb$ and $^{207}Pb/^{204}Pb$ in ore leads from same or connected localities.

magma relative to ^{204}Pb, to give rise to magmas with varying ratios of ^{204}Pb, ^{206}Pb, and ^{207}Pb.

In view of the susceptibility of computation to measurement errors, the sets in which there is little difference between members have been discarded. Of sets so far reported, we have selected five for estimation of T_0. Our estimates of T_0 fall within the range from 4·0 to 5·0 b.y. with an average of 4·55 b.y. (Table 1, Fig. 1). This average value has been calculated from the geometrical mean, 1·667, of β_t reduced to the present. Because of the exactness of geological information on young deposits, young sets are suitable for this computation. Although each of the last three sets listed in Table 1 does not include ores from the same mine, each set could be used to estimate T_0 because it consists of young (Miocene) deposits and because of their intimate occurrence. It must be added that there is no destined tendency for this calculation to be either overestimated or underestimated.

All previous treatments, except Russell and Allan's, failed to yield a reliable age of the earth, giving figures of the order 3·0–3·5 b.y. Russell and Allan's tables show that without Vinogradov's (1952) data they also could not have secured a fair result. Their treatment of data other than Vinogradov's yielded figures of the order of 3·6–4·0 b.y., with 3·2–3·6 b.y. as their result from

North American samples. On the other hand, no sets listed in Table 1, including North American samples, show values lower than 4·0 b.y., although some data are derived from the same sources as used by Russell and Allan. These facts favour the present point of view.

Isotopic Composition of Primeval Lead

In the section above, we have obtained a slope of an isochron corresponding to the present time (giving the earth's primeval age of 4·55 b.y.). This isochron will be assumed to pass a point which represents the ratios of 1 : 18·93 : 15·73 for

Table 1. Estimates of primeval age of the earth in billion years

Locality	Age of ore deposition	T_0	References
Lucky Strike, Utah	Early Tertiary	4·06	(Cited by Faul, 1954)
Chr. Lewin, Germany	Late upper Carboniferous	4·28	Geiss (1954)
Dirty Devil, Utah	Early Tertiary	4·50	(Cited by Faul, 1954)
Cougar mine, Colo.	Early Tertiary	4·89	(Cited by Faul, 1954)
Vesuvius	Recent	5·01	Begemann, Geiss, Houtermans, and Buser (1954)
Bolivia	Miocene	4·43	Vinogradov, Zadorozhnyi, and Zykov (1952); Collins, Farquhar, and Russell (1952)
Japan	Miocene	4·52	Sakai, Honda, and Minami (1955)
Arizona	Miocene	4·92	Nier (1938); Nier, Thompson, and Murphey (1941)

^{204}Pb, ^{206}Pb, and ^{207}Pb. (These ratios have been obtained by averaging the values on lead in manganese nodule and red clay from the Pacific Ocean bed, as reported by Patterson 1953). Thus we have an isochron corresponding to the youngest geological time. Primeval lead should be somewhere on this line. Therefore $^{206}Pb_0$ or $^{207}Pb_0$ will be determined by assuming either. An assumption of certain value for $^{206}Pb_0$ (or $^{207}Pb_0$) will enable us tentatively to date all samples with the exception of abnormal lead.

Assigning the most reasonable value to $^{206}Pb_0$ or $^{207}Pb_0$ is the crux of our problem. At this point we must return to the fundamental hypothesis on the initial state of the earth's lithosphere, previously referred to, according to which the three elements in question were distributed in different amounts at various places during the process of lithosphere formation. Owing to the fixed heterogeneity of thorium and uranium which decay to lead, it can be predicted that the distribution area in a plot of ^{208}Pb against ^{206}Pb would get broader with elapsed time or with increase of ^{206}Pb. In other words, a moderate variation of Th : U ratios could be expected to bring about such a fan-shaped spread. It follows, in turn, that the points in such a distribution would converge at some point ($^{206}Pb_c$, $^{208}Pb_c$) which implies a primeval point. Any estimation of the convergent point,

however, presents a formidable problem because no method of estimation has yet been established. Therefore a new attempt is necessary.

From equations (1) and (3′) we have

$$^{208}Pb_T = {}^{208}Pb_0 + \kappa({}^{206}Pb_T - {}^{206}Pb_0) \times \frac{(1 - e^{-\lambda_{232}T})}{(1 - e^{-\lambda_{238}T})}$$
$$= {}^{208}Pb_0 + \kappa Z$$

where $Z = ({}^{206}Pb_T - {}^{206}Pb_0) \times \frac{(1 - e^{-\lambda_{232}T})}{(1 - e^{-\lambda_{238}T})}$. The term Z as used here enables us to prepare a linear function. As stated previously, the numerical value of $^{207}Pb_0$ can be determined for a given $^{206}Pb_0$. Thus, T for any sample can be evaluated for a given pair of $^{206}Pb_0$ and $^{207}Pb_0$. Consequently the value of Z can be determined for given value of $^{206}Pb_0$. A ^{208}Pb vs. Z plot is employed to get a convergent point.

A random sampling from all geological phases (temporal and spatial) is found to pose a question difficult to answer and so far beyond our reach. Consequently the plotting diagram is divided into small sections, and where two or more points are in a section, they are replaced by one average point to do away with an excessive concentration of points. In the diagram thus arranged, a straight line m is drawn based upon the least squares method*; then lines u_1 and l_1 are drawn for the points lying, respectively, above and below line m, and additional lines u_2 and l_2 are drawn for points above u_1 and below l_1, respectively, and so forth. Two conditions for all lines above m must be fulfilled: (1) κ for u_{i+1} must be greater than κ for u_i; (2) any point below line u_i must not be above line u_{i+1}. For lower lines, the corresponding conditions must hold conversely.

In this way the uppermost and lowermost lines have been drawn, the intersection of which is taken as a convergent point. A logical consideration requires that $^{206}Pb_c$ and $^{206}Pb_0$ be identical. This means that Z-co-ordinate of the convergent point must be zero. It is the eventual $^{206}Pb_0$ that yields convergence at $Z = 0$. The required approach to the ultimate value is by trial and error because it is impossible to obtain a self-consistent value by a direct calculation. In Table 2, for comparison, the resultant values are tabulated together with prior estimates and the troilite lead composition. (Fig. 2 is the final self-consistent diagram with $^{206}Pb_0 = 9{\cdot}05$.) It can be seen that the new estimates do not differ essentially from the troilite lead. This is the first conclusion which substantially endorses the presumption that the primeval lead of the earth should be the same as the troilite lead.

The method used in this paper involves such intricate procedures that it is hard to determine the accuracy of the values obtained. Nevertheless it is sure that, so long as use is made of the method delineated above, the values as obtained by HOLMES, HOUTERMANS, etc. are far from probable. Here are the aspects which distinguish the present work from the previous ones as relate to the primeval lead of the earth. The former requires no knowledge of the time of ore deposition

* If we suppose $y = ax + b$, then a is calculated here as $\pm\sqrt{\{n\Sigma y_i^2 - (\Sigma y_i)^2\}/\{n\Sigma \hat{x}_i^2 - (\Sigma x_i)^2\}}$, where n is the number of measurements. The plus or minus sign should be chosen according to the case. Mathematical meaning of this formula will be argued elsewhere (MASUDA and MATSUO). b is calculated in the usual way.

except for the sets to be used to estimate T_0, while for the latter such knowledge is indispensable for every sample. In the former, variation of the Th : U ratio is utilized in conjunction with that of the U : ^{204}Pb ratio, while in the previous works just the U : ^{204}Pb variation is utilized. Accordingly ^{208}Pb in this paper plays an important part, while it was previously kept out of any essential role. Here estimation of T_0 is separated from that of primeval lead, formerly both were combined.

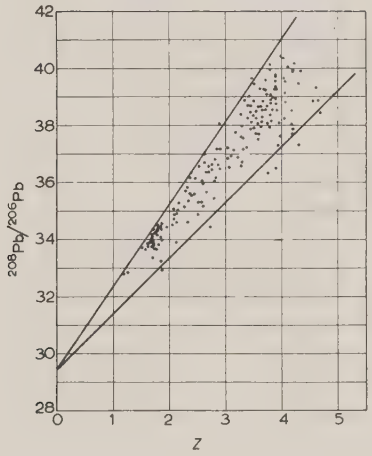

Fig. 2. Plot of ^{208}Pb/^{204}Pb against Z with the self-consistency,

$$Z = (^{206}\mathrm{Pb}_T - {}^{206}\mathrm{Pb}_0) \times \frac{(1 - e^{-\lambda_{232}T})}{(1 - e^{-\lambda_{238}T})}.$$

There is another approach to the primeval lead which also dispenses with the knowledge of geological time. As noted at the beginning of this section, we have only one isochron which corresponds to the youngest geological time. If a set of Precambrian ores from the same mine, however, should have a variation in lead isotope composition, then the straight line passing through the points representing them in ^{206}Pb–^{207}Pb diagram could be assumed an isochron even without any knowledge of their age. The converging point of actual and assumed isochrons

Table 2. Estimated isotopic composition of primeval lead of the earth and the isotopic measurement of troilite lead

^{206}Pb	^{207}Pb	^{208}Pb	Author
10·95	13·51	—	Holmes (1947)
11·52	14·03	31·60	Houtermans (1947)
11·86 ± 1·47	13·86 ± 0·56	—	Bullard and Stanley (1949)
11·33	13·55	31·10	Collins, Russell, and Farquhar (1953)
9·05	9·81	29·45	Present author
9·50	10·36	29·49	Patterson (1955): troilite lead

(^{204}Pb = 1·00)

would represent the primeval lead. Of course, it should be decided after deliberation if "from the *same* site" means "of the *same* age". At present, however, we cannot adopt this approach formally because we have only two such sets if any. These two sets are from Broken Hill, N.S. Wales and from McKim, Ontario. Although the present author has no detailed information on their geological settings, it seems nevertheless of interest here to make some estimation for these sets. The time (A) calculated from isotopic variation in each set itself is listed below and compared to time (B) calculated from the primeval lead composition just obtained.

	$t(A)$	$t(B)$	References
Broken Hill	1·39 b.y. ($\beta_t = 1{\cdot}32$)	1·62 b.y. ($\beta_t = 1{\cdot}26$)	Nier (1938)
McKim	1·92 b.y. ($\beta_t = 1{\cdot}18$)	1·85 b.y. ($\beta_t = 1{\cdot}20$)	Russell *et al.* (1954)

Taking into account the small differences (for Broken Hill, $\Delta^{206}\mathrm{Pb} = 0{\cdot}145$, $\Delta^{207}\mathrm{Pb} = 0{\cdot}11$; for McKim, $\Delta^{206}\mathrm{Pb} = 0{\cdot}13$, $\Delta^{207}\mathrm{Pb} = 0{\cdot}11$) and at the same time any statistical error in the experiment, the agreement between the calculations for both cases may appear accidentally fortunate. In view, however, of the verity found in small differences of some sets in Fig.1, this fair agreement is not necessarily a fortuitous one. It might not only support the present estimate on primeval lead, but might also promise the development of "assumed isochron" method.

Source of Lead Ores

Coefficient κ in equation (3′) is the primeval ratio of $^{232}\mathrm{Th}_0$ to $^{238}\mathrm{U}_0$. It is of particular interest to compare this with the ratio actually observed in igneous rocks because κ is the ratio characteristic of the parent rock from which the original magma and hydrothermal solution came.

The value of κ ranges from 1·9 to 2·9 with a range from 2·3 to 2·9 as indicated by the more crowded dots in Fig. 2. These ranges are 3·1–4·7 and 3·8–4·7 respectively when they are recalculated in reference to the present time.

Evans and Goodman (1941), and Senftle and Keevil (1947) determined the contents of thorium and uranium for a variety of igneous rocks. Most of the values thus actually observed coincide with the values estimated from the isotopic compositions of lead ores (Table 3). The only exceptions are for basalt and diabase determined by Evans and Goodman.

As reviewed by Rankama (1954), the meaning of this ratio concerning the origin of ore lead has long been disputed. It has been widely accepted that ordinary igneous rocks are the source of ore lead, with granitic rocks generally favoured as the source material. McCrady (1952) notes that either granite or basalt alone is unsatisfactory to explain all the results hitherto obtained. Conforming to his idea, the results calculated suggest that rocks with a composition varying between the two extremes, silicic and ultra-mafic, are the source of lead ore.

One characteristic is that, in view of the frequencies of κ's, ultra-mafic or mafic rocks become more significant when Senftle and Keevil's data are considered. Another characteristic is that the upper limit of κ is clear, while the lower limit

Table 3. Ratio of content of thorium to uranium in rocks

Rock type	Th (p.p.m.)	U (p.p.m.)	$^{232}Th : ^{238}U$*	Author
Gabbroic	3·9	0·96	4·20	Evans and Goodman (1941)
Intermediate	4·4	1·4	3·25	Evans and Goodman (1941)
Intermediate	9·97	2·61	3·93	Senftle and Keevil (1947)
Granitic	13·45	3·963	3·50	Senftle and Keevil (1947)
Basalt	5·0	0·83	6·21	Evans and Goodman (1941)
Diabase	2·0	0·83	2·49	Evans and Goodman (1941)
(Estimated)	—	—	4·7—3·1	Present author

* Atomic ratio computed by the present author.

is comparatively vague. These features may be in agreement with the continental growth theories. We can see that the lead ore is a product of magma arising from a deep seat and contaminated to some extent by the overlying rocks. The distribution of minor elements in the deep-seated mafic or ultra-mafic rocks may be more even than in the *shallow*-seated silicic rocks. The extent of contamination may be variable. We can understand such a state and circumstance to be reflected on features of frequencies and range of κ. But it must not be overlooked that the range of the ratios for one category of rocks overlaps that for another category of rocks.

Acknowledgements—The writer expresses his sincere appreciation to Prof. J. T. Wilson of the University of Toronto, Canada, for his gifts of isotopic analyses of common leads, and to Assistant Prof. G. L. Bate of Wheaton College, Illinois, for his good offices in forwarding his thesis.

Acknowledgement is also made of correspondences with Mr. H. Sakai of Tokyo University. The writer is also indebted to Prof. S. Oana for advice and comments, to Assistant Prof. K. Nagasawa for discussions on geological subjects, to Assistant Prof. Y. Shimazu for reading the manuscript, and to Prof. K. Sugawara for reviewing the English text. The encouragement of Mr. S. Matsuo and Mr. R. Sugisaki is gratefully acknowledged.

References

Ahrens L. H. (1955) *Geochim. et Cosmochim. Acta* **8,** 1.
Allan D. W., Farquhar R. M. and Russell R. D. (1953) *Science* **118,** 486.
Bate G. L. (1955) Ph.D. thesis, Columbia Univ., New York.
Begemann F., Geiss J., Houtermans F. G. and Buser W. (1954) *Nuovo Cim.* **11,** 663.
Bullard E. C. and Stanley J. P. (1949) *Veröff. Finn. Geod. Inst.* No. 36, 33.
Collins C. B., Farquhar R. M. and Russell R. D. (1952) *Phys. Rev.* **88,** 1275.
Collins C. B., Russell R. D. and Farquhar R. M. (1953) *Canad. J. Phys.* **31,** 402.
Collins C. B., Farquhar R. M. and Russell R. D. (1954) *Bull. Geol. Soc. Amer.* **65,** 1.
Ehrenberg H. Fr. (1953) *Z. Phys.* **134,** 317.
Evans R. D. and Goodman C. (1941) *Bull. Geol. Soc. Amer.* **52,** 459.
Faul H. (Ed.) (1954) *Nuclear Geology* (see Table 9.1). John Wiley, New York.
Geiss J. (1954) *Z. Naturf.* **9a,** 218.

Holmes A. (1946) *Nature, Lond.* **157,** 680.
Holmes A. (1947) *Nature, Lond.* **159,** 127.
Houtermans F. G. (1947) *Z. Naturf.* **2a,** 322.
Houtermans F. G. (1953) *Nuovo Cim.* **10,** 1623.
Masuda A. and Matsuo S. In preparation.
McCrady E. (1952) *Trans. Amer. Geophys. Un.* **33,** 156.
Nier A. O. (1938) *J. Amer. Chem. Soc.* **60,** 1571.
Nier A. O., Thompson R. W. and Murphey F. B. (1941) *Phys. Rev.* **60,** 112.
Patterson C. (1955) *Geochim. et Cosmochim. Acta* **7,** 151.
Patterson C., Brown H., Tilton G. and Inghram M. (1953) *Phys. Rev.* **92,** 1234.
Patterson C., Goldberg E. D. and Inghram M. (1953) *Bull. Geol. Soc. Amer.* **64,** 1387.
Rankama K. (1954) *Isotope Geology* p. 395. Pergamon Press, London.
Russell R. D., Farquhar R. M., Cumming G. L. and Wilson, J. T. (1954) *Trans. Amer. Geophys. Un.* **35,** 301.
Russell R. D., and Allan D. W. (1955) *Mon. Not. R. Astr. Soc. Geophys. Suppl.* **7,** 80.
Sakai H., Honda M. and Minami E. (1955) *Bull. Chem. Soc. Japan* **28,** 533.
Senftle F. E. and Keevil N. B. (1947) *Trans. Amer. Geophys. Un.* **28,** 732.
Vinogradov A. P., Zadorozhnyi I. K. and Zykov S. I. (1952) *Dokl. Akad. Nauk SSSR* **85,** 1107.
Wilson J. T., Farquhar R. M., Gretener P., Russell R. D. and Shillibeer H. A. (1954) *Nature, Lond.* **174,** 1006.

Geochimica et Cosmochimica Acta, 1958, Vol. 13, pp. 153 to 212. Pergamon Press Ltd., London

Chemistry of Pacific pelagic sediments*

E. D. Goldberg and G. O. S. Arrhenius
Scripps Institution of Oceanography, La Jolla, Calif., U.S.A.

(*Received* 26 *July* 1957)

Abstract—The chemical and mineralogical composition of pelagic sediments from the East Pacific Ocean has been determined with the aim of defining the ultimate sources and the mechanisms of formation of the solid phases. The distribution of elements between sea-water, the pore solution and the various solid components of the sediments permits interpretations of the variations in time and space of the gross chemical composition of pelagic clays. For example, manganese, present in sea-water in a divalent form, is apparently oxidized at the sediment-water interface to tetravalent species which subsequently become a part of the group of ferromanganese oxide minerals which are found in the marine environment. It is suggested the rate of manganese accumulation in sediments is some function of the length of time the sediment surface is in contact with sea-water. The contribution of chemical species from the different geospheres is considered. The quantitative importance of pelagic clays in the major sedimentary cycle is studied on the basis of the distribution of the weathered igneous rock products between continental and pelagic deposits and sea-water. These analyses of a wide variety of pelagic clays allow a reformulation of the geochemical balance and it is concluded that pelagic clays account for approximately 13 per cent of the total mass of sediments produced over geologic time.

Contents

1. Introduction 153
2. Methods 154
   2.1 Preparation of sediments 154
   2.2 Separation of constitutuents 155
      2.21 Dialysis 155
      2.22 Ion exchange 155
      2.23 Separation according to settling velocity 155
      2.24 Separation according to density and magnetic susceptibility . . 155
      2.25 Chelative dissolution 158
   2.3 Elemental analysis 161
3. The Nature of Dissolved Chemical Species in the Ocean 162
4. Distribution of Elements in the Dissolved and Sorbed Phases of the Sediment 166
5. Distribution of Elements in the Solid Phases 169
   5.1 Silicon, aluminium and gallium 172
   5.2 Sodium, potassium and lithium 173
   5.3 Magnesium, calcium and strontium 176
   5.4 Barium 179
   5.5 Boron 187
   5.6 The rare-earth elements, yttrium, scandium and thorium 188
   5.7 Titanium 188
   5.8 Zirconium 191
   5.9 Vanadium 192
   5.10 Chromium 192
   5.11 Iron 193
   5.12 Manganese, cobalt, nickel, lead and molybdenum 193
   5.13 Copper 200
6. Comparative Chemistry of Pelagic Sediments in Space and Time . . . 201
7. The Geochemical Balance 203
   References 209

* Contribution from the Scripps Institution of Oceanography New Series No. 952. The major portion of this work was performed under contract Nonr-233(17) between the University of California and the Office of Naval Research. Support was also received from the Institute of Geophysics, UCLA, and from the Geological Society of America.

1. Introduction

The mineral components of pelagic sediments have their origin in all of the geospheres and in outer space. From the concentration and grouping of different elements in the minerals, inferences can be drawn regarding the sources of the solid phases. For example, the boron content of clay minerals crystallizing in the marine environment is approximately two orders of magnitude higher than the value for terrestrial clays (Goldschmidt and Peters, 1932a, b). There are several indications that boron proxies for silicon in the tetrahedral sheets of the mineral structure. Hence, terrestrial clays could be detected in the pelagic environment by their low boron content, as a secondary exchange of the tetrahedral group probably is excluded for energetic reasons.

Changes in space and time of the contribution of minerals from different sources may be revealed by the proportions of the sedimentary components and by their structure and chemical composition. While in a number of clay cores from the Pacific Ocean, the stable proportions between marine hydrogenous and terrestrial detrital minerals indicate a relatively constant supply of both of these, other sequences bear witness of radical changes in the rate of accumulation of one or both of these components. A high manganese, phillipsite, and apatite content, and a large crystal size of phillipsite and barite, for example, characterize many of the Tertiary sediments of the north Pacific, in contrast to the overlying Quaternary deposits. An understanding of the processes responsible for such differences is of utmost importance in studies of the past history of the earth.

Finally, in geochemical balance computations of the type first used by Joly (1899), the concentrations of elements in ocean sediments enter as important constants, influencing the final values for the proportions of different rock types making up the earth's crust. Two well-known balance computations (Goldschmidt, 1954; Kuenen, 1950) are in disagreement as to the total mass of pelagic clays produced in the major sedimentary cycle. Kuenen concludes that the pelagic clays represent 50 per cent of the total mass of sediments, while Goldschmidt considers pelagic clays quantitatively unimportant. Further evaluation of assumptions involved in geochemical balance computations, combined with additional data on the chemical and mineralogical composition of sediments, should reveal which, if either, of the two extremes is right.

This paper is an attempt to contribute to the knowledge of the localization of elements in the mineral phases of the pelagic sediments and to investigate the sources of the components of the deposits and their processes of formation. Further, upon the basis of new evidence, a modified geochemical balance is presented.

2. Methods

2.1. *Preparation of sediments for analysis*

In general the sediments were treated as indicated by Arrhenius (1952, 4.1.) However, the sampling method was changed in order to smooth out gradients in the composition caused by the activity of benthonic animals, and in order to make possible stratigraphic summation without interpolation. Instead of cutting 1·5 cm thick sample slices every 10 cm, the entire length of the core was thus sampled in consecutive slices, each one 4 cm long.

Density and water content were determined in all samples. One segment of the sample slice was ground and used for chemical analysis, the other one was saved intact and used for the separation of different minerals or mineral groups which were subsequently analysed.

In the designation of the samples the first word refers to the name of the expedition, and the following number and symbols to the core number, the ship, and the type of core. The final number refers to the depth of the sample in cm below the sediment surface. A brief description of the samples is given in Table 1 (see also Fig. 1).

2.2. *Separation of constituents of the sediment*

In order to establish the distribution of different elements between the different constituents of the sediment, attempts were made to separate these. The separation processes include dialysis, exchange of sorbed ions, chelation, separation according to settling velocity, density, and magnetic properties. It should be noted that while bulk analyses of sediments reported in this paper include the sorbed solids, and the dissolved solids of the pore water, analyses of fractions of the sediment, given in the following, refer to material freed from interstitial salts and with exchange positions saturated with ammonium ion. The compositions of the interstitial solids and of the sorbates are given separately.

2.21. *Dialysis.* The wet sample was churned with distilled water, transferred to a thin-walled cellophane tube and dialysed in a volume of distilled water approximately five times the volume of the suspension. The water was changed every 6 hr and the first three dialysates combined and evaporated. The evaporate forms the sample referred to as the dialysate. Dialysis of the suspension was carried on until no chloride could be observed upon the addition of silver nitrate.

2.22. *Ion exchange.* In the samples Cap. 50 BP 812–817, and Cap. 33 BG, sorbed cations were exchanged by boiling the sample with 3 per cent LiOH. In the remaining samples the dialysis tubing with suspension was transferred to a beaker containing an approximately five times larger volume of N ammonium acetate. After heating to 80°C for 6 hr the solution was exchanged against distilled water. The resulting solution was separated after another 6 hr period, combined with the first solution, evaporated and ashed. The ash forms the sample.

2.23. *Separation according to settling velocity.* The mineral powders and the ammonium or lithium saturated sediment samples were suspended in 0·01 N ammonia, and successively finer grain size fractions were separated by repeated settling and decantation. The fractions so prepared had limiting equivalent diameters of spherical quartz grains of 32, 10, 3·2 and 1 μ. A CEPA continuous flow supercentrifuge with an electronic speed regulator, modified according to JASMUND (1948), was employed for the further subdivision of the sediment fractions with grain sizes smaller than 1 μ. The fractions thus obtained had the equivalent size limits 1, 0·32, 0·1 and 0·03 μ. For monomineralic suspensions the known density of the mineral in question was used for the computation of settling velocities; in the case of sediment suspensions a grain density of 2·60 was assumed.

2.24. *Separation according to density and magnetic susceptibility.* Mineral separation on the basis of differences in density and magnetic properties was

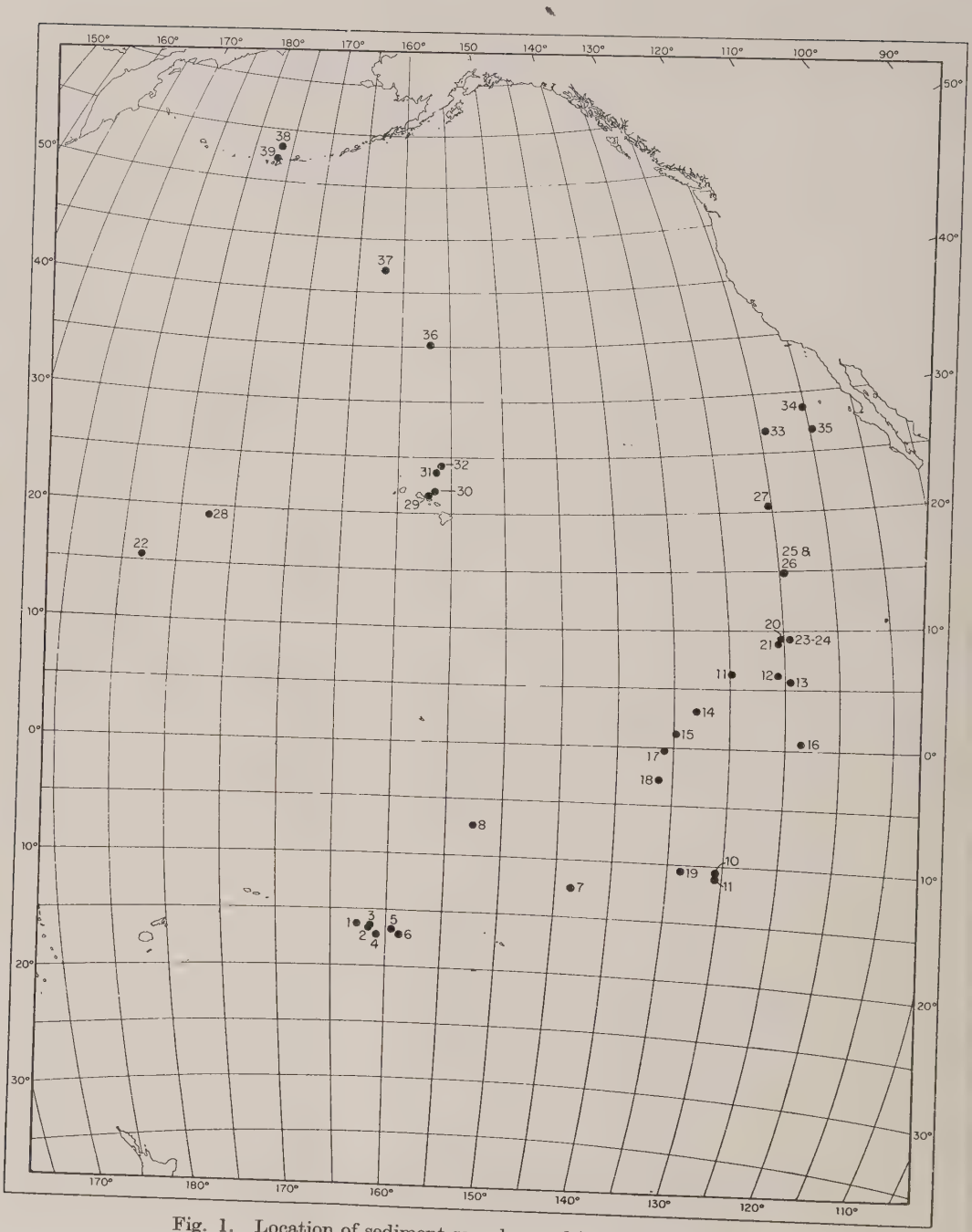

Fig. 1. Location of sediment samples used in the investigation.

Table 1. Description of samples

	South equatorial clays	
1	Capricorn 21 HG	Lat. 16°36′S, long. 162°43′W (NW of Cook Islands). Depth 5125 m. Dark brown clay with manganese micronodules, phillipsite and fish debris.
2	Capricorn 23 HG	Lat. 16°58·5′S, long. 161°35′W (NW of Cook Islands). Depth 5140 m. Dark brown clay as above.
3	Capricorn 24 HG	Lat. 16°44′S, long. 161°22′W (NW of Cook Islands). Depth 4685 m. Dark brown clay as above.
4	Capricorn 30 BG	Lat. 17°28′S, long. 160°59′W (N of Cook Islands). Depth 4710 m. Dark brown clay abundant in manganese nodules and phillipsite and with moderate amounts of fish debris, mica and quartz.
5	Capricorn 25 HG	Lat. 16°53′S, long. 159°8′W (N of Cook Islands). Depth 5040 m. Dark brown clay as Capricorn 31 BG.
6	Capricorn 31 BG	Lat. 17°29′S, long. 158°40′W (W of Society Islands). Depth 4890 m. Dark brown clay, abundant in manganese nodules, in augite, feldspar, and other igneous minerals, with moderate amounts of quartz and phillipsite and small amounts of fish debris.
7	Capricorn 33 BG	Lat. 12°46′S, long. 143°33′W (Tuamotu-Marquesas). Depth 4380 m. Similar in composition to Capricorn 30 BG.
8	Swedish Deep-sea Expedition 71	Lat. 7°38′S, long. 152°53′W (N of Society Islands). Depth 4990 m. Dark brown phillipsitic clay with radiolaria and fish debris.
	Calcareous oozes from the east Pacific rise	
9	Capricorn 32 HG	Lat. 11°00′S, long. 130°24′W (E of Marquesas Islands). Depth 4245 m. Foraminiferal ooze high in ferromanganese oxide minerals.
10	Capricorn 33 HG	Lat. 10°58′S, long. 130°30′W (E of Marquesas Islands). Depth 4040 m. Foraminiferal ooze high in ferromanganese oxide minerals.
	Equatorial calcareous-siliceous oozes and clays	
11	Swedish 58	Lat. 6°44′N, long. 129°28′W. Depth 4440 m (see further Arrhenius, 1952, 2·58).
12	Chubasco 23	Lat. 6°12′N, long. 125°27′W. Depth 4500 m.
13	Capricorn 48 BG1	Lat. 5°45′N, long. 124°02′W. Depth 4125 m.
14	Swedish 59	Lat. 3°05′N, long. 133°06′W. Depth 4370 m (*op. cit.*, 2·59).
15	Swedish 60	Lat. 1°35′N, long. 134°57′W. Depth 4540 m (*op. cit.*, 2·60).
16	Capricorn 47 BG	Lat. 0°40′N, long. 123°33′W. Depth 4230 m.
17	Swedish 61	Lat. 0°06′S, long. 135°58′W. Depth 4437 m (*op. cit.*, 2·61).
18	Swedish 62	Lat. 3°00′S, long. 136°26′W. Depth 4510 m (*op. cit.*, 2·62).
19	Capricorn 36 BG1	Lat. 10°45′S, long. 133°35′W. Depth 4490 m.
	Tertiary sediments	
20	Chubasco 15	Lat. 8°31′N, long. 125°25′W. Depth 4462 m. Tertiary clay.
21	Chubasco 40	Lat. 8°6′N, long. 125°26′W. Depth 4415 m. Tertiary coccolith ooze.
22	Mid-Pac. 40	Lat. 15°35′N, long. 177°30′E. Depth 4060 m. Tertiary coccolith ooze.
	North equatorial clays	
23	Capricorn 49 BG	Lat. 9°17′N, long. 124°9′W. Depth 4410 m. Buff siliceous clay with fine silt of quartz, feldspar and other detrital minerals, alternating with grey clay of similar composition but higher in manganese.
24	Capricorn 49 BP	Position and depth as 49 BG. Sediment as in 49 BG. Lower part of core grey from manganese micronodules. Sequence similar to core 54 of the Swedish Deep-Sea Expedition (Arrhenius, 1952 2·54).
25	Capricorn 50 BG2	Lat. 14°55′N, long. 124°12′W. Depth 4270 m. Sediment similar to Capricorn 49.

Table 1—*continued*

26	Capricorn 50 BP	Location and depth as Capricorn 50 BG2. Buff clay as in Capricorn 50 BG2, unconformally resting on dark reddish brown, partly phillipsite rich, Tertiary clay.
27	Yoyo 2P, 3G, 7P	Lat. 20°49·5′N, long. 125°15′W. Depth 4550 m. Brown, homogeneous clay with relatively high content of quartz, plagioclase, biotite and muscovite.
28	Mid-Pac. 38	Lat. 19°01′N, long. 177°19′W (foothills of Mid-Pacific Mountains). Depth 4774 m. Alternating dark and light brown clay.
	Hawaiian clays and volcanic mud	
29	NH (Navy-Hawaii) 9	Lat. 21°41·2′N, long. 157°28·5′W. Depth 3027 m. Globigerina ooze with abundant sand-silt sized pyroclastics.
30	NH 12	Lat. 22°49·0′N, long. 156°50·3′W. Depth 4484 m. Dark brown clay.
31	NH 13	Lat. 23°21·8′N, long. 156°28·7′W. Depth 4254 m. Dark brown clay.
32	NH 14	Lat. 24°07·5′N, long. 156°03·8′W. Depth 4466 m. Dark brown clay.
	Clays from Baja California Seamount Province	
33	Wigwam 5	Lat. 27°37·8′N, long. 124°25·7′W. Depth 4400 m. Dark brown, homogeneous clay.
34	NG (Navy-Guadelope) 2	Lat. 28°42′N, long. 120°12′W. Depth 3550 m. Dark brown, homogeneous clay.
35	NG 3	Lat. 27°09·N, long. 119°29′W. Depth 4100 m. Dark brown, homogeneous clay.
	North Pacific sediments	
36	Ck (Chinook) 2	Lat. 35°09′N, long. 157°17′W. Depth 5600 m. Brown clay alternating with dark brown clay.
37	Ck 4	Lat. 42°30′N, long. 162°08·2′W. Depth 5350 m. Brown clay, alternating with dark brown clay.
38	Ck 8	Lat. 53°01′N, long. 176°15′W. Depth 3660 m. Bering Sea. Diatomaceous sediment with volcanic ash layers.
39	Ck 9	Lat. 52°25′N, long. 176°24′W. Depth 3440 m. Bering Sea. Similar to Ck 8.

successfully undertaken on fractions with grain sizes larger than 3·2 μ. Tetrabromoethane was used as a heavy liquid and benzene as a diluent, in order to permit subsequent collection of the minerals on membrane filter pads (Millipore Type HA). The magnetic separation was carried out with a Franz Isodynamic Separator, using the normal feeding method along an inclined chute for grain size fractions larger than 32 μ. Magnetic separation of finer particles was achieved by settling of a dilute suspension through a glass tube, mounted vertically between the pole shoes of the separator.

2.25. *Chelative dissolution.* A separation method based on the preferential dissolution of oxyde-aquate minerals in solutions containing chelating agents was devised by Tamm (1932), who used oxalate ion as the complexing group.

In recent years water soluble chelating agents have been found (see, for example, Martell and Calvin, 1952) with stability constants of the metal chelates, which are generally much larger than the stability constants of the corresponding oxalate metal chelates (Table 2).

In connection with investigations of the mineral chemistry of fine grained sediments where detrital igneous minerals are present together with authigenic

phases, it is of interest to establish the partition of different elements between the sedimentary components. For this purpose the present authors attempted to use chelative dissolution with ethylene diamine tetra-acetate ion (EDTA) and a survey was made of the solubilities of a number of minerals in EDTA. The aim of the treatment of sediment samples with EDTA was to remove the readily soluble phases completely, leaving the rest of the minerals as intact as possible. To test to what an extent the latter aim was fulfilled, a series of experiments were performed, where the minerals, expected to be resistant to chelative dissolution were

Table 2. Stability constants for oxalate and EDTA chelates (from MARTELL and CALVIN, 1952)

Metal ion	Log K (oxalate)	Log K (EDTA)
Mg^{+2}	2·6	8·7
Ca^{+2}	3·0	10·6
Sr^{+2}	2·5	9·6
Ba^{+2}	2·3	7·8
Mn^{+2}	3·9	13·4
Fe^{+3}	10·0	25·1
Co^{+2}	4·7	16·1
Ni^{+2}	5·3	18·4
Cu^{+2}	8·3	18·3
Zn^{+2}	4·7	16·1

suspended in EDTA and their rate of dissolution determined. The conditions were such that non-resistant phases were completely dissolved. The soluble minerals present in the samples investigated were mainly the manganese oxide minerals (BUSER and GRÜTTER, 1956) and microcrystalline apatite (ARRHENIUS, BRAMLETTE, and PICCIOTTO, 1957).

Five per cent EDTA buffered to a pH of 8 with ammonia was used as a standard solution for the dissolution experiment. The minerals were ground and samples prepared with a comparatively narrow grain size range by settling and decantation. The size range used was 3·2–10 μ equivalent diameter, except in the case of titanite, where the range was 1·0–3·2 μ. The surface area exposed to the solvent was therefore approximately known, and although varying shape factors involve a minor uncertainty, the results can at least roughly be expressed in mass dissolved per unit surface area and unit time. The mineral sample powder was suspended in the EDTA solution and kept at 100°C for 2 hr, agitated by a magnetic stirrer. After filtering and determination of the weight loss, the powder was again suspended and the dissolution experiment repeated in order to establish any change of the dissolution rate with time.

The results (Table 3) show that there is indeed a progressive decrease of the dissolution rate with time in most cases, probably due to the formation of structurally disturbed and therefore more easily soluble surface layers on the mineral grains at grinding. The formation, during the experiment, of a leached surface

layer progressively slowing down diffusion of the solvent and the solute, may also contribute to this effect.

Arranged in approximate order of increasing rate of dissolution, the minerals investigated appear as follows: biotite, titanite, goethite, magnetite, rutile, hematite, lepidocrocite, nontronite, and augite. Calcite appears to have a still higher rate than the most rapidly soluble of these minerals, but was not investigated quantitatively. The very rapid dissolution occurring in the ferromanganese oxide minerals and microcrystalline apatite depends primarily on the large interior surface area of these minerals; this was found to be of the order 150–200 m^2g^{-1}

Table 3. Weight loss by dissolution in EDTA

Mineral or rock	Run No.	Weight loss (mg m^{-2} hr^{-1})
Titanite	1	39
	2	15
	3	11
Rutile	1	42
Augite No. 2 [a]	1	98
Augite No. 3 [b]	1	470
	2	340
Hematite	1	70
	2	46
Magnetite	1	36
	2	32
Lepidocrocite [c]	1	175
	2	90
Goethite [d]	1	25
	2	24
Biotite	1	17
	2	1
Nontronite A [e]	1	100
	2	62
Nontronite B [e]	1	100
	2	160
Balsaltic glass [f]	1	96
	2	112

[a] Hybia, Ont., U.S. Nat. Hist. Mus.
[b] Franklin, N.J., U.S. Nat. Hist. Mus.
[c] Princetown, Pa., U.S. Nat. Hist. Mus.
[d] Pikes Peak, Colo., U.S. Nat. Hist. Mus.
[e] API standard
[f] Douglas Creek, Wash., U.S. Nat. Hist. Mus.

both for the composite manganese nodule material as determined by Buser and Grütter (1956), employing gas adsorption technique, and for the apatite by Arrhenius, Bramlette, Picciotto, Chodos and Godijn (in preparation) from X-ray diffraction data. Due to the high rate of dissolution of these two minerals, accurate rate values could not be determined with the technique employed, but approximate values of 100–200 mg m^{-2} hr^{-1} were obtained, using the surface area data quoted above.

In the study of the distribution of elements, reported in the following, chelative dissolution was used in some cases to indicate the localization of the elements in question in a mineral or in a group of minerals. The procedure is exemplified by the results given in Table 4. From this it is evident that the amount of insoluble magnesium, boron, copper, and vanadium increases with increasing content of clay minerals, and it is therefore assumed that most of the insoluble fractions of these elements are constituents of these minerals. Conversely, the soluble fractions of the same elements are believed to be the amounts sorbed to

Table 4. Percentage loss of the total amount of individual elements at treatment with EDTA of fractions of sample Cap. 33 BG. The original percentage concentrations of the elements in the sample fractions are shown in the column marked "Orig."

Oxide	Grain size fraction							
	>32 μ		10–32 μ		3–10 μ		1–3 μ	
	Loss	Orig.	Loss	Orig.	Loss	Orig.	Loss	Orig.
MgO	100	0·8	45	0·9	35	2·2	30	4·6
SrO	100	0·14	100	0·11	83	0·08	57	0·08
B_2O_3	100	0·022	43	0·028	33	0·021	6	0·080
CuO	66	0·068	58	0·077	20	0·120	19	0·310
V_2O_5	50	0·026	25	0·015	15	0·020	7	0·054
Most frequent minerals	Apatite Phillipsite (MnO_2)		Phillipsite Apatite (MnO_2)		Amorphous ferric iron oxide–silicates, and clay minerals Phillipsite Apatite (MnO_2)		Phillipsite (MnO_2)	

or structurally bonded in apatite, phillipsite, and in this case to a lesser extent, ferromanganese oxide minerals. Further references to similar interpretations are given in Section 5.

2.3. *Elemental analysis*

In order to obtain a maximal coverage of elements in a large number of samples, most of the analyses reported herein were made by emission spectrographic techniques. The methodology is fully described by Harvey (1950), who carried out most of the analyses. Each sample was subjected to both an a.c. spark and d.c. arc analysis for the major and minor elements respectively. Some of the determinations of barium, titanium, and zinc required either greater accuracy or were outside of the limits of assay of the emission method. Such analyses were made by X-ray fluorescence analysis and the procedures and accuracy of measurement are given by Lewis and Goldberg (1956). For the elemental analysis of microscopic crystals and aggregates the Castaing X-ray microanalyser was used (Castaing, 1952).

Although the utmost in accuracy and reproducibility was sacrificed for a large number of analyses in using the emission spectrographic technique, the errors in the results have placed but minor limitations upon the interpretation of

the data. A number of tests for the reproducibility of results were made to ascertain the differences in values from one series of runs to another which may have been several years apart. Two samples, 49 BP 120 and 50 BP 108, were analysed at intervals of over a year. The analyst was unaware that he was performing duplicate analyses. The results are given in Table 5. Only four elements showed variations in either of the samples by a factor of 2 (strontium, barium, boron, and zirconium)

Table 5. Duplicate analyses of sediment samples by emission spectroscopy

	49 BP 120		50 BP 108	
	Series A	Series B	Series A	Series B
SiO_2	56	57	61	57
Al_2O_3	16·5	21	15	20
Fe_2O_3	5·7	6·4	6·6	7·0
TiO_2	0·63	0·65	0·72	0·60
MgO	2·6	3·3	2·1	2·9
CaO	2·6	2·3	1·5	2·2
Na_2O	5·9	5·5	3·5	5·1
K_2O	4·1	2·6	3·2	3·3
SrO	0·030	0·064	0·23	0·055
BaO	1·25	0·35	0·58	0·260
B_2O_3	0·046	0·110	0·05	0·120
MnO	0·20	0·16	0·91	0·69
Ga_2O_3	0·002	0·0037	0·0018	0·0027
NiO	0·019	0·017	0·023	0·020
CuO	0·19	0·15	0·14	0·14
Co_2O_3	0·006	0·007	0·015	0·013
Cr_2O_3	0·006	0·008	0·009	0·007
V_2O_5	0·016	0·028	0·025	0·023
ZrO_2	0·016	0·033	0·017	0·022
Y_2O_3	0·01	0·008	0·012	0·008

and the variations were in the same direction by essentially the same factor. The majority of elements show variations of under 25 per cent.

To test the accuracy of the measurements, thirty-two different glauconite samples were analysed by precision chemical techniques (the methods will be described elsewhere) and by emission spectrography. The data are presented in Fig. 2 and Table 6 and represent three separate series of analyses made over a 3 year period. The iron values are consistently low by 20 per cent, and this fact is reflected in the higher number of positive deviations from the true value of silicon, aluminium, calcium, and potassium. The magnesium values were low by an average of 25 per cent.

Wedepohl (personal communication) re-ran nine of our samples and found the average nickel contents of his precision spectrographic analyses to be similar to our average, while his average vanadium value was about one-half of the one reported herein. This discrepancy will be discussed in Section 5.9.

3. The Nature of the Dissolved Chemical Species in the Ocean

Studies on the types of dissolved chemical species of elements in marine waters can provide important criteria for the interpretation of the behaviour of elements in the major sedimentary cycle. Two elements that show a similar quantitative distribution of positively, negatively and uncharged species of the same type may have like geochemical paths. On the basis of available thermochemical data the nature of the dissolved chemical species of some of the metals can be described with confidence; on the other hand there is a nearly complete lack of data for the transition elements.

The basis of computing the speciation of elements in aqueous solutions depends upon the formation of complex ions and ionic associations (an excellent survey

Table 6. Accuracy of the spectrographic analysis of thirty-two different glauconite samples

Element	Positive deviations from true value			Negative deviations from true value	
	Av. wt.% in samples	No.	Average deviations in element percentage	No.	Average deviations in element percentage
Si	24	21	2·0	11	1·1
Al	5·5	26	1·7	6	0·5
Fe	17	0	—	32	3·7
Ti	0·10	26	0·03	6	0·03
Mg	2·8	4	0·3	27	0·7
Ca	1·0	25	0·42	5	0·61
Na	0·60	12	0·32	17	0·27
K	5·2	22	1·1	6	0·64

of our present knowledge of these phenomena may be found in Robinson and Stokes, 1955). Non-associated electrolytes exist in the form of simple anions and cations, probably solvated. The associated electrolytes include those solutes that exist as undissociated, covalent molecules as well as ions; and the ion-pair electrolytes in which association arises as a result of purely electrostatic attraction between oppositely charged ions.

With respect to the major cations of marine waters, sodium, potassium, magnesium and calcium, it is of interest to consider the possible existence of associated electrolytes with the major anions, chloride and sulphate. Considerations on possible combinations of the alkali and alkaline earth metals with chloride ion may be neglected inasmuch as no evidence for such associations has been reported. Denney and Monk (1951) tabulate the dissociation constants of the associated electrolytes formed between the metals sodium, potassium, magnesium, and calcium and sulphate. Using these constants ($K_{Na_2SO_4} = 0{\cdot}19$ and $K_{K_2SO_4} = 0{\cdot}11$) and the values of the activity coefficients for uni-divalent salts from Latimer (1952, p. 354) of 0·4 for solutions with an ionic strength of 0·7, similar to that of sea-water, it is readily calculated that for the oceanic waters (Na = 0·45 M and $K = 0{\cdot}01$ M) much less than 1 per cent of either of these metals can be associated

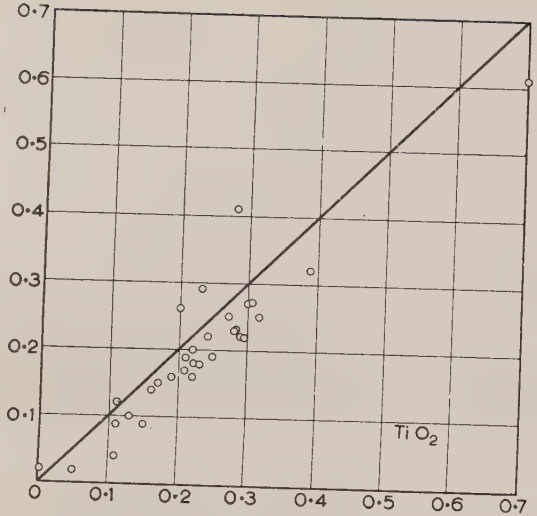

2(a)

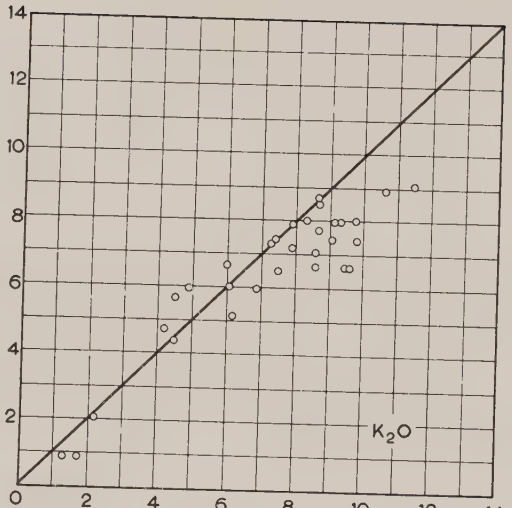

2(b)

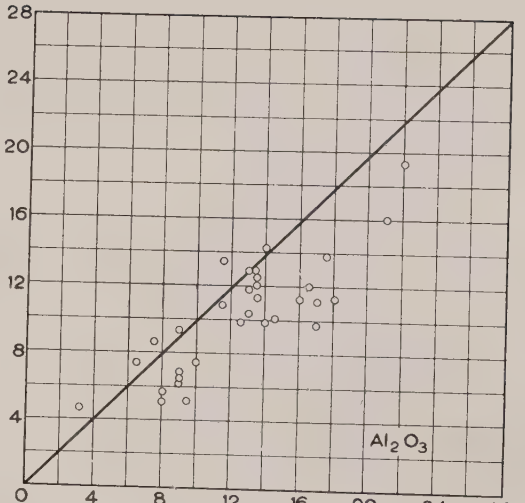

2(c)

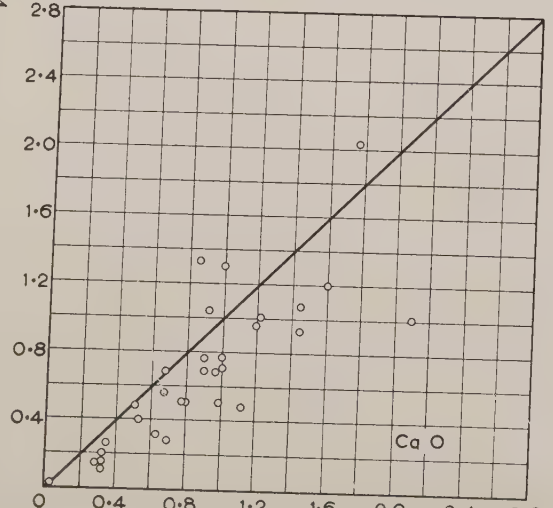

2(d)

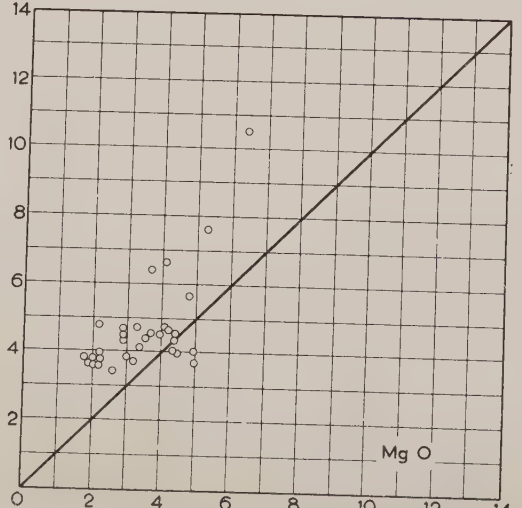

2(e)

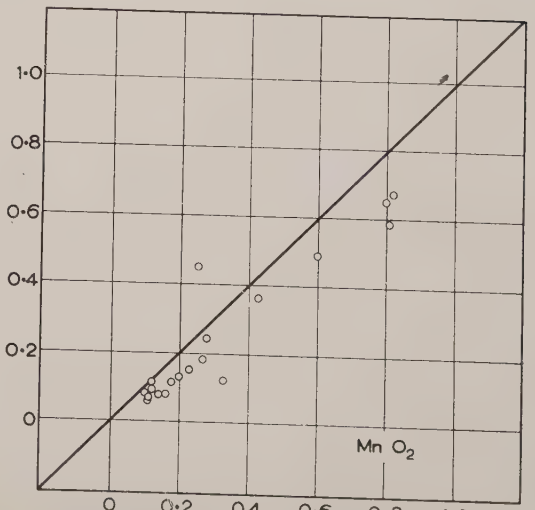

2(f)

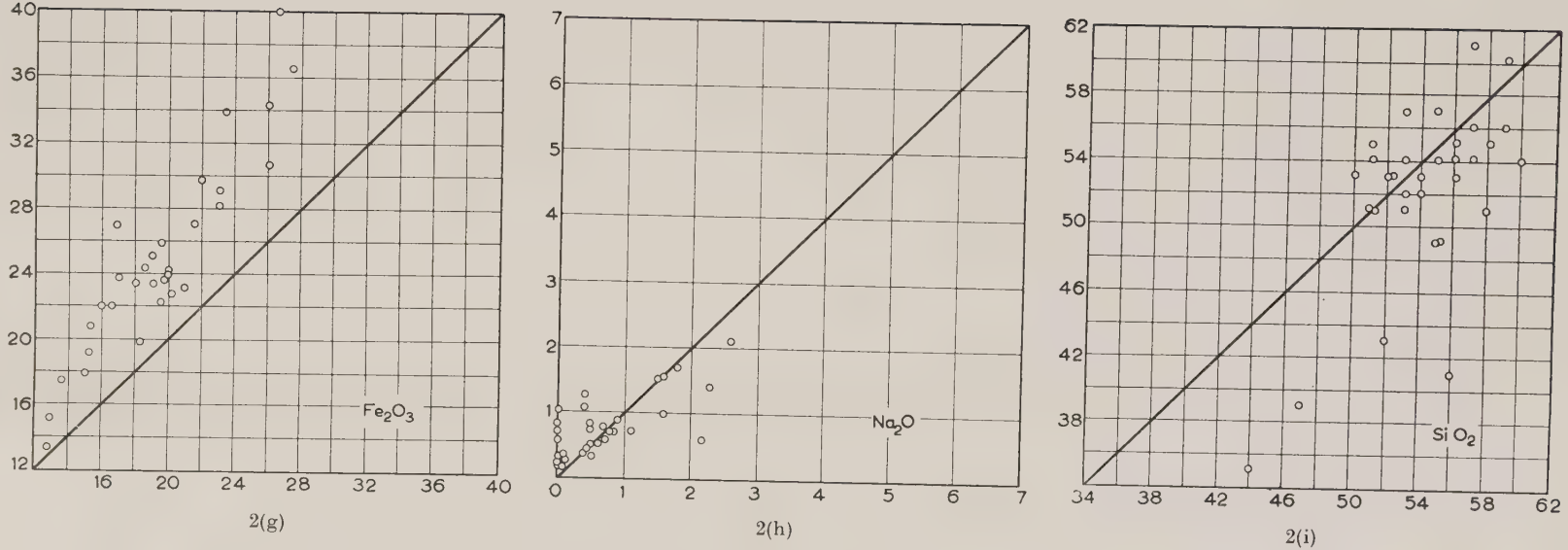

Fig. 2. Comparison of percentage yields obtained by spectrographic methods (abscissae) and colorimetric, volumetric, X-ray spectrometric or gravimetric methods (ordinates).

with sulphate ions. Further, the sulphate ion concentration (0·028 M) would not be significantly affected by such minor interactions.

Higher amounts of the alkaline earth sulphates probably exist in marine waters on the basis of such calculations. The dissociation constants of all divalent ions cluster about 0·005 for the sulphates (Robinson and Stokes, 1955, p. 405) and hence it appears justifiable to consider the magnesium and calcium as a single element for simplicity in calculations. Taking the sum of these ions in sea-water as 60 m moles/l., the sulphate concentration as 28 mM, and the activity coefficients for di-divalent salts as 0·12 (Latimer *op. cit.*), the amount of alkaline earth sulphates is 4 mM and accounts for about 7 per cent of the total content of these elements.

For the divalent group B metals such as nickel, copper, cobalt, and zinc, whose sea-water concentrations are of the order of 10^{-7}–10^{-8} M, approximately 10 per cent of the total amounts will be as associated sulphates. This observation complements those of Goldberg (1954) and Krauskopf (1956), who have emphasized the quantitative importance of the chloro-complexes of these elements. For copper, over 90 per cent of the non-sulphate associated forms would exist as the hydrated divalent ion or the $CuCl^+$ complex with but minor amounts of $CuCl_2$, $CuCl_3^-$, and $CuCl_4^{--}$. Similar speciation is expected for the other divalent group B metals whose hydrated ions have similar radii (Robinson and Stokes, 1955).

The work of Davies (1930) on the dissociation constant of $LaSO_4^+$ ($K = 2{\cdot}12 \times 10^{-4}$) suggests the existence of this pair and the corresponding ones for other rare earths in the marine environment. However, the absence of adequate concentration values of the rare earths in the oceans and of activity coefficients makes any computation unsatisfactory.

A second group of metals, including gold, silver, and mercury, probably occur principally as chloro-complex anions. Using the stability constant of Jonte and Martin (1952) for $AgCl_2^-$, a silver ion concentration in sea-water of 3×10^{-9} M, chloride ion concentration of 0·54 M, activity coefficients for silver and chloride ions of 0·7, it is readily calculated that over 99 per cent of the silver in sea-water exists as the di-chloro-complex. Similar calculations for mercury and gold suggest the dominance of the forms of $HgCl_4^=$ and $AuCl_4^-$ respectively (Lindgren, Johnson and Sillén, 1947; Bjerrum, 1948).

Other possible ion associations with the less abundant anionic species of sea-water as bromide, iodide, phosphate, bicarbonate, carbonate, hydroxide, and silicate could overshadow any of the above postulated species. However, at the present time dissociation constants are not available. Further, polynuclear complexes as described by Sillén (1954) may well exist in the marine environment. Mention should be made of possible organic complex and chelate formation. Again, we have no knowledge of the types of dissolved carbon compounds in the ocean, which exist at concentration of ca. 5 mg/l. of carbon.

4. Distribution of Elements in the Dissolved and Sorbed Phases of the Sediment

As pointed out in Section 2.21, dialysis of the sediment in distilled water probably changes the equilibrium between the pore solution and the surface of the solid, and the dialysate in this case therefore has to be regarded as representative

of the sum of dissolved and weakly sorbed species. The composition of the dialysate from five sediment samples is compared with the composition of sea-water in Table 7. Concentrations are expressed in mg/kg of pore solution and sea-water respectively.

Due to the high concentration of sodium, this element could not be accurately assayed by the spectrochemical methods used, and is omitted from the table. The composition of the sorbate exchanged against ammonium acetate (Section 2.22) and subsequently separated by dialysis, is shown in Table 8 together with the exchangeable fraction of the total amount of each element.

Within the limits of analytical error and variability, potassium, magnesium, and calcium occur in the same concentration in the dialysate as in sea-salt.

As is evident from Table 8, the proportions of the alkali and alkaline earth elements are drastically different in the sorbed phase from those in sea-water and in the dialysate. Calcium is in the sorbate in excess over magnesium and potassium, and both of these ions are more abundant than, or in one case equally concentrated as, sodium. The reason for the preponderance of calcium over magnesium in the exchangeable phase, in spite of the more than three times higher concentration of magnesium in the sea-water and in the pore solution, may be explained by the greater tendency for fixation of magnesium, shown by the fact that there is about twice as much magnesium as calcium in the colloidal fraction (Fig. 5, Cap. 50 BP) of the sediment after ion exchange and chelative dissolution. The potassium/sodium ratio of the sorbate is especially high in Cap. 31 BG, undoubtedly due to the high content in this sample of the potassium zeolite phillipsite. An amount of aluminium, corresponding to about a hundred times the concentration in the open ocean, is present in the dialysate, but only small additional amounts are exchangeable against ammonium ion, and appear in the sorbate. A considerable fraction of the chromium in the sediment gel appears to be loosely bound, so that a thousandfold concentration above sea-water occurs in the dialysate, and an amount, varying between 0·1 and 5 per cent of the total chromium is exchangeable against alkali cations (Table 8).

Iron and manganese are concentrated fifty to a few hundred times above the sea-water contents in the dialysate. Only small additional amounts of iron are present as exchangeable ions on the solid surfaces, whereas in the case of manganese a tenth of a per cent to a few per cent of the total amount appear to be in alkali-exchangeable positions. More detailed and significant exchange experiments on manganese minerals have been carried out by Buser and Grütter (1957, in press), employing solutions of divalent radioactive manganese.

Copper shows a still higher concentration in the dialysate and a half of a per cent to a few per cent exchangeable from the mineral surfaces.

Of yttrium, scandium, and the rare-earth elements none has been detected in the dialysate, and only yttrium in the sorbate. This indicates that these elements do not occupy exchange positions. They may partly have become fixed as phosphates on the surface of the microcrystallites of the apatite and partly are relatively strongly bonded in the manganese minerals.

Titanium and vanadium also are below detectability in the pore solution, but at least a few tenths of a per cent of the total amount of these elements are exchangeable.

Table 7. Concentration (c) of elements in mg/kg of dialysate (dissolved and weakly bonded species) and in sea-water, and concentration ratio (c/S) between dialysate and sea-water

Sample	K		Mg		Ca		Sr		Ba		B	
	c	c/S	c	c/S	c	c/S	c	c/S	c	c/S	c	c/S
Cap. 31 BG	390	1·0	860	0·7	240	0·6	1·4	0·11	0·6	100	22	4·9
Cap. 21–25 HG	315	0·8	1400	1·1	550	1·4	2·9	0·22	0·3	50	15	3·3
Yoyo 7P	315	0·8	480	0·4	220	0·6	3·2	0·25	6·4	1700	11	2·4
Cap. 50 BP 0–30	520	1·4	820	0·6	270	0·7	1·7	0·13	2·7	450	20	4·4
Cap. 49 BP top	500	1·3	1600	1·3	410	1·0	2·6	0·20	0·9	150	17	3·8
Sea-water (S)	380	1	1300	1	400	1	13	1	0·006	1	4·5	1

Sample	Si		Al		Cr		Fe		Mn		Cu	
	c	c/S	c	c/S	c	c/S	c	c/S	c	c/S	c	c/S
Cap. 31 BG	40	10	0·45	45	0·05	1000	0·26	52	—	—	1·4	470
Cap. 21–25 HG	36	9	3·40	340	0·05	1000	1·4	280	0·21	105	1·1	340
Yoyo 7P	84	21	0·67	67	0·05	1000	0·24	48	—	—	0·6	200
Cap. 50 BP 0–30	40	10	0·72	72	—	—	0·24	48	0·13	65	1·4	470
Cap. 49 BP top	40	10	1·10	110	—	—	0·26	52	1·06	530	0·8	270
Sea-water (S)	4	1	0·01	1	0·00005	1	0·005	1	0·002	1	0·003	1

Table 8. Percentage concentration of elements in sorbate (k); and fraction (q) of element in sorbate in per cent of total amount of element in sample (solid + dissolved + sorbed phases)

Sample	Na		K		Mg		Ca		Sr		Ba		B	
	k	q	k	q	k	q	k	q	k	q	k	q	k	q
Cap. 31 BG	1·8	1·0	11	12	7	6·5	15	7·0	0·15	8·0	0·9	16	10·038	6·3
Yoyo 7P	1·7	1·1	8·7	5·0	9	11	14	21	0·25	5·3	16	63	0·016	1·1
Cap. 50 BP 0-30	6·4	4·1	6·5	4·5	5	7	10	17	0·10	5·0	6	20	0·036	4·5
Cap. 49 BP top	1·5	0·8	9·5	7·5	8	9	12	12	0·23	13	16	27	0·016	2·3

Sample	Si		Al		Y		Ti		V		Cr		Fe	
	k	q	k	q	k	q	k	q	k	q	k	q	k	q
Cap. 31 BG	1·0	0·09	0·003	0·0009	0·002	0·4	0·09	0·15	0·018	1·6	0·0012	0·22	0·019	0·006
Yoyo 7P	0·6	0·02	0·007	0·001	0·002	0·4	0·07	0·31	0·008	0·4	0·0055	2·2	0·017	0·007
Cap. 50 BP 0-30	2·1	0·08	0·003	0·0009	0·003	0·8	0·04	0·22	0·003	0·5	0·0006	0·1	0·013	0·005
Cap. 49 BP top	0·4	0·01	0·004	0·0007	0·009	1·5	0·08	0·42	0·018	3	0·0090	5	0·012	0·005

Sample	Mn		Ni		Pb		Mo		Cu	
	k	q	k	q	k	q	k	q	k	q
Cap. 31 BG	0·04	0·05	0·017	1·7	—	—	—	—	0·62	2·0
Yoyo 7P	0·02	0·05	0·008	0·5	—	—	0·073	2·7	0·095	2·4
Cap. 50 BP 0-30	0·45	1·9	0·023	2·8	—	—	—	—	0·062	1·0
Cap. 49 BP top	0·12	0·13	0·007	0·4	0·007	1·2	0·018	2·2	0·036	0·4

Nickel, lead, and molybdenum likewise are missing in the pore solution. Nickel was found in the sorbate in all four cases investigated, lead in one, and molybdenum in two. The exchangeable fraction of these metals appears to vary from half a per cent to a few per cent of the total amount in the sample.

Gallium, cobalt, silver and zirconium were detected neither in the dialysates nor in the sorbates.

Strontium is five to ten times depleted in the pore solution, and a rather large fraction of the total amount of this element is sorbed to the solid phases (Table 8).

The relatively large amounts of barium in the dialysate and in the sorbate may be explained at least partly as resulting from dissolution of microcrystalline barite during dialysis, when the sulphate ion concentration is decreased by a factor of 30–60, and during the ion exchange in ammonium acetate. A considerable fraction of the barium found in the sorbate (Table 8) is, however, certainly originally present as exchangeable cations sorbed in the zeolite structure (Section 5.4), and probably on the clay minerals, which in contact with barite are known to be able to retain enough barium to fill about 20 per cent of the exchange positions (Bradfield, 1932).

Boron shows a 2- to 5-fold excess in the dialysate over sea-water, and 1–7 per cent of the total amount originally present is removed from the solids at ion exchange.

Silicon as the univalent ion of monosilicic acid, or other species small enough to pass through the dialysis membrane, is ten to twenty times more concentrated in the dialysate than in sea-water. If the dissolved species are separated by centrifugation, and a less strict size limitation thus applied, still higher relative concentrations are obtained (of the order 200 mg/kg—Arrhenius and Rotschi unpublished). A steep gradient in the silicon content of the near bottom water was found by these authors at all South Pacific stations investigated, indicating a flow of dissolved silica from the bottom sediments back into the ocean.

5. Distribution of Elements in the Solid Phases

Table 9 gives the average chemical composition of 22 pelagic sediment cores from the eastern Pacific along with various igneous rock types and the average crustal composition of the earth. Cores Cap. 32 HG, 33 HG, NH 9, and MP 38 are calcareous oozes and the analyses are given both on a calcium carbonate-free basis and on the total material. The core descriptions and locations are presented in Table 1. Figs. 3 and 4 are a graphic representation of the data of Table 9. The ranges of the ratio of the concentration of the element in pelagic sediments to the concentration in igneous rocks are plotted for each element. The mode is noted by a small vertical line.

Fig. 5 shows some features of the chemical composition of sediment samples, which have been fractionated according to grain size, and to a limited extent according to density. Separation according to grain size corresponds to a rough fractionation of different minerals and mineral groups, and indications of the mineral localization of different elements can thus be obtained from analysis of these fractions. The details of the construction of the diagrams are given in the caption, and the conclusions drawn from the distributions are found in the paragraphs on different elements below.

Table 9. Chemical compositio

No.	Core	Si	Al	Fe	Ti	Mg	Ca	Na	K	Sr	Ba	B	Mn	C
1	Cap. 21 HG	21·3	10·8	6·2	0·78	1·8	3·3	4·5	2·6	0·050	0·069	0·029	1·5	0·00
2	Cap. 23 HG	20·6	11·6	6·0	0·75	1·8	4·0	4·7	2·5	0·047	0·062	0·030	1·0	0·00
3	Cap. 24 HG	21·4	10·3	6·2	0·84	1·9	4·7	3·8	2·4	0·055	0·093	0·030	1·2	0·00
4	Cap. 30 BP	23·4	8·8	5·7	0·56	1·3	4·4	3·6	3·4	0·027	0·057	0·011	1·8	0·00
5	Cap. 25 HG	22·9	8·7	6·8	1·44	2·3	3·1	3·9	2·2	0·063	0·128	0·033	1·3	0·00
6	Cap. 31 BG	22·4	9·4	6·7	1·22	2·1	4·2	3·5	1·8	0·035	0·11	0·012	1·7	0·00
7	Cap. 33 BG	22·0	7·8	6·2	0·36	1·9	5·9	4·4	2·2	0·041	0·26	0·0096	3·0	0·00
8	Sw. 71	23·5	8·1	4·6	0·38	2·2	3·5	6·3	2·2	0·048	0·14	0·028	1·4	0·00
9	Cap. 32 HG	12·0	4·4	9·2	0·39	1·5	16·3	3·7	—	0·072	0·69	0·022	2·2	–
	Cap. 32 HG ($CaCO_3$ free)	16·2	6·2	12·9	0·49	2·1	—	5·7	1·9	0·14	0·99	0·03	3·2	0·00
10	Cap. 33 HG	3·6	1·0	3·7	0·05	0·60	3·2	2·4	—	0·076	0·30	0·012	1·2	–
	Cap. 33 HG ($CaCO_3$ free)	13·4	3·3	14·0	0·23	2·4	—	10·4	—	0·35	1·3	0·049	4·5	–
24	Cap. 49 BP	26·2	8·4	4·6	0·38	1·7	2·0	3·9	2·5	0·035	1·2	0·014	0·87	0·00
26	Cap. 50 BP	27·5	8·0	5·0	0·43	1·5	1·1	3·1	2·9	0·021	0·60	0·016	0·48	0·00
27	Y3G	25·8	9·9	4·9	0·50	1·8	1·1	2·6	3·5	0·038	0·37	0·034	0·58	0·00
27	Y2P	25·7	9·4	4·6	0·45	1·6	1·3	3·2	3·5	0·047	0·51	0·030	0·82	0·00
28	MP 38	28·7	10·3	3·5	0·43	2·4	5·8	4·1	3·1	0·061	0·16	0·031	1·6	0·00
29	NH 9	8·1	3·9	5·0	1·06	1·6	23·9	1·5	0·71	0·093	0·078	0·032	0·12	0·00
	NH 9 ($CaCO_3$ free)	18·7	9·0	11·6	2·5	4·3	—	3·5	1·6	0·23	0·17	0·076	0·27	0·00
30	NH 12	22·1	11·9	6·4	1·1	2·0	3·1	3·1	1·7	0·043	0·19	0·031	0·30	0·00
31	NH13	23·2	11·4	5·9	0·90	2·1	2·3	2·9	2·5	0·044	0·25	0·035	0·31	0·00
32	NH 14	23·4	11·5	5·8	0·78	1·8	1·9	2·9	2·7	0·041	0·23	0·037	0·33	0·00
33	WW 5	26·9	9·4	4·6	0·49	2·4	1·2	2·8	2·2	0·040	0·60	0·029	0·46	0·00
34	NG 2	25·8	8·9	5·1	0·50	1·8	1·6	3·1	2·4	0·054	0·59	0·028	0·38	0·00
35	NG 3	25·9	10·1	5·1	0·50	1·8	1·3	3·0	2·5	0·049	0·54	0·029	0·41	0·00
36	Ck 2	24·7	7·8	5·7	0·44	2·2	2·1	2·6	2·9	0·030	0·11	0·032	1·6	0·00
37	Ck 4	28·1	8·7	4·7	0·49	2·1	1·1	2·6	2·7	0·019	0·38	0·032	0·51	0·00
38	Ck 8	31·2	6·0	4·0	0·33	2·3	2·9	2·6	1·1	0·036	0·10	0·014	0·14	0·00
39	Ck 9	33·3	4·9	2·4	0·25	1·7	3·0	2·3	1·2	0·028	0·10	0·017	0·11	0·00
1–35	Average	23·0	9·2	6·5	0·73	2·1	2·9	4·0	2·5	0·071	0·39	0·030	1·25	0·00
	Pelagic Deposits[m]	—	—	—	0·40	—	—	—	—	0·06	0·81	—	—	–
	Basalts	23·3[a]	8·5[a]	8·8[a]	0·84[a]	3·8[a]	6·5[a]	2·4[a]	1·2[a]	0·05[b]	0·007[c]	0·0005[c]	0·15[a]	0·00
	Polynesian basalts[n]	22·0	7·9	9·0	1·7	5·5	6·3	2·1	1·2	0·086	0·04	—	0·14	0·00
	Granites	33·1[a]	7·7[a]	2·5[a]	0·25[a]	0·54[a]	1·4[a]	2·6[a]	3·4[a]	0·02[b]	0·048[c]	0·001[c]	0·1[a]	0·00
	Igneous rocks	27·0[f]	8·0[f]	—	0·5[f]	2·0[f]	3·5[f]	2·8[f]	2·5[f]	0·03[f]	0·025[f]	0·003[f]	0·1[f]	0·00
	Igneous rocks[m]	—	—	—	0·44	—	—	—	—	0·022	0·099	—	—	–

[a] Daly (1933).
[b] Turekian (1955).
[c] Goldschmidt (1954).
[d] Sandell (1949).
[e] Turekian (1956.
[f] Sandell and Goldich (1943).
[g] Sandell (1952).

pelagic sediments in weight per cent

Ni	Cu	Co	Cr	V	Pb	Be	Mo	Zr	Yb	Y	La	Sc
0·028	0·077	0·031	0·006	0·043	0·017	—	0·0065	0·020	0·0019	0·016	0·010	0·0018
0·034	0·063	0·023	0·008	0·047	0·016	—	0·0058	0·019	0·0021	0·024	0·014	0·0023
0·043	0·072	0·029	0·007	0·046	0·020	—	0·0066	0·020	0·0023	0·028	0·016	0·0022
0·031	0·068	0·019	0·0048	0·014	0·021	0·00036	0·0036	0·0096	0·0034	0·031	0·016	0·0049
0·030	0·071	0·023	0·014	0·060	0·017	—	0·0051	0·026	0·0017	0·016	0·012	0·0021
0·019	0·064	0·017	0·011	0·023	0·026	0·00061	0·0021	0·016	0·0014	0·013	0·0044	0·0026
0·039	0·14	0·024	0·014	0·020	0·021	0·00036	0·0008	0·013	0·0039	0·039	0·025	0·0044
0·047	0·011	0·027	0·002	0·042	0·011	—	0·0101	0·018	0·0029	0·039	0·024	0·0030
0·048	0·087	0·013	0·002	0·033	0·012	—	0·0087	0·019	0·0022	0·026	—	—
0·064	0·105	0·018	0·004	0·060	0·018	—	0·0107	0·026	0·0032	—	0·023	0·0019
0·016	0·010	0·005	0·0015	0·037	—	—	—	0·008	—	0·009	—	—
0·056	0·038	0·019	0·007	0·18	—	—	—	0·039	—	0·031	—	—
0·031	0·20	0·011	0·0037	0·012	0·012	0·0003	0·0017	0·012	0·0013	0·013	0·0040	0·0037
0·017	0·12	0·0098	0·0062	0·013	0·011	0·00036	0·0011	0·013	0·0011	0·0094	0·0029	0·0028
0·025	0·050	0·012	0·009	0·042	0·008	—	0·0044	0·018	0·0008	0·005	0·005	0·0017
0·035	0·077	0·019	0·005	0·043	0·009	—	0·0055	0·022	0·0012	0·010	0·008	0·0021
0·083	0·093	0·031	0·005	0·025	0·008	—	0·011	0·017	—	0·0038	0·033	0·0040
0·009	0·008	0·001	0·019	0·041	—	—	—	0·010	—	—	—	—
0·028	0·017	0·004	0·04	0·097	—	—	—	0·022	—	—	—	—
0·014	0·035	0·005	0·12	0·045	—	—	0·0022	0·016	—	0·003	—	0·0018
0·014	0·037	0·005	0·013	0·040	—	—	0·0021	0·017	—	0·003	—	0·0014
0·014	0·040	0·005	0·010	0·038	—	—	0·0021	0·017	—	0·003	—	0·0012
0·016	0·066	0·009	0·010	0·031	—	—	0·0037	0·018	—	0·005	—	0·0022
0·014	0·035	0·003	0·006	0·035	—	—	0·0024	0·014	—	0·002	—	0·0022
0·013	0·041	0·004	0·007	0·034	—	—	0·0028	0·014	—	0·002	—	0·0010
0·026	0·038	0·009	0·008	0·021	0·010	—	—	0·023	—	0·017	—	0·0028
0·016	0·027	0·006	0·010	0·012	0·005	—	—	0·020	—	0·004	—	0·0031
0·003	0·010	0·001	0·006	0·014	0·012	—	—	0·010	—	0·002	—	0·0020
0·002	0·009	0·001	0·004	0·012	0·012	—	—	0·010	—	0·002	—	0·0018
0·032	0·074	0·016	0·0093	0·045	0·015	—	0·0045	0·018	0·0021	0·015	0·014	0·0025
0·026	—	0·009	0·0082	0·015	—	—	—	0·013	—	—	0·022	0·0031
0·013[e]	0·0087[e]	0·0025[f]	0·0172[e]	0·02[c]	0·0006[l]	0·0001[g]	0·0001[h]	—	—	—	—	—
0·04	—	0·006	0·044	0·05	—	—	—	0·023	—	0·002	—	—
0·005[f]	0·003[f]	0·008[c]	0·001[c]	0·005[c]	0·0019[l]	0·0003[g]	0·0001[h]	—	—	—	—	—
0·004[k]	0·004[k]	0·002[i]	0·02[i]	0·015[i]	0·0015[l]	0·0002[g]	0·0001[h]	0·0156[h]	0·003[i]	0·003[i]	0·002[i]	0·0005[i]
0·0079	0·0020	—	0·010	0·02	—	—	—	—	—	—	0·0045	0·0020

[b]) Kuroda and Sandell (1954).
[j]) Fleischer (1953).
[l]) Degenhardt (1957).
[g]) Morita (1955).
[f]) Wedepohl (1956).
[m]) Young (1954).
[n]) Nockolds and Allen (1956).

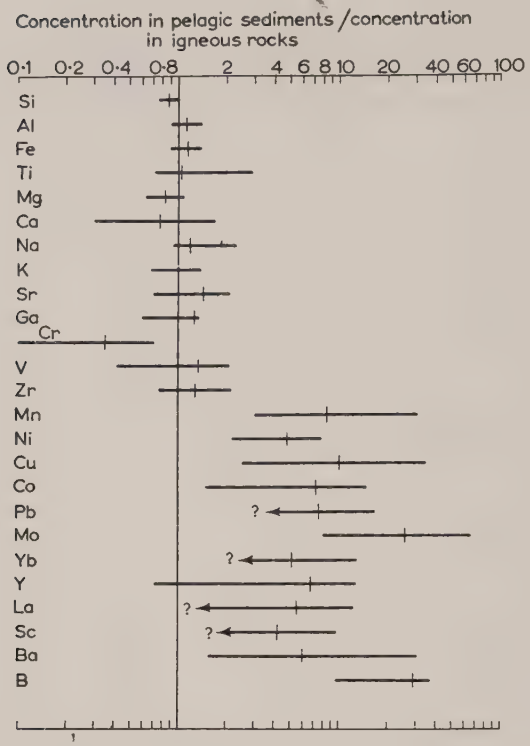

Fig. 3. Ratios of average elemental abundances in Pacific pelagic sediments and igneous rocks. Ranges are indicated by the lengths of the horizontal lines, and modes by a short vertical line.

5.1. *Silicon, aluminium, and gallium.* The overall range of silicon values is somewhat lower than in igneous rocks, and this probably results from a large portion of the silicon being incorporated into siliceous oozes and into continental sediments high in quartz. The silicon is mainly contained in the clay minerals and further in phillipsite in cores Cap. 31 BG; opal, quartz, and feldspar in Cap. 49 BP; quartz, feldspar, and opal in Cap. 50 BP; and quartz, feldspar, biotite, and muscovite in Y3G and Y2P. The quartz contents of some of these cores (49 BP, 50 BP, Y3P, NH 12, NH 13, and Wigwam 5) varies between 9 and 16 per cent. Both quartz and feldspar are on the average coarser in the north equatorial Pacific (cores Yoyo 7P and Cap. 50 BP), than further south and concentration of quartz is also higher in the northern area. More elaborate investigations upon the distribution and characteristics of detrital minerals have been carried out by Rex and Goldberg (in preparation).

A proportionality is observed between average crystal size and concentration of phillipsite. This probably depends on the longer time available for individual crystals to grow in areas of a low rate of deposition, where high concentrations of phillipsite and other marine hydrogenous minerals are found.

The aluminium concentrations show a small variation about the igneous rock average. In the sediments, only a fraction of a per cent of the aluminium can be

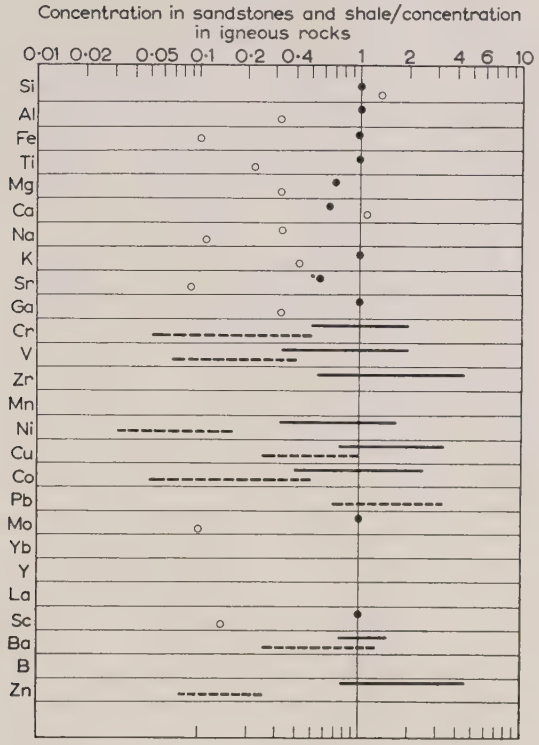

Fig. 4. Ratios of average elemental abundances in sand stones and igneous rocks (ranges marked by dashed lines, averages by open circles), and in shales and igneous rocks (solid lines and circles). Data for igneous rocks from FLEISCHER (1953) and for sandstones and shale from GOLDSCHMIDT (1954), RANKAMA and SAHAMA, (1949), and KRAUSKOPF (1956).

removed by chelative dissolution. The main occurrence of aluminium is in the aluminosilicates listed above.

A high organic productivity in the surface layer of the ocean should result in a high content of diatomaceous and radiolarian silica relative to inorganic constituents in the bottom deposit. This distribution has been verified in a north–south profile through the east equatorial Pacific (ARRHENIUS, 1952, 1.3), and is further illustrated by the data in Table 10, which presents the average ratio Si/Al in sediment cores as a function of latitude. The general increase of the ratio in the equatorial zone of high productivity is evident. Another area with high values for the ratio Si/Al is the sub-arctic productivity zone, where, in the absence of calcium carbonate, diatomaceous remains are the dominant component in the deposits (core Ck 8 and Ck 9, Table 10).

The gallium content of the clays is for all practical purposes constant and corresponds to the igneous rock value.

5.2. *Sodium, potassium and lithium.* Both sodium and potassium occur in concentrations comparable to those of igneous rocks. It should be emphasized that the unfractionated sediment samples contain the salts of the pore solution. The principal mineral group, the clays, contain the bulk of the potassium, and

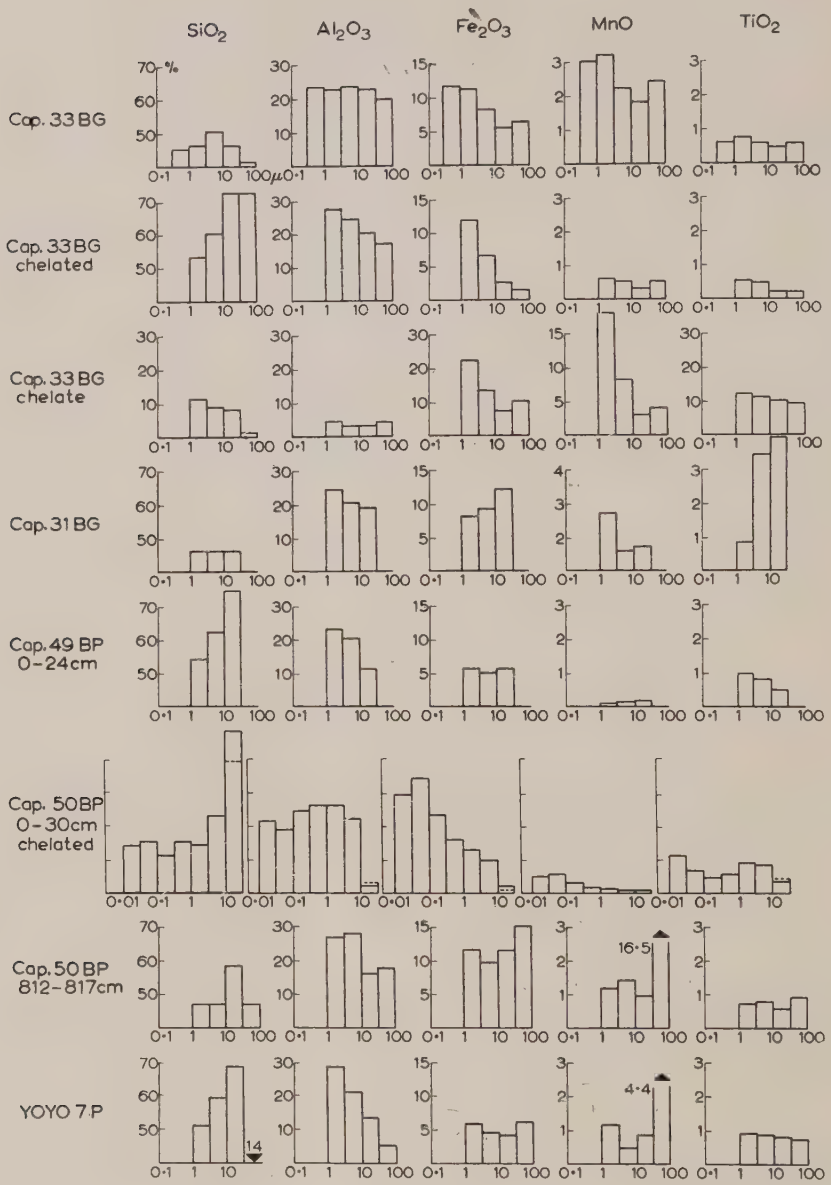

Fig. 5(a).

Fig. 5. Composition of grain size fractions of pelagic clay sediments. The different samples are grouped vertically, and the distributions of properties horizontally. Within the histograms concentrations of element oxides in percent, and size frequencies in percent, are represented by the ordinates. The particle size in μ, on a logarithmic scale, is indicated by the abscissae.

For location and type of samples, see Table 1. For explanation of the chelation procedure (see Section 2.25).

In the sample Cap. 50 BP 0–30 cm, the size fraction 10–32 μ has been subdivided into two density fractions, one mainly containing grains with a density less than 2·5 (full line in

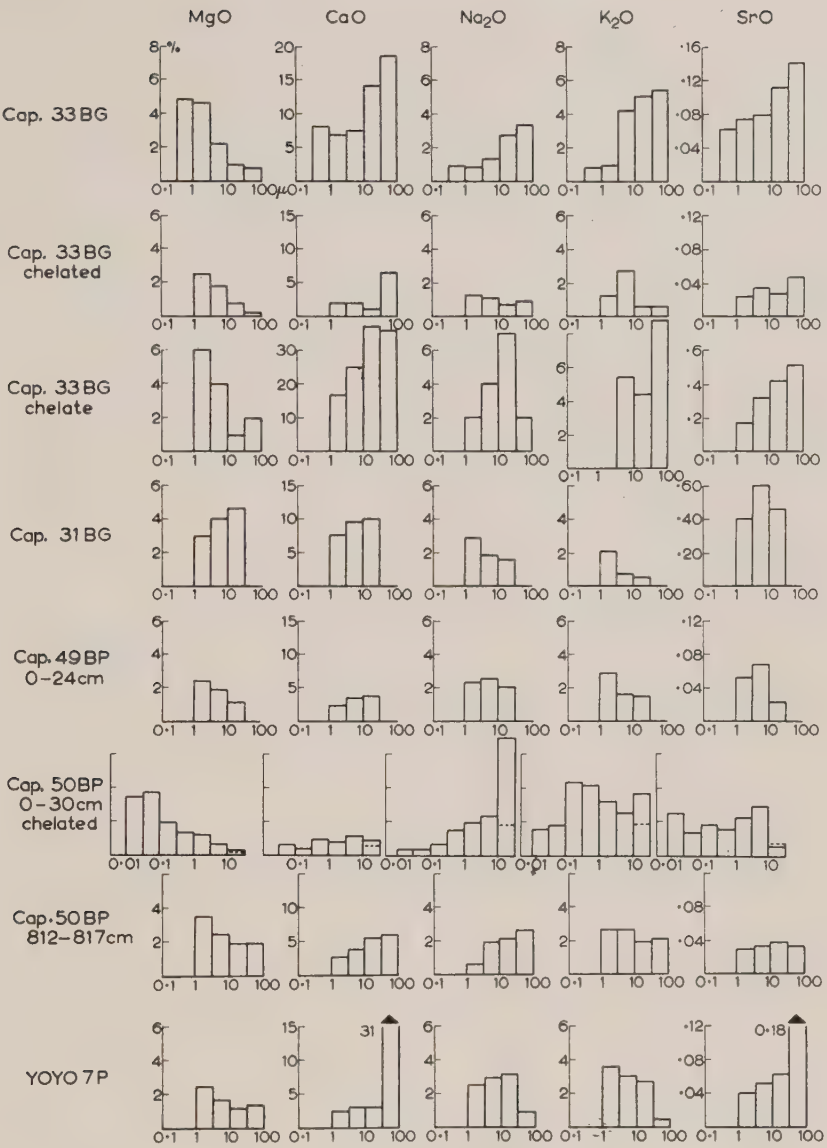

Fig. 5(b).

histograms), the other mainly with particles denser than 2·5 (dashed line in histograms). In this sample ordinate units have been omitted for space reasons. The ordinate scale is in this case always the same as in the corresponding histograms for the adjacent sample Cap. 50 BP, 812–817.

In cases where off-scale high concentrations occur, these have been indicated by a number drawn at the side of an open histogram rectangle, marked by an arrow, pointing upward (ex. BaO in Yoyo 7P, 32–100 μ).

Arrows pointing downward indicate concentrations below the sensitivity limit (ex. Co_2O_3 in Cap. 33 BG) or if a figure is simultaneously given, below the range of the scale (ex. SiO_2 in Yoyo 7P, 32–100 μ).

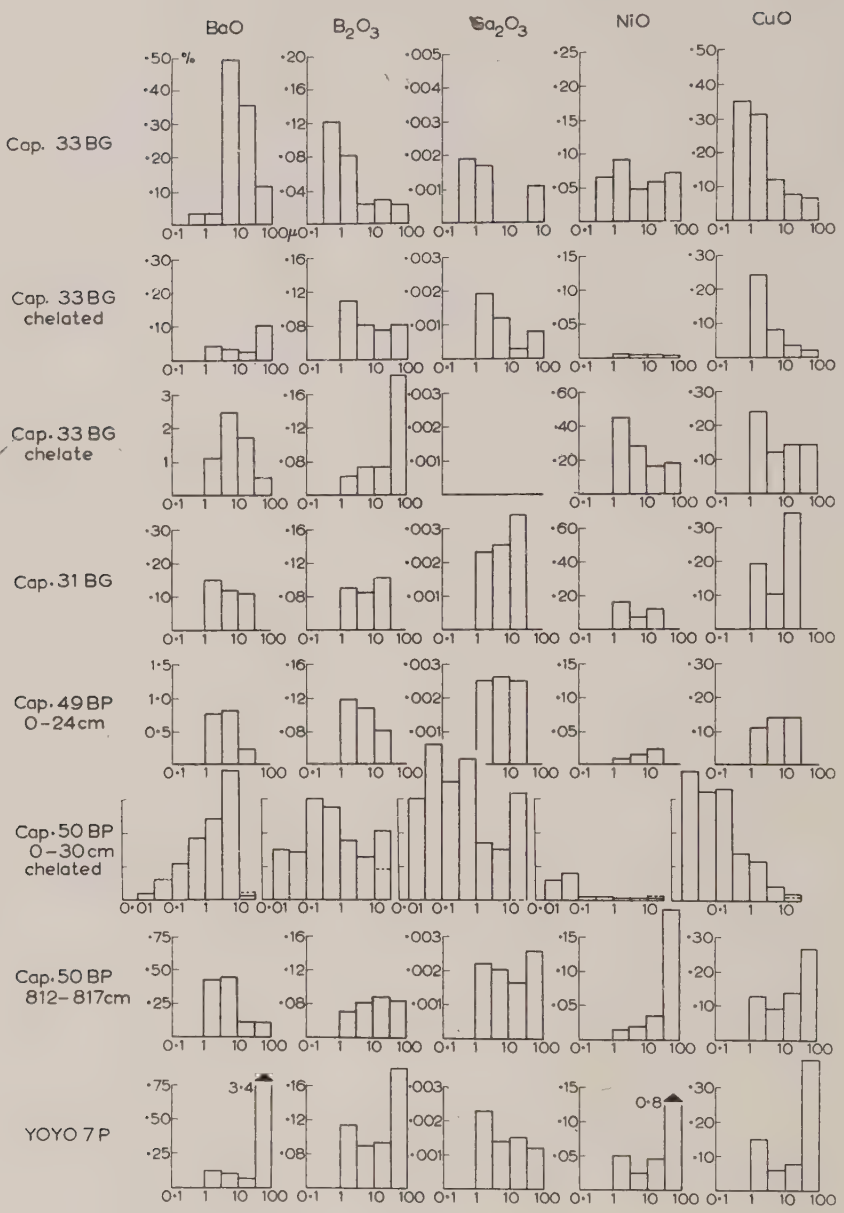

Fig. 5(c).

much of the sodium, yet individual minerals often show higher concentrations. Potassium appears concentrated in phillipsite,* and sodic feldspars contribute significantly to the total sodium content.

* The composition of a mixture of phillipsite and apatite is shown by the analysis of the coarse fraction of Cap. 33 BG (Fig. 5) which consists practically entirely of these two minerals. The difference in composition of apatite and phillipsite can be judged by comparing the above mentioned fractions with the 32–100 μ fraction of Yoyo 7P (Fig. 5), which in addition to the ferromanganese oxide minerals in the form of micronodules and barium-bearing pellets contains large amounts of apatite but no phillipsite.

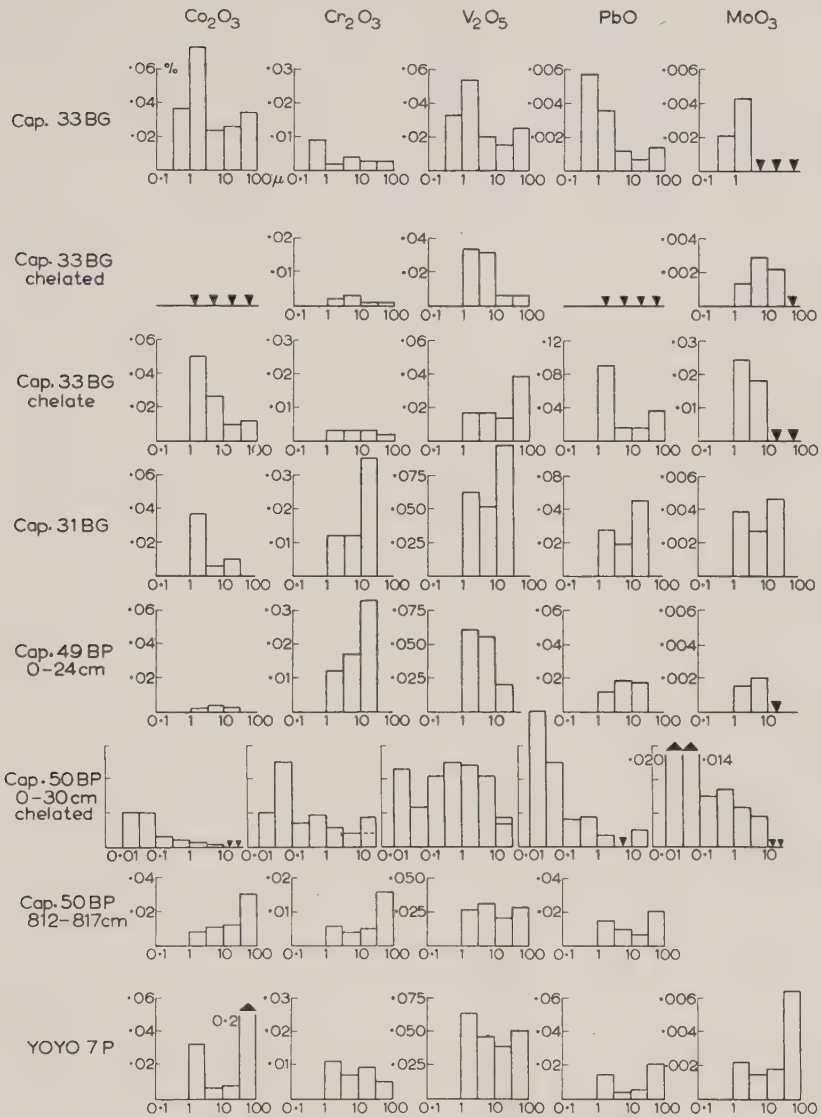

Fig. 5(d).

The lithium contents of a selected group of sediments (Table 11) fluctuate around the igneous rock value of 65 p.p.m. (Rankama and Sahama, 1950, p.143).

5.3. *Magnesium, calcium, and strontium.* The concentration of fixed magnesium increases with decreasing grain size, indicating that the main part of this element is bonded in the clay minerals. An exception is core 31, where large amounts of igneous ferromagnesian minerals occur.

In slowly depositing carbonate-free pelagic clays, comparatively large quantities of calcium (approximately 10 per cent) are stored in phillipsite and biogenous apatite. This calcium is largely removable by chelation. The amounts proxying

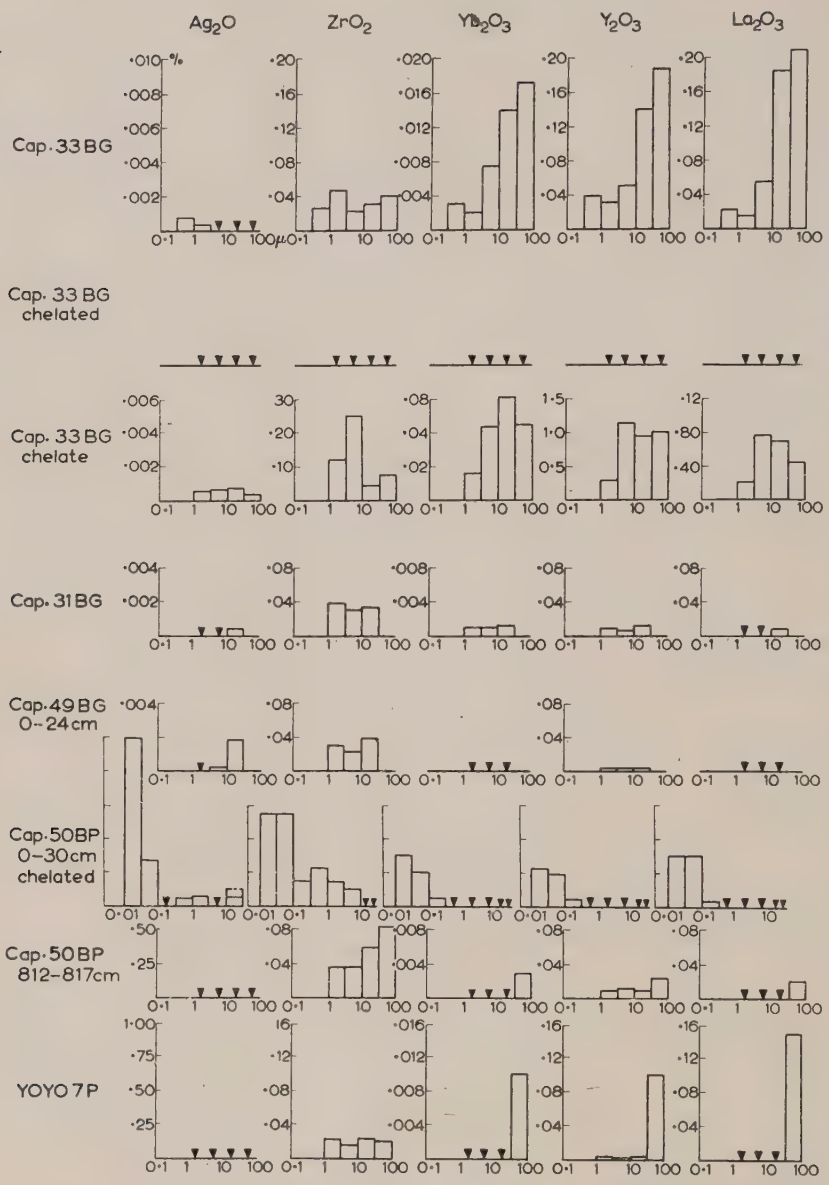

Fig. 5(e).

in ferromanganese oxide minerals are unknown, but may be important. A minor source of calcium is feldspar, whereas the clay minerals appear to be low in calcium. Pyroxenes contribute significantly in cores with a high content of pyroclastics.

The calcium/magnesium ratio is higher in the calcareous oozes than in clays as is evidenced by cores Cap. 32 HG and 33 HG. This is expected as magnesium is usually less abundant than calcium by an order of magnitude in calcareous tests (Clarke and Wheeler, 1922; Chave, 1954). The low values of both calcium

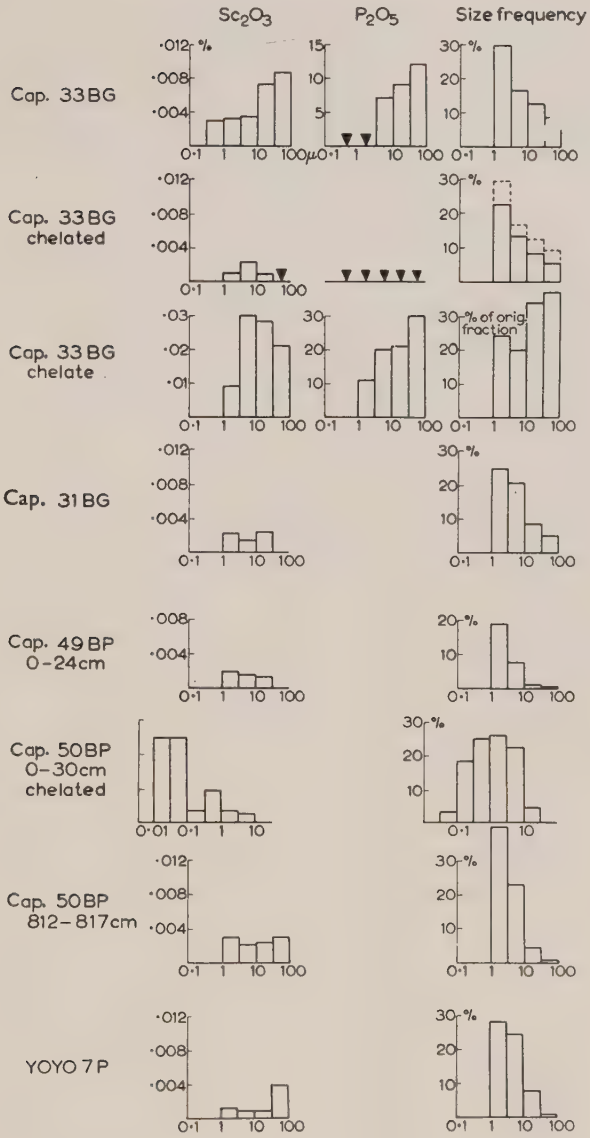

Fig. 5(f).

and magnesium in clays as compared to igneous rocks are compensated by the high concentrations of these elements in the calcareous oozes.

In the minerals, which are quantitatively important in the sediments investigated, high concentrations of strontium are found in the apatite phase of the fish debris (Arrhenius *et al.*, *op. cit.*) where it ranges between 0·2 and 0·7 per cent, and in calcite of pelagic planktonic fossils (0·1–0·2 per cent) (Thompson and Chow, 1955). High concentrations might also be expected in phillipsite and in the ferromanganese oxide minerals, whereas the sediment fractions $<3{\cdot}2\ \mu$, which

Table 10. Silicon/aluminium ratios of Pacific sediments

Core	Lat.	Long.	Si/Al	Average ratio
Ck 8	53°02′N	176°15′W	5·2	6·0
Ck 9	52°25′N	176°25′W	6·8	
Wigwam 5	27°38′N	124°26′W	2·6	
NH 14	24°08′N	156°04′W	2·0	
NH 13	23°22′N	156°29′W	1·9	
NH 12	22°49′N	156°50′W	1·9	2·3
NH 9	21°41′N	157°29′W	2·1	
Y3G	20°49′N	125°15′W	2·6	
Y2P	20°49′N	125°15′W	2·7	
MP 38	19°01′N	177°19′W	2·8	
Cap. 50 BP	14°55′N	124°12′W	3·4	
Cap. 49 BP	9°17′N	124°9′W	3·1	
Sw 71	7°38′S	152°53′W	2·9	3·1
Cap. 33 HG	10°58′S	138°30′W	3·8	
Cap. 32 HG	11°00′S	130°24′W	2·7	
Cap. 33 BG	12°46′S	143°33′W	2·8	
Cap. 21 HG	16°36′S	162°43′W	2·0	
Cap. 23 HG	16°58′S	161°35′W	1·8	
Cap. 25 HG	16°53′S	159°8′W	2·6	
Cap. 24 HG	16°44′S	161°35′W	2·1	2·3
Cap. 30 BG	17°28′S	160°59′W	2·7	
Cap. 31 BG	17°29′S	158°40′W	2·4	

Table 11. Lithium concentrations in Pacific pelagic clays*

Sample	Li (p.p.m. by weight)
Cap. 31 BG 16	58
Cap. 50 BP 44	67
Cap. 50 BP 108	70
Cap. 50 BP 376	51
Cap. 50 BP 760	49

* These analyses were performed by precision emission spectrography by Mr. Arthur Chodos, California Institute of Technology.

consist mainly of clay minerals, have strontium contents of the order 0·05 per cent. The highest concentrations relative to aluminium consequently are found in calcareous oozes (Cap. 32 and 33 HG and NH 9, Table 9).

5.4. *Barium.* The high content of barium in the east equatorial Pacific sediments was first demonstrated by Steiger and Revelle (Revelle, 1944, pp. 66, 68). The correlation between calcium carbonate and barium concentrations was pointed out by the latter author (p. 68), who suggested that the barium in these sediments has been precipitated as the carbonate.

From previous results on the relation between the organic productivity in the surface layer of the ocean and the composition of the sediment below (ARRHENIUS, 1952, *loc. cit.*), it appeared probable that the rate of accumulation of barium, if this element is precipitated by organisms, would be a function of the rate of organic production in the euphotic zone. To check this assumption, the barium content

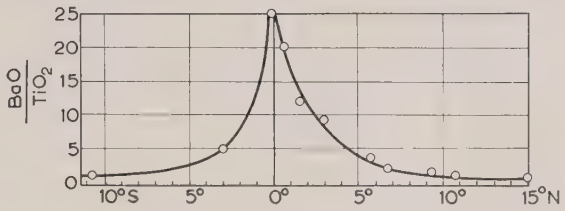

Fig. 6. Relative rate of accumulation of barium as a function of latitude, across the equatorial zone of high organic productivity. The rate is represented by the ratio BaO/TiO_2.

Table 12. Rate of accumulation of barium expressed as the ratio BaO/TiO_2 in a meridional profile through the Glacial and Postglacial strata under the equatorial zone of high productivity, and in a diatomaceous ooze from the Bering Sea

Core	Stratum (cm)	Lat.	Long.	BaO/TiO_2
Cap. 50 BG	0–30	14°58′N	124°12′W	0·8
Cap. 49 BG	0–30	9°17′N	124°9′W	1·5
Sw 58	0–30	6°44′N	129°28′W	2
Cap. 48 BG 1	0–50	5°45′N	124°2′W	3
Sw 59	0–80	3°05′N	133°6′W	9
Sw 60	0–150	1°35′N	134°57′W	11
Cap. 47 BG	0–80	0°40′N	123°33′W	20
Sw 61	190–200	0°6′S	135°48′W	25
Sw 62	0–56	3°0′S	136°26′W	5
Cap. 36 BG 1	9–108	10°45′S	133°35′W	1
Ck 8 (diatomaceous)	5–20	53°1′N	176°15′W	0·6

of the surface layer of the sediment was determined by X-ray spectrometry (Section 2.3) in a meridional profile at approximately long. 125°W, extending from the north Pacific clay area over the zone of high productivity in the equatorial divergence (ARRHENIUS, 1952, STEEMAN-NIELSEN, 1952) and into the south equatorial Pacific (Fig. 6). The amount of titanium per unit surface area is known to be practically constant within each time-rock unit of the Late Pleistocene-Recent series in the calcareous basin sediments of this profile (ARRHENIUS, 1952, 1.2.5) and an expression for the rate of accumulation of barium is therefore given by the ratio BaO/TiO_2, which is plotted as a function of latitude in Fig. 6. The corresponding data are also compiled in Table 12. As is seen from these, the rate of accumulation of barium is more than twenty times higher under the productivity zone of the equatorial divergence than outside the zone 10°N–10°S, and the increase toward the equator is remarkably regular.

The relationship between the present productivity of the surface layer of the

ocean and the recent rate of accumulation of barium on the ocean floor below, thus appears beyond doubt.

Marked variations in time of the organic productivity are inferred from the stratification of the sediments below and near the equatorial divergence (Arrhenius, *op. cit.*, 1.1.6, 1.9). A number of cores, displaying the typical alternation of calcareous and clayey strata, were therefore analysed for calcium carbonate,

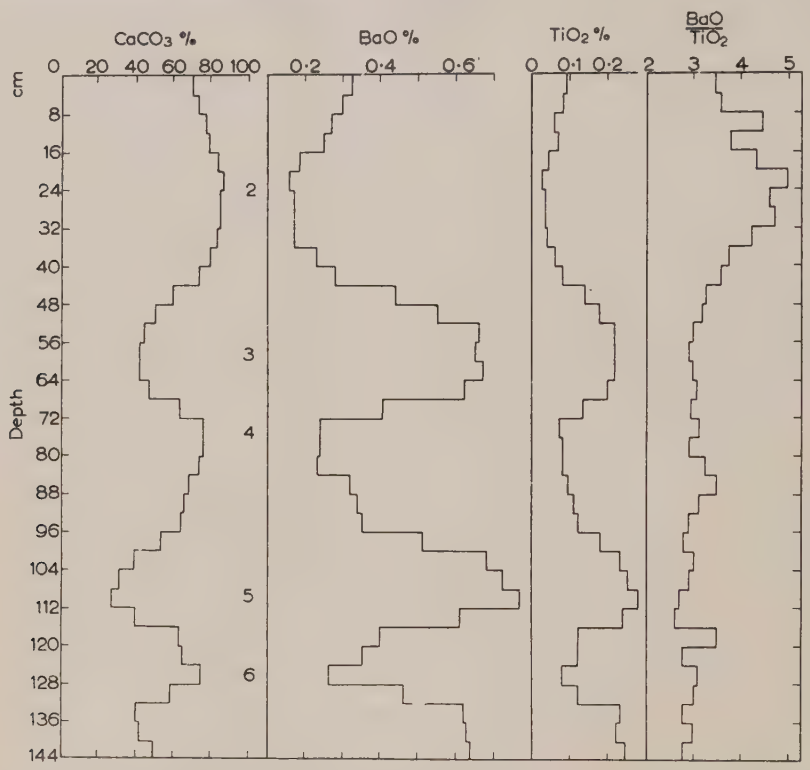

Fig. 7. Vertical distribution of calcium carbonate, titanium oxide and barium oxide, and the ratio BaO/TiO_2 in the core Cap. 48 BG1 (Table 12). The figures at the carbonate maxima and minima refer to the culmination of the stages earlier described (Arrhenius, 1952, 1.1.5.).

titanium, and barium. An example of the vertical distribution of these parameters is shown in Fig. 7. A relatively high barium/titanium ratio occurs only in the last productivity maximum (2). The penultimate productivity maximum, which, judging from paleotemperature distribution (Emiliani, 1955) and rate of accumulation of diatoms, coccoliths, and foraminifera (Arrhenius, *op. cit.*, 3.3.1, 3.4.2), was the highest of all, the increase in the Ba/Ti ratio is hardly noticeable, and in still older strata corresponding to ages of high productivity in the equatorial divergence, no increase whatsoever can be found in this ratio.

It appears from these results that a slow post-depositional migration of barium takes place in the sediments; this has completely levelled the original gradients of the Ba/Ti ratio in strata with an age of the order of 200,000 years or more. The relatively high mobility of barium in the deposit is further evidenced by the high

content of alpha-active nuclides, presumably radium and its successors, in the microcrystals of the barium-bearing pellets (Arrhenius, Bramlette and Picciotto, 1957). These occur at such depths in the cores that the radium cannot have been taken up from sea-water but must have been released from adjacent ionium carrying minerals (cf. Arrhenius and Goldberg, 1955). The concentration of radium together with barium in the excreta of benthonic animals appears also to be reflected by the frequent concentration of alpha-activity to digging structures in the sediment (Picciotto and Arrhenius, in preparation). The similarity in chemical behaviour of barium and radium emphasizes the importance of the chemistry and mineralogy of barium in pelagic sediments for the understanding of the final distribution of radium and its use for geochronological purposes.

The redistribution results in the smoothing out of the original gradients in the amount of barium per unit non-biogenous matter, represented by titanium, but leads to gradients steeper than the original ones, in the concentration of barium. This can readily be understood on the basis of the fact, evidenced below, that the clay minerals, the zeolites, and the ferromanganese oxide minerals, together constituting the bulk of the inorganic phases, have a high capacity to bond barium, in contrast to the calcite which cannot retain this element.

Analyses of diatomaceous oozes from the north Pacific and the Bering Sea (Ck 8, Table 12) indicate a low barium/titanium ratio in this environment, in spite of the supposedly high rate of organic production in the surface layer of the ocean. This may be explained either by assuming that barium is precipitated by an organism or a group of organisms abounding in the equatorial zone, or by assuming a larger contribution of titanium in the form of detrital and pyroclastic minerals in the sub-arctic areas, which are stratigraphically less known than the east equatorial Pacific. This latter explanation is suggested by the fact that the diatomaceous oozes investigated contain considerable amounts of glacial marine detritus and layers of volcanic ash.

It is not known whether the barium is concentrated from sea-water by planktonic or benthonic organisms in the areas in question. In littoral areas brown, red, and green algae are enriched in barium relative to calcium by factors of 16–78 (Bowen, 1956). As is indicated by the results of Wedepohl (1955) and further shown below, the calcite of foraminifera and coccolithophoridae is practically free from barium, whereas the protoplast of live foraminifera appears to contain considerable amounts of this element (Arrhenius, Bradshaw, Chodos and Wisner, in preparation). The occurrence of the major part of barium in aggregates which probably are faecal pellets (see below) indicates that at least a mechanical concentration of barite is brought about by the benthonic animals.

In order to establish the mineral forms of barium in the sediments, material from the core Cap. 50 BP (Table 1) was divided into settling velocity fractions by decantation and centrifugation (cf. Section 2.2.3).

Analysis of the fractions (Fig. 5) demonstrated that the barium concentration is highest in the group with the velocity limits 85×10^{-5} and 85×10^{-4} cm/sec in water at 18°C (corresponding to diameters of 3·2 and 10 μ of spherical quartz grains). This fraction (sample 374) was selected for continued work and was further

Table 13. Distribution of barium in density fractions of fine pelagic silt (sample 374)

Fraction No.	Density	Mass percentage of total sample 374	BaO*%	TiO_2* Rel. units	Percentage of total Ba-content of sample 374	Major mineral components
1	<2·14	0·9	2·4	2	1·5	Opal, phillipsite, yellow aggregates (quartz, feldspar)
2	2·14–2·49	24·5	4·4	6	72·0	Opal, phillipsite, yellow aggregates, quartz feldspar
3	2·49–2·94	71·0	0·5	40	24·0	Quartz, feldspar, phillip site
4	>2·94	3·5	1·1	704	2·5	Augite, apatite, hornblende.
Total sample		100	1·7		100	

* By X-ray spectrometry.

subdivided in density groups by repeated centrifugation in tetrabromoethane, adjusted to the proper density with diethyllpthalate. The results of the analysis of the density fractions are shown in Table 13. The marked differentiation in mineral composition, which is also demonstrated by the titanium content, confirms that a satisfactory density separation was obtained, although quartz and feldspar still contaminate the light fractions.

Barium occurs in considerable concentration both in the light and the heavy minerals, especially in the former. As a result of the relatively high frequency of minerals in the density range 2·14–2·49 and their very high barium content, this fraction contains 72 per cent of the total amount of barium. Heavy minerals are responsible only for a small fraction of the barium present (2·5 per cent). In spite of this, it was regarded as a matter of interest to identify also the heavy components. For this purpose a larger quantity of mixed material from the core Cap. 49 BP (Table 14) was fractionated with regard to settling velocity of the grains in the same way as the sample from core Cap. 50 BP. The velocity group 85×10^{-5}–85×10^{-4} cm/sec was further split in two density groups, one heavier, the other lighter than 2·94. The heavy minerals were freed from manganese oxide minerals and manganite by chelative dissolution. The residue, constituting sample no. 564, was divided according to magnetic susceptibility into three fractions, one non-magnetic, one weakly and one strongly magnetic. The properties of these fractions are shown in Table 14.

Table 14. Properties of magnetic fractions and EDTA-soluble fraction of heavy minerals (Sample 564)

Fraction No.	Description	Mass mg	Ba Rel. units*	Ti Rel. units*	Major mineral components
1	Non-magnetic	19·5	270	3 2	Barite, apatite, quartz, pyroxene anatase
2	Weakly magnetic	29·7	68	n.d.	Pyroxene, hornblende, biotite, apatite, quartz, barite
3	Strongly magnetic	3·7	24	124	Pyroxene, hornblende, biotite
4	Residue of fraction 1 after acid treatment	9·0	0	336	Quartz, pyroxene, anatase
5	Acid soluble components of fraction 1 recovered by evaporation	10·5	54	10	(by difference) Barite, apatite
6	EDTA-soluble components of total sample 564 recovered by evaporation and ignition	65	160	63	Manganese oxide minerals

* By X-ray spectrometry.

The major part of the barium is concentrated in the non-magnetic and weakly magnetic fractions. It prevails as barite and to some extent in apatite (approx. 5 per cent, ARRHENIUS *et al.*, 1957) and is completely removed by boiling in concentrated HCl for 5 min. About twice as much barium is found among the components of the heavy mineral fraction soluble in EDTA. It appears reasonable to assume that this part of the barium is bound in the structure of the manganese oxide minerals.*

For the investigation of the quantitatively much more important barium-carrying minerals and aggregates with a low density, material was used from 165–170 cm depth in the core Ch 23 (Table 1), located in the equatorial high productivity zone, where the relative amount of barium in the sediment is high.

The barium content was determined by X-ray spectrometry. Table 15 shows the concentration in the original sample (no. 159), in the dialysate (no. 713), in the material exchanged and dissolved by N ammonium carbonate at 90°C during 2 hr (no. 714), and in different fossil groups, separated by size, density, and acid solubility† (nos. 159–1.1 to 2.6). From Table 15 it is seen that the barium contained in foraminiferal tests is negligible (sample 159–1.2) and that the amounts dissolved in the pore solution of the sediment or weakly sorbed (sample 713) or exchangeable against ammonium ion (sample 714) are relatively small.

* An experiment carried out with barite crystals of 3–10 μ size, demonstrated that less than 2 per cent of this mineral is dissolved in EDTA under the conditions indicated above.

† The calcareous components were dissolved in acetic acid, added dropwise to the sample suspension.

Table 15. Distribution of barium in a Pleistocene pelagic equatorial calcareous clay (Chubasco 23, 165–170 cm, sample 159) and in a Miocene pelagic coccolith ooze (MP 40, 34–45 cm, sample 569)

Sample No.	Description	Mass mg	% BaO	% Mass	Main constituents
159	Original	50,000	2·0	100	—
713	Dialysate from original	2475	0·005	—	—
714	Sorbate from original	1712	0·030	—	—
159–1.0	>62 μ, fraction of original	1640	0·080	3·3	Foraminifera radiolaria
159–1.1	>62 μ, residue after treatment with acetic acid	256	0·25	0·5	Radiolaria
159–1.2	>62 μ, components dissolved in acetic acid, recovered by evaporation and ignition	720	0·005	—	Foraminifera
159–2.0	3·2–62 μ, fraction of original	—	0·90	—	Unidentified calcareous fragm., coccoliths, foraminiferal fragm., diatoms, radiolaria
159–2.1	3·2–62 μ, residue after treatment with acetic acid	—	1·63	—	Diatoms, radiolaria, yellow aggregates (phillipsite)
159–2.2	3·2–62 μ, components dissolved in acetic acid, recovered by evaporation and ignition	—	0·12	—	Calcareous and phosphatic components of 159–2.0
159–2.3	3·2–62 μ, residue after acid treatment, density fraction >2·22	—	1·25	30% of 2·1	Diatoms, radiolaria, yellow aggregates, phillipsite
159–2.4	3·2–62 μ, residue after acid treatment, density fraction <2·22	—	1·97	70% of 2.1	Diatoms, radiolaria, yellow aggregates, phillipsite
159–2.5	Residue of sample 159–2.3 after 5 min treatment with boiling conc. HCl	—	0·24		Diatoms, radiolaria (degraded phillipsite)
159–2.6	Components dissolved from sample 159–2.5 recovered by evaporation	—	10	1·3% of 159–2.5	Yellow aggregates and part of phillipsite (by difference)
159–3	0·3–3·2 μ, fraction of original	—	1·26	—	—
159–4	<0·3 μ, fraction of original	—	0·48	—	—
569–0	MP 40, 35–45 cm, coccolith ooze	—	0·020	99·5	Coccoliths
569–1	Residue of 569–0 after treatment with acetic acid	—	1·6	0·5	Siliceous remains
569–2	Components, soluble in acetic acid, recovered by evaporation and ignition	—	0·001	—	Dissolved coccoliths

Nor are any considerable quantities of barium found in that part of the 3–62 μ fraction which is soluble at pH 5–6 (sample 159–2.2) and which largely consists of carbonates, mainly in the form of coccoliths. The insoluble residue of the same size fraction, however, has a very high barium content (sample 159–2.1). This residue consists mainly of diatom frustules and other remains of siliceous organisms, with a minor amount of rounded, yellow aggregates. The heavier fraction of this material ($\rho > 2{\cdot}22$, sample 159–2.4) contains a larger amount of barium than the lighter fraction (sample 159–2.3).

After 5 min treatment with boiling conc. HCl, 80 per cent of the barium is removed from 159–2.5. As the yellow aggregates are simultaneously dissolved, a localization of barium in these is indicated. However, on the basis of the experimental evidence, the possibility could not be excluded that the barium is bonded in the opal or zeolite structure, and is removed by hydrochloric acid, although the opal is left intact and the phillipsite is only degraded to a certain extent. In order to check the distribution of barium between radiolarian and diatomaceous silica, the yellow aggregates and phillipsite in the barium-rich fractions of the sample 159, the sample was subjected to a particle by particle analysis* by means of the Castaing X-ray microanalyser, which has a resolution of 2 μ^2. The sample powder was distributed over a bright polished metal surface and coated with a 20 Å film of copper by condensation to make it electrically conducting. The spectrometer was set to the $L\alpha_1$ line in the barium spectrum, and the counter connected to a loudspeaker. During a preliminary scanning of the sample under visual control by the mirror microscope, the audible pulse-rate was used as a rough indication of the concentration of barium in each grain brought under the cross hair. A large number of grains were rapidly checked and it became evident that the aggregates were far higher in barium than were the other components. A number of quantitative measurements gave: for diatoms and radiolaria, 0–2 per cent; for phillipsite crystals, 3–15 per cent; and for the aggregates, 2–47 per cent BaO. Marked variations were noted in the concentration inside the aggregates, indicating that the barium is locally concentrated, probably in the highly refractive microcrystals occurring in varying amounts in the aggregates.

Additional experiments were carried out to check that the calcareous coccoliths lack importance as barium carriers. For this purpose was used the sample MP 40, 35–45 cm (Table 1), a coccolith ooze of high purity. The amount of the sediment soluble in weak acetic acid is 99·5 per cent, and the carbonate prevails almost entirely as coccoliths. The insoluble residue (0·5 per cent) consists mainly of siliceous fragments. As is seen from samples 569–0, 569–1, and 569–2 in Table 15, practically all the barium contained in the sample is retained in the residue, insoluble in weak acid.

The nature of the transparent, isotropic, greenish yellow or yellow matrix of the aggregates has not yet been revealed. The aggregates are rounded with a smooth or slightly irregular surface. They generally fall in a size range of 5–15 μ, although larger specimens have been observed in some north Pacific clays. Due to their low bulk density, the equivalent diameter of spherical quartz grains, which is used for a size scale in Fig. 5, is somewhat smaller (3–10 μ). The crystalline

* This analysis was carried out by one of the present authors in the laboratories of the Office National d'Études et de Recherches Aéronautiques, Chatillon-sous-Bagneux (Seine), France.

inclusions, which vary in size from barely visible under the microscope to a few micra, are highly refractive, and are therefore supposed to have a high density. The density of the matrix of the aggregates is therefore supposed to have a density well below 2·2. It appears reasonable on the basis of the evidence given above to assume that the crystalline inclusions consist of barite, and that the aggregates are faecal pellets of benthonic animals.

Larger euhedral crystals of barite with an average length of 10–40 μ have been observed (Bramlette, personal communication) in a number of sequences of pelagic clays. Their occurrence appears to be limited to the surface of Tertiary outcrops, unconformities, and strata with extremely high contents of manganese, indicating a low total rate of deposition. These crystals may result from the decomposition of the aggregate matrix by degradation of organic matter at the sediment-water interface, and subsequent growth of the included barite micro-crystals.

5.5. *Boron.* As has been suggested by Urey (1953), the high boron content of ocean water is explained by its introduction into the major sedimentary cycle as an "excess soluble". The high oceanic concentration of this element results in a correspondingly high content in marine sediments (several hundred p.p.m.), whereas in non-marine argillaceous sediments the boron content is generally at least one order of magnitude lower (Goldschmidt and Peters, 1932(a) and Landergren, 1945). The concentration of boron in marine sediments was assumed by Landergren (*op. cit.*) to be due to adsorption of the borate ion to detrital clay minerals. A closer examination of the bonding of this element in pelagic clay sediments, briefly reported on earlier (Arrhenius, 1954) indicates, however, that in this case only a minor fraction, roughly corresponding to the amount dissolved in the interstitial solution, is removed when the sediment is washed with distilled water. Less than 10 per cent of the remaining boron is removed at exchange of sorbed ions. The major part thus appears to be relatively strongly bonded in the authigenic minerals of the sediment. Upon chelative dissolution of the manganese and phosphate minerals, which are concentrated in the coarse grain size fractions (Fig. 5) a part of the remaining boron is released. Separate analyses of the phosphates (Arrhenius *et al.*, *op. cit.*) give low boron contents (0·003–0·01 per cent) for this material, which indicates that the main part of the boron released at solution in EDTA, occurs in the structure of the ferromanganese oxide minerals. The amount of this element which remains in the solid phases after this treatment, and which is quantitatively most important (Fig. 5, Cap. 33 BG chelated, and Cap. 50 BP 0–30 cm, chelated), resists dissolution at boiling 0·1 N hydrochloric acid, but is released at boiling in strong alkali. These results suggest that boron is proxying for silicon in the tetrahedral sheets of the clay minerals. If this is true, at least a fraction of these minerals appear to have formed from true solution of ionic species of boron, silicon and aluminium in sea-water (Arrhenius, 1954).

5.6. *Yttrium, scandium, thorium and the rare-earth elements.* All of these elements show a close similarity in their behaviour in the major sedimentary cycle, and appear to concentrate mainly in two groups of minerals, the ferromanganese oxide minerals (Goldberg, unpublished work; Goldberg and Picciotto, 1955) and the biogenous apatite (Arrhenius *et al.*, 1957). This distribution is illustrated

by Fig. 5 where the very high concentrations of Yb, Y, La and Sc are shown in the coarse fractions of Cap. 33 BG and Yoyo 7P which are in the former case dominated by apatite and phillipsite, in the latter by apatite, ferromanganese oxide minerals and barium carrying aggregates. Separated samples of phillipsite showed the absence in this mineral of the elements in question in amounts above the sensitivity limit of the X-ray spectrometric method used (approx. 0·01 per cent). The manganese minerals previously investigated were derived from permanently exposed manganese nodules, where any apatite accumulating on the surface would have been redissolved. The ferromanganese oxide phases of such nodules could have inherited the heavy metals originally adsorbed to the apatite surface, in addition to the amount originally adsorbed directly from sea-water to the surface of the δ-MnO_2. Analyses of manganese micronodules from pelagic clays, and of apatite separated from the same sediment samples indicate a fractionation between the apatite and the manganese oxide phases with an excess of cerium in the latter (Arrhenius *et al.*, in press). A similar fractionation was obtained experimentally by Eräметsä *et al.* (1940) through differential adsorption of the carbonate complexes of the rare earths.

Beside the fraction of this group, which is localized in manganese oxide minerals and on the surface of the biogenous apatite, and which is completely removed by chelative dissolution (Fig. 5, Cap. 33 BG, chelated), quantitatively important amounts, insoluble in EDTA, are found in the colloidal fraction of the sediment (Fig. 5, Cap. 50 BP 0–30 cm). The nature of the host mineral is not known in this case.

5.7. *Titanium.* On the average the titanium content of the pelagic sediments investigated is similar to that of igneous rocks. High concentrations in the sediments are invariably due to the presence of basaltic pyroclastics. This is the case for example in Cap. 31 BG (Table 9) where the excess titanium occurs mainly in augite in the coarse mineral fraction (Fig. 5). The decreasing influence of basaltic pyroclastics with increasing distance from the source is illustrated by the decreasing titanium content of the sediment in a series of cores, extending northward from the Hawaiian Islands (Fig. 8 and Table 16). Similar distributions have been demonstrated in the Atlantic Ocean by Correns (1937, 1954).

A minor fraction of the titanium is readily soluble in EDTA, and probably prevails as colloidal oxyde aquate, dispersed through the manganese oxide minerals.

Goldberg's (1954, p. 255) investigations show a covariance between iron and

Table 16. Metal/aluminium ratios as a function of distance from Hawaiian Islands

Core	Number in Fig. 1	Normal distance from Island chain (naut. miles)	$1000\frac{Ti}{Al}$	$1000\frac{V}{Al}$	$1000\frac{Cr}{Al}$
NH 9	29	26	270	11	4·5
12	30	100	91	4·2	1·0
13	31	137	77	3·9	1·1
14	32	188	66	3·3	0·87
Y3G	27	1820	50	4·3	0·91

titanium in manganese nodules, with an average ratio Fe/Ti of about 18. It is not known if this titanium is a structural component of the ferric manganite, of the goethite, or of another iron mineral, or if it prevails as an independent phase, with a tendency to occur in high concentration under the same conditions as the iron minerals. It is interesting to note that the ferromanganese oxide minerals

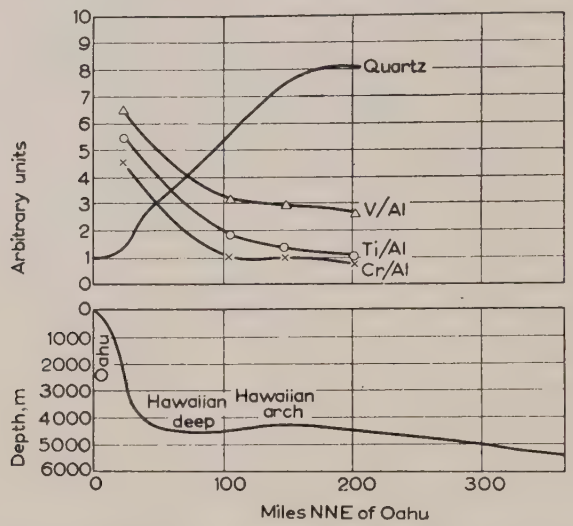

Fig. 8. Relative concentrations of titanium, vanadium and chromium and concentration of quartz in sediments off Hawaiian Islands (upper graph) compared with bottom topography (lower graph).

Flow along the bottom of sediments high in basaltic pyroclastics results in high concentrations of titanium, vanadium and chromium in the sediments of the apron around the islands and in the surrounding depression, the Hawaiian deep. The flow is efficiently stopped by the periferal rise, the Hawaiian Arch, and the pelagic sediments outside of the Arch contain only little of these elements in excess above the average for north Pacific pelagic clays, represented by Y3G in Table 16.

The content of eolian quartz silt is high in pelagic sediment of the lower and middle latitudes in the Northern Hemisphere, due to the vast arid areas in this zone. Near the islands, the concentration of quartz is lowered by the influx of detrital basaltic material.

The absolute concentrations and ratios of the three elements, given in arbitrary units in the figure, are found in Tables 16 and 9. Quartz data from Rex and Goldberg (in press). Topographic data from Dietz and Menard (1953).

dispersed through the calcareous sediments of the east Pacific rise (cf. Section 5.11 and Revelle, 1944, Table 9) have considerably higher iron/titanium ratios than the manganese nodules referred to above, viz. of the order 30–100, as compared to 18 in the nodules.

Euhedral anatase and rutile appear to account for a large part of the approx. 0·8 per cent titanium occurring in such pelagic clays which do not have an appreciable pyroclastic contribution (Correns, 1954; Bramlette, personal communication; this paper, Table 14), and at least the anatase is certainly authigenic in the sediment. As pointed out by Correns (*loc. cit.*) the parent material of the authigenic titanium minerals may at least partly be weathering silicate minerals, glass and ilmenite.

The importance of formation of the hydrogenous titanium minerals from titanium in true solution in sea-water has been stressed by Goldberg (1954) on

the basis of the association of titanium with hydrogenous iron minerals mentioned above and on GRIEL and ROBINSON's data (1952) for dissolved titanium in seawater (approx. 1 μg/l.).

ARRHENIUS (1952) studied the distribution of titanium in sediment profiles from the east equatorial Pacific, and found only small variations in the titanium

Table 17. Concentration of TiO_2 as a function of depth; mean concentration and the standard deviation from the mean in the clay core Cap. 49 BG (Fig. and Table 1) adjacent to the equatorial area of carbonate sediments.

Depth below surface (cm)	$TiO_2 \times 10^4$	Depth below surface (cm)	$TiO_2 \times 10^4$
0–4	58	76–80	59
4–8	60	80–84	65
8–12	58	84–88	57
12–16	63	88–92	57
16–20	60	92–96	53
20–24	54	96–100	66
24–28	62	100–104	75
28–32	64	107–111	69
32–36	63	108–112	63
36–40	63	112–116	65
40–44	63	116–120	59
44–48	62	120–124	61
48–52	61	124–128	64
52–56	53	128–132	62
56–60	57	132–136	65
60–64	63	136–140	65
64–68	58	140–144	66
68–72	60	144–148	56
72–76	60	148–152	67
	$m = 61{\cdot}3$ $\sigma = \pm 4{\cdot}5 = \pm 7{\cdot}3$ per cent		

m = mean concentration
σ = standard deviation

content of unit cross-section columns through the same time rock units of different latitudes. These results indicate uniformity in space of the accumulation of titanium in the sedimentary basins investigated. On the basis of the lack of stratification of adjacent Pleistocene clay sediments it was concluded that the accumulation had been uniform also in time through the major part of the Pleistocene, as any change in the proportions of the biogenous, hydrogenous and lithogenous contribution would be reflected by a corresponding change in composition of the sediment. The titanium content in core Cap. 49 BG, which includes the Recent and approximately the upper half of the Pleistocene, is shown in Table 17. The standard deviation, 7 per cent of the mean value, is close to the analytical error. The assumption of an approximate uniformity of the titanium accumulation during the corresponding time is thus not in disagreement with

these results. However, if it is assumed that the genetic component group, in which the main part of the titanium falls is a very large proportion of the sediment, even relatively large changes in the rate of accumulation of this component would not markedly influence its absolute concentration in the sediment. That this might possibly be the case is suggested by the relatively large variations in concentration of manganese in core 49 BG (by a factor of 9) whereas the concentrations of iron and of quartz show the same invariability as titanium. Further experiments, preferably based on absolute age determinations from the ionium/thorium ratio, are needed before the variability in time of the accumulation rate of the inorganic components can be quantitatively determined.

Goldberg (1954, p. 259) indicated the possibility that biogenous titanium may form a considerable fraction of the total amount of this element in pelagic sediments. This suggestion was based on the observation (Collier, 1953) of concentration of titanium by planktonic dinoflagellates. The absence of an increase in the titanium/aluminium ratio in sediments with a large biogenous component like Cap. 32 and 33 HG (Table 9), however appears to rule out biogenous titanium as an important component, at least in the equatorial pelagic zone.

Correns (1954) pointed out, that the occurrence of microscopic authigenic anatase in the sediment requires the titanium to have prevailed in true solution, at least for a short time, and that the original distribution therefore might have been changed by migration. The maximum average mass transport by diffusion of titanium through the deposit can be estimated from Arrhenius' data (1952, 1.2.4, 1.2.5, Fig. 1.1.6.1) if it is assumed that the observed deviations from constancy in space of the titanium content of each time-rock unit is entirely due to this effect. Using the values $\bar{\Delta}d = 8{\cdot}5$ mg, $\bar{d}_0 = 13$ mg, and $\bar{a} = 16{\cdot}3$ cm for the cores 59, 60, 61 and 62 (Arrhenius *op. cit.*, Table 1.2.5) the maximum displacement of TiO_2 is 0·52 mg/cm^3 or 0·65 of the average titanium content of a stratum. The present authors believe, however, that convective displacement by benthonic animals, stratigraphic correlation errors, variations in the titanium content of the inorganic components of the sediment, and temporary, local variations in the rate of accumulation of titanium contribute to this effect at least as much as diffusive displacement.

5.8. *Zirconium.* This element occurs in the pelagic sediments investigated in concentrations which are on the average 0·8 of the average for crustal rocks. (Fig. 3, Table 9). This supports Goldschmidt's (1954, p. 426) opinion that the resistance of the zirconium minerals to weathering has been over-estimated and that considerable amounts of this element pass through the hydrosphere in true solution. Further evidence for this is provided by the results of Degenhardt on the distribution of zirconium in sediments (1957), and by the fact that a large part of the zirconium found in pelagic sediments appears to be localized in the authigenic ferromanganese minerals (Goldberg, 1954), and is soluble in EDTA (Cap. 33 BG, Fig. 5). Another appreciable part of the zirconium occurs in the colloidal fraction, and is resistant to chelative dissolution (Cap. 50 BP 0–30 cm, Fig. 5).

5.9. *Vanadium.* The average concentration of vanadium found in the sediments investigated is about $2\frac{1}{2}$ times the average for igneous rocks. However, the

apparent discrepancy results from a systematic analytical error of a factor of 2 which was found by WEDEPOHL (personal communication) who made precision analyses of duplicate samples.

These vanadium contents in pelagic sediments are consistant with the observations of previous authors (JOST, 1932; LANDERGREN, 1956; GOLDSCHMIDT, 1954) who found no marked enrichments or deficiencies of this element in marine deposits as compared to igneous rocks.

The relatively even distribution of vanadium through the sediment fractions (Fig. 5.) indicates its simultaneous occurrence in high concentration in several of the main mineral constituents. The reduction of the vanadium content in the coarse grain fractions of Cap. 33 BG (Fig. 5) through chelative dissolution indicates a localization of the element in either biogenous apatite or in phillipsite. The former alternative is excluded by the low contents found upon analyses of separated apatite and the accompanying organic phase (ARRHENIUS *et al.*, in press). Also inorganically precipitated marine apatites are shown by the same authors to be low in vanadium confirming the results of JACOB *et al.* (1933).

A large fraction of the vanadium found is resistant to chelative dissolution, and occurs throughout the finest grain size fractions of the sediments. Following the authors quoted above and HARDER (1951), one might guess at a distribution of this fraction of the element between the clay minerals, the iron oxide minerals, and possibly the authigenic titanium minerals. A definite indication of a concentration in the iron oxide minerals is the high vanadium content of the carbonate-free fractions of cores Cap. 32 and 33 HG (Table 9).

Another important source of vanadium in the Pacific are igneous ferromagnesian minerals, magnetite and ilmenite, which are concentrated in core Cap. 31 BG and which probably are responsible for the high vanadium content of the fractions $>1\ \mu$ in this core. The decreasing influence of basaltic pyroclastics with increasing distance from the Hawaiian Islands is reflected by a decreasing content of vanadium in the series of cores NH 9–NH 14 (Fig. 8 and Table 16).

5.10. *Chromium.* RANKAMA and SAHAMA (1950, p. 620) point out that the igneous rock average values reported by various workers differ by an order of magnitude, the highest value being 530 p.p.m. (HEVESY, MERKEL and WÜRSTLIN, 1934) and the lowest 35 p.p.m. (LUNDEGÅRDH, 1946). SHAW (1954) finds for shales and their metamorphic equivalents 59 to 190 p.p.m. and similar values have been reported for sandstones (GOLDSCHMIDT, 1937). An intermediate value for the average igneous rock concentration of chromium, 100 p.p.m. has been reported by YOUNG (1954) without specification of the method of computation. The average found by us for Pacific pelagic sediments is close to this value by YOUNG, which has been adopted as a basis for the computation in Figs. 3 and 4.

High chromium concentrations occur in sediments containing considerable amounts of basaltic pyroclastics (Cap. 25 HG, 31 BG, 33 BG, NH 9, in Table 9). The decreasing content of chromium bearing minerals with increasing distance from the Hawaiian Islands is illustrated by the falling chromium content in the series of Cores NH 9, NH 12, NH 13 and NH 14, ranging from latitude 21 to 24°N (Table 16 and Fig. 9). As is seen from Cap. 33 BG in Fig. 5, chromium, like titanium, vanadium, copper and magnesium is strongly concentrated in the 10–32 μ fraction,

which is in this core dominated by ferromagnesian minerals, mainly augite. The distribution in Cap. 50 BP 0–30 indicates concentration of chromium also in the colloidal fraction, which is dominated by clay minerals. The lack of volcanic glass even in samples containing large amounts of ferromagnesian phenocrysts, and the high content of montmorillonite in such samples, indicate that basaltic glass is unstable in this environment, and decomposes to form montmorillonite. The colloidal chromium may be derived from the decomposed glass, and is probably present in the octahedral layers of the authigenic clay minerals.

The distribution of chromium suggests that an excess of this element above approximately 0·01 per cent in pelagic sediments, is a useful indication of the presence of altered or unaltered basaltic pyroclastics.

5.11. *Iron.* Largely due to the poor crystallinity of the authigenic iron minerals, little has been known about their character and relative distribution until the appearance of the recent work by Buser and Grütter (1956) and Grütter and Buser (1957). These workers demonstrated that the main iron-containing phases in manganese nodules are ferric manganite (see 5.12), goethite, and colloidal FeOOH. Goldberg (1954), on the basis of Cooper's (1948) and his previous (1952) results, pointed out that the primary phase deposited from the sea-water probably is colloidal iron oxide aquate. The present authors (section 5.12) interpret the information furnished by Buser and Grütter on the basis that the iron oxide aquate colloid, after discharge at the sediment-water interface, forms a highly active surface, which catalyses the oxidation of dissolved manganous ion to MnO_2. Upon precipitation as δ-MnO_2, part of this solid may combine with the catalyst, forming the double layer structure, described by Buser and Grütter as ferric manganite. Excess iron oxide aquate colloid may by ageing be transformed to goethite. In addition to these phases, nontronite has been observed on manganese nodules (Bramlette, personal communication).

It appears reasonable to assume that the same iron minerals are predominant also in other pelagic sediments; however, little is so far known about their relative proportions. Thus it is uncertain whether the very high iron concentrations in the colloidal fraction of pelagic clays (e.g. Cap. 50 BP 0–30 cm, Fig. 5) are due mainly to nontronite or goethite.

In sediments with a large pyroclastic contribution, considerable amounts of iron occurs as augite and hornblende, and further as magnetite and probably ilmenite, all concentrated in the coarse fraction (Fig. 5, Cap. 31 BG).

5.12. *Manganese, cobalt, nickel, lead and molybdenum.* These five elements display a similar behaviour in the marine part of the minor cycle (Goldberg, 1954). In sea-water they most probably prevail as dissolved species mainly as manganous, cobaltous, nickelous and plumbous ions, as either aquato- or chloro-complexes. In the solid phases precipitated from this solution a large part of the manganese occurs as δ-MnO_2* and as manganese and iron manganite, and much of the cobalt, nickel and lead is bound in the structure of these minerals, mainly in the disordered layer of the manganite (Buser and Grütter, 1956). The manganese, and associated

* δ-MnO_2 and manganite are throughout this work employed in the same sense as the one used by Buser and his co-workers, namely as a chemical term. A discussion of the proper mineral names for the species discovered by these workers will follow elsewhere.

metals, occurring in these ferromanganese oxide minerals, are readily soluble in EDTA, and can thus be separated from resistant phases. (cf. Fig. 5 and section 2.25). Another part of the manganese occurs together with iron, cobalt, nickel, copper, rare earths, zirconium and large amounts of lead, molybdenum and silver in the colloidal fraction of the sediment (Cap. 50 BP 0–30, Fig. 5), and is resistant to chelative dissolution. It is not known, what mineral carries this fraction of the manganese, which is quantitatively less important in sediments with a high manganese content, but approaches unity in manganese-poor strata of the buff clays from the north equatorial Pacific (Tables 1 and 9).

The high concentration of manganese in many pelagic deposits has motivated a number of speculations as to the source and mechanisms of accumulation of this element. It is generally accepted that the manganese has been brought into solution by the weathering of igneous rocks, transported in solution to the site of deposition and precipitated there. However, there is a difference of opinion as to the location of the source rocks and the modes of transport and deposition of the dissolved manganese.

Although an obvious source of manganese is the crustal rocks of the continents, as first pointed out by Renard (Murray and Renard, 1891), Murray suggested volcanic debris on the ocean floor as more important. Murray was impressed by the association of manganese nodules and pyroclastics in many of the same samples of the Challenger Expedition. Confronted with the observation that the manganese/iron ratio in nodules is much higher than in the pyroclastics, he amended his ideas (Murray and Irvine, 1894) by suggesting a diffusion of manganese from deeply buried strata of the decomposing rocks. The remnants of such weathered lavas, depleted in manganese, and approximately ten times the volume of the totality of the pelagic sediments, have never been found. In view of the obvious necessity of separating the source of the manganese from the deposits, the emphasis upon volcanic debris on the ocean bottom does not any longer seem to be needed.

Several processes bringing manganese to the sediment, other than oceanic mixing, have been proposed. Beside diffusion through the pore water of the sediments (Murray, *loc. cit.*), Gümbel (1878) suggested transport via submarine springs; in the latter two cases the source of the manganese is presumed to be below the sediment surface. Correns (1941) has indicated the possibility of a biological extraction of manganese from the sea-water into foraminiferal tests. At the partial dissolution of these after deposition, manganous ions are released in the pore water of the surface layer of the sediment. Pettersson (1945) has suggested the inability of this process to account for all the manganese in sediments. He pointed out that the necessary rates of accumulation of foraminifera and the subsequent rates of dissolution would be higher than is probable. A second criticism is based upon his belief that the relatively high manganese contents of the foraminifera, reported by Correns, are brought about after deposition. However, these values have been confirmed recently (Arrhenius, Bradshaw, Chodos and Wisner, in preparation) by analysis of planktonic foraminifera caught by tow-net. Thus it appears reasonable to accept Correns' suggestion as a contributing transport process. The outcome of all of these mechanisms is

to increase the activity of manganous ion at the sediment-water interface.

The following processes of transfer of the manganese from dissolved to solid phases have been suggested: the deposition of manganous sulfide with subsequent oxidation (Buchanan, 1890); adsorbtion on volcanic glass particles (Pettersson, 1945); bacterial oxidation (Dieulafait, 1883; Dorff, 1935; Butkewitsch, 1928); and inorganic oxidation and precipitation (Murray and Renard, 1891; Boussingault, 1882; Kuenen, 1950). All of these hypotheses suffered at the time they

Table 18. Distribution of manganese between particulate and dissolved species on Trans-Pacific Station 129 (lat. 26°28·5′N, long. 170°23·0′W)

Depth in m	Dissolved manganese μg/l.	Particulate manganese μg/l.
0	2·8	0·22
200	4·7	0·08
1000	5·0	0·06
1500	2·0	0·05
2000	2·1	0·09
2500	1·2	0·02
3000	1·7	0·12
3500	0·4	0·07

were presented by inadequate knowledge of the nature of manganese in the ocean and in the solid phases of the sediment. It therefore appears worthwhile to consider some newer aspects of the geochemistry of manganese.

The following lines of evidence point to the existence of manganese in the divalent state in sea water. Buser and Grütter's (1956) study of the mineral composition of manganese nodules indicates the main constituents to be δ-MnO_2 and manganites with double layer structures. The manganites contain, beside MnO_2, mainly divalent manganese 5–25 per cent, iron, calcium and sodium. It is difficult to conceive of a process of reduction of any tetravalent manganese in the oxidating environment where these concretions are found. Chemical analyses of manganese in Pacific Ocean waters indicate a distribution (Table 18) in which less than 10 per cent of the manganese occurred in phases that were retained by a molecular filter with a pore size of 0·5μ. Experiments with a filter of pore size of 5–10 millimicra yielded about the same amount of retained manganese, suggesting that 85 per cent or more of the element prevails in true solution. If one assumes that manganese is present as the divalent ion and that manganous carbonate rather than a silicate of manganese (for which data are lacking) is the least soluble compound that would form, the manganese is undersaturated by a factor of 200 ($K_{MnCO_3} = 8{\cdot}8 \times 10^{-11}$ [Latimer, 1952, p. 236]. CO_3^{--} and Mn^{++} in sea-water have respective concentrations of 5×10^{-4} M and 4×10^{-8} M and assumed activity coefficients of the divalent ions of 0·12).

The manganites described by Buser and Grütter (*op. cit.*), and Grütter and Buser (1957) consist of a double layer structure where layers of MnO_2 alternate

with disordered layers of $Mn(OH)_2$-aquate in the case of manganous manganite, and of $Fe(OH)_3$-aquate in the case of the ferric manganite. Thus, the main part of the manganese prevails in the tetravalent form. The ions in the disordered layers appear to be exchangeable and at least minor amounts of other ions can proxy for the manganous, ferric, calcium and sodium ions. In the manganese nodules examined by GOLDBERG (1954) the iron/manganese ratio varied between 0·26 and 1·04. The lowest value reported for this ratio (0·018) is derived from a nodule from the Atlantic Ocean (BUSER and GRÜTTER *op. cit.*).

One of the results of the important work of BUSER and his collaborators was the observation of the large surface areas of the nodule materials. Values ranged between 6 and 190 $m^2\ g^{-1}$, and the highest values are found in nodules with a large fraction of δ-MnO_2 or FeOOH. BUSER and GRÜTTER on the basis of these observations explain the high concentration of the accessory metals in manganese nodules. It is well known that such polyvalent ions with a high charge density as copper, the rare earths, zinc, lead, etc. more readily enter into sorption reactions than the alkali or alkaline earth metals (GOLDSCHMIDT, 1954, p. 67). The relative amounts of these metals in the ferromanganese oxide minerals probably reflect the activity in sea water of the corresponding ions. These activities may be enhanced at the sediment-water interface by the dissolution from the ocean floor of other phases high in the elements in question such as microcrystalline apatite (ARRHENIUS, BRAMLETTE and PICCIOTTO, 1957). Additional confirmation that these accessory metals are directly or indirectly derived from sea-water is given by the work of PATTERSON, GOLDBERG and INGHRAM (1953) on the isotopic composition of lead in manganese nodules.

Apparently the only non-biological agent in marine waters in appreciable concentrations that is capable of oxidizing manganese is oxygen. The reaction

$$2\ OH^- + Mn^{++} + \tfrac{1}{2}\ O_2 = MnO_2 + H_2O \qquad \Delta F^\circ = -38{\cdot}2\ \text{kcal}$$

has a free energy of $^-9$ kcal at 25°C at a pH of 8, a manganous ion concentration of 10^{-9} M and a partial pressure of oxygen of 0·25 atm (data from LATIMER, 1952).

The fact that the tetravalent manganese is not found in the sea-water but accretes at the sediment-water interface indicates that a surface is necessary for the reaction. The well known catalytic properties of iron oxides, coupled with the frequent presence of large amounts of iron in the manganese nodules, suggests that ferric oxides may provide the most important initial active surface. Assuming that the oxidation requires catalysis on the oxide surface, the amount of manganese deposited will be related to the length of exposure of a given surface to sea-water and to the rate of supply of ferric oxides. Thus, for high rates of accumulation of iron, the active surfaces will be continually replaced and high rates of manganese accumulation will be expected, although the mass concentration of manganese will be low.

Indirect indications, as well as direct measurements, point at a low total rate of accumulation in most localities where the manganese concentration of the sediment is high. The abundance of manganese nodules on topographic highs is greater than in sediments in adjacent depressions. Manganese nodules are

commonly found accreting on top of outcrops of pre-Pleistocene sediments (Hamilton, 1956). The rate of accretion of manganese nodules has been estimated to be 1 mm/10^3 years* whereas the rates for Pacific clays and calcareous and siliceous oozes range from several mm to several cm in 1000 years (Arrhenius, 1952). Sedimentary components, which are diluted at high total rates of deposition, like fish debris, are highly concentrated to manganese sediments. The crystal size of authigenic minerals like barite and phillipsite tends to be large in sediments high in manganese (Bramlette and Arrhenius, in preparation).

In areas with a low total rate of deposition, and a high content of dissolved oxygen in the bottom water, oxidation of dissolved manganous ion at a suitable surface, and subsequent accretion of ferromanganese oxide minerals may thus become the dominant accumulation process. The forming δ-MnO_2 acts as a scavenger of high charge density ions in sea-water, which are probably accommodated in the disordered layers of the resultant manganite (Buser and Grütter, 1956).

Goldberg (1954) postulated that manganese nodules were formed by electrophoretic deposition of oceanic colloidal particles of iron and manganese. The iron colloids are known to be electropositive and the manganese colloids electronegative. The electro-potentials were attributed to the flow of ocean water, a good electrical conductor, through the earth's magnetic field. The natural electrodes would correspond to the nuclei about which manganese and iron accumulate such as pumice, clay aggregates, sharks' teeth or earbones of whales. Such electrodes must either possess a conductance greater than that of the surrounding sediment or project above the water-sediment interface. The positively charged iron particles and the negatively charged manganese particles would be electrophoretically deposited when the electrodes were negatively and positively charged respectively. Potential charge reversal could result if the water movement were tidal in nature. Since the majority of the manganese in sea-water has been observed to be in a dissolved state, such a mechanism appears unlikely for this element.

Some observations on a pair of recently dredged inshore nodules may be of interest from the point of view of deposition of iron from sea-water. Two nodules with metallic nuclei were obtained from dredge hauls taken in the San Clemente Basin (lat. 32·5°N; long. 118°W) at an approximate depth of 2000 m. The specimens consist of coatings of ferric oxides about pieces of steel and have gross features similar to manganese nodules. A section of one of the iron nodules is shown in Fig. 9. In the same figure, for the sake of comparison, is shown a cross-section of the Horizon manganese nodule, recovered from a depth of 5500 m at 40°14′N and 155°15′W.

The composition of the iron oxide coating appears to be indicative of its origin. The coating possesses, like the ferromanganese minerals of manganese nodules, such a low degree of crystallinity, that the structure could not be revealed with ordinary parafocusing methods of X-ray diffraction. A small amount of quartz

* This value from Pettersson (1943) and von Buttlar and Houtermans (1950) may in fact be much too high. It is based on the assumption that the radium in the nodules is unsupported, i.e. derived from sea-water. The unusually high amounts of thorium (Goldberg and Picciotto, 1955) which is directly or indirectly sorbed from the sea-water, suggest that the ionium in sea water, resulting from uranium decay, is collected by these concretions. If all of the radium is ionium supported, that is the extreme case, the rate of deposition given above is too high by a factor of 50, the ratio of ionium to radium half-lives.

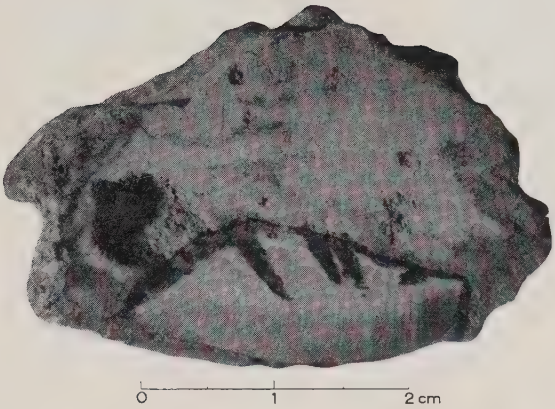

9 (a)

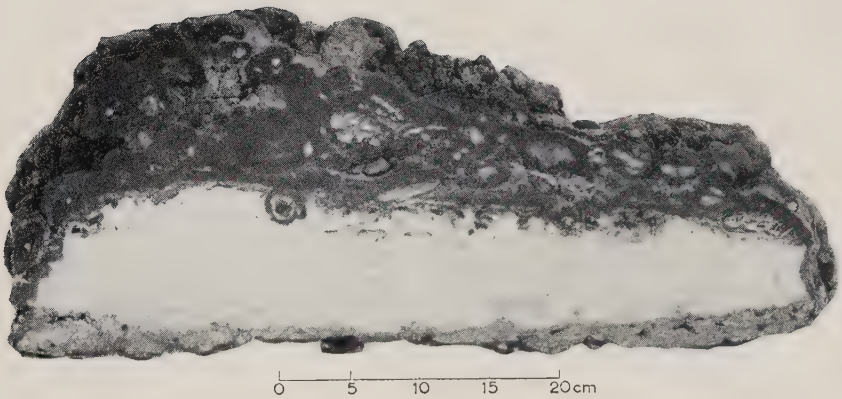

9 (b)

Fig. 9. Sections through one of the San Clemente nodules (top) and the Horizon nodule (bottom).

is indicated by the diffraction pattern. The chemical composition of the oxide coating (Table 19) shows concentrations of zirconium and titanium, abundant elements in the hydrogenous ferromanganese oxide minerals (GOLDBERG, 1954; WISEMAN, 1956). The oxide coating also contains large amounts of magnesium, barium and boron, whereas the steel shows little or none of these elements. Conversely, the relatively high contents of manganese, chromium and vanadium in

Table 19. Minor constituents in the San Clemente iron concretion and its metallic core

Element	Oxide phase	Metallic phase
	wt. %	wt. %
B	0·004	—
Ba	0·02	—
Ca	0·2	—
Co	0·005	0·01
Cr	0·002	0·01
Cu	0·05	0·05
Mg	0·5	—
Mn	0·1	1·0
Ni	0·02	0·1
Sn	—	0·005
Sr	0·002	0·005
Ti	0·02	—
V	—	0·005
Yb	0·0002	0·002
Zr	0·001	—

the steel core are not found in the coating, indicating that the metal was not the source material for the oxide accretion. Some oxidation of the steel fragment probably occurred during the initial period in which the metal lay at the sediment water interface but probably resulted only in a thin coating. The waters overlying the sediments in the San Clemente area contain around 2 ml of dissolved oxygen per litre of water (EMERY and RITTENBERG, 1952).

Any process, for example the rapid flow of ocean water through the earth's magnetic field, causing the steel to be cathodic with respect to sea-water would attract the positively charged iron colloidal particles from the sea-water. Such a precipitation has been produced in the laboratory with a potential difference of 0·5 V/cm in a colloidal solution containing a 100 μg of iron per l. of sea-water. Another precipitation mechanism could be the preferential discharging of the iron oxide colloid at conductive surfaces, where the stabilizing colloidal charge is readily dissipated to ground.

The steel nucleus appears to be a shell fragment and was probably deposited during the last 50 years when the San Clemente area was used as a U.S. Naval Target Range. Hence the rate of accumulation is at least of the order of mm per year. This high rate of accretion allows relatively short times for a given iron

surface to be in contact with the sea-water containing the manganous iron. The iron content is 75 per cent and the manganese concentration 0·1 per cent. The iron-manganese ratio attains a value of 750.

In the more slowly accumulating pelagic clays (order of magnitude mm/1000 years) this ratio varies between 2 and 60. In the extreme case of pelagic manganese nodules, which accrete at a rate of 1 mm/1000 years or less, and where the iron oxide surfaces thus have time to attain a high degree of saturation with manganese oxide, the iron/manganese ratio accordingly reaches very low values, varying between 0·02 and 1.

The rate of accretion of manganese as expected appears to be highest in the San Clemente nodule, viz. a minimum of 200 μg cm^{-2} year $^{-1}$ (assuming a total rate of growth of 100 cm in 1000 years). The average accretion rate is estimated to be 4 μg cm^{-2} year^{-1} in pelagic clays (assuming a manganese content of 1 per cent and a total rate of sediment growth of 2 mm in a thousand years). For manganese nodules with a content of 10 per cent manganese and rates of growth varying between 0·02 and 1·0 mm in 10^3 years, the computed accumulation rate of manganese ranges between 0·4 and 20 μg cm^{-2} year^{-1}.

The present interpretation of the mechanism of formation of nodules of manganese and iron oxide minerals in the ocean can be summarized as follows: Manganous ions brought to the sediment-water interface by oceanic mixing, by deposition and redissolution of organic remains, and possibly by other processes are oxidized to tetravalent manganese by the catalytic action of the discharged iron oxide colloid in the presence of oxygen. The tetravalent manganese oxide in the form of δ-MnO_2 associates with the catalyst, and to a smaller amount with divalent manganese oxyde-aquate to form the ferric and manganous manganites discovered by Buser and Grütter. The lower the total rate of accumulation the more complete is the utilization of the iron oxide as a structural element in the manganite. The concentration ratio between the free iron oxide left over in over in this process, on one hand, and tetravalent manganese in the nodules on the other, might therefore be indicative of the rate of growth of these polymineral aggregates.

Further, manganese and associated heavy metals occur in relatively large amounts in the most fine grained part of the sediment (Fig. 5) in a form that is resistant to dissolution in EDTA. The absence of a tendency to formation of soluble complexes, together with the fact that clay minerals are the only crystalline species which were found by X-ray diffraction technique in these fractions of the sediment, indicates that the insoluble manganese, nickel, copper, cobalt, lead, silver, zirconium, scandium, chromium and molybdenum in the colloidal range possibly proxy for the main cations in clay minerals. The amount of manganese and associated metals bound in this way is of the order of 0·1 per cent of the total sediment, whereas the amount present in ferromanganese oxide minerals varies between wide limits (approx. 0·1–25 per cent).

5.13. *Copper*. Copper prevails in sea-water as Cu^{++}, $CuCl^{+}$ and $CuSO_4$, ionic species similar to those of the transition divalent metals. Like such elements as nickel, cobalt, lead and molybdenum it appears in δ-MnO_2 and manganite, 0·2–2 per cent (Goldberg, 1954; see further the covariance of copper and manganese in

Fig. 5), however, the relationship between copper and manganese is much less distinct than between nickel, cobalt, lead and molybdenum and manganese. This suggested other independent sources of copper.

The well known combination of copper with the organic molecules in the protein hemocyanin and the exceedingly strong ability of copper to complex with most organic functional groups (SCHUBERT, 1954) pointed to a biological origin. For a large number of organic complexes, containing bivalent metals, the order of stability is $Pd > Cu > Ni > Pb > Co > Zn > Cd \gg Mg; Ca > Sr > Ba > Ra$. The stability of the complex is apparently directly related to the basicity of the metal.

It is thus not surprising to find that copper appears in the organic phase of fish debris (ARRHENIUS, BRAMLETTE and PICCIOTTO, 1957; ARRHENIUS, BRAMLETTE, PICCIOTTO, CHODOS and GODIJN, in preparation) in amounts of 0·1–0·5 per cent of the mineral aggregate, and 2–10 per cent of the organic phase. That the concentration takes place after the death of the organism, is indicated by the fact that the skeletal ash of bathypelagic fish, caught alive, contains only one tenth of the amount of copper found in the skeletal remains of bathypelagic fish in the deposits.

Assuming both a biogenous and a hydrogenous source of copper in pelagic sediments, the total copper concentration can be expressed as the sum of these two components, with the hydrogenous copper equated to a constant times the manganese concentration. Such a computation was made by REVELLE *et al.* (1955) who found a remarkable covariance between the biogenous copper and barium, this latter element presumed to be dominantly associated with organic phases (see section 5.4).

Copper also occurs in igneous ferromagnesian minerals, abundant in Cap. 31 BG (Fig. 5). The pyroclastic material of the coarse fractions of this sediment which contain 0·2–0·3 per cent copper are high in augite, possibly indicating the proxying of copper for ferrous iron in this mineral as suggested by RAMDOHR (1940).

Finally, copper is found in the fine grained ($<1\ \mu$) fractions of the sediment, in an unidentified form, resistant to chelative dissolution (Cap. 33 BG and 50 BP 0–30 cm, Fig 5). This copper occurs in concentrations of 0·2–0·4 per cent of the mass of the sediment fraction and may possibly be localized in the clay minerals.

6. Comparative Chemistry of Pelagic Sediments in Space and Time

Interpretations of the observed differences in the composition of pelagic deposits from different areas and of different ages may be proposed on the basis of the mechanics of formation of recent pelagic sediments in the Pacific.

A modest number of chemical analyses have been performed upon sediments from the Atlantic Ocean (WEDEPOHL, 1955; HUTCHINSON, BENOIT, COTTER and WANGERSKY, 1955; LANDERGREN, 1956; SMALES, MAPPER and WOOD, 1957) and these data have been collated in Fig. 10 together with the comparable elemental assays of Pacific clays and manganese nodules (GOLDBERG, 1954 and previously unpublished results).

The composition of the manganese nodules is characterized by high concentrations of the ferromanganese oxide minerals and by higher concentrations of

manganese and other divalent transition elements than either the clay sediments from the Atlantic or Pacific Oceans. Accepting the assumption that the rate of deposition of marine deposits is inversely related to the manganese content (Section 5.12), it is apparent that accumulation rates in the Atlantic are higher than in the Pacific from Fig. 10. Seismic refraction studies of the thickness of the first layer encountered on the ocean floor, presumed to be a blanket of unconsolidated sediments, may be taken to support such an hypothesis. Raitt (1956) gives values for 37 stations in the central Pacific area ranging between zero and

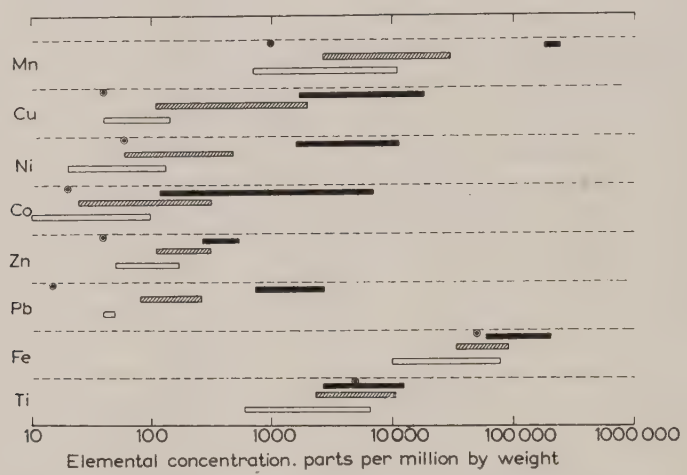

Fig. 10. Ranges of concentration of manganese and associated metals in manganese nodules (black rectangles), Pacific pelagic sediments stippled and Atlantic pelagic sediments (open). Filled circles represent igneous rock concentrations.

2·12 km with a mode of 0·34 km and an average of 0·43 km. On the other hand, Worzel and Shurbet (1955) find a sedimentary layer of 1·0 km thick for a standard oceanic crustal section in the Atlantic.

The observation that the rate of accumulation of sediments is higher in the Atlantic than in the Pacific is not suprising. Revelle *et al.* (1955) point out that the larger Pacific Ocean has a much smaller area of river drainage and a lower number of large rivers than the Atlantic. The sedimentation basins of the Pacific are to a great extent protected against turbidity transport of material from the continents by rises and trenches running parallel to the coast.

The more rapid decrease of calcium carbonate with increasing depth in the Pacific, compared to the Atlantic, might be explained by the lower rates of accumulation which would allow the carbonate to be in contact longer with the corrosive bottom waters.

In all of the cores from the north east Pacific Ocean that penetrate from Quaternary into Lower or Middle Tertiary strata, the quartz content rises markedly at the transition from the older to the younger system (Rex and Goldberg, in preparation). This has been interpreted by postulating either an increased rate of accumulation of quartz, which is presumed by the authors to be dominantly of eolian origin in the pelagic areas, or a decreased deposition of diluting materials

during Quaternary as compared to Tertiary time. Further, in Quaternary clays from the south equatorial and equatorial Pacific, the quartz concentrations are much lower than in clays from the adjacent northern regions.

The changes in quartz content in the north equatorial Pacific deposits with depth are accompanied by changes in gross chemical and mineralogical composition.

Table 20. Ratios of chemical constituents between the Tertiary and Quaternary sections of a north equatorial Pacific core and between a recent south equatorial core and the north equatorial Quaternary section

	Cap. 50 $BP_{300-760\ cm}$ / Cap. 50 $BP_{0-300\ cm}$	Cap. 33 BG / Cap. 50 $BP_{0-300\ cm}$
SiO_2	0·97	0·80
Al_2O_3	0·83	0·98
Fe_2O_3	1·3	1·22
TiO_2	0·69	0·83
MgO	0·96	1·3
CaO	1·41	5·3
Na_2O	1·2	1·4
K_2O	0·89	0·77
SrO	1·6	1·9
BaO	1·5	0·43
B_2O_3	0·93	0·60
MnO	2·9	6·3
Ga_2O_3	0·70	0·65
NiO	1·2	2·4
CuO	1·1	1·1
Co_2O_3	0·50	2·4
Cr_2O_3	0·44	0·24
V_2O_5	1·1	1·5
PbO	1·3	1·9

Revelle *et al.* (1955) found that the manganese/nickel and iron/titanium ratios in core Cap. 50 BP (Table 1) were markedly different in the Quaternary and Tertiary strata which are separated by a discontinuity. This observation is expanded in Table 20 which provides the ratios of the elemental abundances of the lower and upper parts of Cap. 50 BP, and for comparison the same ratio for the south equatorial Pacific core 33 BG and the upper part of Cap. 50 BP. Similar differences between Quaternary and Tertiary sediments have been observed in cores Cap. 49, Ck 2 and Ck 4 (Table 1). High manganese, calcium and sodium concentration in the Tertiary part of 50 BP and in the south equatorial deposits, as compared to the upper levels of 50 BP, result from the presence of ferromanganese oxide minerals and authigenic phillipsite, minerals indicative of low rates of accumulation.

It is tempting to relate these observed similarities to similar conditions in Tertiary times in the north central Pacific and at present in the south equatorial Pacific. The qualitative inference that the accumulation of solids was much less, appears grounded on the basis of both chemical and mineralogical evidence. However, it must be remembered that changes of other parameters directly or indirectly

related to the total rate of accumulation may have contributed to the observed differences in properties of the sediments. The temperature of the deep and bottom water of the ocean is known to have decreased by 10–12°C since Early Tertiary (Emiliani and Edwards, 1953), a change that may have markedly affected the rate of formation of authigenic minerals on the ocean floor directly, and in the case of ferromanganese oxide minerals indirectly through changes in the activities of the reactants.

Further, the solubility of calcium carbonate decreases with temperature. Any temperature change in the bottom waters could significantly influence the dissolution of calcium carbonate and concurrently the activity of calcium ion in the pore waters of the deposit. Other phenomena, as weathering and river influx, wind patterns and eolian transport, and possibly volcanism were quite different in extent between these two geological periods. Their influences upon the composition of the sediments can as yet not be definitively judged but future work may well reveal their significance.

7. The Geochemical Balance

The quantitative study of the changes of state of substances over the surface of the earth has attracted many contributions since the initial modern work of Joly (1899). The goals of the calculations generally have been the determination of the total amounts of sediments formed and of the complementary amount of igneous rocks decomposed. The starting points are the tabulations of average elemental abundance in igneous rocks, in the various classes of sediments and in the oceans. These data are fed into a number of simultaneous equations relating the unknowns, the amount of weathered igneous materials and the amounts of sediments produced.

The general pattern for geochemical balance computations was set by Clarke (1924) and Goldschmidt (1937) and was based to a large extent on the chemical composition of rock classes as given by Clarke. Although modifications and attempts to increase the accuracy of the calculations have appeared (see for example Correns (1948) and Wickman (1954)), the basic conclusions initially reached have remained unaltered. There have been between 150 and 200 kg of igneous rocks weathered to produce a similar mass of sandstones and shales and around 15 kg of carbonate rocks for every cm^2 of earth's surface. These figures show marked differences from the relative percentages of sedimentary rocks from field measurements in which the sandstones and limestones are proportionally much higher. Such discrepancies are attributed to difficulties in respresentatively measuring and averaging sediments throughout the geological column on a worldwide basis and in determining the proportions of the basic constituents in mixed formations (Pettijohn, 1957, p. 11).

Although there is fundamental agreement as to the average composition of the earth's crust and of sea-water, there is no concurrence with respect to the relative proportions of the main types of sedimentary rocks. Goldschmidt (1954, p. 61) states "The regions of deposition of the great sedimentary masses are, as a rule, not the deep sea basins but chiefly those parts of the continental block which at the time happened to belong to the shelf region of the coastal sea". On

this basis GOLDSCHMIDT considers the pelagic clays of negligible importance in his calculations and derives his average composition of sedimentary materials solely on the basis of shales, phyllites, mica schists and terrigenous mud (CLARKE's data from which the sea salts were removed—see below). He arrives through his balance calculations at an average thickness of sediments of 638 m over the surface of the earth. Since one can assume a conservative minimal figure for the depth of pelagic sediments of 300 meters (WORZEL and SHURBET, 1955; RAITT, 1956) in both the Atlantic and Pacific Oceans, since red clays now cover about 28 per cent of the sea floor (KUENEN, 1950, p. 362) and the sea floor constitutes about 70 per cent of the earth's surface, the red clays account for at least 60 m or 10 per cent of GOLDSCHMIDT's figure. More important they would be the second most abundant sediment type inasmuch as shales and sandstones (according to GOLDSCHMIDT) have a thickness of 585 m while limestones and dolomites have computed depths of 38 and 15 m respectively.

KUENEN (*op. cit.*, p. 389), on the other hand arrived at the conclusion that the ratio of red clay, blue mud and globigerina ooze is 8:2:1 and that the total mass of pelagic and hemipelagic sediments is three times the mass of the continental and epicontinental sediments. The mass of red clay is thus made to account for over 50 per cent of the mass of sediments. Although both authors arrive at not significantly different figures for the amounts of igneous rock weathered and sediments produced, the question of the proportion of pelagic deposits remains unresolved. Thus, a closer scrutiny of both the assumptions involved in such balance computations and the validity of the data used appears warranted.

In order to ascertain the relative contribution of pelagic clays to the totality of sediments, general equations, based upon the principles of GOLDSCHMIDT and CLARKE, have been used in this work:

$$A_x X - B_x Y - C_x Z - D_x S = M_x$$

where X, Y, Z and S are the total quantities of igneous rocks, pelagic clays, limestones and globigerina oozes, and shales and sandstones, expressed as kg/cm^2 of earth's surface. The coefficients, A_x, B_x, C_x and D_x represent the per cent concentration of the element x in each respective class, while M_x is the amount of the element in sea-water in units of kg/cm^2 of earth's surface multiplied by 100.

The equations are most sensitive for products of the major sedimentary cycle whose chemical compositions show marked variations from those of igneous rocks. (CORRENS, 1948, has already discussed the minor changes observed in the results for modest alterations of the concentrations of elements in igneous rocks and sediments.) The uncertainties inherent in the estimate of average elemental abundances in different rock types exert a great influence on the solution of the equations when the constants approach each other in magnitude, i.e. when the differentiation of elements between the different rock types is small. To obtain results of maximum significance, such elements must therefore be chosen which display a maximum differentiation between igneous rocks, the sedimentary rock types and sea-water. GOLDSCHMIDT considered in his primary calculations two major fractionations—the accumulation of calcium and magnesium in carbonates in which the enrichment of both elements is of one order of magnitude and the

relative enrichment and depletion of the elements in the sea-water reservoir. In his computations, shales and sandstones were considered alike enough in composition not to warrant placing them initially in separate groups, and for the same reasons limestones and globigerina oozes were combined.

A third major fractionation occurs in the formation of the pelagic clays in which manganese and certain associated metals are enriched over their igneous rock values by factors of five to ten. Kuenen (1950, p. 390) noted in his balance sheet that the manganese contents of the red clays are far too high in relation to igneous rock values for a derivation of this element from magmatic source materials. He explained this discrepancy by stating that the slowly accumulating pelagic sediments are rich in manganese and such samples are overemphasized in the composite sample given in Clarke (1924).

The four elements used for the present computation were chosen with respect to the major fractionations: sodium and potassium because of the depletion of potassium relative to sodium in sea-water; calcium because of its concentration in carbonate sediments; and manganese due to its enrichment in pelagic sediments.

The igneous rock data are taken from Fleischer (1953); the data on shales and limestones from Clarke (1924); the data on pelagic clays from this paper; and the sea-water abundances from Sverdrup, Johnson and Fleming (1946). The manganese value in shales is Minami's average, quoted in Goldschmidt (1954, p. 652).

The data for pelagic clays include sorbed and interstitially dissolved solids and the assumption is made that these solids are a part of the sediments rather than a part of the hydrosphere. Clarke's data for red clays and terrigenous sediments refer to samples in which the sea-salts have been washed out (Clarke, *op. cit.* p. 517). Whether one considers the pore solution as a part of the hydrosphere or of the sediment may be simply a matter of definition, but both operationally and theoretically there are compelling reasons to include them as a part of the pelagic clays. First of all, there is no evidence to indicate that at least the water of the Cenozoic system has been returned to the major sedimentary cycle. Arrhenius (1952) has shown that even in the most advanced stage of diagenesis observed in indurated Tertiary pelagic clays, no marked expulsion of water has taken place. Secondly, the ion-exchange characteristics of the minerals of these clays make it very difficult by any washing technique to remove solely the sea-salts without altering the composition of the solids.

The so-called hemipelagic sediments are in the present paper regarded as a part of the shales due to the similarity in origin and composition.

As Kuenen has pointed out, the use of the arithmetic average of the manganese concentrations in pelagic clays introduces an error in the balance computation by overemphasis of the slowly accumulating deposits. It appears reasonable, in the absence of measured rates of accumulation for all samples involved, to assume that the manganese concentration is inversely related to the rate of accumulation. The use of the reciprocal average should under these conditions compensate for this over-representation. The reciprocal average of all Pacific clays reported herein is 0·77 per cent Mn whereas the arithmetic average is 0·95 per cent. Correns (1937) gives an arithmetic average of 0·25 per cent for the carbonate-free fraction

of around 180 Atlantic sediment samples. This value has been reduced to 0·19 per cent such that the ratios of the arithmetic to reciprocal average are the same in both oceans. To obtain an average for all oceans these two values were combined with a weighting factor of one for the Atlantic Ocean and three for the Indo-Pacific oceanic area. The resulting average manganese content thus obtained is 0·4 per cent.

Even with due regard to the rate effect pointed out by KUENEN, the manganese content of pelagic clays is still significantly higher than that of igneous rocks. Further, a whole suite of heavy metals, including copper, nickel, cobalt and lead, display a similar concentration pattern such that the red clay values are much higher than those of the igneous rocks from which they were presumably derived. Therefore, either KUENEN's estimate of the amount of red clays must be too large, or there is another source of entry of manganese and associated heavy metals into the major sedimentary cycle.

The system of equations can be written as follows:

$$\begin{aligned}
\text{Na} \quad & 2{\cdot}8\,X - 3{\cdot}4\,Y - 0{\cdot}04\,Z - 0{\cdot}97\,S = 297{\cdot}5 \\
\text{K} \quad & 2{\cdot}5\,X - 2{\cdot}5\,Y - 0{\cdot}27\,Z - 2{\cdot}7\,S = 10{\cdot}7 \\
\text{Ca} \quad & 3{\cdot}5\,X - 2{\cdot}6\,Y - 30{\cdot}4\,Z - 2{\cdot}2\,S = 11{\cdot}3 \\
\text{Mn} \quad & 0{\cdot}1\,X - 0{\cdot}4\,Y - 0{\cdot}038\,Z - 0{\cdot}062\,S = 0
\end{aligned}$$

The solution of these equations gives: $X = 185$, $Y = 23$, $Z = 8{\cdot}5$ and $S = 145$ in units of kg/cm^7 of earth's surface. Thus, the contribution of pelagic clays appears to be approximately 13 per cent of the total amount of sediments and somewhat greater than that of the carbonates.

The importance of balance calculations of this kind lies not in sharply delimiting the amounts of each sediment class but rather in the elucidating the general features of the major sedimentary cycle. Too many assumptions of doubtful validity and uncertainties in the values for the composition of the geological domains deny a strictly quantitative interpretation of the results.

It is, for example, normally assumed that the ultimate source of pelagic sediments is the weathering products from the continents. A number of authors have pointed out that the pyroclastics and their subsequent weathering products may significantly contribute to pelagic clays. This point has been considered at great length by MURRAY in the case of submarine volcanism. Quantitative estimates of contributions of supramarine pyroclastics have been suggested by KUENEN (1941, p. 166). He took as the composition of the source material, one part of plutonic and one part of volcanic rocks, the latter with a composition of rhyolite: andesite: basalt as 1:2:4.

The values for pelagic sediments are obtained from the samples of the surface layer of the sedimentary carpet beneath the oceans. Most analyses are from columns extending less than 20 m into the deep-sea floor. Thus, the assumption that materials from the present pelagic sediment surface are representative of weathering processes and sedimentation throughout geologic time must be considered. Changes in the rate of deposition of several elements, amounting to

one order of magnitude have been demonstrated to be common in the Tertiary and Quaternary of the east Pacific and the relative extent of calcareous sediments appears now to be considerably smaller than in Tertiary time (Arrhenius, 1952). The quartz content measured in a number of profiles shows a change between two geological periods by factors of three or four (Rex and Goldberg, in press). The amplitude in regional concentrations is also considerable (Revelle, 1944; Hutchinson, 1947; Goldberg, 1954) which makes it very difficult to decide upon an average compositional value for any element. Ocean to ocean variations in minor and trace elements have been clearly demonstrated (Fig. 10) and must be taken into account. Differences in the relative and absolute amounts of rock types exposed to weathering during geologic time are difficult to assess and present a further uncertainty in computations of a geochemical balance.

The residence times of elements in the ocean can be calculated on the basis of the values derived for the amounts of elements introduced into the major sedimentary cycle and for the rates of accumulation of pelagic clays.

Kuenen (1950, p. 362) gives the area of pelagic deposition as 268×10^{16} cm^2. Accepting an average accumulation rate of hydrogenous and lithogenous matter over this area of 0·1 cm/10^3 years and a density of the clay fraction of 2 with a water content of 50 per cent by weight, calculation of the total mass of pelagic clay accumulated in one year gives $26{\cdot}8 \times 10^{13}$ g. Division of this value with the fraction of pelagic clays in the totality of sediments (0·13), derived above, gives 2×10^{15} g/year as the amount of weathering products and pyroclastics. It is assumed in the present computation that practically all of this material enters the oceans.

If it is further assumed that the present chemical composition of the oceans represents a steady state system in which the amount of material introduced per unit time is compensated by an equal amount deposited as sediments, and that there is complete mixing of materials introduced into the oceans in times that are short with respect to the residence times. The residence time in years of an element in sea-water is then given by

$$T = \frac{A}{dA/dt}$$

where A is the total amount of the element in suspension or solution in the oceans and dA/dt is the amount introduced into the oceans per year. Values for the residence times of a selected group of elements are given in Table 21.

A remarkable agreement is observed between these values and those of Barth (1952), who made a similar set of calculations, using values for the rate of supply of elements to the ocean by rivers instead of the rate of removal from the ocean. Barth gives relatively few values, inasmuch as only a few elements have been adequately assayed in river water.

Although many independent assumptions are involved in the calculations, the absolute and relative values obtained for the residence times of the element appear reasonable. The element of longest residence, sodium, has a residence time within an order of magnitude of the age of the oceans, several billion years. The alkali and alkaline earth metals all have residence times in the range of 10^6–10^8

years. Manganese shows a remarkably low value in comparison to the metals associated with it in marine deposits such as zinc and nickel. This relation probably depends on the unique removal of manganese from solution in the oceans by oxidation (Section 5.12), a process that precedes the sorption which accounts for the deposition of the associated metals, and demands a larger amount of manganese than of the sorbed ions.

Silicon and aluminium are among the elements with the shortest residence

Table 21. Residence times of elements in the oceans

Element	Amount in oceans (g)	Residence time in years	
		This work	Barth (1952)
Na	$1{\cdot}47 \times 10^{22}$	$2{\cdot}6 \times 10^{8}$	$2{\cdot}1 \times 10^{8}$
Mg	$1{\cdot}8 \times 10^{21}$	$4{\cdot}5 \times 10^{7}$	$2{\cdot}2 \times 10^{7}$
Li	$2{\cdot}8 \times 10^{17}$	$2{\cdot}2 \times 10^{7}$	
Sr	$9{\cdot}8 \times 10^{18}$	$1{\cdot}6 \times 10^{7}$	
K	$5{\cdot}3 \times 10^{20}$	$1{\cdot}1 \times 10^{7}$	$1{\cdot}0 \times 10^{7}$
Ca	$5{\cdot}6 \times 10^{20}$	$8{\cdot}0 \times 10^{6}$	$1{\cdot}0 \times 10^{6}$
U	$5{\cdot}2 \times 10^{15}$	$6{\cdot}5 \times 10^{5}$	
Zn	$1{\cdot}4 \times 10^{16}$	$1{\cdot}8 \times 10^{5}$	
Cu	$5{\cdot}2 \times 10^{15}$	$6{\cdot}5 \times 10^{4}$	
Co	$7{\cdot}0 \times 10^{14}$	$1{\cdot}8 \times 10^{4}$	
Si	$5{\cdot}2 \times 10^{18}$	$1{\cdot}0 \times 10^{4}$	$3{\cdot}5 \times 10^{4}$*
Mn	$1{\cdot}4 \times 10^{15}$	$7{\cdot}0 \times 10^{3}$	
Fe	$1{\cdot}4 \times 10^{16}$	$1{\cdot}4 \times 10^{2}$	
Ti	$1{\cdot}4 \times 10^{15}$	$1{\cdot}6 \times 10^{2}$	
Al	$1{\cdot}4 \times 10^{16}$	$1{\cdot}0 \times 10^{2}$	

* This value was obtained from the influx value given by Barth (1952) and the amount of silicon in the oceans from this paper. Barth gives only an upper limit for this latter number.

times. Both are reactants in the formation of clay minerals and partly enter the oceans as rapidly settling suspended solids. Iron and titanium, which also pass rapidly through the hydrosphere, probably prevail as solid phases during the major part of their residence, even in the pelagic areas of the ocean. The absolute values for the residence times of these elements are somewhat tenuous as the assumption that these times are small in comparison with the mixing time is invalid in these cases. It may be worthwhile in the future, when values exist for the contribution of solid and dissolved phases of these elements to the total concentrations, to calculate more accurately the residence times of both of these components.

Mention should be made of the importance of the residence time in predicting the increases in concentration of artificial radionuclides introduced into the oceans by nuclear detonations or as wastes from reactors. The isotopes of strontium and caesium, both hazardous to living organisms, would have residence times in the oceans which are very high relative to their half-lives. Hence, the great majority of radionuclides of these elements brought into the oceans would undergo radioactive decay there. Further, it is evident that the bulk of the radioisotopes

introduced into the marine environment during the next few hundred years will build up to values of specific activity for each element that is principally a function of the decay constant of the isotope and the rate of entry, rather than of any sedimentary process.

Acknowledgements—The authors wish to express their gratitude to the sponsors of this research, and to those who gave their help in the work, viz. Dr. M. N. Bramlette who continually contributed with suggestions, observations and criticism; Dr. Harrison Brown in whose institute the research under Section 5.5 was carried out; Dr. R. Castaing, who took an active part in the X-ray micro-analysis reported in Section 5.4; Dr. M. Roy and M. G. de Faget, who kindly put the facilities at the O.N.E.R.A. to disposal for this part of the investigation; Mr. C. Harvey and Mr. A. Chodos, who contributed to the optical spectrographic analysis; and Dr. F. A. Paneth, who gave help and constructive suggestions. The authors are further indebted to Drs. J. R. Arnold, O. Arrhenius, W. Buser, C. W. Correns, H. Craig, G. de Hevesy, M. Fleischer, E. Ingerson, Ph. H. Kuenen, E. Picciotto, R. Revelle and K. H. Wedepohl, for their valuable criticism and comments.

References

Arrhenius G. (1952) Sediment cores from the East Pacific. *Repts. Swed. Deep-Sea Exped.* No. 5.
Arrhenius G. (1954) *Bull. Geol. Soc. Amer.* **65,** 1228–1229.
Arrhenius G. and Goldberg E. D. (1955) *Tellus* **7,** 226–231.
Arrhenius G., Bramlette M. N. and Picciotto E. (1957) *Nature, Lond.* 180, 85–86.
Barth T. W. (1952) *Theoretical Petrology.* John Wiley, New York.
Bjerrum N. (1948) *Bull. Soc. Chim. Belges* **57,** 432–495.
Boussingault F. (1882) *Ann. Chim. Phys.* **27,** 289.
Bowen H. J. M. (1956) *J. Mar. Biol. Ass. U.K.* **35,** 451–460.
Bradfield R. (1932) *J. Phys. Chem.* **36,** 340–347.
Buchanan J. Y. (1890) *Proc. Roy. Soc. Edinb.* **18,** 17–39.
Buser W. and Grütter A. (1956) *Schweiz. Min. Petrogr. Mitt.* **36,** 49–62.
Buser W. and Grütter A. (1957) Radiochemische Untersuchungen an Festkörpern IV.
Butkewitsch W. S. (1928) *Ber. Wiss. Meeresinst. Moscow* **3,** 63–80.
von Buttlar H. and Houtermans F. G. (1950) *Naturwissenshaften* **37,** 400–401.
Castaing R. (1952) *Office National d'Etudes et de Recherches Aéronautiques Publication Nr.* 55.
Chave K. (1954). *J. Geol.* **62,** 266–283.
Clarke F. W. (1924) *U. S. Geol. Survey Bull.* 770.
Clarke F. W. and Wheeler W. C. (1922) *U.S. Geol. Survey Prof. Paper* 124.
Collier A. (1953) *Science* **118,** 328.
Cooper L. H. N. (1948) *J. Marine Biol. Ass. U.K.* **25,** 279–313.
Correns C. W. (1937) *Wiss. Ergebn. Dtsch. Atlant. Exped.* "*Meteor*" 1925–1927 3, part 3.
Correns C. W. (1941) *Nachr. Ges. Wiss. Göttingen Math.-phys. Kl.* 5, 219.
Correns C. W. (1948) *Naturwissenschaften* **35,** 7–12.
Correns C. W. (1954) *Deep-Sea Res.* **1,** 78–85.
Daly R. A. (1933) *Igneous Rocks and the Depths of the Earth.* McGraw-Hill, New York.
Davies C. W. (1930) *J. Chem. Soc.* 1930 2421–2426.
Degenhardt H. (1957) *Geochim. et Cosmochim. Acta* **11,** 279–309.
Denney T. O. and Monk C. B. (1951) *Trans. Faraday Soc.* **47,** 992–8.
Dietz R. S. and Menard H. W. (1953) *J. Geol.* **61,** 99–113.
Dieulafait L. (1883) *C. R. Acad. Sci., Paris* **96,** 718–721.
Dorff F. (1935) *Biologie des Eisens und Mangankreislaufes* Berlin.
Emery K. O. and Rittenberg S. C. (1952) *Bull. Amer. Ass. Petrol Geol.* **36,** 735–806.

Emiliani C. (1955) *J. Geol.* **63,** 538–578.
Emiliani C. and Edwards G. (1953) *Nature, Lond.* **171,** 887–889.
Erämetsä O., Sahama Th. and Kanula V. (1940) *Ann. Acad. Sci. Fenn. VLIIA* No. 3.
Fleischer M. (1953) *U.S. Geol. Survey Circular* 287.
Goldberg E. D. (1952) *Biol. Bull.* **102,** 243–248.
Goldberg E. D. (1954) *J. Geol.* **62,** 249–265.
Goldberg E. D. and Picciotto E. (1955) *Science* 613–614.
Goldschmidt V. M. and Peters C. (1932a) *Nachr. Ges. Wiss. Göttingen* **27,** 402.
Goldschmidt V. M. and Peters C. (1932b) *Ibid.* **31,** 528.
Goldschmidt V. M. (1937) *J. Chem. Soc.* 1937, 655.
Goldschmidt V. M. (1954) *Geochemistry.* Oxford University Press, London.
Griel J. V. and Robinson R. J. (1952) *J. Mar. Res. Sears Foundation* **11,** 173–179.
Grütter A. and Buser W. (1957) *Chimia* **11,** 132–133.
von Gümbel C. W. (1878) *S. B. Bayer. Akad. Wiss.* **8,** 189–209.
Hamilton E. L. (1956) *Geol. Soc. Amer. Memoir* 64.
Harder H. (1951) *Heidelberg. Beitr. Min.* **2,** 455–476.
Harvey C. E. (1950) *Spectrochemical Procedures.* Applied Research Labs., Glendale, California.
von Hevesy G., Merkel A. and Würstlin K. (1934) *Z. Anorg. Chem.* **219,** 192.
Hutchinson G. E. (1947) *Ecol. Mon.* **17,** 299–315.
Hutchinson G. E., Benoit R. J., Cotter W. B. and Wangersky P. J. (1955). *Proc. Nat. Acad. Sci. U.S.* **41,** 160–162.
Jacob K. D., Hill W. L. *et al.* (1933). *U.S. Dept. Agric. Tech. Bull.* 364.
Jasmund K. (1948) *Heidelberg. Beitr. Min.* **1,** 341–380.
Joly J. (1899) *Trans. Roy. Dublin Soc.* **7,** 23.
Jonte J. H. and Martin D. S. (1952) *J. Amer. Chem. Soc.* **74,** 2052–2054.
Jost K. (1932) *Chem. d'Erde* **7,** 177.
Krauskopf K. B. (1955) *Econ. Geol.* (*Fiftieth Anniv. Vol.*) 411–463.
Krauskopf K. B. (1956) *Geochim. et Cosmochim. Acta* **9,** 1–33.
Kuenen Ph. H. (1941) *Amer. J. Sci.* **239,** 161–190.
Kuenen Ph. H. (1950) *Marine Geology.* John Wiley, New York.
Kuroda P. K. and Sandell E. B. (1954) *Geochim. et Cosmochim. Acta* **6,** 35–63.
Landergren S. (1945) *Ark. Kemi. Min. Geol.* A **19.**
Landergren S. (1956) *Repts. Swed. Deep-Sea Exped.* **7,** No. 2.
Latimer W. M. (1952) *Oxidation Potentials* (Second Edition). Prentice-Hall, New York.
Lewis G. J. and Goldberg E. D. (1956) *Analyt. Chem.* **28,** 1282–1285.
Lindgren B., Johnson A. and Sillén L. (1947) *Acta Chem. Scand.* **1,** 479–88.
Lundegårdh P. H. (1946) *Ark. Kemi. Min. Geol.* A **23,** No. 9.
Martell A. E. and Calvin M. (1952) *Chemistry of the Metal Chelate Compounds.* Prentice-Hall, New York.
Morita Y. (1955) *J. Earth Sci. Nagoya Univ.* **3,** 33–57.
Murray J. and Renard A. (1891) *Challenger Repts.* 525 pp.
Murray J. and Irvine R. (1894) *Trans. Roy. Soc. Edinb.* **37,** 712–242.
Nockolds S. R. and Allen R. (1956) *Geochim. et Cosmochim. Acta* **5,** 245–785.
Patterson C. C., Goldberg E. D. and Ingram M. G. (1953). *Bull. Geol. Soc. Amer.* 1387–1388.
Pettersson H. (1943) *Medd. Oceanogr. Inst. Göteborg* B **2.** 1–39.
Pettersson H. (1945) *Ibid.* **3,** 1–37.
Pettijohn F. J. (1957) *Sedimentary Rocks* (Second Edition). Harper and Brothers, New York.
Raitt R. W. (1956) *Bull. Geol. Soc. Amer.* **67,** 1623–39.
Rankama K. and Sahama Th. (1950) *Geochemistry.* University of Chicago Press.
Ramdohr P. (1940) *Abh. Preuss. Akad. Wiss.* No. 2.
Revelle R. (1944) *Carnegie Inst. Wash. Publ. No.* 556.
Revelle R., Bramlette M., Arrhenius G. and Goldberg E. D. (1955) *Geol. Soc. Amer. Special Paper* 62, 221–236.
Robinson R. A. and Stokes R. H. (1955) *Electrolyte Solutions.* Butterworths, London.
Sandell E. B. (1949) *Amer. J. Sci.* **247,** 40–48.

Sandell E. B. (1952) *Geochim. et Cosmochim. Acta* **2,** 211–218.
Sandell E. B. and Goldich S. S. (1943) *J. Geol.* **51,** 161–189.
Schubert J. (1954) *Chemical Specificity in Biological Interactions* (Ed. F. R. N. Gurd). Academic Press, New York.
Sillén L. G. (1954) *Acta. Chem. Scand.* **8,** 318–335.
Shaw M. (1954) *Bull. Geol. Soc. Amer.* **65,** 1151–1166.
Smales A. A., Mapper D. and Wood A. J. (1957) *Analyst* **82,** 75–88.
Steeman-Nielsen E. (1952) *J. Cons. Int. Explor. Mer.* 18, 117.
Sverdrup H., Johson M. and Fleming R. (1946) *The Oceans.* Prentice Hall, New York.
Tamm O. (1932) *Medd. Statens Skogsförsöksanst. Stockh.* **27,** 1–20.
Thompson T. G. and Chow T. J. (1955) *Deep-Sea Res.* (Suppl. to Vol 3) 20–39.
Turekian K. (1955) *Trans. Amer. Geophys. Un.* **36,** 523.
Turekian K. (1956) *Ibid.* **37,** 361.
Urey H. C. (1953) *Proc. Roy. Soc.* **219,** 281–292.
Wedepohl K. (1955) *Nachr. Ges. Wiss. Göttingen Math. physik Kl.* 79–86.
Wedepohl K. (1956) *Geochim. et Cosmochim. Acta* **10,** 69–148
Wickman F. E. (1954) *Geochim. et Cosmochim. Acta* **5,** 97–110.
Wiseman J. D. (1956). *Advanc. Sci., Lond.* **49,** 579–588.
Worzel J. L. and Shurbet G. L. (1955) *Geol. Soc. Amer. Special Paper* 62, 87–100.
Young E. J. (1954) *Bull. Geol. Soc. Amer.* **65,** 1329.

Geochimica et Cosmochimica Acta, 1958, Vol. 13, pp. 213 to 217. Pergamon Press Ltd., London

Some data on diagenesis obtained from Soviet literature: A summary

George V. Chilingar*
Los Angeles, California

Moisture Content of Recent Sediments

The high moisture content in the recent sediments plays an important role in the early processes of diagenesis. According to Strakhov (1953, p. 13), in the upper layers of recent sediments sands contain 20–25 per cent moisture, siltstones—30–60 per cent, and clays—60–80 per cent. The recent clayey sediments of fresh-water

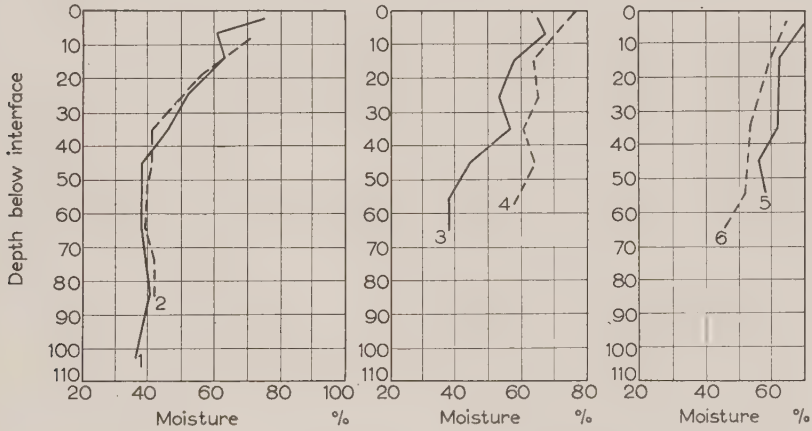

Fig. 1. Change in moisture content of Caspian Sea sediments with depth below the depositional interface (after Bruevich and Vinogradova, 1947).
1—Station G × 92, Tyub-Karaganskiy Bay; 2—Station G × 83, Tyub-Karaganskiy Bay; 3—Station no. 57, northern Caspian Sea; 4—Station no. 1, central Caspian Sea; 5—Station no. 26, southern Caspian Sea; and 6—Station no. 28, southern Caspian Sea.

lakes contain even higher amounts of moisture—86–95–96 per cent by weight. As shown in Fig. 1, however, the moisture content decreases with depth below the depositional interface.

Chemical Composition of Interstitial Solutions of Caspian Sea Sediments (Bruevich and Vinogradova, 1947)

The results obtained by Bruevich and Vinogradova (1947, Table 1) clearly show that the concentration of some elements in the interstitial waters is many times greater than it is in the bottom waters. According to Strakhov (1953, p. 16) the maximum concentrations of these elements occur in the fine-grained sediments (muds).

The variation in composition and properties of the interstitial solutions of

* University of Southern California, Petroleum and General Engineering Departments.

Table 1. Average content of some elements in the interstitial solutions of Caspian Sea sediments. Depth up to 100 m. (After Bruevich and Vinogradova, 1947)

Areas of Caspian Sea	Muds	Sandy muds and silty sands	Silty sands with coquina (northern Caspian); mud with coquina (southern Caspian)	Coquina	Bottom water
			Cl (%)		
Northern	5·54	5·47–5·15	—	—	5·42
Central	5·37	—	5·43	5·46	5·37
Southern	5·42	—	5·43	5·44	5·42
			pH		
Northern	7·91	7·64–7·45	—	—	8·36
Central	7·7–7·8	—	7·66–7·89	7·82–7·89	8·26–8·31
Southern	—	—	7·76	7·99	8·11–8·25
			Alkalinity (mg/equiv.)		
Northern	35·8–18·8	15·6–6·4	5·4	—	3·6–3·7
			Mineral phosphorus (mg/m^3)		
Northern	1100	35–45	32	33	2·73
Central	200	—	150	24	5
Southern	360	—	26	34	7
			Silica (mg/m^3)		
Northern	23,700	6900	6700	4500	100–200
Central	17,400	—	12,100	1000	200–240
Southern	13,000	—	6600	1600	250–36
			Ammonium nitrogen (mg/m^3)		
Northern	17,800	2500	2100	1200	84–36
Central	8500	—	2500	310	31–17
Southern	1500	—	1000	1300	34–43
			Oxidizability in neutral medium O_2 (mg/l.)		
Northern	6·1	4·7	—	—	1·7–2·5
			Iron (mg/l.)		
Northern	—	700–210	310(?)	—	—

Caspian Sea sediments with depth below the depositional interface is shown in Fig. 2.

Vertical Distribution of Biogenous Elements in the Interstitial Solutions of Bering Sea Sediments in 1950 (Zaytseva, 1954)

The vertical distribution of biogenous elements in the interstitial solutions of Bering Sea sediments is presented in Tables 2 and 3. On the basis of her findings, Zaytseva arrived at the following conclusions:

(1) The values for alkalinity (which is indicative of the mineralization of organic carbon) and ammonium nitrogen content in the interstitial solutions increase with depth below the depositional interface; and show definite similarity in trend.

(2) In the majority of cases, the phosphate phosphorus exhibits systematic increase with depth below the interface. This increase, however, is less pronounced than that for ammonium nitrogen.

(3) The silica content does not show any systematic increase with depth of burial, and varies within relatively narrow limits for each station. Emery and Rittenberg (1952), on the other hand, found that the silica dissolved in the interstitial waters of California Basin sediments increases with depth of burial.

(4) The quantitative increase in the content of biogenous elements and alkalinity varies markedly from station to station. In some places they increase rapidly with depth below the interface, whereas at others, slowly.

Table 2. Variation in composition (alkalinity and nitrogen content) of the interstitial solutions in sediments of Bering Sea with depth (after Zaytseva, 1954, p. 290)

Station no.	Total N in upper horizon %	Depth below depositional interface in metres											
		0	1	2	4	8	16	0	1	2	4	8	16
		Alkalinity (mg-equiv/l.)						Ammonium nitrogen (mg/l.)					
							Depth 0–150 m						
568	0·038	2·75	12·8	—	—	—	—	3·6	—	—	—	—	—
565	0·037	10·9	26·9	—	—	—	—	11·4	25·4	—	—	—	
557	0·14	2·5	8·6	17·5	—	—	—	1·2	7·6	17·0	—	—	—
553	0·29	41·7	66·2	72·7	(73·7)	—	—	45·0	111·0	159·0	(145·0)	—	—
							Depth 1000 m						
612	0·17	2·9	3·0	6·3	(21·9)	—	—	0·92	1·3	7·5	(23·4)	—	—
							Depth 2000 m						
617	—	(2·6)	4·2	6·0	8·6	—	—	(1·6)	2·5	4·8	7·1	—	—
							Depth 3000 m						
614	—	3·0	5·2	6·5	(11·0)	—	—	0·68	2·9	3·8	(11·6)	—	—
540	0·092	(3·5)	3·8	5·7	13·5	29·2	38·5	1·7	1·8	3·6	10·5	21·5	31·8
619	0·084	(3·8)	3·8	5·9	16·8	24·4	(32·0)	(2·8)	3·2	5·9	12·4	16·5	(18·6)
615	—	(6·6)	7·5	8·8	9·4	12·2	—	(4·3)	4·5	4·9	5·4	(6·4)	—
537	0·086	2·6	5·6	8·2	(15·9)	—	—	0·24	5·3	6·0	(15·0)	—	—
618	0·088	2·6	3·3	4·3	6·5	—	—	0·61	1·9	3·0	5·0	—	—
533	—	(1·73)	10·52	—	—	—	—	(1·6)	4·1	—	—	—	—

(5) With increasing organic matter content in the solid phase of sediments, there is a corresponding increase in the content of biogenous elements in the interstitial solutions. The comparison of sampling localities having considerable quantities of organic matter (such as station no. 553) with those low in organic matter (most of the stations) clearly demonstrates this.

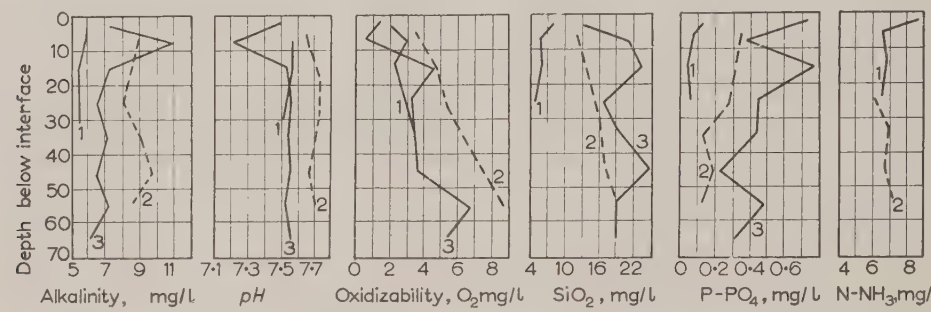

Fig. 2. Variation in composition and properties of the interstitial solutions of southern Caspian Sea with depth below the depositional interface (Bruevich and Vinogradova, 1947).

1—Station no. 16, 100 m depth; 2—Station no. 26, 960 m depth; and 3—Station no. 28, depth of 460 m.

Table 3. Variation in composition (phosphorus and silica contents) of the interstitial solutions in sediments of Bering Sea with depth (after Zaytseva, 1954, p. 290)*

Station no.	Total *N* in upper horizon %	Depth below surface of sea bottom in metres											
		0	1	2	4	8	16	0	1	2	4	8	16
		Phosphate P (mg/l.)†						Silica (mg/l.)†					
						Depth—0–150 m							
568	0·038	1·6	4·0	—	—	—	—	14·5	12·2	—	—	—	—
565	0·037	6·3	3·2	—	—	—	—	11·0	—	—	—	—	—
557	0·14	0·35	1·8	1·7	—	—	—	13·7	—	—	—	—	—
653	0·29	2·5	4·5	4·7	(7·5)	—	—	26·8	14·0	16·0	23·2	—	—
						Depth—1000 m							
612	0·17	0·25	0·26	0·67	—	—	—	12·7	16·2	17·2	—	—	—
						Depth—2000 m							
617	—	0·20	(0·21)	0·40	0·77	—	—	(17·7)	16·5	12·6	13·0	—	—
						Depth—3000 m							
614	—	0·25	0·38	0·43	(1·2)	—	—	15·5	17·0	16·2	(15·2)		—
540	0·092	(0·17)	0·17	0·25	0·70	1·9	3·0	—	14·7	14·7	17·5	20·7	17·5
619	0·084	(0·43)	0·39	0·46	4·4	4·4	5·4	(17·7)	17·7	17·7	13·8	14·4	15·7
615	—	(0·27)	0·50	0·79	0·69	0·35	—	(14·0)	14·0	14·1	14·6	16·8	—
537	0·086	0·17	0·17	0·68	(1·6)	—	—	15·5	26·8	30·9	29·8	—	—
618	0·088	0·22	0·26	0·31	0·95	—	—	13·5	18·0	12·4	12·7	—	—
533	—	(0·65)	1·3	—	—	—	—	(19·0)	14·2	—	—	—	—

* The values in parentheses indicate that samples were not obtained from the exact localities described. Station no. 553 is located in a bay with large biologic productivity.

† The contents of silica and phosphate phosphorus were determined by A. V. Fotiev.

(6) The interstitial solutions in sediments of shallow-water stations, as compared to deep-water stations (1000–4000 m), are characterized by considerably higher values for alkalinity and biogenous elements (N, P); and a higher absolute increment with depth of burial as compared to the upper horizons.

(7) The process of decomposition of organic matter does not stop in the upper layers of sediments (16 m), and continues with decreasing intensity to greater depths.

Conclusions

The findings of Zaytseva (1954) indicate that the diagenetic processes go on in the marine sediments for hundreds of thousands of years after their deposition.

For a comprehensive review of Soviet literature on diagenesis, the reader is referred to an excellent article by Strakhov (1953, pp. 12–49), who is considered one of the best geologists in U.S.S.R. It is interesting to note that the results obtained by Emery and Rittenberg (1952) are extensively quoted in Soviet literature, and referred to as "the first work overseas on the quantitative distribution of silica and ammonium nitrogen in the interstitial solutions".

References

Bruevich S. V. and Vinogradova E. G. (1947) Chemical composition of interstitial solutions of Caspian Sea. *Gidrokhim. Mat.* **13,** Reports 1 and 2.

Emery K. O. and Rittenberg S. C. (1952) Early diagenesis of California Basin sediments in relation to origin of oil. *Bull. Amer. Ass. Petrol. Geol.* **36,** 5, 735–806.

Strakhov N. M. (1953) Diagenesis of sediments and its significance for sedimentary ore formation. *Izv. Akad. Nauk SSSR Geol. Ser.* No. 5, 12–49.

Zaytseva E. D. (1954) Vertical distribution of biogenous elements in interstitial solutions of Bering Sea. *Dokl. Akad. Nauk SSSR* **99,** No. 2, 289–91.

Geochimica et Cosmochimica Acta, 1958, Vol. 13, pp. 218 to 219. Pergamon Press Ltd., London

GEOCHEMICAL NOTE

The solid solubility of $MgCO_3$ in $CaCO_3$: A revision

(*Received* 24 *May* 1957)

In a paper entitled, "Dolomite–magnesian calcite relations at elevated temperatures and CO_2 pressures" (Graf and Goldsmith, 1955), data were presented on the Mg-content of calcite in equilibrium with dolomite, and with MgO and CO_2. The data are shown in Tables 2–5 of the above publication, and Figs. 4 and 5 are based on some of these data. The X-ray method by which these Mg-calcites were analysed is described by Goldsmith *et al.* (1955). The primary standards for determining the curves of X-ray spacing vs.

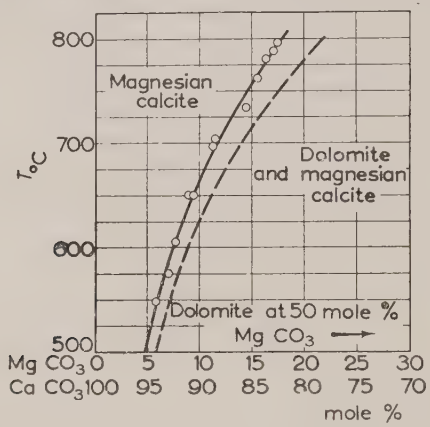

Fig. 1. A portion of the exsolution curve in the system $CaCO_3$–$MgCO_3$, determined at CO_2 pressures sufficient to prevent decomposition. The broken curve is the one published previously (Graf and Goldsmith, 1955).

magnesium content of the calcites were natural magnesian calcites, and the precision of the method depended on the following:

(1) The analytical accuracy (spectrochemical or chemical) in determining the composition of the magnesian calcite;

(2) The assumption that all of the Mg was present in solid solution in the calcite, and that none was tied up in small quantities of dolomite or as an adsorbed phase on the fine-grained algal or skeletal carbonates;

(3) The accuracy of the X-ray spacing measurements, particularly on rather poorly crystallized material of high Mg-content, such as the algal calcite.

A more detailed study of the X-ray spacings of calcite, dolomite, and magnesite, along with the preparation and examination of a series of synthetic magnesian calcites (Goldsmith *et al.*, in press) has produced more precise data on the cell constants of these materials. It is felt that attention should be called to the revised curves derived from the more accurate data.

The X-ray patterns of the runs used in determining Fig. 4 (Graf and Goldsmith, 1955) were remeasured and re-evaluated. The revised data corresponding to the first and second columns of the old Table 3 are given here as Table 1, together with the redrawn exsolution curve. Fig. 5 is not redrawn here, but the numerical values for the vertical iso-Mg lines in that figure are directly taken from the exsolution curve, and the Mg contents in the field of dolomite decomposition can be lowered by subtracting 1 mole per cent $MgCO_3$ for each 6 mole per cent present.*

Table 1. Revised values of $MgCO_3$ solid solubility in calcite, upon which the solid curve of Fig. 1 is based

T°C	Mole % $MgCO_3$	T°C	Mole % $MgCO_3$
584	5·9	704	11·5
575	7·0	734	14·4
605	7·7	762	15·6
650	9·0	780	16·4
650	9·5	788	17·1
697	11·3	796	17·5

It may be noted from column 4 of the old Table 3 that the solid solution data are based upon runs which, with one exception, were made at CO_2 pressures of 10,000 lb/in^2 or less. Not only are these pressures in all cases equal to or greater than the partial pressure of CO_2 required to prevent decomposition, but they are also total pressures in the system. The effect of significantly greater total pressures upon solid solubility will be discussed by Goldsmith in a subsequent note.

Illinois State Geological Survey, Urbana, Ill. Donald L. Graf

Department of Geology, The University of Chicago. Julian R. Goldsmith

References

Goldsmith J. R., Graf D. L. and Joensuu O. I. (1955) The occurrence of magnesian calcites in nature. *Geochim. et Cosmochim. Acta* **7**, 212–230.

Goldsmith J. R. and Graf D. L., with additional analytical determinations by Chodos A. A., Joensuu O. I. and McVicker L. D. (1957). The relation between lattice constants and composition of the *Ca–Mg* carbonates. *Amer. Min.* In press.

Graf D. L. and Goldsmith J. R. (1955) Dolomite–magnesian calcite relations at elevated temperatures and CO_2 pressures. *Geochim. et Cosmochim. Acta* **7**, 109–128.

Harker R. I. and Tuttle O. F. (1955) Studies in the system CaO–Mg–OCO_2: Part 2. Limits of solid solution along the binary join, $CaCO_3$–$MgCO_3$. *Amer. J. Sci.* **253**, 274–282.

* Harker and Tuttle (1955) published a graph (their Fig. 3) also showing the solid solubility of $MgCO_3$ in $CaCO_3$. Their results were in good accord with ours, but our revised results are in even closer agreement.

Geochimica et Cosmochimica Acta, 1958, Vol. 13, pp. 220 to 222. Pergamon Press Ltd., London

LETTERS TO THE EDITORS

Hydrothermale und röntgenographische Untersuchungen an gesteinsbildenden Mineralen—II

Über hydrothermale Untersuchungen in Druckbomben mit Temperaturgefälle

(*Received* 21 *July* 1957)

Viele Gesteinsumwandlungen in der Natur gehen nicht unter konstanten Temperaturen vor sich. Es enstehen zum Beispiel Temperaturgefälle im Nebengestein durch das Eindringen intrusiver Magmenkörper und durch das Eindringen pneumatolytischer und hydrothermaler Phasen.

Um ähnliche Bedingungen bei hydrothermalen Untersuchungen erhalten zu können, wurden Druckbomben hergestellt, deren Versuchsraum eine Länge von 100–110 mm hat. Versuche wurden an Gesteinsleisten durchgeführt mit einer Grösse von etwa 3 × 3 × 100 mm. Mit diesen Bomben konnte ein Temperaturgefälle von z.B. 700°/500°C oder 400°/280°C eingestellt werden. Sämtliche Versuche wurden bei 1000 bar H_2O-Druck durchgeführt.

Zunächst wurden Untersuchungen an Gesteinsleisten vorgenommen, die aus Paragneisen des Schwarzwaldes (Gelbachtal und Frohnbachtal) herausgeschnitten wurden. Die mittlere Zusammensetzung dieser Paragneise beträgt 45% Plagioklas ($\approx An_{35}$), 30% Quarz, 20% Biotit, Rest Akzessorien. In einem Temperaturgefälle 800°/600° bzw. 700°/500°C wanderte vor allem der Quarz zu der Seite der Bombe, an der die tiefere Temperatur herrschte. Dabei schied sich das SiO_2 auf der Gneisleiste als Quarz ab, z.Tl. als Rosenquarz, während unmittelbar am Bombenverschluss Cristobalit röntgenographisch nachgewiesen wurde. Zurück blieb von dem Teil der Leiste, der bei der höheren Temperatur lag, ein Restgewebe aus Biotit und Plagioklas. An weiteren Neubildungen wurden Hämatit, Rutil, Cordierit und ein milarit-ähnliches Mineral, alle in idiomorpher Ausbildung, erkannt. Im Temperaturgefälle 600°/400°C wuchsen Quarzkristalle in demjenigen Teil der Bombe, welcher tiefere Temperaturen hatte, weiter; am anderen Ende der Bombe (bei höherer Temperatur) schieden sich auf einer Goldfolie und auf der Gesteinsleiste Alkalifeldspäte ab. Die Alkalifeldspäte dürften auf Kosten des Biotits unter gleichzeitiger Neubildung von Cordierit entstanden sein. Die Na-Komponente der Feldspäte muss aus dem Plagioklas stammen. Die neugebildeten Alkalifeldspäte setzen sich nach röntgenographischen Untersuchungen mit der Guinierkamera unter Verwendung der Linie ($\bar{2}01$) nach Bowen und Tuttle (1950) aus zwei verschiedenen Phasen zusammen; der kalireiche Feldspat hat die Zusammensetzung $Ab_{30}Or_{70}$, der natriumreiche Feldspat $Ab_{90}Or_{10}$. Tempert man die vorher gepulverten Feldspäte zusammen bei 1050°C einen Tag lang, so erhält man *einen* Feldspat mit der Zusammensetzung $Ab_{60}Or_{40}$. Bisher gelang es nur, Einkristalle der einen Phase zu finden, deren Zusammensetzung $Ab_{90}Or_{10}$ auch aus Precession-Aufnahmen mit Hilfe der Werte von $d_{(100)}$ nach Laves (1952) bestimmt wurde. An diesen Kristallen wurden die Flächen (010), (110), (001), ($\bar{1}01$) beobachtet.

Aus diesen Versuchen geht hervor, dass Quarz und Alkalifeldspat die leichtbeweglichen Komponenten von Paragesteinen sind. Im Temperaturgefälle 600°/400°C wandert der Alkalifeldspat zu dem Teil der Bombe, an dem die höhere Temperatur herrscht. Der Quarz kristallisiert in dem Teil der Bombe mit der tieferen Temperatur. Hieraus darf man qualitativ

schliessen, dass die Kurve der Kristallgrösse der Alkalifeldspäte bei etwa 600°C, die des Quarzes bei etwa 400°C oder tiefer ein Maximum hat. Die Kristallgrösse ist nach Winkler (1949)

$$\text{Kristallgrösse} \sim \sqrt[4]{\left(\frac{\text{Wachstumsgeschwindigkeit}}{\text{Keimbildungshäufigkeit}}\right)}$$

Ganz ähnliche Verhältnisse finden wir im Nebengestein vor, wenn ein saures Intrusivmagma kristallisiert. Im Nebengestein entsteht ein Temperaturgefälle, das durch den Wärmeinhalt des Intrusivkörpers und durch das Eindringen der magmatischen Restlösungen verursacht wird. Auffallend ist, dass im Nebengestein in der Nähe eines Intrusivkörpers (z.B. Randgebiete der Schwarzwälder Granite) Alkalifeldspatmegablasten gebildet werden, dass aber ein Wachsen des Quarzes in diesen Gebieten nicht gleichzeitig beobachtet wird.

R. Euler
E. Hellner

Mineralogisches Institut der
Universität Marburg/Lahn

Literatur

Bowen N. L. und Tuttle O. F. (1950) *J. Geol.* **58**, 493.
Laves F. (1952) *J. Geol.* **60**, 553.
Winkler H. G. F. (1949) *Heidelberg. Beitr. Min.* **1**, 86–104.

Hydrothermale und röntgenographische Untersuchungen an gesteinsbildenden Mineralen—III

Über einen hydrothermal hergestellten Granat (Andradit)

(*Received* 21 *July* 1957)

Über die Herstellung von Granaten in Laboratorien sind zahlreiche Arbeiten bekannt geworden. Über Hydro-Granate informiert die Grossular-Arbeit von Yoder (1950). In einer zusammenfassenden Arbeit über "Investigations under hydrothermal conditions" berichten Roy und Tuttle (1956) über die Herstellung von verschiedenen Granaten bei hohen Drucken und Temperaturen (15.000–30.000 kg/cm^2 und 600°–900°C) durch L. Coes. Es wurde auch der Andradit aufgeführt, ohne dass die Ausgangssubstanzen bei diesen Versuchen und die optischen Eigenschaften sowie die Gitterkonstanten mitgeteilt wurden. Über die Herstellung eines wasserfreien Granats (Almandin) bei niedrigeren Drucken (1.000–10.000 bar) berichtet Yoder (1955a und 1955b).

Bei Untersuchungen über das hydrothermale Verhalten von Weilburgiten im Temperaturgefälle wurde unter anderem auch der Granat Andradit synthetisiert. Weilburgite sind Gesteine, die im Mittel aus 60% Alkalifeldspäten und 35% Chlorit sowie Akzessorien bestehen. Der Granat bildete sich in folgenden Versuchen jeweils am Ende der Bombe mit der höheren Temperatur (600°C):

Intermediärer Weilburgit, das Temperaturgefälle in der Bombe betrug 600°/380°C;
Na-Weilburgit, das Temperaturgefälle in der Bombe betrug 600°/410°C.
Alle diese Versuche wurden bei 1.000 bar H_2O-Druck durchgeführt.

Die Andraditkristalle bildeten sich als idiomorphe goldgelbe Rhombendodekaeder auf einer Goldfolie und hatten eine Grösse bis zu 0,2 mm. Sie sind unter dem Mikroskop in anomal doppelbrechende Felder aufgeteilt und haben die Brechzahl $n_D = 1{,}87_2$. Aus Guinieraufnahmen mit Cu$K\alpha_1$-Strahlung wurde die Gitterkonstante $a_0 = 12{,}016 \pm 0{,}004$ Å ermittelt. Vergleicht

man diese Werte mit der Darstellung des Systems Grossular—Andradit—$Ca_3Al_2O_6 \cdot 6H_2O$—$Ca_3Fe_2O_6 \cdot 6H_2O$ bei WINCHELL (1951), so erhält man einen wasserfreien Granaten mit etwa 90 Mol-% Andradit, $Ca_3Fe_2[SiO_4]_3$. Hierbei ist zu beachten, dass die Gitterkonstanten bei WINCHELL aus älteren Arbeiten entnommen sind und somit Werte in kX-Einheiten darstellen. Für unsere Gitterkonstante ergibt sich umgerechnet ein $a_0 = 11{,}992$ kX. Zum Vergleich seien in einer Tabelle die neubestimmten Gitterkonstanten von in der Literatur beschriebenen Granaten mit ähnlicher Zusammensetzung mitgeteilt:

Fundort	MENZER (1929)		eigene Werte
	kX	umgerechnet in Å	Å
Andradit (Topazolith) Alatal in Piemont	12,026 ± 0,003	12,050 ± 0,003	12,064 ± 0,005
Andradit Dobschau in Ungarn	12,030 ± 0,003	12,054 ± 0,003	12,060 ± 0,005
Andradit Dognacska in der Woiwodina			12,051 ± 0,006
Hessonit Mussa-Alpe in Piemont	11,89 ± 0,06	11,91 ± 0,06	
Hessonit Elba			11,882 ± 0,004
Andradit hydrothermal hergestellt bei 600°C, 1000 bar, $n_D = 1{,}87_2$			12,016 ± 0,004

Auch aus diesen Untersuchungen geht hervor, dass Granate bei 1000 bar H_2O-Druck und Temperaturen um 600°C gebildet werden können.

Mineralogisches Institut R. EULER
der Universität Marburg/Lahn E. HELLNER
Germany

LITERATUR

MENZER G. (1929) *Z. Kristallogr.* **69,** 300–396.
ROY R. and TUTTLE O. F. (1956) *Physics and Chemistry of the Earth* Vol 1, pp. 138–180. Pergamon Press, London.
WINCHELL A. N. and WINCHELL H. (1951) *Elements of Optical Mineralogy* (Fourth Edition) Part II, p. 493. Wiley, New York; Chapman & Hall, London.
YODER H. S. (1950) *J. Geol.* **58,** 221–253.
YODER H. S. (1955a) *Amer. Mineral.* **40,** 342.
YODER H. S. (1955b) *Carnegie Institution of Washington, Year Book* **54,** 97–99.

News and Notes

Announcement of a new journal, *THE PHYSICS OF FLUIDS*, published by the American Institute of Physics

STARTING with January 1958, the American Institute of Physics will publish a new journal *The Physics of Fluids.*

The new journal will be devoted to original contributions to the physics of fluids covering kinetic theory, statistical mechanics, structure and general physics of gases, liquids and other fluids; as well as certain basic aspects of physics of fluids bordering geophysics, astrophysics, biophysics and other fields of science. The scope of these fields of physics includes: magneto-fluid dynamics, ionized fluid and plasma physics, shock and detonation wave phenomena, hypersonic physics, rarefied gases and upper atmosphere phenomena, physical aeronomy, transport phenomena, hydrodynamics, dynamics of compressible fluids, boundary layer and turbulence phenomena, liquid state physics and superfluidity.

The new journal will consider appropriate for publication original papers containing sufficiently significant results not published in any other recognized publication. *The Physics of Fluids* will start as a bimonthly and will become a monthly as soon as it appears desirable.

Correspondence on editorial matters should be addressed to: F. N. Frenkiel, Editor, "The Physics of Fluids", Applied Physics Laboratory, The Johns Hopkins University, Silver Spring, Maryland.

Subscription information can be obtained from the American Institute of Physics, 335 East 45th St., New York 17, New York.

THE NATIONAL SCIENCE FOUNDATION

The National Science Foundation will award grants to partially defray travel expenses for a limited number of American scientists wishing to participate in the meetings of the International Federation of Electron Microscope Societies. This meeting is to be held in Berlin, Germany, 10–17 September 1958.

Papers to appear in future issues

W. GENTNER und W. KLEY: Argonbestimmungen an Kalium–Mineralien. V. Altersbestimmungen nach der Kalium–Argon-Methode an mineralien und Gesteinen des Schwarzwaldes

R. CASTAING and K. FREDRIKSSON: Analyses of cosmic spherules with an X-ray microanalyser

G. JUNK and H. J. SVEC: The absolute abundance of the nitrogen isotopes in the atmosphere and compressed gas from various sources

G. S. BIEN, D. E. CONTOIS and W. H. THOMAS: The removal of soluble silica from fresh water entering the sea

G. W. REED, H. HAMAGUCHI and A. TURKEVICH: The uranium contents of iron meteorites

P. E. DAMON and J. L. KULP: Inert gases and the evolution of the atmosphere

J. A. S. ADAMS, J. E. RICHARDSON and C. C. TEMPLETON: Determinations of thorium and uranium in sedimentary rocks by two independent methods

F. CUTTITTA and J. J. WARR, JR.: Retention of lead during oxidative ashing of selected naturally occurring carbonaceous substances

H. LEVINE and F. S. GRIMALDI: Determination of thorium in the parts per million range in rocks

E. G. MURRAY and J. A. S. ADAMS: Thorium, uranium and potassium in some sandstones

H. C. UREY: Comments on two papers by John F. Lovering concerning a typical parent meteorite body

A. B. VISTELIUS: Paragenesis of sodium, potassium and uranium in volcanic rocks of Lassen Volcanic National Park, California

W. NICHIPORUK: Variations in the content of nickel, gallium, germanium, cobalt, copper and chromium in the kamacite and taenite phases of iron meteorites

T. C. HOERING and H. E. MOORE: The isotopic composition of the nitrogen in natural gases and associated crude oils

H. SAKAI and K. SATO: Isotopic composition of the common lead of Japan

S. R. TAYLOR and K. S. HEIER: Alkali elements in potash feldspar from the pre-Cambrian of Southern Norway

H. G. MACPHERSON: A chemical and petrographic study of pre-Cambrian sediments

L. CAHEN, P. EBERHARDT, J. GEISS, F. G. HOUTERMANS, J. CAHEN and P. SIGNER: On a correlation between the common lead model age and the trace element contact of galenas

W. O. ROBINSON, H. BASTRON and K. J. MURATA: Biogeochemistry of the rare-earth elements with particular reference to hickory trees

D. H. ANDERSON and H. E. HAWKES: Relative mobility of the common elements in weathering of some schist and granite areas

R. COULOMB, M. GOLDSZTEIN and M. LE MERCIER: L'uranium dans quelques granites français

C. D. KEELING: The concentration and isotopic abundances of atmospheric carbon dioxide in rural areas

A. E. RINGWOOD: The constitution of the mantle—I. Thermodynamics of the olivine-spinel transition

K. R. MEHNERT: Argonbestimmungen an Kaliummineralien—VI. Die geologische Entwicklung des Schwarzwald-Grundgebirges anhand absoluter Altersbestimmungen nach der K-A-Methode

---

IN MEMORIAM

Deceased Members of the Geochemical Society

Dr. GEORGE D. LOUDERBACK
Bacon Hall
University of California
Berkeley 4, California

Professor AUSTIN F. ROGERS
2423 Virginia Street
Berkeley 9, California

Dr. JOHN C. RABBITT
U. S. Geological Survey
Washington 25, D. C.

Professor S. JAMES SHAND
1 Fintry Place
Broughty Ferry
Dundee, Scotland

INFORMATION FOR CONTRIBUTORS

I. GENERAL

1. Papers on geochemistry should be submitted to the editors for the appropriate country or language (*Papers on cosmochemistry should be sent to Prof. F. A. Paneth, F.R.S.*). Papers submitted for publication will naturally be judged from the standpoint of scientific originality and novelty. Technical details of apparatus used in scientific investigation can, however, be presented in brief notes. Critical comments or preliminary results requiring early publication should be submitted as letters to the editors. Where possible, letters should be confined to 500 words. The preparation of progress reports and review articles will be invited by the editors from time to time. The journal appears as independent and complete numbers, which are combined into volumes of about 300 pages.

2. Only papers which have not been previously published can be accepted. Authors must agree not to publish elsewhere a paper submitted to and accepted by *Geochimica et Cosmochimica Acta*.

3. Fifty reprints of each paper are provided free. Additional copies can be purchased if ordered at the time the first proofs are returned. A reprint order form will accompany first proofs.

II. SCRIPT REQUIREMENTS

1. Scripts must be written in one of the three official languages—English, French, or German.

2. The script should be typed (not a carbon copy). The text must be ready for printing and should be carefully checked for errors. Authors will receive proofs for correction.

3. Illustrations should accompany the script, mounted on separate sheets. Line diagrams that require to be redrawn should include all relevant details. Half-tone illustrations should be restricted to the minimum necessary. Photographs should be enlarged sufficiently to permit their clear reproduction, and if words or numbers appear on them, two copies should be sent, one clearly printed and the other without inscription. All illustrations should be provided with descriptive legends, which should be given on a separate sheet.

4. References in the text should be given by quoting the author's name and year of publication, i.e. AHRENS (1952). **Full references should be listed at the end of each paper, in alphabetical order, in the following manner:**

AHRENS L. H. (1952) *Geochim. et Cosmochim. Acta* **2**, 168.

and should include the standard abbreviated title of the journal, year, volume number, and page number.

5. The text of articles submitted should be concise and in a readily understandable style. The technical description of the methods used should only be given in detail when such methods are new. The essential contents of each paper should be briefly recapitulated in an abstract in English. Such an abstract may, however, be submitted by the author in the language of the original typescript for translation into English by the editorial staff.

6. To conserve space, authors are requested to mark less important portions of the paper (such as description of methods, record of experimental results, etc.) for printing in smaller type.

Pergamon Press are also publishers of the following Journals:

JOURNAL OF NUCLEAR ENERGY (*including* THE SOVIET JOURNAL OF ATOMIC ENERGY *on behalf of the Pergamon Institute, a non-profit-making foundation*)
JOURNAL OF INORGANIC AND NUCLEAR CHEMISTRY
TETRAHEDRON (*the International Journal of Organic Chemistry*)
INTERNATIONAL JOURNAL OF APPLIED RADIATION AND ISOTOPES
*BULLETIN OF THE ACADEMY OF SCIENCES OF THE U.S.S.R.; GEOPHYSICS SERIES
*BIOPHYSICS
*JOURNAL OF MICROBIOLOGY, EPIDEMIOLOGY AND IMMUNOBIOLOGY
*PROBLEMS OF HEMATOLOGY AND BLOOD TRANSFUSION
*PROBLEMS OF VIROLOGY
*PROBLEMS OF ONCOLOGY
*SECHENOV PHYSIOLOGICAL JOURNAL OF THE U.S.S.R.
*RADIO ENGINEERING
CHEMICAL ENGINEERING SCIENCE
JOURNAL OF ATMOSPHERIC AND TERRESTRIAL PHYSICS
ANNALS OF THE INTERNATIONAL GEOPHYSICAL YEAR
BULLETIN GÉODÉSIQUE
SPECTROCHIMICA ACTA
JOURNAL OF THE MECHANICS AND PHYSICS OF SOLIDS
ACTA METALLURGICA (*for the Board of Governors of Acta Metallurgica*)
INTERNATIONAL JOURNAL OF THE PHYSICS AND CHEMISTRY OF SOLIDS
DEEP-SEA RESEARCH
JOURNAL OF NEUROCHEMISTRY
JOURNAL OF PSYCHOSOMATIC RESEARCH
JOURNAL OF INSECT PHYSIOLOGY
INTERNATIONAL ABSTRACTS OF BIOLOGICAL SCIENCES (*for Biological and Medical Abstracts Ltd.*)

**Translations of Russian journals published on behalf of the Pergamon Institute, a non-profit-making foundation*

D IN STACKS

THE GEOCHEMICAL SOCIETY

OFFICERS

EARL INGERSON, President
JULIAN R. GOLDSMITH, Vice-President
JOHN C. MAXWELL, Secretary
GEORGE T. FAUST, Treasurer

COUNCILLORS

J. W. GREIG, 1956–1957
WILLIAM W. RUBEY, 1956–1957
WILLARD F. LIBBY, 1956–1958
HATTEN S. YODER, JR., 1956–1958
JOHN A. S. ADAMS, 1957–1959
ALFRED O. NIER, 1957–1959

COMMITTEES

Auditing Committee:

SAM ZERFOSS, Chairman
WILLIAM L. HILL
J. TREGONING

Constitution and By-Laws Committee:

MICHAEL FLEISCHER, Chairman
JULIAN R. GOLDSMITH
DENIS M. SHAW

Education Committee:

JOHN A. S. ADAMS, Chairman
H. D. HOLLAND
K. B. KRAUSKOPF

Membership Committee:

H. R. ALDRICH, Chairman
H. N. FISK
R. M. GARRELS
WILLIAM W. RUBEY

Nominating Committee:

JOHN W. GRUNER, Chairman
LEONARD G. BERRY
S. E. CLABAUGH
WILLIAM T. PECORA
D. E. WHITE

Programme Committee:

O. F. TUTTLE, Chairman
HOWARD T. EVANS
GORDON J. F. MACDONALD

Publications Committee:

ARIE POLDERVAART, Chairman
JULIAN R. GOLDSMITH
E. WM. HEINRICH
JOHN C. MAXWELL
L. R. WAGER

Research Committee:

R. A. ROWLAND, Chairman
CHAS. G. DODD
T. G. THOMPSON
GEORGE W. WETHERILL
(including Regional Vice-Presidents)
Africa: LOUIS H. AHRENS
Asia: KEN SUGAWARA
Australia and Oceania: W. S. FYFE
Europe: C. W. CORRENS
North America: GEORGES ORDONEZ
South America: RUI RIBEIRO FRANCO

Seal Committee:

ALVIN VAN VALKENBURG, JR., Chairman
MARGARET D. FOSTER
ED ROEDDER
JEWELL GLASS

Tellers Committee:

ALLEN SINNOTT, Chairman
T. E. GILLINGHAM
A. S. WILKERSON